

2008-01-01

## The Effects of Posture on Quantitative EEG and End Tidal CO<sub>2</sub> during Standardised Optimal Hyperventilation in Healthy Adults and in Patients with Childhood Absence Epilepsy and Attack Disorders

Ann Coughlan  
Technological University Dublin

Follow this and additional works at: <https://arrow.tudublin.ie/sciendoc>

 Part of the [Medicine and Health Sciences Commons](#)

---

### Recommended Citation

Coughlan, Ann. (2008). *Enhanced absorption metal oxides for photocatalytic applications*. Technological University Dublin. doi:10.21427/D7PW24.

This Theses, Ph.D is brought to you for free and open access by the Science at ARROW@TU Dublin. It has been accepted for inclusion in Doctoral by an authorized administrator of ARROW@TU Dublin. For more information, please contact [yvonne.desmond@tudublin.ie](mailto:yvonne.desmond@tudublin.ie), [arrow.admin@tudublin.ie](mailto:arrow.admin@tudublin.ie), [brian.widdis@tudublin.ie](mailto:brian.widdis@tudublin.ie).



This work is licensed under a [Creative Commons Attribution-NonCommercial-Share Alike 3.0 License](#)

# **The Effects of Posture on Quantitative EEG and End tidal CO<sub>2</sub> during Standardised Optimal Hyperventilation, in Healthy Adults and in Patients with Childhood Absence Epilepsy and Attack Disorders**

**Submitted by: Ann Coughlan PgDip, MSc.**

**Thesis is submitted for the award of PhD to :**

**Dublin Institute of Technology, School of Physics**

**Supervisors: Prof. Pat Goodman, Dr. James Walsh,  
Prof. Matt Hussey (DIT)**

**Prof J. Mc Menamin, Consultant Paediatric  
Neurologist, Prof of Paediatrics RCSI**

**July 2008**

## **Abstract:**

### **The Effects of Posture on Quantitative EEG and End Tidal CO<sub>2</sub> during Optimal Hyperventilation, in healthy adults and in patients with Childhood Absence Epilepsy and Attack Disorders.**

Hyperventilation is used as an activation procedure during EEG. It induces hypocapnia, which elicits changes in brain wave activity that may be diagnostically useful

The mechanism of action by which Hyperventilation (HV) produces slow theta /delta waves on EEG remains conjectural. Four criteria determine the magnitude of HV response: vigorous exchange of air, blood glucose levels, age of subject, and posture. Effects of posture are poorly studied quantitatively.

Objective: A Standardised Optimal Hyperventilation Protocol (SOHVP), which elicited Hyperventilation Induced High Amplitude Rhythmic Slow activity (HIHARS) during EEG controlling for posture seated (stOHV), and supine (spOHV) is presented and validated

Method: Respiratory rate 30/min, producing three fold elevation in total expiratory vol/min (VE), duration 4 minutes. Cohort of 22 healthy adults subjects, 14 females, 8 males, mean age 29.5 years recruited. Digital video EEG, EOG, EMG, Respiration Rate, Heart rate, pO<sub>2</sub>, end tidal pCO<sub>2</sub> and Cerebral Blood Flow are monitored before, during and after OHV performed in sitting (st) and supine (sp) position

Results:

StOHV is more effective than spOHV in eliciting Hyperventilation Induced High Amplitude Rhythmic Slow activity (HIHARS) on EEG of normal adults, significantly

reducing pETCO<sub>2</sub> power density of slow EEG frequencies, and vCBF

Significance: The role of posture is confirmed as one of the factors influencing magnitude of the HV response. The seated posture is significantly more effective than the supine in developing a standardised hyperventilation response

A prospective clinical trial commenced

Objective: Is seated standardized optimal hyperventilation (StOHV) more effective in eliciting positive EEG findings in patients with Childhood Absence Epilepsy (CAE) and Attack Disorders (AD). Method: Two cohorts, a group of patients with Childhood Absence Epilepsy matched for age and sex with a group of patients with undiagnosed events.. 37 patients recruited 19 female 18 male. Mean age 9.7 years. Comparing the number of absence seizures + HIHARS in HV during non standardised(nsHV) and StOHV protocol with those spontaneously occurring during resting, wakefulness, and sleep, using 8-minute epochs as denominators. Results; 7 spontaneous CAE events captured at rest, 10 during nsHV and 27 during StOHV. . Mean. PDR 1.61 Hz slower during StOHV

Discussion: 8.1% patients ( 18.75% of CAE group) would not have been diagnosed with CAE if StOHV exercise not performed

Significance: The StOHV method is statistically and clinically more effective than nsHV at eliciting diagnostic epileptiform abnormalities on EEG. Adoption of standardised operational protocol (SOP) recommended as guideline for best practice for EEG testing in clinical practice. Standardized hyperventilation response can separate seizures from other forms of idiopathic changes in mental status in children. A hypothesis for HV induced EEG rhythmogenesis of slow theta and delta is discussed with a role for neuronal- glial interaction at the network level.

### III



## Declaration

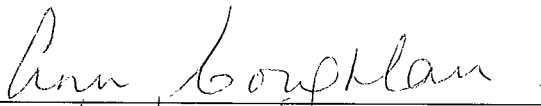
I certify that this thesis which I now submit for examination for the award of PhD is entirely my own work and has not been taken from the work of others save and to the extent that such work has been cited and acknowledged within the text of my work.

This thesis was prepared according to the regulations for post graduate study by research of the Dublin Institute of Technology and has not been submitted in whole or in part for an award in any other Institute or University.

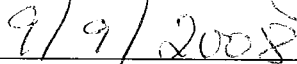
The work reported on in this thesis conforms to the principles and requirements of the Institute's guidelines for ethics in research

The Institute has permission to keep, to lend or to copy this thesis in whole or in part, on condition that any such use of the material of the thesis be duly acknowledged

Signature



Date



## **Acknowledgements**

I wish to thank Prof. Pat Goodman, Dr James Walsh, Prof Matt Hussey and Prof J Mc Menamin for their advice and expertise in the preparation and supervision of this work..

I wish to acknowledge the patience of my long suffering husband John and my children Oisin and Emma, who supplied me with cups of tea, and who had to live with me when I was in “The Zone” and totally impervious to everything happening around me.

Sincere thanks to all of my colleagues in the Children’s Neuroscience Centre in Our Lady’s Children’s Hospital Crumlin, Dublin. They have all been unfailingly supportive throughout. Their good humour and hilarious e-mails kept me sane (almost!).

Last but not least thanks to my mom, whose regular enquiry of “will you be finishing it soon?” kept me motivated when the urge to procrastinate seemed so reasonable.

## Table of Contents

## Chapter 1: Introduction Page 11

- 1.1: Hyperventilation
  - 1.2: The effect of posture on respiratory activity
  - 1.3 : “Optimal” Hyperventilation
  - 1.4: Conventional EEG measurement
  - 1.5: Quantitative EEG (QEEG) measurement
- References Chapter 1

**Chapter 2: Literature Review, Neurophysiological Mechanisms of Hyperventilation.** **Page 25**

## Introduction

- 2.1: The “Neurovascular Unit” Neurons, Glial, and Brain Endothelium
  - 2.1.1 : Neurons and the generation of EEG activity
  - 2.1.2 : Blood Brain Barrier
  - 2.1.3: Glia and the role of glial-neuronal interactions in the hyperventilation response on the EEG
- 2.2: The Astrocyte Neuron Lactate Shuttle Hypothesis (ANLSH)
- 2.3: Neurometabolic and neurovascular coupling
  - 2.3.1: Neurovascular coupling
- 2.4: Review of the potential mechanisms underlying the clinical effects of hyperventilation.
  - 2.4.1: The Cerebral Hypocapnia Theory
    - 2.4.1(a): Divergent views on the Hypocapnia Theory of HV activation
  - 2.4.2 : The Hypoxia Theory
    - 2.4.2(a): Divergent views on the hypoxia theory of HV activation
    - 2.4.2(b): Cerebral Blood flow and Brain hypoxia
  - 2.4.3: Respiratory Alkalosis Theory
  - 2.4.4: The Role of the Autonomic Nervous system : theory of hyperventilation activation
  - 2.4.5: Brainstem and Thalamic Mechanism theory
- 2.5: Excitability of human cortex in hyperventilation
- 2.6: Calcium “wave”

2.7: Contribution of potassium currents and glia to slow potential shifts.

2.8: The concept of a spatial buffering function.

2.8.1:  $K^+$  Siphoning in the Retina, spatial buffer function:

A model for the neocortex?

2.8.2: Synopsis of current knowledge on astrocytes

2.9: Can epilepsy contribute to our understanding of the underlying physiological mechanisms of the EEG hyperventilation response?

2.10: Discussion

2.10.1 A novel hypothesis: the 'hypocapnia cascade' as the basis of the neurophysiological EEG response to spontaneous hyperventilation

2.11: Conclusion

References Chapter 2

## **Chapter 3: Materials, Methods, and Results. Page 151**

Methodology

3.1: Electrode application method

3.2: Physiological signals measured

3.3: Equipment

3.4: EEG Montage

3.5: Capnography

3.6: Oxygen Saturation

3.7: Transcranial Doppler Ultrasonography (TCD) Procedure

3.8: Acquisition of each data set

3.9: Quantitative Analysis

3.10: EEG analysis software

3.10.1: Topograph contour creation

3.10.2: Power Spectrum

3.10.3: Fast Fourier Transform (FFT) Calculation

3.11: Results

3.12: Subjective symptoms

3.13: Analysis

3.14: Box Plots

- 3.15: Comparison of partial end tidal CO<sub>2</sub> (pETCO<sub>2</sub>) following 4 minutes of optimal hyperventilation controlled for posture
  - 3.16: Comparison of EEG Frequency in Hz, following 4 minutes of optimal hyperventilation controlled for posture
  - 3.17: Change in Heart rate with SpOHV and StOHV
  - 3.18: Trans Cranial Doppler ultrasound measurement of the velocity of cerebral blood flow (vCBF)
  - 3.19: Power density of low frequency bands
  - 3.20: Case Presentation, Subject 3 (27 year old male)
  - 3.21: Discussion
- References: Chapter 3

#### **Chapter 4 : Introduction and review of recent literature. Standardized Hyperventilation during EEG in children with absence epilepsy and “funny turns” Page 224**

- 4.1: Aim of Study
  - 4.2: Childhood Absence Epilepsy
  - 4.3: Pathogenesis of absence epilepsy
  - 4.4: Differentiating features of absence seizures and complex partial seizures
  - 4.5: Childhood Absence Epilepsy and Hyperventilation induced high amplitude rhythmic slowing
  - 4.6: Methodology
- References: Chapter 4

#### **Chapter 5**

#### **Results: Standardized Hyperventilation during EEG in Childhood Absence Epilepsy Page 250**

- 5.1 Analysis of the data
- 5.2: “At Rest” EEG
- 5.3: Non Standardized Hyperventilation (nsHV)
- 5.4: Standardized Seated Optimal Hyperventilation (SOHV)
- 5.5: Posterior Dominant Rhythms and hyperventilation
- 5.6: Efficacy of SOHV in induction of Absence Seizures
- 5.7: Spontaneous CAE seizures “at rest” and CAE seizure induction during nsHV

5.8: Gender Differences

5.9: Discussion

5.10: Final conclusions and summation

References Chapter 5

### **Figures, Tables, Equations**

#### **Chapter 1: Figures**

Fig 1.1: EEG sample: HIHARS pattern elicited by hyperventilation

#### **Chapter 2: Figures**

Fig 2.1: A signal propagating down an axon to the cell body and dendrites of the next cell.

Fig 2.2: Locations of barrier sites in the CNS. Abbot et al (2006) after : Astrocyte-endothelial interactions at the blood-brain-barrier. (After Nature Reviews Neuroscience 7:41-53).

Fig 2.3: General interactions among neurons, astrocytes and brain capillaries.

Fig 2.4: Relationship between astrocytes and other brain elements.

Fig 2.5: Neuron with supporting glial astrocytic cell.

Fig 2.6: Astrocytes (red cells) and neurons (blue cells) were labeled with specific antibodies in this fixed rat brain section. ( After Kasischke 2004).

Fig 2.7: Proof of activity-dependent metabolism in two kinds of brain cells, neurons and astrocytes ( After Kasischke 2004).

Fig 2.8: Schematic representation of a neuron, an astrocyte and a capillary.

Histological arrangement and the trafficking of substrates

Fig 2.9: Illustration of the putative Astrocyte–Neuron Lactate Shuttle Hypothesis (ANLSH).

Fig 2.10: Model for neuron-glia metabolic coupling (after Magistretti 2006).

Fig. 2.11: Line graph showing the relationship between cerebral blood flow and pCO<sub>2</sub>.

Fig 2.12: CO<sub>2</sub> as a regulator of cerebro vascular tone.

Fig 2.13: Hyperventilation, pH ,CO<sub>2</sub>, and arterial diameter

Fig 2.14: Relationship between OEF and L/P ratio.

Fig2.15: Hyperventilation and PET parameters.

Fig 2.16: Flow chart “Hypocapnia Cascade”:

## **Chapter 2: Tables**

2.1: The effects of hypocapnia.

## **Chapter 2: Equations**

2.1: Scale of propagation speed of calcium wave.

2.2: Time needed for calcium release.

## **Chapter 3 : Figures**

3.1: International 10-20 system of electrode placement

Fig 3.1.2: International 10/20 system. Electrode positions superimposed on brain image

Fig 3.1.3: MRI slices nearest the international 10/20 electrode positions

Fig 3.2: EEG Montage for Posture Hyperventilation Study

Fig 3.3: Digital Video EEG

Fig 3.4a: TCD the transtemporal window (1), the transorbital window (2) and the transoccipital window.(3)

Fig 3.4b: TCD 3 positions through the transtemporal window

Fig 3.4c: VCBF in MCA with age

Fig 3.4d: Sample of TCD waveform

Fig 3.5: Sample of Topographic plot of delta, theta, alpha and beta EEG frequency bands

Fig 3.6: Sample of Power spectrum (Hz,uV/Hz) of 10-20 scalp electrodes

Fig 3.7: Total of subjective symptoms, seated OHV and supine OHV

Fig 3.8: Box Plot of pETCO<sub>2</sub> at rest and during Sp OHV and StOHV

Fig 3.9: Box Plot of EEG in Hz at rest and during Sp OHV and StOHV

Fig 3.10: Box Plot of heart rate in bpm at rest and during Sp OHV and StOHV  
Y axis units are b.p.m.

Fig 3.11: Box Plot of vCBF in cm s<sup>-1</sup> at rest and during Sp OHV and StOHV.

Fig 3.12: Trial 1 subject 6 trial 1 . TCD of right MCA supine at rest

Fig 3.13: Trial 1 subject 6. TCD of right MCA seated at rest

Fig 3.14: Trial 1 subject 6. TCD of right MCA supine during SOHV, at pETCO<sub>2</sub> of 22mmHg

Fig 3.15: Trial 1 subject 6. TCD of right MCA seated during SOHV, at pETCO<sub>2</sub> of 13 mmHg

Fig 3.16: Box plot of power density of low frequency bands

Fig 3.17: pETCO<sub>2</sub>(mmHg) and EEG (Hz) in both postures at rest and during HV

Fig 3.18: pETCO<sub>2</sub>(mmHg) and Heart Rate (bpm) in both postures at rest and during HV

Fig 3.18: pETCO<sub>2</sub>(mmHg) and Heart Rate (bpm) in both postures at rest and during HV

Fig 3.19: Digital EEG/Video Image, Subject supine and resting. Raw EEG, EOG, Respiration, and ECG data.

Fig 3.20: Power spectrum of Fig 3.19with subject supine and resting

Fig 3.21: Topographic map of Alpha, Beta, Theta, and Delta frequency bands from power spectrum in Fig3.19. supine resting

Fig 3.22: Supine OHV. Digital Video EEG

Fig 3.23: Power spectrum of EEG data in Fig 3.22

Fig 3.24: Topograph of alpha, beta, theta, delta bands of fig 3.22 supine with optimal hyperventilation

Fig 3.25: Comparison of Raw EEG data, supine resting and OHV

Fig 3.26: Raw Digital EEG seated at rest

Fig 3.27: Raw Digital EEG seated and hyperventilating

Fig 3.28: Power spectrum of EEG during seated OHV (Fig3.27)

Fig 3.28: Power spectrum of EEG during seated OHV (Fig3.27)

Note increase in slow wave spectra, ie frequencies under 8Hz, during Seated OHV compared to figure 3.24 (Supine OHV)

Fig 3.29: Topograph of alpha, beta, theta, delta bands of fig 3.27 during seated OHV.

### **Chapter 3: Tables**

Table 3.1: Age and gender of study population

Table 3.2: Subjective symptoms by gender during Seated OHV (StOHV)

Table 3.3: Subjective symptoms by gender during Supine OHV (SpOHV)



Table 3.4: Total subjective symptoms, seated OHV and supine OHV

Table 3.5: Paired Student's *t*-Test: Results End Tidal CO<sub>2</sub>, Supine OHV and Seated OHV

Table 3.6: Paired Student's *t*-Test: Results EEG frequency in Hz, Seated OHV and Supine OHV

Table 3.7: Paired Student's *t*-Test: Results Heart rate in bpm, Seated OHV and Supine OHV

Table 3.8: Paired Student's *t*-Test: Results vCBF in cm s<sup>-1</sup>, Supine OHV and Seated OHV

Table 3.9: Paired Student's *t*-Test: Results Power density of low frequency bands in EEG, Supine OHV and Seated OHV

Table 3.10: Sample from Excel file of data on each subject  
(this is subject 3, trial no. 6)

#### **Chapter 4: Figures**

Fig 4.1: Typical 3 per second (3Hz) Spike and wave discharges seen in CAE

Fig 4.2 : (a)An EEG recording of a generalised absence seizure showing the synchronous spike and wave discharge (SWD) (b) The classic view of absence seizure pathophysiology is shown.

Fig 4.3 : HIHARS during hyperventilation (Sample from EEG dept. OLCHC)

Fig 4.4: Frequency and type of clinical features observed in episodes of HIHARS with altered awareness and in absence seizures (after Lum *et al* 2002)

#### **Chapter 4: Tables**

4.1: Clinical and EEG Findings in Typical and Atypical Absence Seizures

Table 4. 2. Differentiating Features of Complex Partial and Absence Seizures

#### **Chapter 5: Figures**

Fig 5.1: Medication: no. of patients in each group taking AED's

Fig 5.2: Medication by category

Fig 5.3: Medication, percentages

Fig 5.4: HV Effort

Fig 5.5: PDR at Rest

Fig 5.6: No. of EEG changes observed at rest in 37 subjects

Fig 5.7: No. of EEG changes observed during non standardised supine HV

Fig 5.8: No. of EEG changes observed during standardised supine hyperventilation (SOHV) in 37 subjects

Fig 5.9: Box Plot, Range, Mean and Standard Deviation of the change in posterior dominant rhythm in EEG during nsHV (Group A) and SOHV (Group B).

Fig 5.10: Box plot of group means, range and SD of PDR, with 95% confidence intervals

Fig 5.11: Number of Childhood Absence Seizures captured spontaneously “At Rest”, during non standardized HV (nsHV), and during standardized HV (SOHV).

Fig 5.12: Total duration of CAE seizures “At Rest” 101 seconds, during non standardized HV (nsHV) 104 seconds, and during standardized HV (SOHV) 314 seconds .

Fig 5.13: Plot of group means 95% CI. Y axis duration of events in seconds

Fig 5.14: Diagnosis by Gender (Following EEG)

Fig 5.15 : Gender and EEG findings

## **Chapter 5: Tables**

Table 5.1: Comparison of PDR during nsHV and SOHV

Table 5.2: ANOVA of PDR at rest, during nsHV, and SOHV

Table 5.3: No of absence seizures induced during nsHV and SOHV

Table 5.4: Paired *t*-test Duration of CAE seizures, nsHV, SOHV

Table 5.5: ANOVA comparison of duration of CAE events, at rest (A), nsHV (B), SOHV (C)

Table 5.6: Paired *t*-test spontaneous CAE Seizures “at rest” and during nsHV

## **EEG Samples**

EEG 5.1: left frontal polar prominent spike discharge

EEG 5.2: left temporal onset

## **Glossary of abbreviations**

adenosine tri-phosphate	ATP
alternating current	AC
analogue to digital converter	ADC
blood oxygen level dependant fMRI	BOLD fMRI
carbon dioxide	CO <sub>2</sub>
cerebral blood flow	CBF
cerebral blood volume	CBV
cerebral metabolic rate	CMR
cerebral metabolic rate of oxygen	CMRO <sub>2</sub>
cerebrospinal fluid	CSF
direct current	DC
echo planar imaging (MRI)	EPI-MRI
electrocardiograph	ECG
electromyograph	EMG
electro-oculograph	EOG
electroencephalograph	EEG
end-tidal partial pressure carbon dioxide	pETCO <sub>2</sub>
fast Fourier transform	FFT
functional magnetic resonance imaging	fMRI
gamma-aminobutyric acid	GABA
gradient echo MRI	GE-MRI
hertz (cycles per second)	Hz
hypoxia	oxygen deficit
hyperventilation induced high amplitude rhythmical slowing	HIHARS
hyperventilation	HV
magnetic resonance imaging	MRI
measurement unit of acid/base metabolism	pH
middle cerebral artery	MCA
near-infrared spectroscopy	NIRS
optimal hyperventilation	OHV

oxygen	O <sub>2</sub>
oxygen extraction fraction	OEF
partial pressure of arterial oxygen	PaO <sub>2</sub> (P, pressure)
partial pressure of arterial carbon dioxide	PaCO <sub>2</sub>
partial pressure of carbon dioxide	PCO <sub>2</sub>
partial pressure of oxygen	PO <sub>2</sub>
positron emission tomography	PET
posterior dominant rhythm	PRD
quantitative digital EEG	QEEG
saturated partial pressure of oxygen	SpO <sub>2</sub>
silver/silver chloride electrodes	Ag/AgCl
spin echo MRI	SE- MRI
total expiratory volume/minute	VE
transcranial Doppler	TCD
velocity of cerebral blood flow	vCBF

## **CHAPTER 1**

### **INTRODUCTION**

Electroencephalography (EEG) is normally used since its initial discovery in 1929 to record the electrical activity, which is generated in the brain by extra-cellular currents in the cortex, by using electrodes placed on the head. The EEG is recorded as a graph of voltage against time and four main frequency bands are present. These are named after letters in the Greek alphabet, delta 0.5-4.5 Hz, theta 5.0-7.5 Hz, alpha 8.0-12.5 Hz and beta 13.0-20.0 Hz. A routine EEG recording takes about 30 minutes to perform and consists of a “resting” phase (20 minutes) during which the patient lies down quietly with their eyes closed. Following this three separate “Activation Procedures” are carried out. As follows:

- A.       intermittent photic stimulation (IPS)
- B.       the recording of a period of sleep
- C.       hyperventilation (HV).

These activation procedures are used to induce abnormal findings in an otherwise normal EEG, or to accentuate and clarify the origin of abnormalities noted on the resting EEG recording.

During IPS the patient is asked to watch a strobe light that flashes at various different frequencies. This is done to determine whether the patient is photo-

sensitive and susceptible to experiencing epileptic seizures. Standardised protocols for performing IPS have been published by Bickford (1979) and Binnie and Jeavons (1972), and therefore IPS does not form part of the current study.

About 20-25% of patients with epilepsy have seizures exclusively or mainly while sleeping (Janz 1962, Gibberd and Bateson 1974). The relationship between epileptic seizures and sleep, arousal from sleep, and sleep deprivation was extensively reviewed by Broughton (1972, 1984). In brief there is evidence that tonic clonic, tonic, and myoclonic generalised epileptic seizures are activated in non-rapid eye movement sleep (NREM). Typical absence seizures may be seen in rapid eye movement sleep (REM). Achieving a period of sleep recording during EEG is therefore very desirable as it activates latent epileptiform abnormalities - EEG activity which contains sharp waves, frank spikes or spike and wave discharges which support the diagnosis of epilepsy.

Hyperventilation (HV) is the third activation procedure routinely used in EEG recording. HV is particularly effective in eliciting epileptiform discharges. Berger (1933), who recorded the first human EEG, described the effect of hyperventilation on the electrical activity of the human brain. The methodology of the HV activation procedure used during EEG is the focus of this study.

## 1.1 Hyperventilation

Generally the method of hyperventilation (HV) consists of deep and regular respiration at a rate of about 20 per minute for a period of two to five minutes (the average is about three minutes) with the eyes closed and while in a supine position. Post hyperventilation the EEG is monitored for another two to three minutes until the background has returned to baseline. When carried out in adults Morrice (1956) reported that such hyperventilation causes an air exchange of 20-50 litres per minute and a drop in partial pressure of carbon dioxide ( $p\text{CO}_2$ ) in the range of 4-7%. The underlying mechanism of hyperventilation's provocation of slow waves and seizure discharges is not understood fully and has been the subject of studies by several investigators (see chapter 2 section 2.4). The most widely accepted explanation for EEG activation relates a decrease in  $p\text{CO}_2$ , which elicits vasoconstriction leading to a reduction in the velocity of cerebral blood flow (vCBF), and decreased partial pressure of oxygen ( $p\text{O}_2$ ) causing relative brain ischaemia, which produces slowing of activity on the electroencephalogram. In response to this procedure the characteristic EEG "slowing" or "build up" changes, which are more prominent in children, consist of a fluctuating increase of bilaterally synchronous slow theta (5.0-7.0 Hz) and delta activity (i.e. present in both cerebral hemispheres and synchronised together), and also a slowing of the alpha (8.0-12.5 Hz) and Beta (13.0-20.0 Hz) activity. There is also an overall increase in the background amplitude (size) of the recorded waveforms. In most neurophysiology laboratories HV is generally performed with the patient lying down on a couch or bed in the supine position. This recording position is comfortable for the

patient and facilitates relaxation, eye closure and sleep during the “resting” phase of the routine EEG recording, but according to the literature it may not be the optimal posture in which to obtain maximal activation of the EEG during hyperventilation.

The magnitude of the hyperventilation response depends upon: (Takahashi 1998)

- the vigour of the exchange of air,
- the age of the subject
- the subject's blood glucose levels
- the subject's posture.

In adults low blood glucose of less than 80 mg/dl tends to enhance the appearance of slow waves. Conversely a high level of more than 120 mg/dl tends to inhibit or prevent such an effect. Slow waves appear much more abruptly and are more pronounced in children, and this is considered to be related to hypersensitivity to hypocapnic changes in children (Takahashi 1998). It has been reported occasionally that an erect position as opposed to a reclining position enhances the effect of hyperventilation on the EEG (Engel *et al* 1944, Morrice, 1956. Billinger and Frank 1969). *“Erect position as compared with a reclining position enhances the effect of HV; EEG slowing occurs earlier and with greater intensity. This is thought to be a result of relative cerebral anoxia”* (Billinger and Frank 1969)



The position in which hyperventilation was performed by subjects is often mentioned in the literature only as a minor “aside”, and there are only three papers which reported on direct studies on effects of posture on the EEG.

In 1944 Engel *et al.* noted that hyperventilation produced greater EEG slowing when the subjects were in an upright position than when they were in the recumbent position. In 1956 Morrice mentioned position as one of the factors influencing the HV response. Billinger and Frank in 1969 examined the effects of posture on EEG slowing during hyperventilation using analog 8 and 16 channel recording instruments and subjective grading of the responses into four possible categories using three judges scoring the tracings.

The supine position is the most commonly used for clinical EEG recording, as it is desirable to obtain sleep. The work of Engel, Morrice and Billinger and Frank however indicated that it may be more clinically effective to perform hyperventilation (HV) in an upright (sitting) position. There is currently no internationally recognised standard protocol for the performance of HV. Conditions of hyperventilation vary tremendously from one EEG service to another and there is no quantitative “normal” range of EEG slowing produced by hyperventilation. Practice is variable across neurophysiology laboratories. The duration of HV varies, and is generally accompanied by active encouragement by the EEG practitioner and a subjective grading of the effort made by the patient. Developing a standardised operational protocol (SOP) for HV activation, controlling for the posture in which the procedure is performed during EEG is the focus of this research.

## **1.2 The effect of posture on respiratory activity**

Posture is known to affect the activity of the abdominal muscles (Kera and Maruyama 2005). The main difference between hyperventilating in the supine and sitting position is the differential involvement of the diaphragm. Lying down the diaphragm is the primary muscle, while sitting the diaphragm and intercostals operate in tandem. The relative contribution of the different muscles is also a function of age and gender: children and men tend to utilize abdominal muscles to a greater degree than adult females.

Kera and Maruyama (2005) reported the influence of posture on the expiratory activity of the abdominal muscles in a group of 15 young men. EMG activity was examined in the following muscles: external oblique abdominis, internal oblique abdominis, and rectus abdominis muscles. Subjects were placed in the supine, standing sitting and sitting with elbow on knee position. A spirometer was used to measure the lung volume in various postures. Lung volume was observed to change with posture. Activity is not generally observed during respiration at rest; however these are activated during exercise and expiratory effort. De Troyer (1983) reported upper and lower abdominal tonic muscle activities in various tilt positions. However, such activity was not observed in the supine position. This tonic activity is reported to result from an increase in intra-abdominal pressure attributed to gravity, serving to prevent a shift in the length-tension relation by shortening the diaphragm. Lung volumes changes with changes in posture, particularly when affected by gravity (D'Angelo and Agostini 1995). Vital capacity and Total Lung Capacity (TLC) shows a relative

decrease in the supine position as compared to the standing position. In the supine position, the abdominal contents push the diaphragm into the thoracic cavity, thus raising the diaphragm and decreasing the Functional Residual Capacity (FRC) relative to standing / sitting conditions (D'Angelo and Agostini 1995). The determining factor for FRC is the elastic recoil pressure of the rib cage and the reduced pressure in the lungs. The FRC is affected by changes in pressure over and under the diaphragm

Although the maximal effort is possible in the standing position this is not a safe position in which to perform a hyperventilation exercise, as it carries risk of falling and injury to the subject should they become faint, dizzy or lightheaded.

During a preliminary pilot study of 5 patients (2 male and 3 female ) by the author the end tidal volume was measured at rest and during seated hyperventilation using full body plethysmography to confirm a three fold increase in VE using the optimal hyperventilation method described by Konishi (1987). These measurements could not be repeated for the supine position as the instrumentation does not accommodate supine measurements.

All of the subjects in this study reported that they found performing the OHV exercise easier and felt they could make a greater effort in the seated position. Therefore the contributions of abdominal muscles which are only used during respiratory effort in the sitting position could be a factor in the achievement of lower pETCO<sub>2</sub> in the seated position.

### 1.3 “Optimal” hyperventilation

In order to measure the effect of a single variable, posture, on the EEG a standardisation of the method of hyperventilation is required. In 1987 Konishi published the optimal conditions for adequate HV activation in a study group of thirty seven children (Konishi 1987 part 1). These were:

- a respiratory rate of 30 per minute
- a three-fold elevation of total expiratory volume/minute (VE)
- a duration of 4 minutes.

With this activation the degree of EEG slowing was found to be nearly inversely proportional to the age (range 6-17 years). In the paper Konishi postulated that the difference in the hyperventilation response between children and adults may be due to age related CNS (central nervous system) sensitivity to CO<sub>2</sub> and /or cerebral vascular CO<sub>2</sub> responsiveness. There is no indication as to the position or posture in which hyperventilation was performed by the subjects. Optimal hyperventilation has been demonstrated to produce hyperventilation induced high amplitude rhythmical slowing (HHARS) (Fig 1.1) in adult subjects with end-tidal pCO<sub>2</sub> (pETCO<sub>2</sub>) of 2.0 +/- 0.1 kPa (15.4 +/- 0.8 mm Hg) (Zwiener *et al* 1998), (see chapter 3 section 3.16). Lum *et al* (2002) used the following criteria to define HHARS (in a video EEG study on HHARS with altered awareness)

1. high amplitude (> 100µV)
2. ~2.5-5.0 Hz generalised rhythmic slowing
3. duration of greater than or equal to 3 seconds.

This criterion was used to define an epoch of HIHARS in this study.

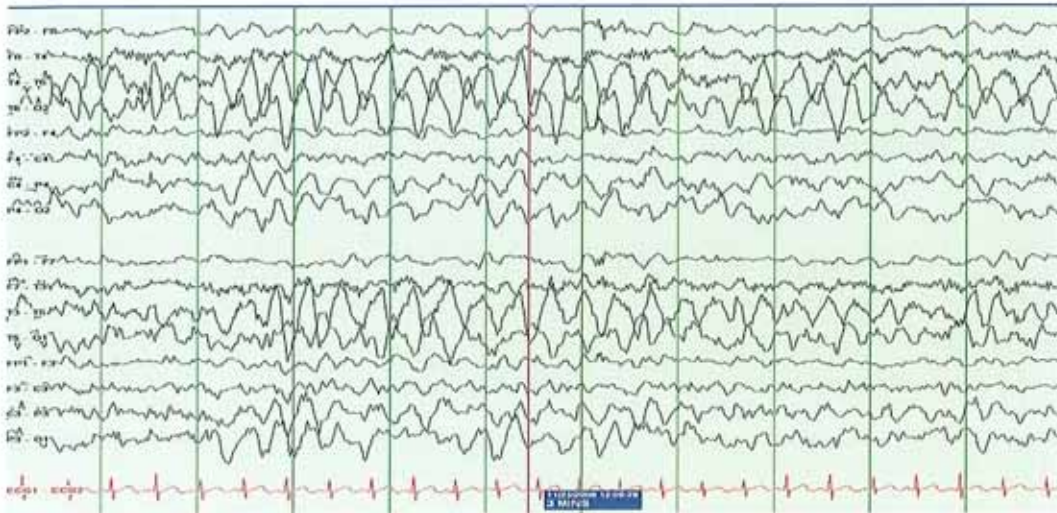


**Fig 1.1 EEG sample: HIHARS pattern elicited by hyperventilation in a 26-year-old female (from EEG dept. Our Lady's Hospital Crumlin, Dublin)**

## 1.4 Conventional EEG measurement

EEGs are generally still interpreted by the electroencephalographer “reading” the trace and giving a subjective interpretation of the various EEG frequencies present, their topography, amplitude, inter-hemisphere symmetry, and the presence of “abnormal” or suspicious EEG activity. Measurements are made using cursors of the dominant background frequencies. The effort made by the subject and the changes induced on the EEG by 3 minutes of hyperventilation are also subjectively assessed and usually graded as mild, moderate, or marked depending upon the amount of theta and delta activity induced by the procedure. Gilbert *et al* (2003) carried out a meta-analysis of EEG test performance. They

carried out a Medline search from 1970 to 2000 of English language studies, reviewing 25 studies involving 4,912 EEGs. They found that the specificity (range 0.13 to 0.99) and sensitivity (range 0.20 to 0.91) of interpretations by electroencephalographers (EEGers) were very diverse. They reported that the diagnostic accuracy of EEG and the thresholds for classifying EEG as positively epileptiform varied widely. In their multivariate model, differences in the readers' thresholds accounted for 37% of the variance in the EEG diagnostic accuracy. No other reported factors were found to be significant. They concluded that there is wide inter-reader variation in sensitivity and specificity of non-quantitative EEG interpretations.

### **1.5 Quantitative EEG (QEEG) measurement**

QEEG involves the use of fast Fourier transform (FFT) and spectral analysis of the digital EEG signal to facilitate objective analysis of the data. FFT significantly simplifies the computation of spectral coefficients. The EEG contains regular patterns, which may be defined by their spectral (frequency) content. Bursts of sinusoidal type waves occur and recur in a predictable fashion. These bursts may correspond with mental states, primarily inattention or inactivity, or with physiological states such as hyperventilation activation or sleep. The advent of digital technology facilitated the conversion of the analog EEG signal into a digital format. The rapid development of this technology over the past 10 years has placed QEEG technology in the hands of clinicians. QEEG can now be combined with functional magnetic resonance imaging (fMRI) for a 3-dimensional view of brain activity. QEEG analysis of clinical digital EEG

recordings and transformation to alternative domains assists in the interpretation and contributes to more objective interpretations. A recent study by Greene *et al* (2008) on a comparison of QEEG features for neonatal seizure detections yielded a sensitivity of 81% and a specificity of 82.2%.

For the purpose of this study the baseline EEG activity, the peri-hyperventilation and post-hyperventilation changes in the frequency, amplitude, topography (brain mapping), and symmetry of EEG waveforms are analysed using QEEG methods (Konishi 1987 Part 2, Zweiner *et al* 1998, Van Der Worp *et al* 1991). Topographical quantitative EEG changes in the mean spectral power density of the delta, theta, alpha and beta frequency bands during and after optimal hyperventilation (OHV) may be analysed and compared to the resting baseline activity. Changes in the power ratios between the four frequency bands are investigated and related to changes in the end tidal  $pCO_2$  and  $pO_2$ , (See Chapter 3 section 3.9 and 3.10).

The null hypothesis is that posture has no effect upon measured physiological variables during a standardised hyperventilation exercise.

The data are analysed to establish if a particular postural position for HV proves statistically significantly better at inducing HIHARS in normal adults. A positive relationship, demonstrating increased sensitivity and specificity related to the posture in which a standardised optimal hyperventilation exercise is performed, and the degree of EEG activation would support the adoption of the standardised method during routine hyperventilation testing in EEG laboratories.

Therefore the specific aims of this study are:

Specific Aim 1

1.a To examine the impact of standardised optimal hyperventilation (SOHV) in healthy adult volunteers during EEG performed in two different postures, sitting and supine.

1.b To measure these changes using quantitative methods

1.c To determine if posture has a statistically significant impact on the effectiveness of hyperventilation.

1.d To propose a standardised operational hyperventilation protocol (SOHV) which optimises activation of the EEG during hyperventilation

Specific Aim 2,, applying the findings of Aim 1 in three situations

2.a To apply the SOHV method, controlling for posture in a clinical trial of patients with childhood absence epilepsy (CAE) and patients with attack disorder

2.b To determine whether or not SOHV has a statistically significant impact on the number of epileptic absence attacks and epileptiform changes on EEG elicited in the CAE cohort

2.c To determine whether or not SOHV has a statistically significant impact on the production of HIHARS and is more effective in eliciting events and electrographic changes in patients with attack disorders.



## References: Chapter 1

- Berger H, 1933, Uber das Electrenkephalogram des Menschen IX (translated as “about the human EEG”) *Arch Psychiatr. Nervenkr.* 101: 452-469
- Bickford RG, 1979, Activation procedures and special electrodes. In *Current Practice of Clinical Electroencephalography*. Eds. Klass DW, Daly DD, pp.269-305. New York: Raven Press
- Billinger T W, Frank G S, 1969, Effects of posture on EEG slowing during hyperventilation. *Am. J. EEG Technol* 9(1): 22-27
- Binnie CD , Jeavons PM, 1992. Photosensitive epilepsies. In *Epileptic Syndromes in Infancy, Childhood, and Adolescence*. 2<sup>nd</sup> ed, Eds. Roger J, Bureau M, Dravet FE, Dreifuss FE, Perret A, Wolf P. pp 299-302, Amsterdam: Elsevier
- Broughton R, 1972, Sleep and neurological states. In *The Sleeping Brain*, Ed. Chase M. pp 363-376. Los Angeles: Brain Information Service/Brain Research Institute
- Broughton R, 1984, Epilepsy and sleep: A synthesis and prospectus. In *Epilepsy-Sleep-Sleep Deprivation*, Eds. Degan R, Neidermeyer E. pp 317-356. Amsterdam: Elsevier
- De Troyer A(1983) Mechanical role of the abdominal muscles in relation to posture. *Respir Physiol* 53: 341-353
- D’Angelo EG, Agostoni E 1995. Statistics of the chest wall. In Roussos C, Macklem PT eds. *The Thorax* 2<sup>nd</sup> ed, Dekker, New York, 457,493
- Engel GL, Romano J *et al*, 1944, A simple method of determining frequency spectrums in the electroencephalogram. *Arch. Neurol, Psychiat.*, Chicago, 51: 134-146
- Gibberd FB, Bateson MC, 1974, Sleep Epilepsy: Its pattern and prognosis. *Br Med J* 2: 402-405
- Gilbert DL, Sethuraman G, Kotagal U, Buncher CR, 2003, Meta-analysis of EEG test performance shows wide variation among studies. *Neurology* 60(4): 564-570
- Greene BR, Faul S, Marnane WP, Lightbody I, Korotchikiva I, Boylan GB, 2008, A comparison of quantitative EEG features for neonatal seizure detection.

*Clin Neurophysiol* 119(6): 1248-61, Epub 2008 Apr 1

Janz D, 1962, Grand mal epilepsies and the sleeping-waking cycle. *Epilepsia* 3: 69-109

Kera T, Maruyama H, 2005. The effects of posture on respiratory activity of the abdominal muscles. *J Phys Anthropol and Appl Human Science* 24: 259-265

Konishi T, 1987 Part 1, The standardization of hyperventilation on EEG recording in childhood Part I: The quantity of hyperventilation activation. *Brain Dev.* 9 (1): 16-20

Konishi, T, 1987 Part 2, The standardization of hyperventilation on EEG recording in childhood Part 2: The quantitative analysis of build-up *Brain Dev.* 9 (1): 21-25

Lum LM, Connolly MB, Farrell K, Wong PKH, 2002, Hyperventilation – Induced High Amplitude Rhythmic Slowing with altered awareness: A video EEG Comparison with absence seizures. *Epilepsia* 43(11): 1372-1378

Morrice, J.K, 1956, Slow wave production in the EEG with reference to hypernoea, carbon dioxide, and autonomic balance. *Electroenceph. Clin. Neurophysiol* 8: 49-72

Takahashi T, 2004, 5<sup>th</sup> Ed. Chapter 14: Activation Methods , in *Electroencephalography: Basic Principles, Clinical Applications, and Related Fields*. Eds. Neidermeyer E, Lopes da Silva F. pp 261-262. Lippincott Williams and Wilkins  
ISBN-13: 9780781751261

Van der Worp, H.B. *et al.* 1991, Quantitative EEG during progressive hypocarbia and hypoxia. Hyperventilation–induced EEG changes reconsidered. *Electroencephalogr. Clin. Neurophysiol.* 79 (5): 335-41

Zwiener U, Lobel S. *et al*, 1998, Quantitative topographical analysis of EEG during non-standardized and standardized Hyperventilation. *J Clin. Neurophysiol.* 15(6): 521-8

## **CHAPTER 2**

# **NEUROPHYSIOLOGICAL MECHANISMS OF HYPERVENTILATION**

The term *homeostasis* is used by physiologists to mean maintenance of steady or constant conditions in the internal environment. Hyperventilation (HV) simply means breathing in excess of the body's needs for oxygen at a particular moment. Hans Berger a German psychiatrist working in Jena in Germany, first described the effect of voluntary hyperventilation on the electrical activity of the brain in 1933. He wrote the first paper on the human EEG in 1929. By encouraging a subject to hyperventilate during EEG the aim is to transiently disturb homeostasis, activating previously unseen abnormalities or accentuating those already present for the purposes of aiding diagnosis and treatment.

During hyperventilation carbon dioxide is “blown off”. Hyperventilation is a condition existing when the rate and depth of respiration exceed demands for oxygen delivery and carbon dioxide removal, which gradually leads to hypocapnia (low partial pressure of carbon dioxide,  $\text{PaCO}_2$ ). Hypocapnia can make the heart pound, vision blur, ears ring or may induce dizziness lightheadedness or fainting (Gardner 2003). These physiological changes are all related to the fact that during hyperventilation a deficit of  $\text{CO}_2$  develops.  $\text{CO}_2$  is a

waste gas, and a byproduct of metabolism, primarily due to muscle activity; it is given off by tissues and carried in the bloodstream to the lungs, to be exhaled. Production of CO<sub>2</sub> is normally in equilibrium with O<sub>2</sub> intake. This equilibrium is important because CO<sub>2</sub> has an essential physiological function as a prime regulator of vascular tone in the cerebral cortex (Busija and Heistad 1984).

There is a large body of data in the medical literature on voluntary hyperventilation in humans, mechanical ventilation in brain injured patients, in animal models of hyperventilation under anesthesia, and in *in vitro* preparations of hippocampal slices (Thomas *et al* 2002, Golanov *et al* 2000, Corfield *et al* 1995, Balzamo *et al* 1991, Toda *et al* 1989, Balestrino and Somjen 1988, Busija and Heistad 1984, Granholm 1971, Granholm and Seisjo 1971). Clinically hyperventilation has been used either to activate the EEG in order to identify epileptic patients (Drury 2000, Gabor and Marsan 1969, Morgan and Scott 1970, Miley and Forster 1977), which is the case in the work described in this thesis, or to reduce pressure in the brain after traumatic brain injury (Thomas *et al* 2002). Despite the almost universal use of hyperventilation as an “activating” procedure in clinical EEG, its mechanism of action remains conjectural. Substantial controversy persists in the literature concerning the physiological consequences of voluntary hyperventilation. The theory most broadly quoted in the literature is that the “activation” is related to ischaemic-hypoxic changes within the brain secondary to systemic hypocapnic vasoconstriction associated with respiratory alkalosis resulting in increased neuronal excitability leading to the appearance of “slow waves” in the theta (4.0-7.0 Hz) and delta (0.5-4.0 Hz) frequencies in the EEG (Bickford 1979, Cooper *et al.* 1980). A 1987 review

found “*no substantive evidence to support the theory that EEG slowing with hyperventilation is due to cortical hypoxia secondary to cerebral vasoconstriction and/or secondary to hypocapnia*” (Patel and Mulsby 1987). In fact, the intact thalamus is necessary for the hyperventilation response and hypocapnia produces decreased activity in the mesencephalic reticular formation. They proposed that these two phenomena are associated with the slow wave states found during EEG activation by hyperventilation, which are similar to drowsiness, or an “edge of sleep” state. The most common EEG response to hyperventilation in a normal individual consists of diffuse slowing; in adults this response is most prominent at the vertex of the brain. Slowing will disappear within a minute after stopping hyperventilation. In patients prone to epilepsy, focal slow wave activity is enhanced, particularly in the temporal region and a 3 Hz spike and wave activity may be detected only during hyperventilation. In the normal brain hyperventilation produces a nearly linear decrease in cerebral blood flow (CBF) and a 3 mmHg decrease in PaCO<sub>2</sub> (Muller et al 1977).

## **2.1 The “Neurovascular Unit” Neurons, Glia, and Brain Endothelium**

The cellular components of the brain are neurons, glia and vascular cells of the brain endothelium. These three entities form a metabolic network to sustain brain activity. In this review of the current literature pertaining to hyperventilation and EEG the “neurovascular unit” is an important component. The cerebral microvascular endothelium, together with astrocytes, pericytes, neurons, and the

extracellular matrix, constitute a "neurovascular unit" that is essential for the health and function of the CNS. In this thesis the disturbance of homeostasis by hyperventilation is hypothesised to be of particular importance in the neurovascular unit. Therefore the physiological mechanisms which underlie these interactions, including some very recent discoveries, are outlined in sections 2.1.1 –2.1.3 and section 2.2.

.

### **2.1.1 Neurons and the generation of EEG activity**

In 1906 the Nobel Prize for Physiology and Medicine was awarded to the Spanish anatomist Santiago Ramón y Cajal, “in recognition of his meritorious work on the structure of the nervous system”. Cajal's great contribution to the history of science is undoubtedly the postulation of neuron theory. Cajal proposed that neurons were discrete cells that communicated with each other via specialized junctions, or spaces, between cells. This became known as the “neuron doctrine”, one of the central tenets of modern neuroscience. The neuron doctrine is the now fundamental idea that neurons are the basic structural and functional units of the nervous system (Santiago Ramon y Cayal 1928).

Neurons are electrically excitable cells in the nervous system that process and transmit information. Neurons are the core components of the brain, and spinal cord and peripheral nerves. Neurons are typically composed of a soma or cell body, a dendritic tree and an axon (Fig 2.1). The majority of vertebrate neurons receive input on the cell body and dendritic tree, and transmit output via the axon. However, there is great heterogeneity throughout the nervous system. Neurons communicate via chemical and electrical synapses in a process known

as synaptic transmission, where the axon terminal of one cell impinges upon another neuron's dendrite, soma or, less commonly, axon. Synapses can be excitatory or inhibitory, and will either increase or decrease activity in the target neuron. In the human brain each of the  $10^{11}$  neurons has on average 7,000 synaptic connections to other neurons. Afferent neurons convey information from tissues and organs into the central nervous system and are sometimes also called sensory neurons. Efferent neurons transmit signals from the central nervous system to the effector cell and are sometimes called motor neurons. Interneurons connect neurons within specific regions of the central nervous system. Afferent and efferent can also refer generally to neurons which, respectively, bring information to or send information from the brain region (Guyton and Hall 2000).

Excitatory neurons excite their target neurons. Excitatory neurons in the central nervous system, including the brain, are often glutamergic. The carboxylate anion of glutamic acid is known as glutamate. Glutamate is the most abundant swift excitatory neurotransmitter in the human nervous system. Glutamergic neurons respond specifically to glutamate.

Inhibitory neurons inhibit their target neurons. Inhibitory neurons are often interneurons. The primary inhibitory neurotransmitters are gamma-aminobutyric acid (GABA) and glycine. GABA is an amino acid and the chief inhibitory neurotransmitter in the human nervous system. As such GABA plays an important role in regulating neuronal excitability throughout the nervous system

Modulatory neurons evoke more complex effects termed neuromodulation. These neurons use such neurotransmitters as dopamine, acetylcholine, serotonin

and others. The neurotransmitters diffuse across the synaptic cleft and activate receptors on the postsynaptic neuron. The fundamental process that triggers synaptic transmission is the action potential, a propagating electrical signal that is generated by exploiting the electrically excitable membrane of the neuron (Fig 2.1). This is also known as a wave of depolarization (Guyton and Hall 2000). A scalp EEG measures summated activity of excitatory and inhibitory post-synaptic currents. An action potential in a pre-synaptic axon causes the release of neurotransmitter into the synapse. The neurotransmitter diffuses across the synaptic cleft and binds to receptors in a post-synaptic dendrite. The activity of many types of receptors results in a flow of ions into or out of the dendrite. This results in compensatory currents in the extracellular space. It is these extracellular currents which are responsible for the generation of EEG voltages. The EEG is not sensitive to axonal action potentials.

While it is post-synaptic potentials that generate the EEG signal, it is not possible to determine the activity within a single dendrite or neuron from the scalp EEG. Surface EEG is the summation of the synchronous activity of thousands of neurons. Scalp EEG activity is composed of multiple oscillations. These have different characteristic frequencies, spatial distributions and associations with different states of brain functioning, such as the waking and sleeping states. These oscillations represent synchronized activity over a network of neurons.



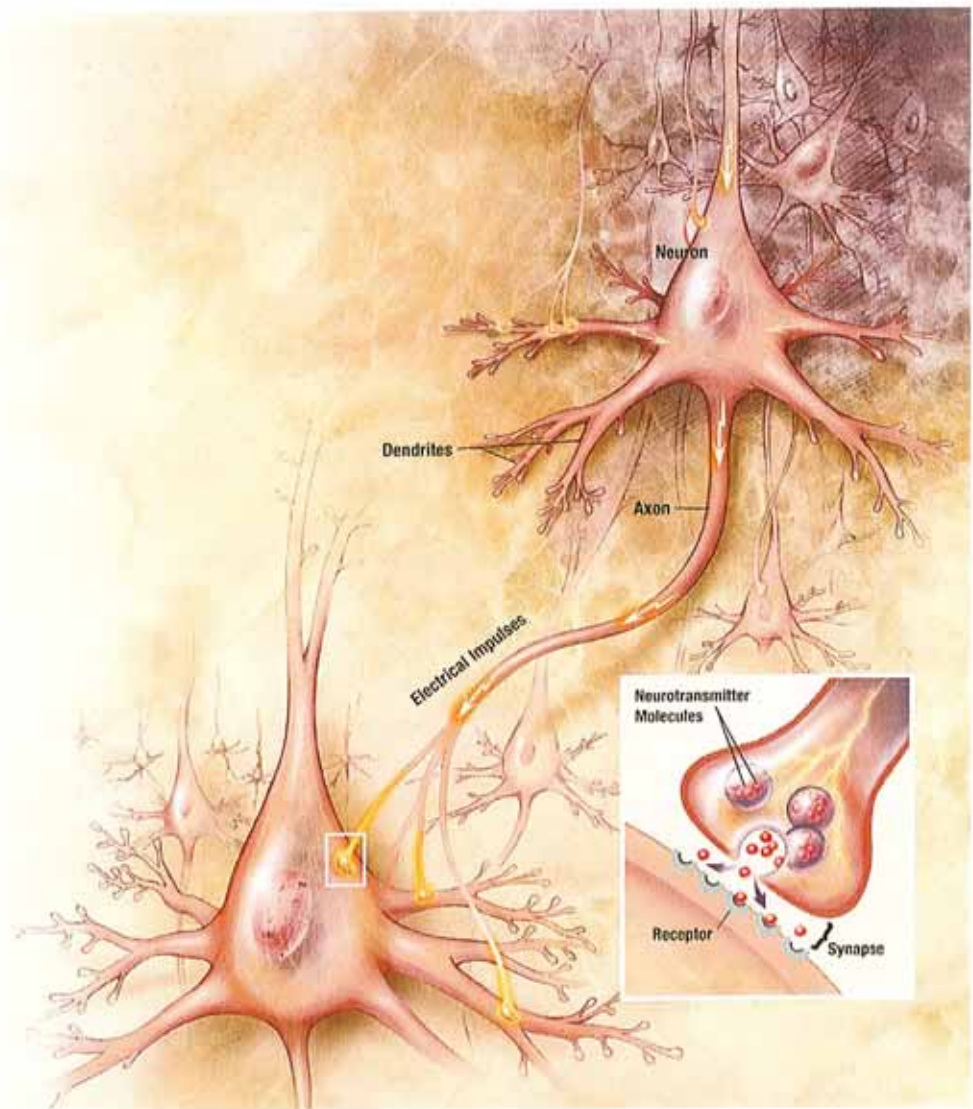


**Fig 2.1 : A signal propagating down an axon to the cell body and dendrites of the next cell. (from <http://carsguide.110mb.com/?l=Neuron>)**

### **2.1.2 Blood brain barrier (BBB)**

Brain endothelial cells lining the cerebral microvasculature form the blood brain barrier. The BBB is a membranous structure that acts primarily to protect the brain from chemicals in the blood, while still allowing essential metabolic functions. It is composed of endothelial cells, which are packed very tightly in brain capillaries. This higher density restricts passage of substances from the bloodstream much more than endothelial cells in capillaries elsewhere in the body. The tight packing of the endothelial cells in the brain is due to what are called tight junctions. These make the blood-brain barrier block the movement of all molecules except those that cross cell membranes by means of lipid solubility, such as oxygen, carbon dioxide, ethanol and steroid hormones, and those that are allowed in by specific transport systems such as sugars and some amino acids. Substances with a molecular weight higher than 500 daltons generally cannot cross the blood-brain barrier, while smaller molecules often can. In addition to tight junctions acting to prevent transport between endothelial cells, there are two mechanisms to prevent passive diffusion through the cell membranes. Glial cells surrounding capillaries in the brain pose a secondary hindrance to hydrophilic molecules, and the low concentration of interstitial proteins in the brain prevent access by hydrophilic molecules.

Astrocyte cell projections called astrocytic feet surround the endothelial cells of the BBB, providing biochemical support to those cells. It is the tight junctions and basal lamina of the cerebral endothelial cells that play the most substantial role in maintaining the barrier. The barrier plays an important role in the

homeostatic regulation of the brain microenvironment necessary for the stable and co-ordinated activity of neurons and for the healthy functioning of the CNS(Fig 2.2). There are a number of specific transport and enzyme systems which regulate molecular traffic across the endothelial cells. Specific carriers mediate the efflux from the CNS of potentially toxic metabolites such as glutamate. Astrocytes and other cells can release chemical factors that modulate endothelial permeability over a time scale of seconds to minutes. Endothelial cells are involved in both long and short term chemical communications with neighbouring cells, with the perivascular end feet of astrocytes being of particular importance. The endfeet of astrocytic glia form a lacework of fine lamellae closely apposed to the outer surface of the endothelium. *In vitro* cell culture models have provided a great deal of information about the induction of the BBB phenotype in brain endothelium, and have generally confirmed the key inductive role of astrocytes (Reinhart and Gloor 1997, Bauer and Bauer 2002). Endothelial cells have a reciprocal inductive influence on astrocytes (Abbot 2002). The regulation of endothelial transport by astrocytes may play a key role in modulating the energy supply supporting neuronal function (Magistretti and Pellerin 1999). Thus these three entities form a metabolic network to sustain brain activity. Disturbance of this homeostatic balance by the changes in availability of carbon dioxide and alterations in brain pH, such as that induced by voluntary hyperventilation during an EEG test, may have a significant effect on the electrophysiological state of the brain.

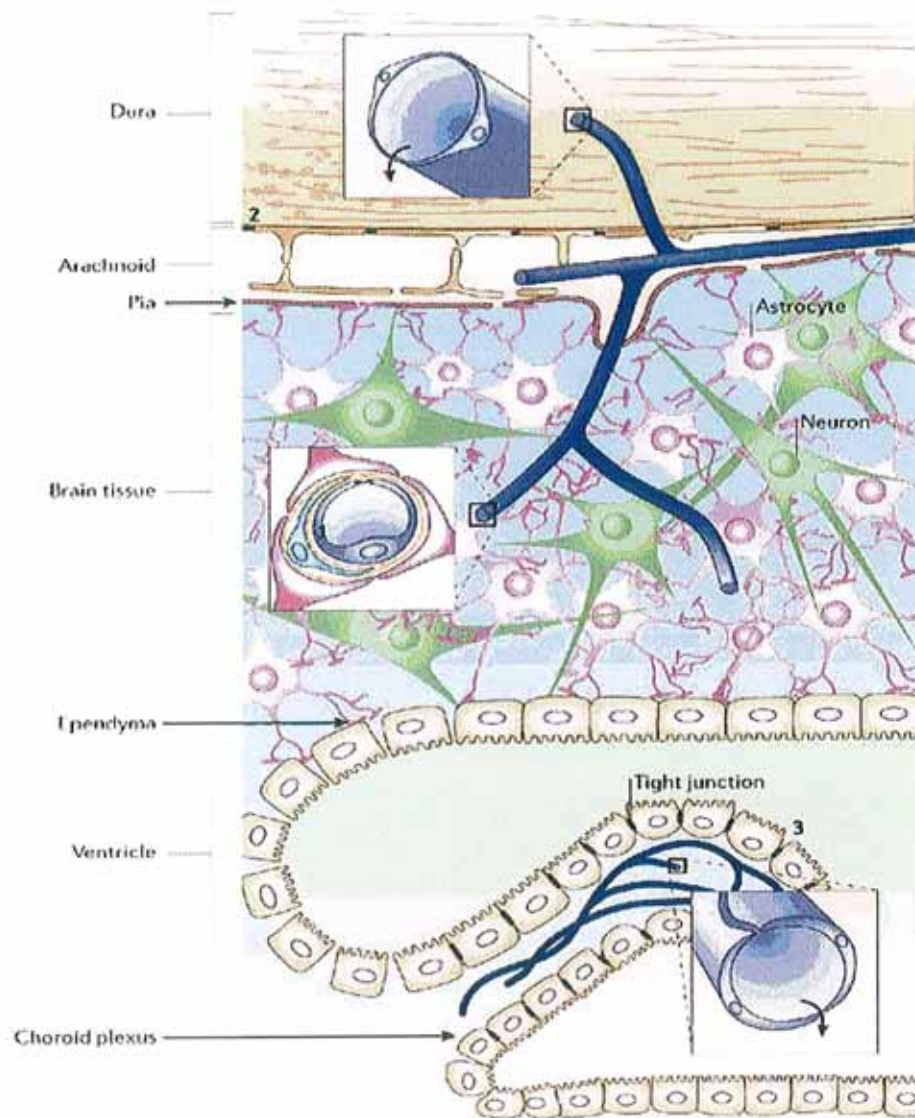


**Fig 2.2: Locations of barrier sites in the CNS. Abbot *et al* (2006) after : Astrocyte-endothelial interactions at the blood-brain-barrier. After Nature Reviews Neuroscience 7:41-53.**

### **2.1.3 Glia and the role of glial-neuronal interactions in the hyperventilation response on the EEG**

The neuronal irritability elicited during HV is considered to be due to brainstem-mediated cerebral vasoconstriction and pH changes induced by hypocapnia. The possible role of the glial cells in the EEG HV response has not received wide consideration. This is probably because when we think about the brain and the EEG we usually think about neurons

Neurons have long been thought to represent the sole "information-processing" elements of the central nervous system (CNS). However, the anatomical proximity of the non-neuronal elements, called neuroglia, to the neuronal cells, makes these elements particularly suited for taking active roles in the functions of neural information processing, and contributing to the alteration in rhythmogenesis of the EEG during HV. Glia were discovered in 1856 by the pathologist Rudolf Virchow in his search for a 'connective tissue' in the brain. Glial cells, commonly called neuroglia or simply glia (Greek for "glue"), are non-neuronal cells, which provide support and nutrition, maintain homeostasis, form myelin, and participate in signal transmission in the nervous system. In the human brain glia are estimated to outnumber neurons by about 10 to 1. Glial cells provide support and protection for neurons, the other main type of cell in the nervous system. It is inaccurate to consider glia as a passive 'glue' in the nervous system as the name implies, rather it is more of an active partner to neurons.

There are two broad subgroups of glial cells: the macroglia which consists of astrocytes, oligodendrocytes and ependymal cells, and the microglia. In recent years, an array of neurotransmitters, receptors, ion channels, adhesion molecules, and trophic factors have been revealed to be associated with glial cells. Knowledge on neuroglia has rapidly accumulated in the last decades, and an extensive body of evidence has now been assembled by different investigators from all fields of neuroscience, supporting a key role for the glia in neuronal physiopathology and thus questioning the “Neuron Doctrine”. From a structural perspective, the most abundant type of macroglial cell, astrocytes (also called astroglia) have numerous projections that anchor neurons to their blood supply (Fig 2.3).

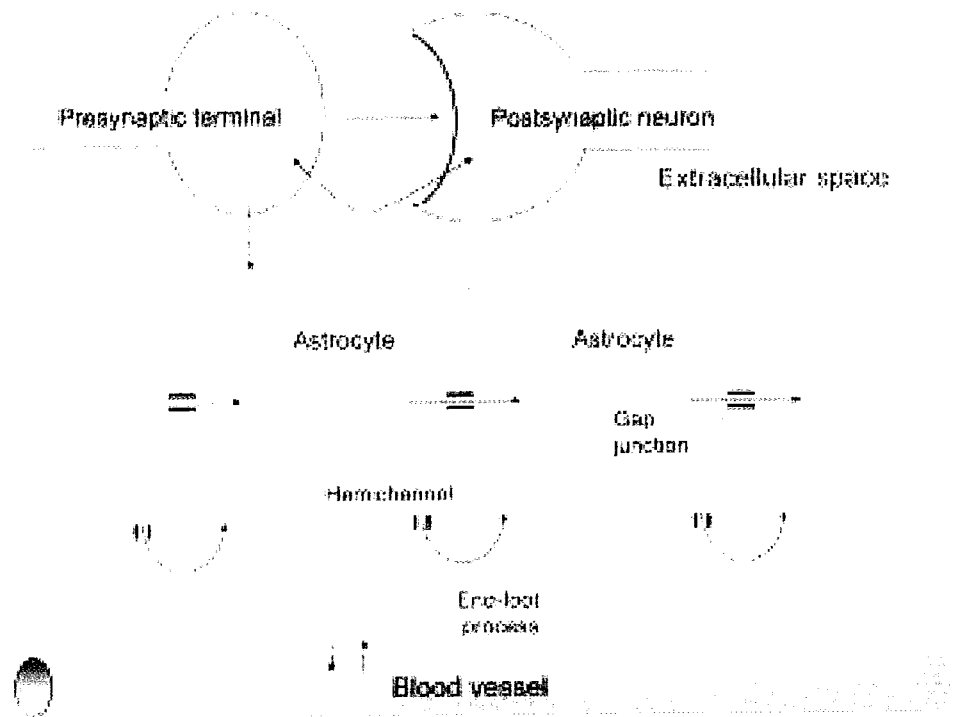


**Fig 2.3: General interactions among neurons, astrocytes and brain capillaries.** The astrocytes both face the synapses and form the astrocytic end-foot processes that abut the capillaries. Astrocytes are connected extensively by gap junctions, forming a syncytium-like organization, connecting via connexin 43 hemichannels. There are reciprocal interactions between the astrocytes and the pre- and post-synaptic elements.

## Relationship of Astrocytes and Other Brain Elements

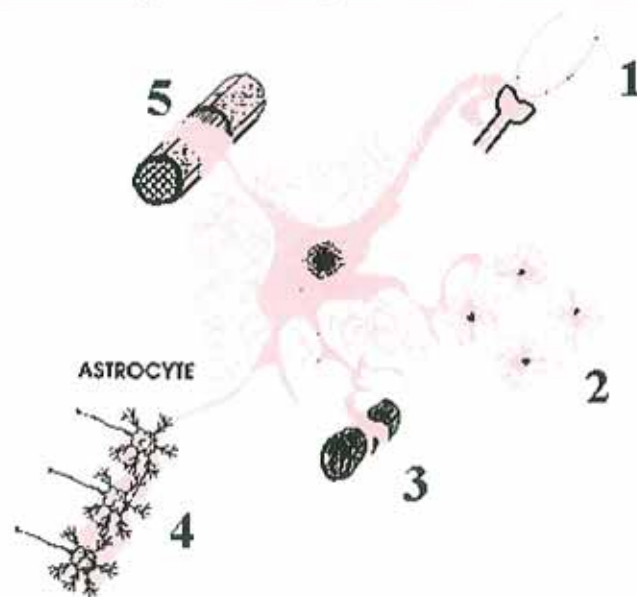


**Fig 2.4: Relationship between astrocytes and other brain elements.** The schematic drawing illustrates several possible contacts between the astrocyte and 1: a synaptic cleft 2: Other astrocyte networks 3: Capillary/blood vessel 4: Neuronal cell bodies 5: Nodes of Ranvier (After Morale *et al*, *Immun Cell Biol*)

A gap junction or nexus is a junction between certain animal cell-types that allows different molecules and ions, mostly small intracellular signalling molecules to pass freely between cells. The junction connects the cytoplasm of the cells. One gap junction is composed of two connexons, or hemichannels, which connect across the intercellular space. At gap junctions, the intercellular space narrows from 25 nm to 3 nm and unit connexons in the membrane of each cell are lined up with one another. Channel composition is thought to influence the function of gap junction channels but it is not yet known how.



There is now evidence that astrocytes are strongly coupled by gap junctions (Fig 2.3). Gap junctions formed from two identical hemichannels are called homotypic, while those with differing hemichannels are heterotypic. In turn hemichannels of uniform connexin composition are homomeric, while those with differing connexins are heteromeric. A naming system based on the molecular weight of the proteins which make up gap junctions is popular, for example connexin 43 in astrocytes. There is also now considerable evidence that glial cells play a role in  $K^+$ , pH and neurotransmitter homeostasis. The glial membrane transport systems involved in the regulation of these substances, like most homeostatic processes, are mostly reversible negative feedback systems.

Astrocyte ion channels include voltage gated calcium ( $Ca^{2+}$ ), sodium ( $Na^+$ ) and potassium ( $K^+$ ).  $K^+$  channels constitute the largest and most diverse family of ion channels and are abundantly expressed in astrocytes. Inward rectifier ( $K_{ir}$ ) channels are thought to adjust the level of neuronal excitability and have been shown to couple electrical activity to the metabolic state of the cell (Reimann and Ashcroft 1999). Astrocytes are the only cells in the mammalian brain that contain significant glycogen (Cataldo and Broadwell 1986). There is an intimate structural association between neurons and glial cells (astrocytes) which now appears to have significant functional implications. Glia are not simply the matrix in which neurons are embedded. Rather, they are endowed with a diverse assortment of ionic channels, neurotransmitter receptors, and transport mechanisms that both enable the glia to respond to many of the same signals that act on neurons and also to modulate the neuronal response.

In the astrocyte, glutamate serves both as a metabolic fuel and as precursor of glutamine and glutathione. The synthesis of glutamine in astrocytes is critical for two fundamental processes: replenishment of the glutamate pool in the neurons and ammonia detoxification in the nervous system. Astrocyte synthesis of glutathione is the major mechanism for ammonia detoxification in the nervous system (Bennarroch 2005). Glutamine synthetase synthesises the glutamine from glutamate and ammonia in the presence of ATP. This glutamate-glutamine cycle between neurons and astrocytes is critical for replenishment of the neuronal glutamate pool for neurotransmission. Disorders affecting ammonia metabolism, such as hepatic failure result in morphologic and functional changes that contribute to cerebral edema and neuronal and astrocytic dysfunction in these conditions. Metabolic encephalopathies produce significant electrographic abnormalities and hepatic encephalopathy has distinctive triphasic EEG slow wave abnormalities.

The anatomic relationship between neurons and astrocytes dictates opportunities for these cells to interact and sets limits on how they might do so. Because neurons and glial cells make no functional synaptic or gap junctional contacts with one another, interactions between the two cell types must occur via the narrow separating extracellular space (ECS) by volume transmission (Nicholson 1995). The average width of the space between brain cells is about 20 nm, a distance small enough that molecules released from one cell can diffuse to immediately adjacent cells with only a small time delay. Astrocytes are uniformly distributed throughout the central nervous system (CNS) and virtually every neuron shares common ECS with astrocyte neighbours (Peters *et al* 1991).

Some astrocyte processes seem to enwrap synapses. It has been estimated that peri-synaptic processes constitute 70-80% of astrocytic plasma membrane (Wolff 1970). Many astrocyte processes terminate in specialised endfeet that cover the entire surface of intraparenchymal capillaries. Astrocyte endfeet express glucose transporters (Vanucci *et al* 1997), water channels called aquaporins (Nielsen *et al* 1997) and a high density of potassium channels (Newman 1986). These endfoot specialisations suggest that astrocytes may play important roles in glucose uptake and in water and ion balance in the brain (Nedergaard *et al* 2003). The widespread and uniform distribution of astrocytes throughout the brain coupled with their inevitable intimacy with neuron neighbours makes them ideally suited for homeostatic or supportive type relationships. During an optimal hyperventilation exercise the aim is to intentionally disturb homeostasis. Astrocytes are designed to keep K<sup>+</sup> uptake around 3 mM (Ransom and Sontheimer 1992).

There is increasing evidence that glia play a dynamic role in regulating synaptic transmission. Experiments conducted in both culture and intact-tissue preparations demonstrate that transmitters released from neurons can stimulate glia, leading to the release of glutamate, ATP and other neuroactive substances from the glia. These gliotransmitters can feed back onto the presynaptic terminal to either enhance or depress the further release of neurotransmitter. Gliotransmitters released from glia can directly stimulate postsynaptic neurons as well, evoking either excitatory or inhibitory responses in these cells (Volterra 2002, Zonta *et al* 2003).

In contrast to the serial flow of information along chains of neurons, glia communicate with other glial cells through intracellular waves of calcium, and via intercellular diffusion of chemical messengers. By releasing neurotransmitters and other extracellular signaling molecules, glia can affect neuronal excitability and synaptic transmission and perhaps coordinate activity across networks of neurons. Astrocytes express receptors for many neurotransmitters, and their activation leads to oscillations in internal  $\text{Ca}^{2+}$  (calcium wave). These oscillations induce the accumulation of arachidonic acid and the release of the chemical transmitters, D-serine, ATP, and glutamate. Astrocytic  $\text{Ca}^{2+}$  changes signal the cerebral microvasculature and this communication occurs through the suppression of arteriolar  $[\text{Ca}^{2+}]_i$  oscillations and corresponding vasomotion

Sodium-dependent glutamate uptake leads to a secondary astrocytic sodium wave, accompanied by a wave of increased glucose uptake and metabolism. This metabolic wave may enable astrocytes to provide lactate as an energy source to neighboring active neurons and perhaps to more distant neurons as well. Thus, one function of long-range intercellular calcium signaling in astrocytes may be to spatially coordinate their function in supporting neuronal metabolism (Charles 2005). Neurons and astrocytes now appear to represent an integral unit that has a distinctive role in different fundamental events in brain function. The regulation of glutamate homeostasis by astrocytes is key to normal synaptic transmission and co-ordination of neural networks (Fellin 2006).

The astrocyte is positioned to regulate synaptic transmission and neurovascular coupling: the processes of one astrocyte contact tens of thousands of synapses, while other processes of the same cell form endfeet on capillaries and arterioles (Haydon and Carmignoto 2006) (Fig 2.3). They help to regulate the external chemical environment of neurons by removing excess ions, notably potassium, and recycling neurotransmitters released during synaptic transmission. Perisynaptic astrocytic processes ensheath the central excitatory synapses, extend into the synaptic cleft and express clusters of glutamate transporters and receptors. Glutamate binding to these molecules triggers complex bi-directional neuron-astrocyte interactions that affect energy metabolism, excitability and transmission of signals within and between the neuronal and astrocytic networks (Newman 2003, Hertz and Zeilke 2004).

Neurons activate glial cells by release of neurotransmitters, including glutamate, GABA, Acetylcholine, ATP and nitric oxide. Glial cells in turn modulate synaptic transmission by a number of mechanisms. They directly activate pre- and post-synaptic neurons by release of glutamate and ATP. They also modulate synaptic efficiency and plasticity by the uptake of glutamate from the synaptic cleft, by release of D-serine, and by regulating extracellular  $K^+$  and  $H^+$  levels.

The rapid temporal resolution of the EEG reflects real time excitability in these networks, which show significant change during altered physiological states including hypocapnic hyperventilation. Astrocytes signal to each other using calcium. The gap junctions between astrocytes allow the messenger molecule inositol 1,4,5-triphosphate (IP3) to diffuse from one astrocyte to another. IP3 activates calcium channels on cellular organelles, releasing calcium into the

cytoplasm. This calcium may stimulate the production of more IP<sub>3</sub>. The net effect is a calcium wave that propagates from cell to cell. Extracellular release of ATP, and consequent activation of purinergic receptors on other astrocytes, may also mediate calcium waves in some cases. There is an association between genetic mutations in CACNA1H (gene locus), which encodes T-type calcium channels, and childhood absence epilepsy (CAE).

Glial cells and neurons interact at the synapse. Neurons activate glial cells by release of neurotransmitters, including glutamate, GABA, Acetylcholine, adenosine triphosphate (ATP) and nitric oxide. Glial cells in turn modulate synaptic transmission by a number of mechanisms. They directly activate pre- and postsynaptic neurons by release of glutamate and ATP. They also modulate synaptic efficiency and plasticity by the uptake of glutamate from the synaptic cleft, by release of D-serine, and by regulating extracellular potassium (K<sup>+</sup>) and hydrogen (H<sup>+</sup>) ion levels. The concept of a more central and significant position of astrocytes in the metabolism and functioning of the CNS is now accepted. Indeed, the anatomical proximity of astrocytes to neuronal synapses and the blood brain barrier (Fig. 2.4) makes these cells ideally suited for taking an active role in the ion, water and neurotransmitter metabolism of the CNS during both normal and abnormal neuronal functioning. Neurons depend on some biochemical reactions which can only occur in glia, due to their unique production of key enzymes not available to neurons. These three key enzymes are pyruvate carboxylase, glutamine synthetase and carbonic anhydrase. Pyruvate carboxylase is a catalyst for the binding of CO<sub>2</sub> with pyruvate to produce the 4-carbon oxaloacetate. This is the starting point for the tricarboxylic acid cycle and gluconeogenesis where glucose is synthesized from two

molecules of oxaloacetate with a corresponding decarboxylation. This astrocytic glucose can then be polymerised to form glycogen, found almost exclusively in astrocytes as energy reserves for the brain. The glutamate-glutamine cycle is a sequence of events by which an adequate supply of the neurotransmitter glutamate is maintained in the central nervous system. Initially, glial cells release glutamine, which is then taken up into pre-synaptic terminals and metabolised into glutamate by glutaminase (a mitochondrial enzyme). Glutamate can also be produced by transamination of 2-oxoglutarate, an intermediate in the citric acid cycle. The glutamate that is synthesized in the pre-synaptic terminal is packaged into synaptic vesicles by the transporter VGLUT. Once the vesicle is released glutamate is removed from the synaptic cleft by excitatory amino acids transporters (EAATs), of which there are five types. Glutamate taken up by glial cells is then converted into glutamine by glutamine synthetase and transported out of the cells into the nerve terminals. This allows synaptic terminals and glial cells to work together in order to maintain a proper supply of glutamate (Purves et al 2008).

The carbonic anhydrases form a family of enzymes that catalyse the rapid conversion of carbon dioxide to bicarbonate and protons, a reaction that occurs rather slowly in the absence of a catalyst. The oxidation of carbohydrates by CNS cells results in the formation of bicarbonate and  $H^+$ , under the influence of carbonic anhydrase, located within the cytoplasm or cell membrane of glial cells.

It has become progressively more apparent that glia are major partners in determining the brains operations (Laming *et al* 1998 in their book: Glial Cells:

Their Role in Behavior) The role of glial cells as managers of communications in the synaptic gap, has been discovered only very recently( Kasischke *et al* 2004). The current theory suggests that astrocytes may be the predominant "building blocks" of the blood brain barrier. Astrocytes may regulate vasoconstriction and vasodilation by producing substances such as arachidonic acid whose metabolites are vasoactive. The functioning of the nervous system depends upon a continuous and sophisticated interrelationship between neuronal and glial cells (Fig 2.5). The global change in the EEG seen during hypocapnic hyperventilation may reflect the disturbance of the homeostatic relationships in the neural/glial network.

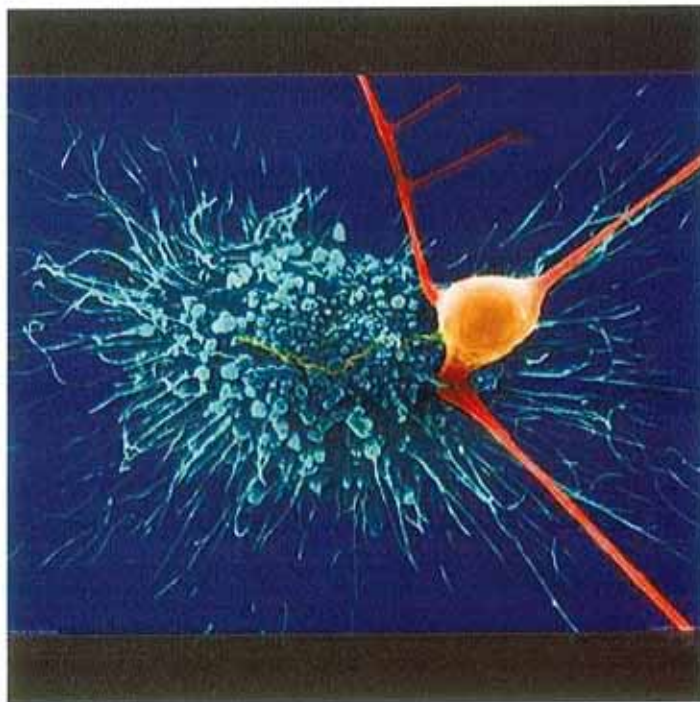


**Fig 2.5: Neuron (orange) with supporting glial astrocytic cell (blue)**  
(from [www.astrographics.com](http://www.astrographics.com))



## **2.2 Astrocyte neuron lactate shuttle hypothesis (ANLSH)**

In 1994 Pellerin and Magistretti made the first observation that glutamate stimulates, in a dose-dependent manner, glucose uptake into cultured astrocytes. The second observation was that glucose was mainly metabolized to lactate, indicating net aerobic glycolysis. The latest set of data defined the signaling pathway as glutamate acting via its transporter not its receptors. The hypothesis that was put forward by Pellerin and Magistretti suggested that 'glutamate uptake-induced aerobic glycolysis into astrocytes is the cellular mechanism coupling neuronal activity to glucose utilization'.

Chih *et al* (2001 and 2003) raised the following concerns related to this astrocyte neuron lactate shuttle hypothesis (ANLSH).

1. Why do neurons not satisfy their energy needs by using more glucose?  
Neurons, like all brain cells, possess a glycolytic pathway that is tightly coupled to energy demand. Low levels of ATP activate hexokinase and accelerate glycolysis. This control mechanism would allow active neurons to rapidly increase glucose uptake to meet their energy needs.
2. The pathway for increasing lactate import, if via lactate dehydrogenase (LDH) and increased energy demand, does not activate this enzyme.
3. If glucose were available in the ECS, it would essentially compete with lactate for access to the energy metabolism pathways for kinetic and thermodynamic reasons.

Despite the subsequent vigorous debate of the ANLS hypothesis, there is no alternative signaling pathway that links neuronal glutamatergic activity to glucose use that would fit with what has been observed using *in vivo* brain imaging. It is not yet known with certainty which signaling pathway enables a tight adjustment of glucose use to meet the increasing needs of the glutamatergic synapse. Almost all recent experiments performed *in vitro* or *in vivo* have provided data which are supportive of the lactate shuttle. There is now “proof of principle” of the ANLSH in the extreme circumstance of hypoglycaemia. A model can be constructed showing how glycogen protects axons during glucose removal or when intense neural activity causes excess energy demands to exceed the availability of glucose (Wender *et al* 2000, Brown *et al* 2003).

Recent multi-photon fluorescence imaging studies by Kasischke *et al* (2004) at Cornell University provide strong evidence that in a hippocampal brain slice preparation *energy metabolism is compartmentalised between astrocytes and neurons especially during increased neuronal activity*. Using multi-photon microscopy scans of living brain tissue the authors claimed to have both confirmed and redefined the controversial “astrocyte-neuron lactate shuttle” hypothesis for brain energy metabolism. Multi-photon microscopy is a technology that produces high-resolution, three-dimensional images of tissues (e.g. in the central nervous system), with minimal damage to living cells, while resolving metabolic signatures in processes of astrocytes and neurons. (Fig 2.6, Fig 2.7) The laser based microscopy technique is based on imaging of two different energy states of nicotinamide adenine dinucleotide, a coenzyme involved in brain-cell metabolism (NADH). Studies revealed how and when

neurons and astrocytes interact to burn oxygen and glucose, after astrocytes make lactate brain glucose in the bloodstream, to meet the extraordinary energy demands of the brain (Fig 2.8, Fig 2.9).

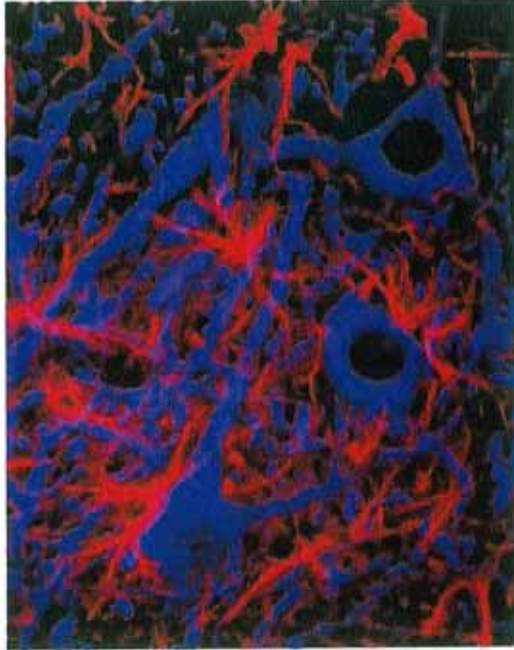


**Fig 2.6** Astrocytes (red cells) and neurons (blue cells) were labeled with specific antibodies in this fixed rat brain section. Because NADH, the coenzyme involved in brain metabolism, fluoresces differently in astrocytes and neurons in living brain tissue, biophysicists at Cornell University could determine precisely when astrocytes were providing extra lactate "fuel" to neurons, confirming the controversial astrocyte-neuron lactate shuttle hypothesis. (After Kasischke 2004)

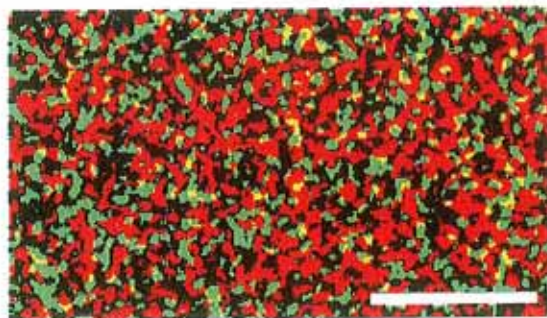


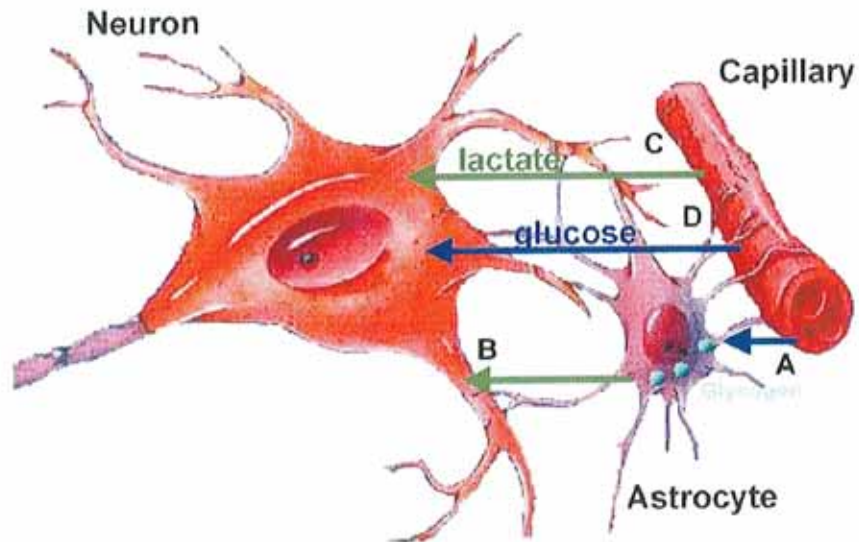
**Fig 2.7** Proof of activity-dependent metabolism in two kinds of brain cells, neurons undergoing oxidative metabolism show up as green speckles while astrocytes with glycolytic metabolism are red in this multiphoton microscopy scan of living rat brain tissue. (After Kasischke 2004)

Multi-photon microscopy imaging of intrinsic fluorescence in NADH shows that early oxidative metabolism in neurons is eventually sustained, after about 10 seconds, by late activation of the astrocyte-neuron lactate shuttle. Neurons, even at rest, are always burning glucose and they continue to do so when a signal begins to pass through the neurons. Then the astrocytes 'kick in' to provide lactate fuel that they have converted from glucose. This model integrates existing views of brain energy metabolism and is in accord with known macroscopic physiological changes *in vivo*.

These findings imply that PET and functional magnetic resonance imaging (fMRI) are not recording neural activity directly, but rather surrogates for activity; changes in blood flow (in the case of PET) and blood oxygenation (fMRI). Kasischke *et al* found that under resting conditions cytoplasmic NADH was elevated in astrocytes compared to neurons. Astrocytes therefore have higher glycolytic capabilities. Activation of the Schaffer collateral pathway in the hippocampus induced a biphasic metabolic response. This consisted of an early NADH decrease (the “dip”) in dendrites of neurons, followed by an increase (the “overshoot”) in astrocytes. These observations had been already noted *in vivo*. Due to the high temporal resolution of this technique it became possible to reconcile previous contradictory results and suggest a revised sequence of events of the ANLSH (Pellerin and Magistretti 2004), i.e. neuronal oxidative and then astrocytic nonoxidative glycolysis. In his paper Kasischke compared PET and fMRI scans to pictures from cameras with slow shutter speeds and

wide-angle lenses, producing a broad view over a relatively lengthy time span. A very different picture emerges from multi-photon microscopy, which can record millisecond changes in microscopic detail. The ultra-fast microscopic technique can image individual nerve cells and even their finest extensions, where important steps in brain-cell metabolism take place.

The astrocyte neuron lactate shuttle hypothesis promises to help unravel important cellular and molecular aspects of neurometabolic and neurovascular coupling, particularly relevant to investigation of the biological basis of brain imaging (Bonvento *et al* 2005) (Fig 2.8, Fig 2.9, Fig 2.10). (See section 2.10.1 for discussion of a novel “hypocapnia cascade” which involves the ANLSH))



- (A) **FIG 2.8: Schematic representation of a neuron, an astrocyte and a capillary, showing histological arrangement and the trafficking of substrates** The lactate shuttle implies that part of the glucose taken up by astrocytes maintains a glycogen level
- (B) Neuronal activity induces breakdown of glycogen to provide instant energy for the neuron as lactate is released
- (C) During exercise, lactate taken up from the blood may be provided directly to the neuron.
- (D) The neuron requires glucose for de novo synthesis of neurotransmitters such as glutamate



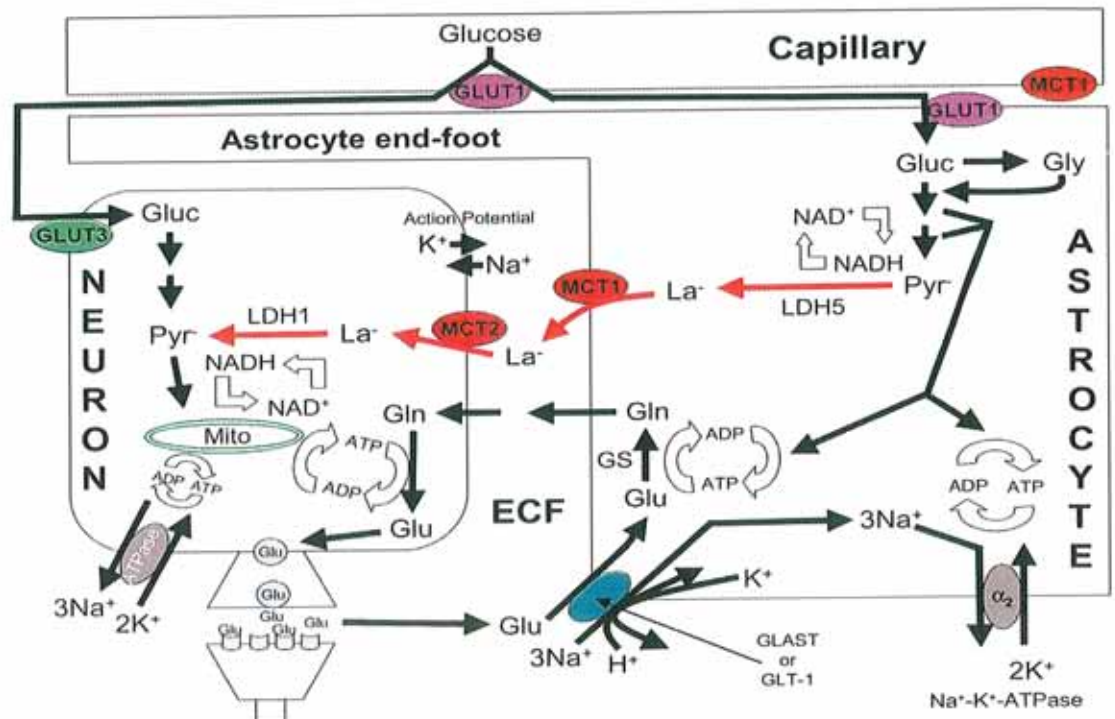


**Fig 2.9: Illustration of the putative astrocyte-neuron lactate shuttle hypothesis (ANLSH)**

The basic outline of the astrocyte-neuron lactate shuttle hypothesis is as follows. Blood glucose is a major energy substrate that can be taken up by both neurons and astrocytes via their specific glucose transporters (GLUT3 in neurons and GLUT1 in astrocytes); note that GLUT1 is also present in the plasma membrane of endothelial cells making up capillaries. Blood glucose may be more readily available to astrocytes because the surface of intraparenchymal capillaries is covered by specialized astrocytic end-feet. Release of the neurotransmitter, glutamate, at glutamatergic synapses leads to glutamate uptake into surrounding astrocytes via glutamate transporters GLT-1 and GLAST to terminate the action of glutamate on post-synaptic receptors. Glutamate entry into astrocytes is powered by the  $\text{Na}^+$  concentration gradient and current evidence suggests that one glutamate enters with three  $\text{Na}^+$  and one  $\text{H}^+$  while one  $\text{K}^+$  is simultaneously extruded. The resulting increase in intra-astrocytic  $[\text{Na}^+]$  activates a glia-specific  $\text{Na}^+-\text{K}^+-\text{ATPase}$   $\alpha_2$  subunit. Glutamate is converted to glutamine by glutamine synthetase. Both the ATPase pump activation and the glutamine synthesis activate astrocytic glycolysis that is possibly compartmentalized with these processes; presence of LDH5, the muscle form of LDH, is argued to promote  $\text{La}^-$  formation. The end result is  $\text{La}^-$  accumulation and efflux into the extracellular fluid, facilitated by MCT1. Subsequently,  $\text{La}^-$  is taken up into neurons via MCT2. Glutamine also diffuses from astrocytes into the extracellular fluid and on into neurons where it is used to resynthesize glutamate.  $\text{La}^-$  taken up into neurons is preferentially converted to pyruvate, arguably because of pyruvate utilization as an aerobic fuel and the presence of LDH1, the heart form of LDH. In this hypothesis, the energy metabolism of neurons is largely aerobic with  $\text{La}^-$  serving as the major fuel. GLUT1 and GLUT3: specific glucose transporters located in the membranes of brain endothelial cells and astrocytes (GLUT1), and neurons (GLUT3); MCT1 and MCT2: specific monocarboxylate transporters located in the membranes of brain endothelial cells and astrocytes (MCT1), and neurons (MCT2); Gluc: glucose; Gly: glycogen;  $\text{Pyr}^-$ : pyruvate;  $\text{La}^-$ : lactate; Glu: glutamate; Gln: glutamine; GS: glutamine synthetase; LDH1 and LDH5: specific forms of lactate dehydrogenase in neurons (LDH1) and astrocytes (LDH5); ECF: extracellular fluid; GLT-1 and GLAST: glutamate transporters;  $\alpha_2$ : glia-specific  $\text{Na}^+-\text{K}^+-\text{ATPase}$  subunit.

After Pellerin, 2003, Lactate as a pivotal element in neuron-glia metabolic cooperation, *Neurochemistry International* 43, 331-338

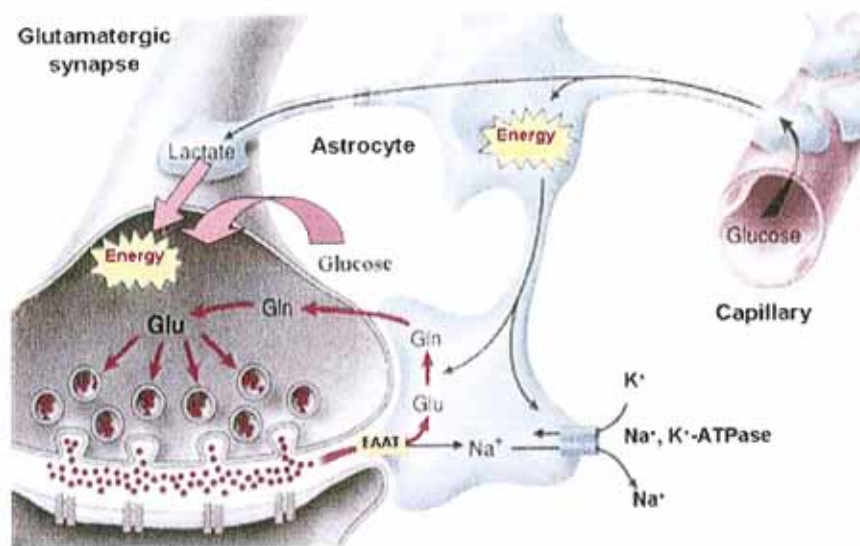


Fig 2.10: Model for neuron-glia metabolic coupling (after Magistretti 2006)



## **2.3 Neurometabolic and neurovascular coupling**

Cerebral blood flow is tightly coupled to neuronal metabolic activity (functional hyperemia). Brain energy metabolism, neural organisation, cell signalling and vascular regulation provide the basis for functional imaging and the EEG. Technologies to measure blood flow and metabolism with high spatial and temporal resolution are available. The regulation of brain energy metabolism during neuronal activation is poorly understood. Specifically, the extent to which oxidative metabolism rather than glycolysis supplies the additional adenosine triphosphate (ATP) necessary to sustain neuronal activation is a source of active debate.

The brain is a major energy consumer and dependent on carbohydrate and oxygen supply. Electrical and synaptic activity of neurons can only be sustained given sufficient availability of ATP. Glial cells, which have long been assigned trophic functions, seem to play a pivotal role in meeting the energy requirements of active neurons.

Astrocytes face the synapses, send end-foot processes that enwrap the brain capillaries, and form an extensive network inter-connected by gap junctions. Astrocytes express several membrane proteins and enzymes that are critical for uptake of glutamate at the synapses, ammonia detoxification, buffering of extracellular K<sup>+</sup>, and volume regulation.

Under normal conditions almost all of the energy required by brain cells is supplied by glucose and oxygen derived from the blood. In a normal person, the blood glucose concentration is narrowly controlled, usually between 80 and 90 mg/100ml of blood in the fasting person each morning before breakfast. This concentration increases to 120 to 140 mg/100ml during the first hour or so after a meal, but the feedback systems for control of blood glucose return the glucose concentration rapidly back to the control levels, usually within 2 hours after the last absorption of carbohydrates. Most body tissues can shift to utilization of fats and proteins for energy in the absence of glucose. Most of the glucose formed by gluconeogenesis (i.e. formation of carbohydrates from proteins and fats) during the inter-digestive period is used for metabolism in the brain.

Neuronal activity is fuelled by glucose metabolism (Fig 2.4) According to the most widely accepted current view, glucose transport into the brain is not rate-limiting; thus it cannot exert control over metabolism. However as discussed in section 2.1.4 above the ANLSH links neuronal glutamergic activity to glucose use that would fit with what has been observed using *in vivo* brain imaging. A study by Gjedde and Marrett (2001) concluded that glycolysis in neurons, not in astrocytes, delays oxidative metabolism. They state that neurons increase their oxidative metabolism in proportion to an increase in pyruvate, which is generated by neuronal rather than astrocytic glycolysis, and that the “neuronal and astrocytic pathways of energy metabolism remain as distinct during neuronal excitation as they are at rest”. The Kasischke *et al* 2004 study (section 2.1.4) demonstrated a compartmentalisation of energy metabolism between astrocytes and neurons.

Due to the high temporal resolution of the multi-photon fluorescence microscopy technique it has become possible to reconcile previous contradictory results and suggest a revised sequence of events for the ANLSH (Pellerin and Magistretti 2003) i.e. neuronal oxidative and then astrocytic nonoxidative glycolysis (Figs 2.6 and 2.7, after Kasischke 2004).

Astrocytes participate in detection, propagation, and modulation of excitatory synaptic signals, provide metabolic support to the active neurons, and contribute to functional hyperemia in active brain tissue (Benarroch 2005).

A recent article by Barros (2005) demonstrated that basal transport hovers near its maximum, making metabolic activation unable to increase flux on its own. As astrocytic cells preferentially break down glucose they suggest that fluorodeoxyglucose positron emission tomography (FDG-PET) reports the synergistic activation of glucose transport and metabolism in astrocytes rather than in neurons.

### **2.3.1 Neurovascular coupling**

Neurovascular coupling refers to the relationship between local neural activity and subsequent changes in cerebral blood flow (CBF). The magnitude and spatial location of blood flow changes are tightly linked to changes in neural activity through a complex series of coordinated events involving neurons, glia, and vascular cells. Brain activation is accompanied by a sequence of cellular, metabolic, and vascular processes.

Under normal conditions, cerebral autoregulation maintains a stable CBF in the face of fluctuations in systemic pressure. The limits of autoregulation between 60 and 160 mmHg, can be shifted in chronic disease states (e.g. arterial hypertension). Under normal conditions, the cerebral circulation responds exquisitely to changes in hypercapnia and hypocapnia with concomitant vasodilatation and vasoconstriction respectively. CBF changes linearly from 2% to 4% for every millimetre of mercury (mmHg) change in  $p\text{CO}_2$  (the  $\text{CO}_2$  reactivity coefficient). Hypoxia must be profound, with a  $p\text{O}_2$  less than 60 mmHg to trigger cerebral vasodilation.

As with other body tissues the brain requires oxygen and glucose to supply its metabolic needs. The cerebral vasculature has unique properties because of the metabolic demands of nervous tissue. The brain depends upon aerobic metabolism of glucose and is one of the most metabolically active organs of the body. Although composing only 2% of the body weight, the brain receives approximately 15% of the cardiac output and consumes about 20% of the oxygen utilized by the entire body.

Under resting conditions brain metabolism per unit mass of tissue is about 7.5 times the average metabolism in non-nervous system tissues (Guyton and Hall 2000). Most of this excess metabolism of the brain occurs in the neurons, which pump sodium and calcium ions out, and potassium and chloride ions in through their neuronal membranes. During excessive brain activity, neuronal metabolism can increase by 100 to 150%. As a result of this the brain is not capable of much anaerobic metabolism. The amount of glycogen stores in the neurons is very small. Therefore most neuronal activity depends upon second by second delivery of glucose and oxygen from the blood. A sudden cessation of blood flow to the brain or sudden total lack of oxygen in the blood can cause unconsciousness within 5 to 10 seconds. Cerebral metabolism thus depends on a constant supply of both glucose and oxygen. A continuous supply of these two energy substrates is maintained by cerebral blood flow (CBF), which delivers glucose and oxygen to neural tissue through the complex web of blood vessels in the brain's vascular system. Accordingly, during neural activity, increases in oxygen and glucose consumption are followed by an increase in CBF. Whereas the fractional increases in CBF and glucose consumption are similar in magnitude, oxygen consumption increases much *less* than CBF.

Various cellular processes of neurons, such as the restoration of ionic gradients and neurotransmitter recycling, require energy in the form of adenosine triphosphate (ATP). ATP is synthesized in two steps, first by glycolysis, which does not require oxygen and produces a small amount of ATP, and then by oxidative glucose metabolism, which does require oxygen and produces a large amount of ATP. In the brain, about 90% of glucose is metabolized by the latter mechanism, i.e. aerobically.

The observation that changes in neural activity and metabolism are correlated with changes in CBF suggests that blood flow is controlled directly by energy demand. In fact, this idea was originally proposed over a century ago by Roy and Sherrington (1890): “...*the brain possesses an intrinsic mechanism by which its vascular supply can be varied locally in correspondence with local variations of functional activity.*” In this view, regional blood flow is controlled by mechanisms that are sensitive to variations in the concentrations of ionic and molecular metabolic by-products. These by-products, such as potassium (K<sup>+</sup>), nitric oxide (NO), adenosine and arachidonic acid metabolites, may directly or indirectly alter blood flow by depolarizing (or hyperpolarizing) the vascular smooth muscle cells which trigger vasodilation (or vasoconstriction). The idea that energy supply (i.e. local blood flow) is controlled directly by energy demand (i.e. metabolic activity) may be an oversimplification. An alternative hypothesis (Harder *et al* 1998) is that local blood flow is controlled not by energy demand, but by neuronal signaling processes involving neurotransmitters. Evidence suggests that astrocytes may play an important role in linking neurotransmitter activity to vascular responses. A cascade of chemical events within the astrocyte may then link the rate of glutamate cycling to the production of vasoactive chemical agents (Raichle and Mintun 2006). In this view, neurovascular coupling is mediated by neuronal signaling mechanisms via glial pathways, not by mechanisms that sense energy consumption.

Astrocytes can act as intermediaries between neurons and cerebral arterioles to regulate vascular tone in response to neuronal activity. Release of glutamate from pre-synaptic neurons increases blood flow to match metabolic demands. Recent research into astrocytic neuroglial cells indicates that they metabolise

glucose anaerobically (glycolosis) for energy. Astrocytes can take up glutamate, ship the glutamate to the neuron, ship lactate to the neuron, and also signal capillaries to dilate. Astrocytes are intricately linked in the regulation of synaptic strength and plasticity and provide a pathway for synaptic cross-talk (Zonta *et al* 2003). The precise links between neural activity, metabolism and blood flow continue to be an area of active investigation. This thesis uses clinical measurement modalities including quantitative EEG analysis of spectral power, end tidal CO<sub>2</sub>, pO<sub>2</sub>, heart rate and velocity of cerebral blood flow, to investigate physiological responses to a standardised hyperventilation protocol, and suggests a hypothesis which directly relates the neurovascular unit to the potential mechanisms underlying the clinical effects of hyperventilation.

## **2.4 Review of the potential mechanisms underlying the clinical effects of hyperventilation**

Since the introduction of hyperventilation as an adjunctive test during clinical EEG, a considerable body of literature has accumulated relating to the possible physiological mechanisms which underly the hyperventilation response. However it is still far from clear how the effects of HV are mediated at the cortical level.

Reviews of the experimental work which resulted in these theories have been published by Morrice 1956, Granholm and Siesjo 1971, Paulson and Sharborough 1974, Raess 1974, Bostem 1976 and Patel and Mulsby 1987. The latter reviewed the opinions in the literature at that time. In approximately

chronological order these theories are reviewed below, with inclusion of current research which is relevant to the ANLS hypothesis:

- the cerebral hypocapnia theory
- the hypoxia theory
- respiratory alkalosis
- role of the autonomic nervous system
- brainstem and thalamic mechanisms of activation.

#### **2.4.1 The cerebral hypocapnia theory**

According to this theory the EEG changes seen during hyperventilation result directly from a decrease in cerebral carbon dioxide. In the average healthy person, the amounts of oxygen and carbon dioxide in the arterial blood are kept at remarkably constant levels. The respiratory drive (breathing) is not regulated primarily by the need for oxygen, but by the need to remove carbon dioxide from the blood.

Carbon dioxide is produced in the body through cellular metabolism. At rest, arterial blood normally contains a partial pressure of about 40 mmHg (5.3 kPa) of CO<sub>2</sub>. This corresponds to a normal arterial CO<sub>2</sub> concentration in the blood and in exhaled air of around 5%. Venous blood has a partial pressure of CO<sub>2</sub> of around 46 mmHg (6 kPa). Carbon dioxide is expelled in the lungs through the process of diffusion between blood and the pulmonary capillaries and air in the alveoli.



When CO<sub>2</sub> production is in equilibrium with CO<sub>2</sub> excretion there is a metabolic balance; pH stays at 7.4 and PCO<sub>2</sub> remains in the 35-40 mmHg range. Below 30 mmHg (pH of 7.5) mild hypocapnic symptoms are likely to begin, 20 mmHg is associated with a pH of 7.6, at which symptoms will appear in almost everyone. Alteration of this balance has a global effect on the function of the cerebrum. Restricted circulation in the cerebral cortex leads to light-headedness, dizziness, occasional visual disturbances and paraesthesia in hands and feet.

The underlying mechanism of hyperventilation's provocation of slow (theta and delta) EEG activity remains incompletely explained, as little is known about the physiological changes at the neuronal network level following a period of hyperventilation. The possible role of neuroglia cells and networks in the EEG hyperventilation response has not received general consideration.

Gibbs (1942) published the earliest work suggesting that diffuse EEG slowing is due to inadequate compensatory vasoconstriction of the cerebrum in response to systemic hypocapnia. He described cerebral vasoconstriction as the normal compensatory homeostatic response to hypocapnia to regulate the local PCO<sub>2</sub>, and he stated that the EEG changes occurred as a direct result of a decrease in cerebral carbon dioxide. Sherwin (1967) attributed the diffuse slowing to synchronous activity in the nonspecific thalamocortical projecting systems, which become more active in hypocapnia. Yamatani *et al* (1995), measuring cerebral blood flow in the right carotid artery during hyperventilation, reported that decreased PCO<sub>2</sub> and cerebral blood flow were the fundamental factors causing EEG slowing. Hattunen and Tolvanen (1999), studying the effects of

voluntary hyperventilation on cortical sensory responses, suggested that the reduction noted in long latency cortical sensory responses was probably mediated by hypocapnia rather than by other non-specific effects of hyperventilation.

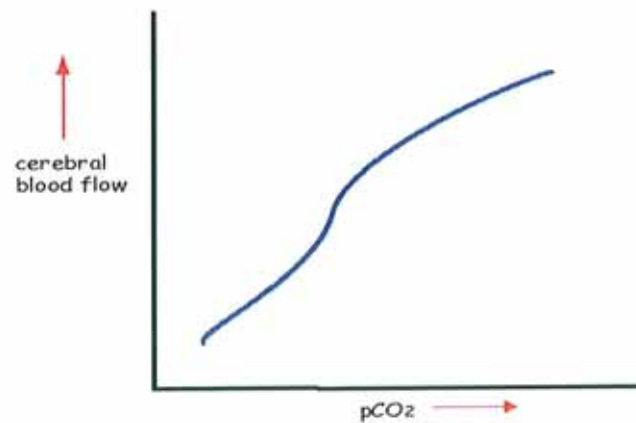


**Fig. 2.11: The relationship between cerebral blood flow and  $p\text{CO}_2$**

$\text{CO}_2$  acts as a regulator of cerebrovascular tone, and cerebral blood flow (Fig 2.11). Breathing volume determines the amount of  $\text{CO}_2$  excreted per unit time. The metabolic demand of the body determines the amount of  $\text{CO}_2$  produced. In hypercapnia (such as occurs with “breath holding”) there is a high level of  $\text{CO}_2$  in the bloodstream, which equates with less oxygen availability. Hypoxia does not have much effect on cerebral blood flow (CBF) until  $\text{PaO}_2$  falls below 60 mmHg at which point vasodilation occurs. Since oxygen deficit (i.e. hypoxia), is dangerous for the brain, vasodilation of blood vessels occurs to maintain normal brain oxygenation. This is probably due to alterations in calcium and/or phosphorus movement through the vessel walls. Arterial walls, when dilated, become more permeable to oxygen molecules (Gilbert 1999, Gardner 2003). The opposite condition, a drop in  $\text{CO}_2$  (hypocapnia) stimulates vasoconstriction and is said to be the “most potent vasoconstrictive agent known” (Raichle and

Plum 1972). When an individual breathes in excess of the bodily needs for oxygen and more CO<sub>2</sub> is exhaled than is being replaced, the regulatory mechanism becomes dysfunctional.

Cerebral blood flow is controlled by five factors: partial pressure of carbon dioxide in arterial blood (PaCO<sub>2</sub>), partial pressure of oxygen in arterial blood (PaO<sub>2</sub>), autoregulation, metabolism and the autonomic nervous system. Autoregulation refers to a process intrinsic to the cerebral vasculature in which changes in transmural pressure affect blood flow. The degree of circulatory loss in the cerebral cortex is around 2% for each 1 mmHg drop in CO<sub>2</sub> partial pressure (Gardner 1996). This loss is visible to the observer if the individual's cortex happens to be uncovered at the time. It has been described by the neurosurgeon Wilder Penfield as a blanching of the surface of the brain. Coughlan and Mc Menamin (2008) describe a marked increase in the spectral power density of theta and delta EEG activity during a standardised hyperventilation exercise, with partial end tidal CO<sub>2</sub> (pETCO<sub>2</sub>) from 15 mmHg to 22 mmHg.

Breathing volume determines the amount of CO<sub>2</sub> excreted per unit time; metabolic demand determines the amount of CO<sub>2</sub> produced. With CO<sub>2</sub> production in equilibrium with CO<sub>2</sub> excretion, homeostasis is maintained, pH stays at 7.4 and CO<sub>2</sub> remains at 35.40 mmHg. However, (Fig 2.12 A), with restricted oxygen intake (breath holding or high CO<sub>2</sub> air), more CO<sub>2</sub> is produced than is exhaled. CO<sub>2</sub> rises, stimulating blood vessel dilation to offset danger of

suffocation (Fig 2.12 B). With hyperventilation more  $\text{CO}_2$  is exhaled than is produced.  $\text{CO}_2$  drops, stimulating blood vessel constriction. As breathing increases beyond metabolic needs,  $\text{CO}_2$  is depleted from the body and alkalinity rises. Smooth muscles such as blood vessels are more likely to constrict (Fig 2.13).

**Fig 2.12: CO<sub>2</sub> as a regulator of cerebrovascular tone** (for illustration only and not to scale)

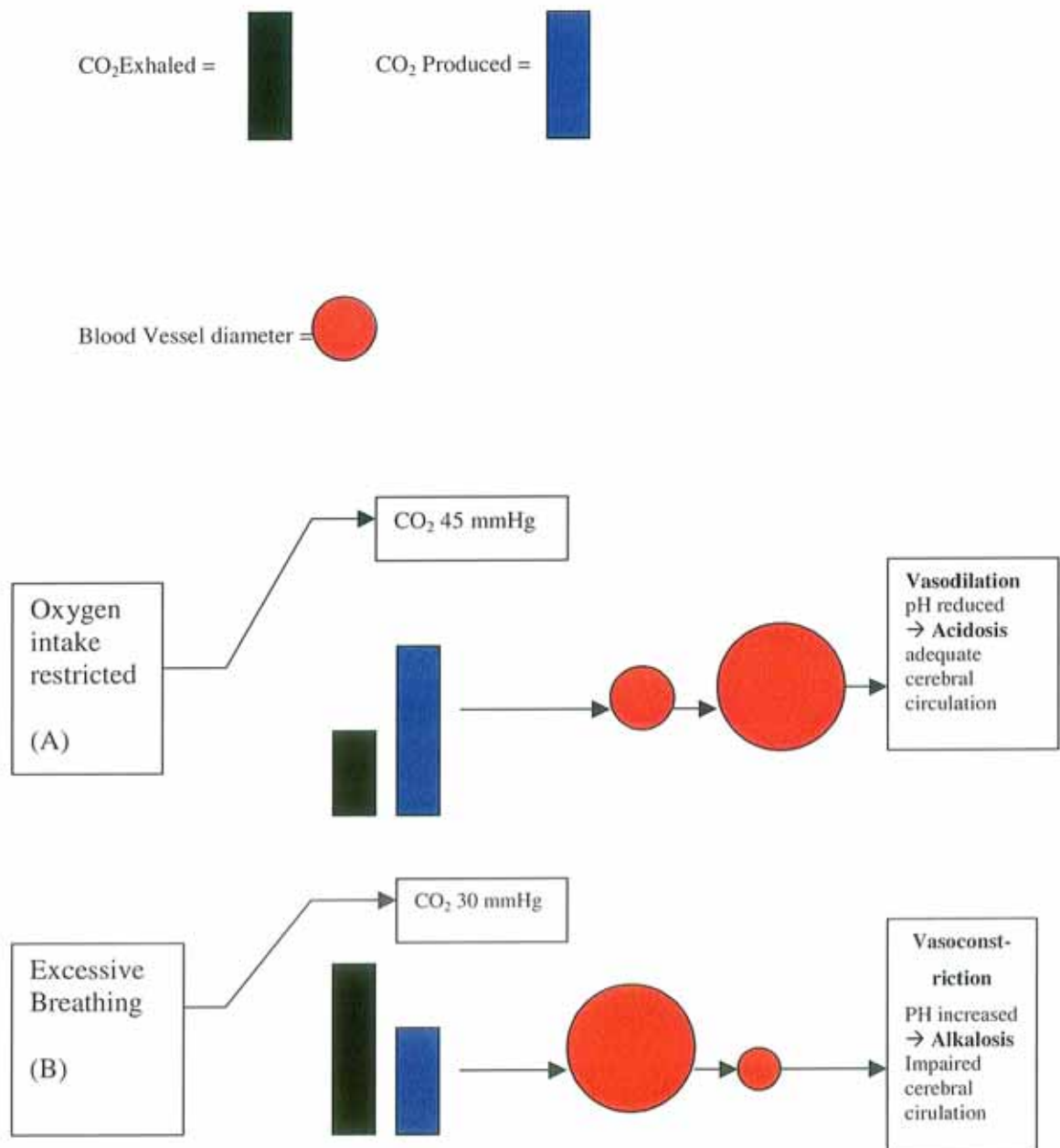


**Fig 2.13: Hyperventilation: (A) = pH (B) = CO<sub>2</sub> (mmHg) (C) = Arterial diameter**  
 (For illustration only not to scale)

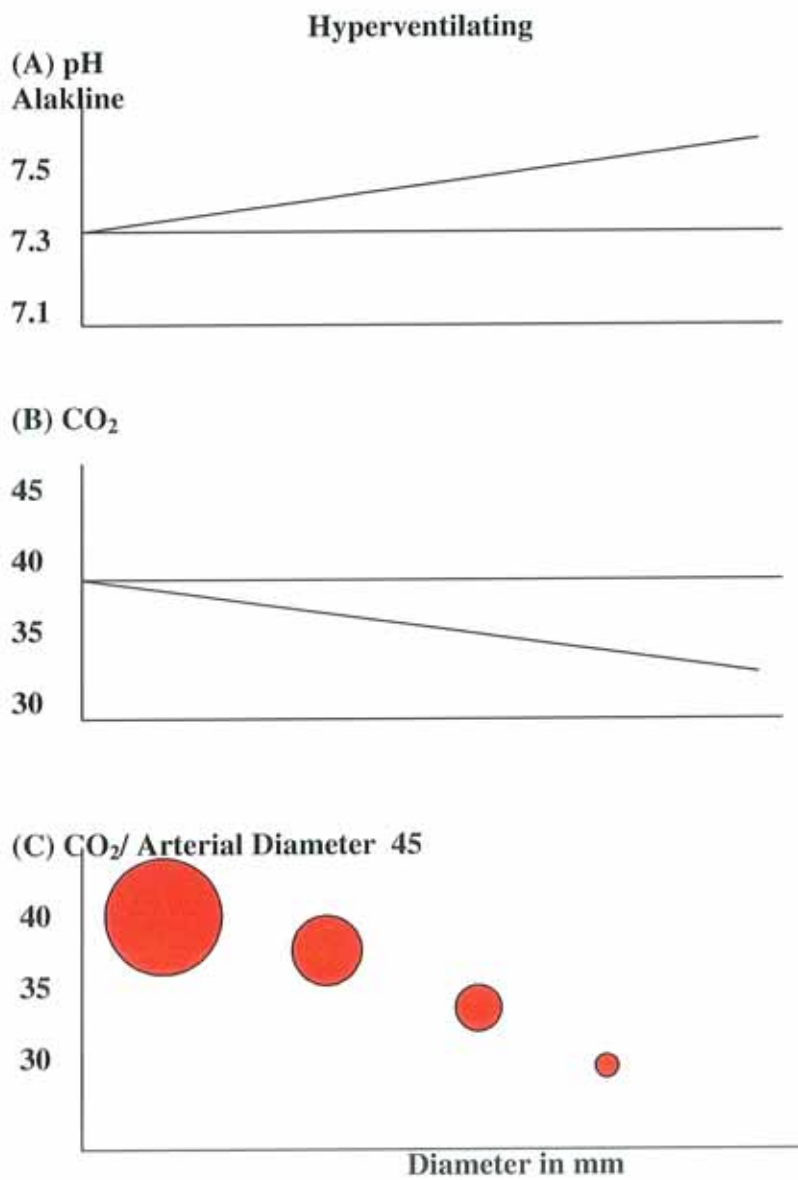


**Table 2.1: Effects of Hypocapnia**

Effects of Hypocapnia
1. Neurological Effects
<p>Increasing neuromuscular irritability (eg paraesthesias such as circumoral tingling and numbness; carpopedal spasm)</p> <p>Decreased intracranial pressure (secondary to cerebral vasoconstriction)</p> <p>Increased cerebral excitability</p> <p>Inhibition of the respiratory drive via the central and peripheral chemoreceptors</p> <p>Increases brain interstitial pH</p>
2. Cardiovascular effects
<p>Alkalosis induces arteriolar constriction and global decrease in cerebro vascular resistance. This cerebral vasoconstriction causes decreased cerebral blood flow [Short term only as adaptation occurs within 4 to 6 hours]</p> <p>Cardiac arrhythmias</p> <p>Decreased myocardial contractility</p>
3. Other effects
<p>Shift of the haemoglobin oxygen dissociation curve to the left (impairing peripheral oxygen unloading)</p> <p>Slight fall in plasma potassium</p>

After Guyton and Hall 2000

A recent study of cerebral haemodynamics measured with simultaneous PET and near-infrared spectroscopy in humans (Rostrup *et al* 2002) showed an average cerebral blood volume (CBV) of  $5.5 \pm 0.74$  ml  $100\text{g}^{-1}$  in normoventilation, with no significant changes seen during hyperventilation. CBF was  $51 \pm 10$  in normoventilation and *decreased* by 25% during hyperventilation. Cerebral blood flow is normally coupled to cerebral metabolic rate (CMR). Hypocapnia rapidly increases brain interstitial pH ( $\text{CO}_2$  is freely diffusible across the blood brain barrier) and alkalosis produces arteriolar constriction and a global increase in cerebral vascular resistance (CVR) (Table 2.1). The resultant decreased CBV lowers intracranial pressure, to a degree which is determined by intracranial compliance. This physiology was first described in cats by Wolff in 1928 and subsequently in humans by Kety and Schmidt in 1948. Therefore hyperventilation decreases  $\text{PaCO}_2$  and the perivascular pH and causes vasoconstriction.



### **2.4.1(a) Divergent views on the hypocapnia theory of HV activation**

The hypocapnia theory, which implies that low levels of carbon dioxide would lead to the predominance of the non-specific thalamic projection system over the activating reticular ascending system (Sherwin 1965, Sherwin 1967) has been put in doubt by observations that the slow waves on the EEGs of patients and normal individuals appear in a wide range of arterial and expired air CO<sub>2</sub> tension.(Morrice 1956, Blinn and Noel 1949). It has also been demonstrated by Kraaier *et al* (1989) that the drug indomethacin produces hypoperfusion similar to that caused by hypocapnia, without provoking any slowing on the EEG. There is some evidence that the HV induced EEG slowing and HV epileptiform activation of the EEG may have independent mechanisms. Neidermeyer (1972) observed that intravenous diazepam prevented activation of epileptiform discharges without affecting the HV induced slow waves. Engel *et al* (1985) showed conversely that following the treatment of absence seizures by anti-epileptic medication the HV slowing persisted.

### 2.4.2 The hypoxia theory

Under resting conditions, the brain is protected against hypoxia because cerebral blood flow increases when the arterial oxygen tension becomes low. However, during strenuous exercise, hyperventilation lowers the arterial carbon dioxide tension and blunts the increase in cerebral blood flow, possibly leading to an inadequate oxygen delivery to the brain and contributing to the development of fatigue. Voluntary hyperventilation rapidly and strongly reduces the CBF, but usually does not decrease cerebral oxygen consumption in healthy individuals.

Having studied 450 aircraft pilots in 1942 Davis and Wallace proposed the hypoxia theory. They concluded that when their subjects hyperventilated using pure oxygen there was a lesser tendency to show delta waves than when the inspired air was at the ambient oxygen content of 20%. According to a study by Gotoh *et al* (1961) diffuse slowing is considered to be the direct result of cerebral ischaemic anoxia resulting from hypocapnic cerebral vasoconstriction

It has been subsequently claimed that the slowing of the EEG during hyperventilation (HV) is caused by ischaemia/hypoxia secondary to hypocapnia-induced vasoconstriction rather than by direct neuronal effects of CO<sub>2</sub> or the associated alkalosis (Takahashi 2004). Kraaier *et al* (1989) found that standardized hyperventilation induces changes in the EEG, a decrease in the velocity of the cerebral blood flow and a decline in cognitive performance, which are comparable to those occurring in patients with cerebral ischaemia. They tested the anti-ischaemia properties of 3-OH aniracetam and found that is

had a pronounced positive effect on HV induced EEG changes and cognitive deterioration.

The immediate physiological effect of HV is to reduce arterial PaCO<sub>2</sub>, which increases perivascular and intra-neuronal pH. Increased neuronal pH produces a shift in the oxidation/reduction state of central nervous system (CNS) tissue and increases neuronal discharge of both motor and sensory fibres and increases glucose consumption and lactate and pyruvate production (Posse *et al* 1997). Rises in perivascular pH induce marked vasoconstriction, which leads to a rapid reduction in CBF, and this is observable by functional magnetic resonance imaging.

Posse *et al* (1997) demonstrated an actual reduction of blood oxygen level dependant (BOLD)-fMRI signals in the grey matter of the brain cortex during hyperventilation. This result lends supports the cerebral hypoxia theory of EEG HV activation. Within 20 seconds of starting hyperventilation, rapid and substantial decreases in the functional MR imaging signal (by as much as 10%) were measured in areas of gray matter, which were significantly greater than the modest changes observed in white matter. They concluded that regional and gray-white matter differences in fMRI signal changes during controlled HV may reflect differences in metabolic activity, vascular regulation, and/or capillary density. BOLD MR imaging has been used in most NMR studies measuring changes in local oxygenation as it is sensitive to deoxyheamoglobin. This method uses differences in the magnetic nature of oxyheamoglobin and deoxyheamoglobin to provide information related to tissue oxygenation.

However the method only reflects changes in haemoglobin saturation and additional information is required to deduce absolute haemoglobin saturation, or oxygen status. Hoshi (1999) re-evaluated the hypoxia theory as the mechanism of HV induced EEG slowing by monitoring relative changes in cerebral oxygenated, deoxygenated, total haemoglobin, and oxydized cytochrome oxidase using near-infrared spectroscopy. EEG slowing was not found to be synchronous with changes in either the cerebral oxygenation or end tidal concentration of carbon dioxide. The EEG slowing persisted at low levels after the EEG had returned to baseline levels. They concluded that the findings did not confirm the hypoxia theory and suggested that more subtle mechanisms were the cause of the EEG slowing.

A subsequent study by Naganawa *et al* (2002) using a 3-Tesla fMRI and 2 minute periods of subject hyperventilation showed that both gradient-echo (GE) echo planar imaging (EPI) and spin-echo (SE) echo planar imaging, when used to evaluate their sensitivity to vascular reactivity in the brain, showed globally significant signal decreases in the cerebral cortex. In GE-EPI the frontal cortex showed a larger signal decrease than other grey matter tissues ( $p < 0.05$ ). Observable blood oxygen level dependent (BOLD) – contrast fMRI signal decreases in grey matter were approximately 30% more in subjects with intermittent rhythmic delta activity (IRDA) than in controls in the first 2 minutes of hyperventilation during EEG in a study by Makiranta (2004). Positron emission tomography (PET) scanning provides measurements of brain tissue oxygenation using non-invasive, quantitative data on global and regional cerebral blood flow (CBF), cerebral blood volume (CBV), cerebral metabolic

rate of oxygen (CMRO<sub>2</sub>) and oxygen extraction fraction (OEF). The availability of regional OEF measurement allows the calculation of regional end capillary PvO<sub>2</sub>. Because PET scanning is the only method available to measure regional OEF at present, it is regarded as the gold standard in comparisons of methods of measuring cerebral oxygenation. A mean value of PvO<sub>2</sub> of 31.2 mmHg in normocapnia was reported by Alpert *et al* (1988) and Gupta *et al* (2002). Hutchinson *et al* (2002), in a PET study using frontal regions of interest in patients and in controls, showed that at resting baseline there was a significant relation between the lactate/pyruvate (L/P) ratio and the OEF (spearman  $r = 0.69$ ,  $p = 0.002$ ). This relationship between the OEF and the L/P ratio was also seen after controlled hyperventilation causing a reduction in the arterial carbon dioxide tension by 0.9 kPa, but shifted to the right (Fig 2.14, 2.15), indicating that HV significantly increases the OEF but does not increase the L/P ratio. This was compatible with the ANLS hypothesis. (Controls in this study showed CBF values (mean  $\pm$  SD) of  $27 \pm 3.4$  ml.100g<sup>-1</sup>.min<sup>-1</sup>, CBV of  $0.03 \pm 0.01$ , OEF of  $0.42 \pm 0.03$ , and CMRO<sub>2</sub> of  $92 \pm 10.5$   $\mu$ mol. 100g<sup>-1</sup>. min)

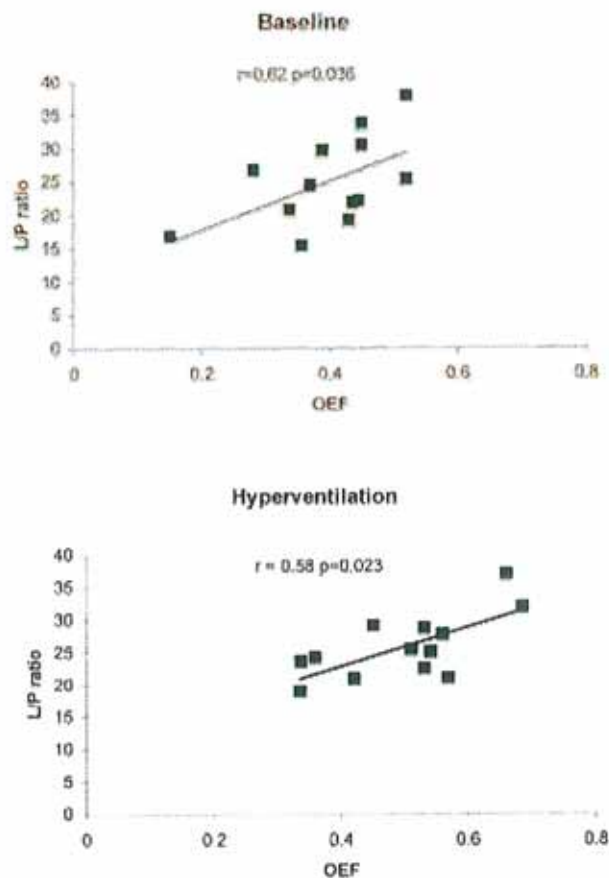


**Figure 2.14:** Scatter/Line graph showing the relationship between oxygen extraction fraction (OEF) and lactate/pyruvate ratio at baseline and after hyperventilation in 13 patients. Note the shift to the right with hyperventilation. The  $r$  value is the Spearman coefficient (after Hutchinson *et al* 2002).

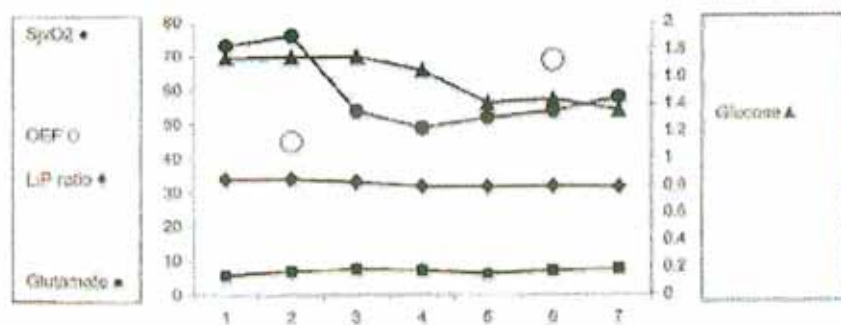


**Figure 2.15:** Effects of HV and PET parameters showing increase in oxygen extraction fraction (OEF%), reduction in jugular venous oxygen saturation (%), reduction in glucose (mmol/L), and no change in the lactate/pyruvate ratio or glutamate (umol/L). Each integer on the horizontal axis (1-7) represents a 20 minute epoch. HV was performed at epoch 2 (after Hutchinson *et al* 2002).

A recent study by Binks *et al* (2007) showed that grey matter blood flow change is unevenly distributed during moderate isocapnic hypoxia in humans. Increases in regional CBF (rCBF) were not uniform and ranged from  $9.9\% \pm 8.6$  in the occipital lobe to  $28.9\% \pm 10.3$  in the nucleus accumbens. Phylogenically (i.e. evolutionary) older regions of the brain tended to show larger vascular response to hypoxia than evolutionary younger regions, e.g. the putamen, brainstem, thalamus, caudate nucleus, nucleus accumbens and pallidum, received greater than average increases in blood flow, while cortical regions, where the EEG is generated, received below average increase. The authors offered no explanation for this result.

Glutamate uptake by astrocytes is fundamentally important in the regulation of CNS function. Disruption of uptake can lead to excitotoxicity as a consequence of hypoxic/ischaemic events and is implicated in various neurodegenerative processes. Dallas *et al* suggested in 2007 that glutamate transporter expression in astrocytes is directly downregulated by hypoxia. Such suppression of glutamate uptake may be an important contributory factor in hypoxic/ischaemic triggered glutamate toxicity. Coughlan and McMenamin (2008) noted no decrease in  $pO_2$  measured using digital oximetry during a standardised hyperventilation study in normal adults. Average  $pO_2$  in the resting state was 98% and this increased to an average of 100% (with a  $pETCO_2$  of 15mmHg)

#### **2.4.2(a) Divergent views on the hypoxia theory of HV activation**

The hypoxia theory which suggests that the EEG slowing seen during hyperventilation is due to vasoconstriction and diminution of oxygen and dextrose supply to the cerebral cortex (Davis and Wallace 1942) has many arguments against it. Van Der Worp *et al* (1991) demonstrated that differences exist in the quantitative EEG changes due to HV and hypoxia. Kennealy *et al* (1986) using spectral analysis in acute hyperventilation showed that the EEG changes were independent of the concentration of inspired oxygen. Konishi (1987) showed that the EEG changes were independent of the reduction of cerebral blood flow.

#### **2.4.2(b) Cerebral blood flow and brain hypoxia**

Cerebral blood flow changes rapidly in direct relationship to changes in arterial pCO<sub>2</sub>. One function served by this response is to counteract changes in brain pH, such as those occurring during hyperventilation-induced alkalosis (Kuschinsky 1982). Hyperventilation reduces cerebral blood flow (CBF) by 40% to 50% (Edvinsson *et al* 1993). However, in both humans and animals, this decrease in CBF does not usually cause metabolic changes indicating brain hypoxia. The increase in brain lactate caused by hyperventilation appears to result from the direct effects of alkalosis on glycolytic flux. (Siesjo 1978, Hood and Tannen 1983, Edvinsson *et al* 1993, Leusen and Weyne 1976, Kauppinen and Williams 1998)



During hyperventilation, CBF reaches its minimum at an arterial  $p\text{CO}_2$  of approximately 25 to 30 mm Hg. (Edvinsson *et al* 1993). Although lower arterial  $p\text{CO}_2$  levels may not further reduce CBF, they impede oxygen delivery by the Bohr effect (the shift in the oxyhemoglobin dissociation curve to the left with increasing pH).. Edvinsson *et al* (1993) stated that "the clinical and experimental evidence for brain hypoxia is somewhat scant." Reviews of experimental studies of brain metabolism during hyperventilation have concluded that hyperventilation leading to a  $p\text{CO}_2$  as low as 14 mm Hg does not produce brain hypoxia (Seisjo 1978, Kuschinsky 1982, Hood and Tannen 1983). The subjective effects of hyperventilation may be the result of altered function of the numerous receptors, channels, transporters, and enzymes in neurons that are highly sensitive to increases in pH, rather than the result of hypoxia (Kaila and Ransom 1998).

In attempting to determine the cause of increased lactate production in response to respiratory alkalosis, Siesjo (1978) noted that it is difficult to distinguish between lactate production that occurs as a result of increased intracellular pH activating phosphofructo kinase (PFK a glycolytic enzyme that catalyzes the irreversible transfer of a phosphate from ATP to fructose-6-phosphate) and lactate production that occurs as a result of decreased oxygen delivery and cellular hypoxia. He concluded that "the most direct way of testing whether or not hypoxia is present is to measure concentrations of labile phosphates in the tissue." van Rijen *et al* (1989) measured brain lactate with proton magnetic resonance spectroscopy (MRS) and additionally measured ATP, ADP, AMP,  $\text{P}_i$ , PCr, and pH with phosphorus-31 MRS in human volunteers who hyperventilated to an average  $p\text{CO}_2$  of 16 mm Hg. Concurrent transcranial Doppler sonography

showed a 42% reduction in left middle cerebral artery flow. Brain lactate increased significantly during and after hyperventilation, but no change was observed in the phosphate compounds, suggesting that hypoxia did not occur.

Hyperventilation causes a large increase in arterial pH but only a small increase in brain pH (Van Rijen *et al* 1989, Petrof *et al* 1985). The relative stability of brain pH results from homeostatic processes, which serve to counteract changes in intracellular pH. One of the most important mechanisms of this defense against intracellular alkalosis in the brain is the increased production of lactic acid via glycolysis (Seisjo 1978, Leusen and Weyne 1976). This mechanism can operate in the presence of fully adequate oxygen tension. Numerous biochemical studies (Granholm *et al* 1969, Granholm and Seisjo 1971, Nilsson and Busto 1973, Carlsson *et al* 1974, Kogure *et al* 1975, Young and Yagel 1984) and more recent spectroscopic studies (Van Rijen *et al* 1989, Petroff *et al* 1985) have shown that high-energy phosphate levels (ATP and PCr) remain unchanged during hyperventilation that produces pCO<sub>2</sub> levels of approximately 14 mm Hg. Only one study, which involved severe hypocapnia in rats (pCO<sub>2</sub>=10 mm Hg), found evidence for decreased PCr and increased ADP, indicating that metabolically significant hypoxia had occurred (Macmillan and Seisjo 1973). Studies of cerebral oxygen consumption (CMRO<sub>2</sub>) during hyperventilation also typically show no reduction in CMRO<sub>2</sub> (Young and Yagel 1984, Macmillan and Siesjo 1973, McHenry *et al* 1965). Overall, the evidence suggests that respiratory alkalosis leading to a pCO<sub>2</sub> of  $\geq 14$  mm Hg produces a rise in brain lactate as a result of increased glycolysis in the service of regulating intracellular pH, and that brain hypoxia does not occur.

### 2.4.3 Respiratory alkalosis theory of HV activation

The body endeavours to preserve a normal pH, particularly in the bloodstream, extracellular fluids and cerebrospinal fluid. The body is optimised for a pH of 7.4, slightly above the neutral 7.0 and towards the alkaline. This supports endocrine, metabolic and other maintenance operations. Respiratory alkalosis results from excessive excretion of CO<sub>2</sub> and occurs when the PaCO<sub>2</sub> is less than 4.5 kPa (34 mmHg). Changes in pH of only one tenth of a point have distinct consequences for the body, altering nerve conduction, the diameter of blood vessels and the contractility of smooth muscle. This balance is easily disrupted by taking deep breaths, i.e. hyperventilating, where pH will rise from 7.4 to 7.5 or 7.6, and CO<sub>2</sub> will fall from normal 40 to 30 or 25 in less than 30 seconds (Figs 2.8 and 2.9). The combination of high pH and low CO<sub>2</sub> causes certain body changes, such as effects on skeletal muscle causing twitches and spasms. Moderate hyperventilation causes motor excitability and hypertonicity, faster reflexes, and suppression of parasympathetic nervous system activity. This is part of the “fight or flight” conditioned response. Therefore a short period (3 minutes) of hyperventilating raises the pH toward alkalosis, directly affecting circulation, muscle tension, smooth muscle, nerve conduction, sensory functions, cerebral functions etc. (Table 2.1).

Gotoh *et al* (1961) suggested that the action of CO<sub>2</sub> was mediated by direct effect of hydrogen ions (H<sup>+</sup>) on cerebrovascular smooth muscles. The majority of experimental studies support the concept that CO<sub>2</sub> regulates the cerebral circulation primarily by changes in pH in the extracellular fluid surrounding the

vessels (Busija 1984). Kontos *et al* (1977) found that marked changes in PaCO<sub>2</sub> did not affect cerebral vessel diameter unless a change in extracellular fluid pH occurred. However, it is not certain whether the effects on cerebral vessels are due solely to changes in extracellular fluid pH, or whether and to what extent changes in intracellular pH also contribute (Harder 1982). Evidence to support the theory that the extracellular pH influences the vasodilatory response to a greater extent than the intracellular pH was published in 1898 by Toda *et al*. They found that hypercapnic vasodilation in dog cerebral artery strips was reversed by infusion of sodium-bicarbonate, i.e. pH was raised, while PCO<sub>2</sub> remained stable. In other experimental studies, blockade of adenosine triphosphate (ATP)-sensitive potassium channels completely inhibited the hypercapnia induced vasodilation (Kontos 1996, Faraci 1998) as well as the hypocapnia-induced vasoconstriction (Wei 1999). Findings suggest that opening and closure of these channels are of importance for the vascular responses to alterations in PaCO<sub>2</sub>.

Recently, Nakahata *et al* (2003) showed that blockade of ATP-sensitive potassium channels with glibenclamide completely abolished hypercapnia-induced vasodilation only when pH was decreased. Thus, CO<sub>2</sub>-induced alteration in pH appears to affect ATP-sensitive potassium channels either by opening (hypercapnia-induced acidosis) or closure (hypocapnia-induced alkalosis) of the potassium channels.

Invasive animal studies have demonstrated large pH increases (>0.25U), phosphocreatine (pCr) decreases (>30%) and adenosine triphosphate (ATP)

decreases (>10%) after hyperventilation to 20 mmHg PaCO<sub>2</sub>. However using magnetic resonance spectroscopy, HV studies in awake humans have demonstrated only small pH changes (approximately 0.05U) and no changes in phosphocreatinine (PCr) or ATP. Using rapidly interleaved phosphorus-proton spectroscopy in a 4 Tesla magnetic field to measure pH, PCr, inorganic phosphate, beta-ATP and lactate changes, a recent study on brain changes due to hypocapnia induced by 20 minutes of HV by Friedman (2007), demonstrated that PaCO<sub>2</sub> reached a minimum of 17 mmHg at 16 minutes. The maximum pH change achieved was +0.047U at 14 minutes. Maximal lactate change was at 15 minutes, PCr maximum change was (-3.4%) at 10 minutes, and inorganic phosphate (+6.4%). No changes in beta-ATP were observed. The peak in pH, despite continued decreases in PaCO<sub>2</sub> suggests active buffering during HV (Friedman 2007). These data and the small magnitude of early PCr and inorganic phosphate changes do not support the suggestion of substantial energy compromise during HV.

Glial cells provide an essential contribution to pH regulation and acid/base transients in the nervous system. The mechanisms of intracellular pH regulation and the transport of neurotransmitters and metabolites across the glial cell membrane also shape extracellular pH shifts. These pH transients can be very brief and local, and may constitute a proton mediated signalling between glial cells and neurons. By modulating and shaping neuronal and synaptic processes, excitation and inhibition in nervous tissue may be affected, producing slow potential shifts (Deitmer and Rose 1996).

Rapid pH transients may actually be signals rather than only a result of inadequate homeostatic acid-base regulation. Analogous to the signaling pattern of other ions, such as calcium and potassium, transient shifts of protons and bicarbonate, together with changes in carbon dioxide (CO<sub>2</sub>), may influence or initiate functional processes in the nervous system. This may include pH induced changes of neuronal excitability, the modulation of gap junctions, and thus of electrical synapses and the glial syncytium. Glial cells actively regulate extracellular pH changes related to neuronal activity (Rose and Deitmer 1994). pH perturbations can induce a variety of changes in cellular functions in nervous systems, from the induction or inhibition of ionic currents, to alterations in the overall neuronal excitability, and to modulation of enzyme activities (Chesler 1990, Deitmer and Rose 1996). In glial cells in particular, pH shifts may be associated with acid/base secretion, lactate transport, cell volume changes, glutamate uptake, alteration in gap junctional communication and metabolic processes. Some of these pH-dependent processes are linked to or might induce a cascade of H<sup>+</sup>-induced signals in nervous systems. pH shifts and brief pH transients may contribute to shape neuronal performance, and hence behaviour, at molecular and cellular levels.

Fast oscillatory EEG activity in the gamma range (fast EEG frequencies from 25.0-80.0 Hz) described in several cortical regions has been interpreted as a form of synaptic network activity which underlies attention and arousal, presumably facilitating associative binding between large ensembles of neurons. In different cortical structures, gamma activity has been related to the synchronous activation of reciprocally connected GABAergic neurons, with and without the simultaneous involvement of excitatory recurrent synapses. It is

interesting to note, that pH has a powerful modulatory action on the GABAergic mechanisms (Kaila, 1994), which suggests a tight link between respiration-mediated regulation of pH/pCO<sub>2</sub> and neuronal functions at the whole-organism level.

Alterations in respiratory activity (if not balanced by simultaneous changes in the production of CO<sub>2</sub>) go along with profound changes in PCO<sub>2</sub>, and have a direct effect on the acid-base status of the brain parenchyma. A wealth of evidence has been accumulated during the last few decades demonstrating that pH is a powerful physiological modulator of neuronal activity, and this has led to the hypothesis that H<sup>+</sup> ions have an important signalling function in brain tissue (Kaila and Ransom 1998). GABA receptors are known to be modulated by pH changes (Kaila 1994), and as described above, the driving force of GABA<sub>A</sub> receptor-mediated currents is also affected by changes in the acid-base status of neuronal tissue. A critical role for GABA<sub>A</sub>-ergic mechanisms has been demonstrated for carbachol-induced gamma oscillations in the hippocampal slice (Fisahn *et al* 1998). The oral stability of gamma oscillations was dramatically enhanced by the extracellular respiratory alkalosis that takes place in 1% CO<sub>2</sub>, and this effect is most likely a result of a selective increase in the amplitude (but not in the decay time constant) of GABA<sub>A</sub> receptor-mediated inhibitory post synaptic current (IPSC) (Stenkamp *et al* 2001).

By artificially and independently changing the PCO<sub>2</sub> and pH in different ways, it has been demonstrated that *negligible EEG changes occur with alkalosis alone* (Davis and Wallace 1942; Lubin and Price 1942; Schieve and Wilson 1953; Swanson *et al* 1958). Hyper-excitability of neurons may be induced by

respiratory alkalosis (Esquivel *et al* 1991). Hyperventilation implies a reduction in tissue CO<sub>2</sub> tension (hypocapnia), which, is known to produce an increase in neuronal excitability. Experiments on *in vitro* preparations suggest that neuronal hyperexcitability associated with hyperventilation is largely attributable to respiratory alkalosis, which takes place within nervous tissue during the net loss of CO<sub>2</sub> (Caspers *et al* 1987, Tombaugh and Somjen 1998). A survey of the pH dependence of a large number of ligand- and voltage-gated channels indicates that a rise in pH will increase both intrinsic neuronal excitability and excitatory (glutamatergic) synaptic transmission while suppressing GABA<sub>A</sub> receptor mediated postsynaptic inhibition (Kaila 1994, Lee *et al* 1996, Tombaugh and Somjen 1998, Traynelis 1998). The hyperventilation induced physiological changes are thought to be a consequence of increased neuronal excitability and alteration of synaptic transmission resulting from the hypocapnia-induced alkalosis. Despite these findings little is known about the physiological changes at the neuronal network level following hyperventilation (Jensen *et al* 2002). Alkalosis induces epileptiform activity in low magnesium rat neo-cortical slices, an effect which is blocked by N-methyl-D-aspartate (NMDA) antagonists (Aram and Lodge 1987). Increasing gap junctional conductance by intracellular alkalinization augmented epileptiform activity in calcium-free hippocampal slices (Perez-Velazques *et al* 1994). These data suggest that alkalinization is at least one mechanism by which HV evokes temporal lobe seizures. Guaranha *et al* 2005 demonstrated the efficacy of HV in activating clinical and electrographic seizures of temporal lobe origin.



#### **2.4.4 The role of the autonomic nervous system: theory of hyperventilation activation**

The autonomic nervous system (ANS), as its name implies, governs or regulates the body's internal environment. Vital signs such as temperature, pulse rate, blood pressure, and rate of respiration mirror the body's internal environment.

As previously mentioned CBF is controlled by five factors:  $\text{PaCO}_2$ ,  $\text{PaO}_2$ , autoregulation, metabolism and the autonomic nervous system. The autonomic nervous system affects the cerebral blood flow by activation of the sympathetic nervous system, which causes vasoconstriction. In a normal adult the ANS maintains the respiratory rate below 18 breaths per minute, preventing hyperventilation. Voluntary hyperventilation induces a fall in systolic and diastolic blood pressure as well as a reflex increase in heart rate. Hyperventilation causes a reduction in cerebral  $\text{PCO}_2$ , which results in cerebral vasoconstriction and consequent hypertension at a bulbar level. The sympathetic inhibition area of the bulbar vasomotor centre then sends impulses along its efferent pathway to cause peripheral vasodilation. Verification of a fall in blood pressure triggered by hyperventilation is a sign that the bulbar vasomotor centre, its efferent pathway and its terminal organ are functioning normally (Sharpey-Schfer 1965). In normal subjects systolic and diastolic pressure drops around 30 mmHg at the end of hyperventilation, and then quickly returns to baseline.

Darrow *et al* (1943, 1944a, 1944b) and Darrow and Pathman (1944) proposed that parasympathetic inhibition during hyperventilation results in the EEG

slowing, stating that “*a supplemental relationship between acetylcholine and CO<sub>2</sub> in homeostatic regulation of cerebral circulation is indicated*”. The role of a cholinergic mechanism received support at that time from Barnes and Amoroso (1947) who stated that, “*slow waves in deep breathing are explained by cerebral vasoconstriction and by destruction of electrogenic acetylcholine in alkalosis of acapnia*”. The irregular breathing observed during hypocapnia may be mediated by the autonomic nervous system, reflecting a fluctuating drive related to changes in the behavioural state (Plum and Leigh 1981).

Maintenance of cerebral perfusion over a wide range of systemic pressures is thought to be carried out through a mechanism of cerebral autoregulation (Strandgaard *et al* 1984, Paulson *et al* 1990). This function counter-regulates systemic pressure changes through cerebrovascular resistance adjustments. Originally, cerebral autoregulation was conceived as encompassing a time scale from minutes to hours, such that changes in cerebral blood flow that fully counteract sustained arterial pressure changes indicate effective autoregulation. As the time resolution of measurement techniques has increased, however, results have suggested that autoregulation works on a much more ‘dynamic’, beat-by-beat basis (Aaslid *et al.* 1989, Newell *et al* 1989). Specifically, the beat-by-beat relationship between pressure and flow has been modelled as a simple high-pass filter (Newell *et al* 1989, Blaber *et al* 1997, Diehl *et al* 1998, Panerai *et al* 2004, Zhang *et al* 1998). This assumes that lower frequency oscillations in pressure (below ~0.07 Hz) are effectively blunted while faster oscillations pass through unaffected (Zhang *et al* 1998). These observations have led researchers to hypothesize that cerebral autoregulation is a frequency-dependent

phenomenon that operates most effectively in the frequency range below 0.07 Hz.

Diehl (1995) demonstrated a phase relationship between cerebral blood flow velocity and blood pressure as a clinical test of autoregulation. Using transcranial Doppler monitoring of both middle cerebral arteries (MCAs) during hyperventilation, the study confirmed the high-pass filter model of cerebral autoregulation. The overall pattern of the pressure–flow relation was of decreasing coherence and gain, and increasing phase with decreasing frequency, characteristic of a high-pass filter. Normal subjects showed predicted positive phase shift angles between cerebral blood flow velocity and arterial blood pressure oscillations. Patients with expected autoregulatory disturbances showed significant decreases in phase shift angles. Close correlations existed between autoregulation and CO<sub>2</sub> induced vasomotor reactivity.

Autonomic nervous system responses to hyperventilation mediated in the rostral and caudal ventrolateral medulla have been demonstrated by Julu *et al* (1992, 1997). They showed evidence of activation of both sympathetic and parasympathetic systems during HV. Papp *et al* (1993) expressed the view that autonomic instability underlies both hyperventilation and panic disorders, although the neurological basis for this remains unresolved.

Julu and Engerstrom (2005) investigated whether brainstem assessment using the “NeuroScope” system could be used for objective and quantitative

monitoring of early development and later progress in Rett syndrome, a dysautonomia, and in normal subjects.. The following cardiovascular vital signs were recorded simultaneously in real-time: cardiac vagal tone (CVT), cardiac sensitivity to baroreflex (CSB), (the baroreflex or baroreceptor reflex is one of the body's homeostatic mechanisms for maintaining blood pressure providing a negative feedback loop in which an elevated blood pressure reflexively causes blood pressure to decrease; similarly, decreased blood pressure depresses the baroreflex, causing blood pressure to rise), heart rate (HR), and mean arterial blood pressure (MAP) and respiratory vital signs: breathing rate and pattern, transcutaneous partial pressures of oxygen ( $pO_2$ ) and carbon dioxide ( $pCO_2$ ). These objective measurements of ANS function have yielded quantitative data on the closely associated function of the brainstem and thalamic mechanisms involved in hyperventilation activation of the ANS/ CNS.

#### **2.4.5 Brainstem and thalamic mechanism theory of HV activation**

The medical literature presents two major groups of disorders in which hyperventilation is a presenting feature, disorders of mood, notably panic disorder, and disorders of brain stem function which include developmental, vascular, traumatic, toxic, metabolic, degenerative or neoplastic disorders (Kerr and Julu 1999).

The respiratory centre located in the medulla and the pons, acts in the regulation of rhythmic, involuntary respiration. The reticular formation (an inner core of

gray matter found in the midbrain, pons and medulla oblongata) of the pontine tegmentum contains multiple cell groups. Output ascending from the reticular formation of the brainstem is relayed to the cerebral cortex by intralaminar thalamic nuclei which are located in laminae separating the medial and ventrolateral thalamic nuclei. The thalamus is involved in the relay and distribution of most, but not all, sensory and motor signals to specific regions of the cerebral cortex. Sensory signals generated in all types of receptors are projected via complex pathways to specific relay nuclei in the thalamus, where they are segregated and systematically organized. The relay nuclei in turn supply the primary and secondary sensory areas of the cerebral cortex. From within the medulla, graded action potentials are discharged in a cyclic pattern, and act to excite respiratory muscles. It is the medullary respiratory centres that receive and integrate input from a variety of sources, which allow the exchange of carbon dioxide at the lungs in response to the body's requirements. Receptors play an important role in the regulation of respiration; these consist of central and peripheral chemoreceptors and mechanoreceptors. Voluntary control of respiration, such as when consciously hyperventilating, is provided via the cerebral cortex, although the chemoreceptor reflex is capable of overriding conscious control. Respiratory inspiration is actively terminated by serotonergic neurones in the brain stem of humans. Central chemoreceptors of the central nervous system, located on the ventrolateral medullary surface, are sensitive to the pH of their environment. These act to detect a change in pH of the cerebrospinal fluid. The respiratory centre responds rapidly to changes in plasma pH or  $\text{PaCO}_2$  and respiratory compensation results in a change in ventilation within minutes.

In the 1950s research interest was generated in the effect of hyperventilation on the ascending reticular activating system and its relationship with the cerebral cortex. The prevailing theory of hypocapnic vasoconstriction leading to hypoxic-ischaemic changes in the cerebrum and thus to EEG slowing was questioned. Bonvallet and Dell (1956) reported that hyperventilation does not modify the EEG characteristics of the *in vitro* brain preparation. They found that hypercapnia produces cortical arousal and hypocapnia produces cortical depression due to a direct effect on mesencephalic structures. They also showed that mesencephalic reticular structures are as sensitive to carbon dioxide as the classic respiratory centres in the brainstem. They postulated that hypocapnia could liberate normally inhibited synchronizing structures of the mesencephalic reticular formation resulting in a slow wave pattern.

Sherwin (1967) attributed the diffuse slowing to synchronous activity in the non-specific thalamocortical projecting systems which become more active in hypocapnia. Patel and Mulsby (1987) raised the possibility that hypocapnia induced by hyperventilation decreased activity in the mesencephalic reticular formation which then caused EEG slowing, just as drowsiness and sleep produce EEG slowing.

Studies by Julu *et al* (1997) and Julu and Engerstrom (2005). showed that voluntary hyperventilation in normal female controls was associated with agitation and autonomic stimulation. Cold extremities and increase in blood pressure and heart rate indicated activation of the sympathetic vasoconstrictors and cardioaccelerators which are situated in the rostral part of ventrolateral

medulla. At the same time there was parasympathetic activation in the caudal part of the ventrolateral medulla, shown by an increase in cardiac vagal tone, which rose to check and control the increase in both heart rate and blood pressure. In normal controls the rise in cardiac vagal tone was adequate, achieving smooth regulation of heart rate and blood pressure. The autonomic responses to hyperventilation suggest that both rostral and caudal ventrolateral medulla, are simultaneously activated during the initiation process. It has been established that the neurones responsible for terminating inspiration are situated at the ventrolateral aspect of the lower pons since a lesion of this area causes apnoea in lower mammals (St. John 1990). The studies indicated that there is a generalised activation of the ventrolateral medulla during hyperventilation, although the origin of this activation is unclear. However Golonov *et al* (2000) demonstrated in the rat that hypoxic excitation of reticulospinal sympathoexcitatory neurons of the rostral ventrolateral medulla (RVLM) in the brain stem mediated cerebrovascular and EEG responses. Seigneur *et al* (2006) in a study aimed at understanding complex interactions between cortical neurons, glia and blood supply demonstrated brainstem cholinergic action on cortical glial cells *in vivo*. Cortical activation was elicited using electric stimulation of cholinergic nuclei, including the pedunculopontine tegmentum in the brainstem. More than 80% of glial cells were hyperpolarized during electrical stimulation, and this was associated with steady neuronal depolarisation, increased CBF, lower extracellular K<sup>+</sup> concentration, increased membrane resistance, decreased membrane capacitance and persistent positive DC field potentials. More than 20% of glial cells displayed sustained depolarising potentials, in parallel with neuronal depolarisation, decreased CBF and more

negative DC field potentials. In animal studies, negative DC shifts have generally been linked to increased neuronal excitability (Caspers *et al* 1987), presumably due to increased excitatory synaptic transmission and enhanced membrane excitability (Balestrino 1988, Caspers 1987, Lee 1996). DC field potentials also contribute to the summated excitatory post-synaptic potentials which are recorded on the scalp as the EEG.

Hyperventilation stimulates vagal afferents to the thalamus, thus exerting powerful effects on the excitability of the cortex as well as producing an 'edge of sleep' state. Vagus nerve afferents synapse in the nucleus tractus solitarius (NTS). The NTS ascends to the parabrachial nucleus which diverges into two pathways, one of which inputs to the hypothalamus, amygdala, stria terminalis and limbic corex, affecting autonomic, endocrine and emotional control. The other pathway from the parabrachial nucleus goes to several thalamic nuclei and thence to the cortex. Thalamic intralaminar and mid-line nuclei project diffusely to the cerebral cortex and probably influence cortical synchronisation or desynchronisation. In animals, lower frequency stimulation (1.0-17.0 Hz), causes EEG synchronisation while high frequency stimulation (greater than 30.0 Hz) results in EEG desynchronisation. Two PET studies performed during stimulation of the vagus nerve reported thalamic activation and inconsistent results in areas of the cortex and subcortical structures (Henry and Votaw 2006, Kanner 2008).



## 2.5 Excitability of human cortex in hyperventilation

The coupling of cerebral blood flow to metabolism ensures that tissues with high metabolic needs have higher flows than low metabolic areas. In human subjects, hyperventilation leads to a negative DC shift in the scalp-recorded EEG (Voipio *et al* 1995). As mentioned in section 2.3.5, negative DC shifts have generally been linked to increased neuronal excitability, (Caspers *et al* 1987). Slow ionic shifts at the blood-brain barrier might also contribute to the DC shift (Lehmenkuhler 1999). It is known that reductions in PaCO<sub>2</sub> increases the excitability of sensory and motor axons in the peripheral nervous system (Macefield and Burke 1991, Mogyros *et al* 2000, Somjen *et al* 1987). Low PaCO<sub>2</sub> levels appear to affect the brain as a whole. This is suggested by the common observation that HV causes a generalised slowing of the EEG (Kujirai *et al* 1993). Lee *et al* (1999), studying the effects of CO<sub>2</sub> on excitatory transmission apparently caused by changes in intracellular pH in the rat hippocampal slice, concluded that the transient changes in the EPSP seen in response to changes in PaCO<sub>2</sub> are mediated by intracellular pH. Magnetoencephalography (MEG) studies by Carbon and Wubbler (2000) and Jensen *et al* (2002) demonstrated that HV enhances cortical excitability in widely distributed networks.

Recently the possible role of gap junctions on interneuronal synchronization has received much attention (Traub and Bibbig 2000). Since the conductivity of gap junctions increases with intracellular pH (Spray *et al* 1981), it is possible that respiratory alkalosis could affect the gap junctions and thus the properties of the

interneuronal network. Extensive theoretical and experimental work on the rat hippocampus suggests that networks of interneurons coupled with GABAergic connections are responsible for rhythmogenesis and neuronal synchronization underlying in particular Gamma oscillations (Palva *et al* 2000).

Tomita-Gotoh and Hayashida (1996) recorded direct shifts in electrical potential from scalp electrodes when they induced hypocapnia and hypercapnia in human subjects. Hyperventilation increased cortical excitability with hypocapnia. Kukumberg *et al* (1996) found increased cortical excitability in ten human subjects, noting changes of motor evoked potential amplitudes following magnetic stimulation after hyperventilation. Seyal *et al* (1998) showed widespread increased excitability as measured by motor evoked potentials with hyperventilation in six human subjects.

Hyperventilation also increases the excitability of skin and motor nerves. In experimental animals, hyperventilation increases excitability of hippocampal neurons. The hippocampus is responsible for attention and orientation. Carbon and Wubler (2000) have shown that fifteen minutes of hyperventilation increased sensorimotor cortex excitability measured by direct current magnetoencephalography. Vidiendal *et al* (1998) demonstrated that the peripheral physical effects of voluntary hyperventilation include modest hypocapnia and normal PO<sub>2</sub> leading to increased cardiac output, increased renal blood flow, increased lithium and sodium excretion, and a minor increase in renal sympathetic activity. Djarova *et al* (1986) showed that three minutes of

hyperventilation produced a brief increase in cortisol and human growth hormone in eleven men.

Diringer *et al* (2000) in a PET scan study demonstrated that brief moderate hyperventilation did not decrease cerebral metabolism in patients with traumatic brain injury. In a rat hippocampal slice model, Stenkamp *et al* (2001) showed that hyperventilation with hypocapnia led to strong stabilization of gamma oscillations in the rat hippocampus, probably due to increased effectiveness of GABA (gamma-amino butyric acid) inhibitory networks in the cortex. Gamma rhythms are necessary in sensory integration and higher cognitive function. Posse *et al* (1997) showed that hyperventilation quieted the frontal and parietoccipital cortex but not subcortical areas on functional MRI imaging. Voluntary hyperventilation does not decrease cerebral oxygen use in normal subjects (Van Rijen 1989). Lee *et al* (1999) studying the effects of CO<sub>2</sub> on excitatory transmission apparently caused by changes in intracellular pH in the rat hippocampal slice, concluded that the transient changes in the excitatory post synaptic potentials (EPSP) seen in response to changes in PCO<sub>2</sub> are mediated by in intracellular pH.

Dulla *et al* (2005) demonstrated that decreasing CO<sub>2</sub> levels reduced extracellular adenosine concentration and increased neuronal excitability via adenosine A<sub>1</sub> receptors, ATP receptors, and ecto-ATPase. They proposed that CO<sub>2</sub>-induced changes in neuronal function arise from a pH-dependent modulation of adenosine and ATP levels. These findings demonstrate a mechanism for the bidirectional effects of CO<sub>2</sub> on neuronal excitability in the forebrain.

Using EEG measures of activity from somatosensory and auditory cortex, Huttunen *et al* (1999) showed that voluntary hyperventilation suppressed long latency evoked responses from the cortex while early short latency responses were less reduced. They suggested that the increased cortical excitability caused by hyperventilation-induced hypocapnia led to spontaneous firing of cortical neurons. They also noted studies showing enhancement of excitatory glutamate synaptic transmission with concurrent suppression of GABA receptor-mediated postsynaptic inhibition. The underlying basis of this cortical excitability, particularly in the sensori-motor cortex, is probably due to thalamic activation. Using PET scans Prevett *et al* (1995) showed that hyperventilation increased blood flow to the thalamus in patients with generalized epilepsy in whom typical absence seizures were induced by voluntary hyperventilation. Marrosu *et al* (2000) showed that single-photon emission computed tomography (SPECT) measures of cerebral blood flow correlated with hyperventilation-enhanced interictal lateralized discharges in epileptic patients. They suggested that hyperventilation-induced slow activity on EEG is probably the result of synchronous activity in non-specific thalamocortical projecting systems, as Patel and Mulsby (1987) also suggest. However, in epileptics other mechanisms also affect transition from slow waves to spike-wave discharges. Acute cognitive effects of hyperventilation have been studied for many years. Hyperventilation is known to lead to alterations in physiological and cognitive functions (Jensen *et al* 2002). The physiological changes are thought to be a consequence of increased neuronal excitability resulting from the hypocapnia-induced alkalosis. A recent review by Van Diest *et al* (2000) showed that hyperventilation briefly decreases attention and cognitive function in a stroop-like task. Reviewing

studies of Pavlovian and operant control of emotion and cognition through modification of breathing behavior, Ley (1999) described the complex interrelationship between breathing and cognition and emotion.

A recent study by Sparing *et al* (2007), using transcranial magnetic stimulation, indicated that HV decreases intracortical inhibition (ICI) without changing intracortical facilitation. They suggested that low PCO<sub>2</sub> levels modulate, in particular the intrinsic neuronal circuits of ICI, which are largely mediated by neurons containing  $\gamma$ -aminobutyric acid (GABA).

## **2.6. Calcium “wave”**

Astrocytes exhibit a form of long distance signalling, communicating with each other by the propagation of calcium elevation, termed Ca<sup>2+</sup> waves (the propagation of Ca<sup>2+</sup> transients within an astrocyte population) (Schipke and Kettenmann 2004). The signalling mechanisms responsible for their propagation are the release of ATP by astrocytes and the gap junction connectivity (Charles and Giaume 2002). Astrocytes can respond to neurotransmitters released at the synapse by generating elevations in intracellular Ca<sup>2+</sup> concentration ([Ca<sup>2+</sup>]<sub>i</sub>) and releasing glutamate that signals back to neurons. This discovery opens new perspectives for the possible participation of these glial cells in actual information processing by the brain and raises the hypothesis that astrocyte activation by neuronal signals plays a key role in distinct, functional events. Depending on the level of neuronal activity, the [Ca<sup>2+</sup>]<sub>i</sub> response that is activated

by neurotransmitters can either remain restricted to an astrocytic process or can propagate as an intracellular  $[Ca^{2+}]_i$  wave to other astrocytic processes in contact with different neurones, astrocytes, microglia or endothelial cells of cerebral arterioles. These  $Ca^{2+}$  waves can spread hundreds of  $\mu m$  thereby activating hundreds of cells. Glutamate release triggered by the  $[Ca^{2+}]_i$  rise at the astrocytic process represents a feedback, short-distance signal that affects synaptic transmission locally. The release of glutamate as well as of other compounds far away from the site of initial activation represents a feedforward, long-distance signal that can be involved in the regulation of distinct processes. For instance, through the release of vasoactive molecules from the astrocytic processes in contact with cerebral arterioles, the neurone–astrocyte–endothelial cell signalling pathway can play a pivotal role in the neuronal control of vascular tone.

Kupferman *et al* (1997) proposed an analytic model for calculation of intracellular calcium wave propagated by calcium feedback at the inositol 1,4,5,-triphosphate ( $IP_3$ ) receptor. The dimensional combination of parameters that gives the scale of propagation speed of calcium waves as:

$$(J_{eff}D_{eff}/C_o)^{1/2} \quad \textbf{(Eq. 2.1)}$$

where  $J_{eff}$  is the effective free  $Ca^{2+}$  influx when the channels are activated,  $D_{eff}$  is the effective diffusion constant of calcium and  $C_o$  is a concentration scale that corresponds to the channel activation threshold. This combination has the form:

$$(D_{eff}/T_r)^{1/2} \quad (\text{Eq. 2.2})$$

Where  $T_r = C_o/J_{eff}$  reflects the time needed for calcium release to activate further release (after Luther's equation in Luther 1906, Jaffe 1991).

The propagation speed is strongly dependent on buffer concentration and buffer kinetics. The presence of fast buffers significantly slows down the wave, whereas the presence of slow buffers does not.

Filosa *et al* (2004) demonstrated calcium dynamics in cortical astrocytes and arterioles during neurovascular coupling, providing the first evidence that in a brain slice preparation, increased neuronal activity by electrical stimulation (ES) is rapidly signaled, within seconds, to cerebral arterioles and is associated with astrocytic  $\text{Ca}^{2+}$  waves. Smooth muscle cells in parenchymal arterioles exhibited  $\text{Ca}^{2+}$  and diameter oscillations ("vasomotion") that were rapidly suppressed by electrical stimulation. The neuronal-mediated  $\text{Ca}^{2+}$  rise in cortical astrocytes was dependent on intracellular (inositol trisphosphate [ $\text{IP}_3$ ]) and extracellular voltage-dependent  $\text{Ca}^{2+}$  channel sources. The  $\text{Na}^+$  channel blocker tetrodotoxin prevented the rise in astrocytic  $[\text{Ca}^{2+}]_i$  and the suppression of  $\text{Ca}^{2+}$  oscillations in parenchymal arterioles to ES, indicating that neuronal activity was necessary for both events. Activation of metabotropic glutamate receptors in astrocytes significantly decreased the frequency of  $\text{Ca}^{2+}$  oscillations in parenchymal arterioles. Filosa's study therefore supports the concept that astrocytic  $\text{Ca}^{2+}$  changes signal the cerebral microvasculature and that this communication occurs through the suppression of arteriolar  $[\text{Ca}^{2+}]_i$  oscillations and corresponding vasomotion.

Di Garbo *et al* (2007), starting from the experimental data on ATP evoked calcium responses in astrocytes, built a biophysical model describing these phenomena. The simulations showed, in agreement with the experimental findings, that the intracellular calcium fluxes mediated by the P2X and P2Y purinoreceptors are responsible for the biphasic ATP evoked calcium response in astrocytes. The modulation effects on the neural dynamics arising from the release of glutamate from astrocyte were also investigated. By using a minimal network model describing a neuron coupled to the astrocyte, they demonstrated that the calcium extrusion rate through the astrocyte membrane is critically involved in the generation of different firing patterns of the neuron.

## **2.7 Contribution of potassium currents and glia to slow potential shifts**

There is no precise, formal, defined boundary between slow EEG waves and sustained potential shifts (SPS). SPS can describe shifts of voltage that last a second or more but do not exceed a few minutes, and in most cases do not repeat or oscillate (Somjen 1973). Measurement of SPS requires DC coupled amplification. The SPS was first described over a century ago. Laming *et al* (1998) defined them thus: “*SPSs are long standing changes in the DC recorded potential of a region of nervous tissue . . . [They] occur in the brains of all vertebrates thus far studied in response to trains of electrical impulses applied . . . or to sensory stimuli.*”



There is growing evidence for the hypothesis that glia cells contribute to the generation of slow shifts in local field potential records and in the EEG. Glia cells are often spatially extended and electrically coupled. They sense rises in  $[K^+]_e$ . Changes in  $[K^+]_e$  are associated with most conditions where slow potential shifts are recorded. Local accumulation of  $K^+$  leads to depolarisation of glial cells, which spreads along the glial syncytium. As a result the local depolarisation in glial membrane potential is smaller than expected from the change in  $[K^+]_e$  and a driving force for  $K^+$  uptake develops while at remote sites  $K^+$  is released from glia. The potassium inward currents into glia are associated with generation of slow negative field potentials, while at remote sites the  $K^+$  outflux leads to generation of positive field potentials (Heinemann and Walz 1998).

The generation of slow potentials by glutamate is not observed when glutamate is injected into gliotic tissue devoid of neurons (Alici *et al* 1996). Therefore it is likely that neurons also contribute to the generation of slow potentials.

In order for glial cells to supply the current for the slow potential shifts, the following four criteria must be met:

- when neuronal elements are active, neighbouring glial cells must always be depolarised
- a large enough population of glial cells has to undergo that depolarisation at the same time
- there has to be electronic continuity of spatially extended glial cells and/or the glial syncytium from the active to the inactive region.

- the length constant of the glial syncytium has to be compatible with the spread of current.

In general, astrocytes have about a 20 mV more negative membrane resting potential than neighbouring neurons (Muller and Somjen 2000). This is mainly due to the relatively reduced  $\text{Na}^+$  permeability of astrocytes compared to neurons. This is also the reason why astrocytes are more sensitive to increases in extracellular  $\text{K}^+$  than neurons. They react with larger depolarisation amplitudes to these extracellular  $\text{K}^+$  increases. Substances other than  $\text{K}^+$  released from active neurons, could also contribute to glial membrane potential changes. *In situ*, all of these substances, kainite (glutamate), GABA, and dopamine cause a depolarisation in the glial cells (Walz 1989, Walz and MacVicar 1988, MacVicar 1989, Jabs, Paterson and Walz 1997). The depolarisation response is mediated by three contributing factors, changes in the extracellular microenvironment, modulation of ion channel conductances and electrogenic uptake. Astrocytes *in situ* sense increases in extracellular  $\text{K}^+$  concentration. During seizure-like events, the glial depolarisations are up to 35 mV, which corresponds to the 10-12 mM ceiling level (Heinemann and Lux 1977). This ceiling level is only increased during spreading depression waves in hypoxia or ischaemia. Under these conditions glia can depolarise very strongly to levels a few mV below zero potential.

The “length constant” of the glial syncytium is the distance along a process to the site where a voltage amplitude has decayed to 37% of its value due to leakage of current across the cell membrane. Low specific membrane resistance

will decrease the length constant and, as a result, the distance a significant amount of current can travel in the glial syncytium. Astrocytes have a relatively low membrane resistance. The issue of a restricted length constant is the major difficulty in examining the glial contribution to slow extracellular potentials (Somjen 1973). The available estimates of the glial length constant suggest that the  $K^+$  depolarisation induced in the glial network at regions that experience elevated extracellular  $K^+$  concentrations does not spread over more than 100  $\mu m$ .

## **2.8 The concept of a spatial buffering function**

In a glial syncytium in which extracellular  $K^+$  is increased in one region the membrane of neighbouring cells has a tendency to iso-potential. Therefore the region experiencing an increased extracellular  $K^+$  current will have a more positive  $K^+$  equilibrium potential than the membrane potential. This leads to an inward driving force for  $K^+$  and since the membrane is highly permeable to  $K^+$  it will enter the cell via a passive current. It is necessary for this current loop to be closed, and the  $K^+$  current will be distributed to the other parts of the syncytium via the gap junctions. In regions further removed from the high  $K^+$  region, the  $K^+$  equilibrium potential is more negative than the membrane potential and therefore there is a driving force for  $K^+$  to flow out of the cell. Thus the current into the cells (at high  $K^+$  regions), inside the syncytium and out of the cells (at regions distance from the high  $K^+$  locations), is almost completely carried by  $K^+$ . The loop is closed by a return current in the ECS. This current is carried mainly

by  $\text{Na}^+$  and  $\text{Cl}^-$  which constitute the bulk of extracellular ions (Heinemann and Lux 1977).

### **2.8.1 $\text{K}^+$ Siphoning in the retina, spatial buffer function: a model for the neocortex?**

The retina is the part of the CNS what is best characterised in terms of spatial buffering due to its easy accessibility and well-layered structure. The major glial element of the retina stretches through all layers starting at the photoreceptors and ending with endfeet at the inner limiting membrane adjacent to the vitreous humour. The inner and outer plexiform layers are the areas of light induced  $\text{K}^+$  increases. This is where  $\text{K}^+$  ions have to enter the muller cells generating a current sink. The endfoot  $\text{K}^+$  channel is tenfold greater than in the other regions (Newman 1986). The endfeet border at a large liquid reservoir, and  $\text{K}^+$  released will quickly diffuse keeping the extracellular  $\text{K}^+$  concentration close to normal. If during light stimulation the plexiform layers accumulated high  $\text{K}^+$  and the muller cell parts in these regions are depolarised, there is a driving force for  $\text{K}^+$  currents to flow into the cell in these areas and towards the hyperpolarized end feet when  $\text{K}^+$  is released. The return current will be carried by  $\text{Na}^+$  and  $\text{Cl}^-$  ions (Newman 1995). This pattern is associated with negative extracellular potentials in the plexiform layers and a large positive potential at the end feet/vitreous humour interface. This is the electroretinogram (ERG) B-wave. Since this mechanism is based on anatomically fixed loops due to the increased endfeet  $\text{K}^+$  channel density, it is also called  $\text{K}^+$  siphoning (Newman 1995). Whether such

siphoning and special endfeet specialisation also applies to astrocytes in the cerebral cortex and other brain structures is still a matter of speculation, but current evidence suggests that spatial buffering and generation of slow field potential does occur in the neocortex (Heinemann and Walz 1998).

### **2.8.2 Synopsis of current knowledge on astrocytes**

The brain is critically dependent on oxygen and glucose supply for normal functioning. Various neurovascular control mechanisms assure that the blood supply of the brain is adequate to meet the energy needs of its components. Emerging evidence shows that neuronal activity can control microcirculation using astrocytes as a mediator.

Astrocytes sense neuronal activity and are involved in signal transmission. Synaptic activity triggers an increase in the intracellular calcium concentration ( $\text{Ca}^{2+}$ )<sub>i</sub> of adjacent astrocytes, stimulating the release of adenosine triphosphate (ATP) and glutamate. The released ATP mediates the propagation of  $\text{Ca}^{2+}$  waves between neighbouring astrocytes, thereby recruiting them to mediate adequate cerebrovascular response to neuronal activation. Simultaneously, sodium dependent glutamate uptake in astrocytes generates  $\text{Na}^+$  waves and subsequently increases glucose uptake and metabolism that leads to the formation of lactate which is then delivered to neurons as an energy substrate. Further, astrocytic  $\text{Ca}^{2+}$  elevations can lead to secretion of vasodilatory substances for perivascular endfeet, such as epoxyeicosatrienoic acid (EETs), adenosine, nitric oxide (NO) and cyclooxygenase-2 (COX-2) metabolites, resulting in increased local blood

flow. Thus by releasing vasoactive molecules astrocytes mediate the neuron-astrocyte-endothelia signalling pathway and play a profound role in coupling blood flow to neuronal activity (Jakovcevic and Harder 2007).

## **2.9 Can epilepsy contribute to our understanding of the underlying physiological mechanisms of the EEG hyperventilation response?**

Idiopathic epilepsies are genetically determined diseases of the central nervous system characterized by typical epileptic seizures and EEG abnormalities but not associated with structural brain lesions. Sleep profoundly influences the sensitivity of the EEG for detecting focal spike wave (FSW) epileptiform discharges (Kellaway 1985, Nobili *et al* 1999). Sleep doubles the detections of FSW in the EEG (Gibb and Gibbs 1942, Blom and Heijel 1975, Degen and Degen 1992) and increases the discharge rate by one or two orders of magnitude (Kellaway 2000).

Generalized nonconvulsive absence seizures are characterized by the occurrence of bilateral, synchronous spike-and-wave discharges (SWDs) on electroencephalographic recordings, concomitant with behavioral arrest. Childhood absence epilepsy (CAE) is a complex polygenic disorder. There is an association between mutations in *CACNA1H* and CAE. These mutations cause increased channel activity and associated increased neuronal excitability. Seizures are believed to originate in the thalamus, where there is an abundance of T-type calcium channels such as those encoded by *CACNA1H*.

Many of the CACNA1H mutations have a measurable effect on channel kinetics, including activation time constant and voltage dependence, deactivation time constant and inactivation time constant and voltage dependence. Many of these mutations should lead to neuronal excitability, though others may lead to hypoexcitability. The full impact of ion channel dysfunction in the idiopathic generalized epilepsies, including absence epilepsy, is however incompletely understood.

The strain of genetic absence epilepsy rats from Strasbourg (GAERS) is an isomorphic, predictive and homologous model of human generalized idiopathic absence epilepsy. The clinical seizures consisting of behavioral arrest with twitching of facial muscles and occurring in all animals have a polygenic origin (Rudolf *et al* 2004). Behavioral expression of seizures is associated with bilateral synchronous spike wave discharges (SWDs) that resemble those of typical absence seizures. Spontaneous absence seizures originating in the cortex and thalamus appear in this strain after the age of 1 month and their frequency is stabilized by 3 to 4 months (Danover *et al* 1998, Meeren *et al* 2005).

Disturbances in GABAergic and glutamatergic neurotransmission in the thalamocortical loop are involved in absence seizures. Pharmacological data propose that both excitatory and inhibitory neurotransmission are involved in triggering and maintaining absence seizures (Danover *et al* 1998).

More recent data are in favor of the existence of a specific balance between excitation and inhibition in the brain of GAERS that would favor the occurrence of absence seizures. This subtle imbalance could reflect some dysregulation in glutamate metabolism in the cortex of GAERS (Dufour *et al* 2001). GAERS display an increase in cerebral glucose utilization throughout the whole brain compared with non epileptic rats (NER) (Nehlig *et al* 1991), paralleled by elevated activities of enzymes coupled to glycolysis, oxidative phosphorylation, and glutamate metabolism (Dutuit *et al* 2000, Dufour *et al* 2003). Furthermore, the expression of the astrocyte-specific glial fibrillary acidic protein (GFAP) is increased in the cortex and thalamus (Dutuit *et al* 2000). Thus, astrocytes may be involved in the regulation of neuronal processes underlying the occurrence of epileptic seizures in this strain.

Amzica and Steriade (2001), studying neuronal and glial membrane potentials during sleep and paroxysmal oscillation in the neocortex of cats, found that slow oscillations in the cortex often evolved into spike wave paroxysms, mimicking sleep-triggered seizures. This transition was associated with increased coupling between the depolarizing events in neurons and glial cells. During seizures, the glial membrane potential displayed phasic negative events related to the onset of the paroxysmal depolarizing shifts in neurons. They proposed a field effect crossing neuron/glial membranes as a function of the state of the cortical network.

Tian *et al* (2005) suggested an astrocytic basis of epilepsy. They attempted to define the cellular basis of hyper synchronous bursting activity in a study of the



occurrence of paroxysmal depolarizing shifts after suppressing synaptic activity. Hypersynchronous neuronal firing is a hallmark of epilepsy. The mechanisms underlying simultaneous activation of multiple neurons remain unknown. Epileptic discharges are in part initiated by a local depolarization shift that drives groups of neurons into synchronous bursting. Two photon imaging of live exposed cortex showed that several anti-epileptic agents, including Valproate, gabapentin and phenytoin reduced the ability of astrocytes to transmit  $\text{Ca}^{2+}$  signalling, indicating a key role for astrocytes in seizure activity.

Recent results (Melo *et al* 2006) from an  $^{13}\text{C}$ - NMR spectroscopy study support the idea that increased cycling of glutamate and glutamine between astrocytes and glutamatergic neurons combined with decreased GABAergic function in the cortex of GAERS may be the underlying cause of absence seizures. These changes are accompanied by enhanced glycolysis and mitochondrial function. They suggest “*this may lead to impaired thalamic filter function*” and that the occurrence of SWD in the thalamocortical loop may be facilitated by reduced sensory input to the cortex.

Childhood absence epilepsy (CAE) may provide an example of the astrocytic etiology of epilepsy. CAE seizures can often be provoked by hyperventilation (for example, by having a child blow repeatedly on a windmill). After several minutes of hyperventilating the pH of the child's blood becomes slightly alkaline as a consequence of the respiratory depletion of carbon dioxide. With this shift toward the alkaline, the CAE seizure begins as evidenced by a characteristic

three-per-second spike-wave pattern on the electroencephalogram. In addition to their many other roles, astrocytes near the capillaries of the cerebral cortex envelop these blood vessels with their cytoplasmic extensions. The exposure of these perivascular astrocytes, which also control synaptic domains of influence, to the sudden alkaline shift in the blood may result in primary perivascular calcium wave activation and secondary perivascular synaptic synchrony. Indeed, the three-per-second spike-wave pattern seen on the electroencephalogram may reflect the synaptic (spike) and astrocytic (wave) oscillations the theory proposes, with unusually high frequency calcium waves resulting from the effects of alkalosis combined with secondarily coordinated neurotransmitter release. Of additional interest is the demonstration that many of the medications used in the treatment of epilepsy are astrocytic calcium wave inhibitors (White 1992, Nilson *et al* 1992).

## **2.10 Discussion**

In principle, every event associated with membrane potential changes of individual cells (neurons and glia) should contribute to the perpetual voltage variability of the extracellular space. Until recently, synaptic activity was viewed as the exclusive source of extracellular current flow or EEG potential. Progress during the 1990s revealed numerous sources of relatively slow membrane potential fluctuations, not directly associated with synaptic activity. Such non-synaptic events may also contribute significantly to the generation of local field potentials (Buzaki *et al* 2003).

The idea that networks of neurons may display patterns of activity that go beyond the sum of each component has been around for about a century since original anatomical studies suggested that the brain constitutes a 'functional syncytium'. Increases in our understanding of the heterogeneity of neuronal subtypes, their intrinsic electrical properties, the immense diversity of interneuronal communication via synapses, and recent developments in understanding of the "tripartite synapse" have led to the generation of a working hypothesis for network function which is critically dependent on the complex interplay between these phenomena.

Evidence for astrocytic participation of neuronal signal processing has accumulated in recent years. In particular, large and long-lasting cytosolic calcium surges in astrocytes, which may result in neurotransmitter release from the astrocytes, have been described in *in vivo* preparations. While the mechanisms for astrocytic calcium events have been extensively studied *in vivo*, their existence and functions in the intact brain (i.e. the *in vivo* condition) have just started to be addressed. Astrocytes are intricately linked in the regulation of synaptic strength and plasticity and provide a pathway for synaptic cross-talk. Impairment of glutamate uptake by the astrocyte in the setting of ATP depletion, as occurs with hypoxia ischaemia or hypoglycaemia, is considered a primary mechanism of excessive accumulation of glutamate in the synaptic space, leading to neuronal injury.

The functional architecture of the brain depends on an intimate neuron-glia partnership. The cortical activity reflected in the EEG results from complex interactions within networks of neurons and glial cells. The dialogue signals

consist of neurotransmitters and various ions, which cross through the extracellular space (Amzica 2002). The normal function of the central nervous system depends on adequate maintenance of the neuronal microenvironment. Complex bi-directional neuron-astrocyte interactions affect energy metabolism, excitability and transmission of signals within and between the neuronal and astrocytic network. The excitatory signals in the brain are transmitted through two parallel and interactive networks, neuronal and astrocytic. This involves synaptically released glutamate, intracellular  $\text{Ca}^{2+}$  waves, and paracrine interactions mediated by glutamate, ATP, Cyclic ADP-ribose, and probably other signals.

During hypoxia, ischaemia or hypoglycaemia there is impairment of glutamate uptake by the astrocyte associated with ATP depletion. Hypoglycaemia is one of the factors governing the extent of the expected EEG HV slow wave response, along with age, effort and posture. The HV response is exaggerated and immediate in a hypoglycaemic patient. This may be considered as “Proof of Principle” for the involvement of astrocytes in the generation of the EEG hyperventilation response. Implicating glial cells as hypoglycaemic sensors is consistent with the observation that glial cell toxins prevent activation of neurons by glucoprivic agents both in the NTS and the hypothalamus (Young *et al* 2000). Other recent observations support the role of glial cell glucose metabolism, probably via glial autonomic outflow, in controlling important systemic processes. Metabolism of glucose to lactate in astrocytes is required to activate neuronal ATP-sensitive  $\text{K}^+$  channels (*via* pyruvate formation) and ultimately mediate the suppressive effects of glucose on hepatic glucose

production (Lam *et al* 2005). This is in line with the concept of an astrocyte-neuron lactate shuttle (Pellerin *et al* 1998), in which metabolism of glucose by astrocytes generates extracellular lactate that serves as substrate for neuronal pyruvate synthesis.

Emerging evidence shows that neuronal activity can control microcirculation using astrocytes as a mediator. By releasing vasoactive molecules astrocytes mediate the neuron-astrocyte-endothelial signalling pathway and play a profound role in coupling blood flow to neuronal activity. Astrocytes enwrap blood vessels with their endfeet and are therefore in the strategic position to convey signals from neurons to the blood system. Zonta (2003) has provided evidence for the functional coupling of neuronal activity, astrocyte  $\text{Ca}^{2+}$  signalling and vessel diameter. In rat cortical slices the dilation of arterioles triggered by neuronal activity is dependent on  $[\text{Ca}^{2+}]_i$  oscillations in astrocytes. Glia can integrate neuronal inputs and modulate synaptic activity. Astrocytes act as sensors of synaptic activity and then send signals to blood vessels about its intensity. Seigneur *et al* (2006) proposed that the glial response to cholinergic activation results from the balance between the direct hyperpolarizing action of acetylcholine and the depolarising modulation of glutamate from the neighboring neurons, in addition to the modulation of the interglial communication pathway and/or the ionic traffic across blood vessels.

Glutamate uptake by astrocytes is fundamentally important in the regulation of the CNS function. Disruption in uptake can lead to excitotoxicity as a consequence of hypoxic/ischaemic events (Dallas 2007). Glutamate homeostasis is pivotal to prevent neuronal death after hypoxic/ischaemic events. The

regulation of glutamate homeostasis by astrocytes is key to normal synaptic transmission and co-ordination of neural networks (Fellin 2006). The EEG activation procedure disturbs the homeostatic balance of the neural/glia/vascular network triad. Astrocytes play a pivotal role in meeting the energy requirements of active neurons. Astrocytes appear to function as a network to ensure coordinated metabolic and vascular responses to neuronal activity. The precise link between neural activity, metabolism, and blood flow continues to be an area of active ongoing research.

What has become increasingly apparent is that interactions within populations of GABAergic interneurons, and between these neurones and glial cells, can provide mechanisms which may underlie some classical EEG rhythms (theta, beta and gamma frequency activity in particular). The transmembrane currents of both types of cells summate in the interstitial space.

Locally projecting GABAergic interneurons are the major providers of inhibition in the neocortex and play a crucial role in several brain functions. Neocortical interneurons are connected via electrical and chemical synapses that may be crucial in modulating complex network oscillations. The particular properties of GABAergic input on different interneuronal subtypes might have important consequences for generation and pacing of cortical rhythms underlying several brain functions. Whatever interneurone sub-type may be shown to be involved in network behaviour, it is the influence of the output from these cells that critically shapes population activity. Kai Kaila (1994) showed that this GABAergic synaptic activity is profoundly modified during brain development. The activity of two factors, the  $K^+-Cl^-$  cotransporter (KCC2) and neuronal

carbonic anhydrase (CA VII) critically control the expression of GABAergic postsynaptic events as either depolarizing, during early development, or hyperpolarizing, in the mature brain (Riviera *et al* 2005). Patterns of synaptic connectivity, intrinsic cell properties and gap-junctional communication have been shown to combine to provide the rich temporal framework of activity typical of thalamocortical function *in vivo* (Traub *et al* 2005).

Amzica (2001) and Amzica and Steriade (2002) collected data from intracellular recordings from pairs of neurons and glia in the cortex of cats. They proposed that the genesis of field potentials results from complex interactions between neurons and glia and that the state of the cortical networks modulates this interaction. During the slow oscillation, which dominates the electric activity of the cortex during quiet sleep, the extracellular milieu undergoes the influence of neuronal and glial potentials. The behavior of glial cells suggested that they are not idle followers of neuronal activity. They postulate that through their uptake mechanisms, glia cells modulate the neuronal excitability and contribute to the pacing of slow oscillations. Electrical stimuli applied to the cortex elicited responses consisting of a biphasic depolarisation in glial cells, which was associated with an EPSP-IPSP sequence in neurons. The transmembrane currents of both types of cells summate in the interstitial space. Paroxysmal oscillations induce glial swelling and the reduction of the extracellular space. Field effects across the touching membranes may be superimposed on the intracellular activities. Large neuronal potentials are expected to be reflected reversed in glia. A reciprocal action would also be justified; however, the slower time course of intragial events makes them less likely to be recognized within

intraneuronal potentials, where they might be included in the neuronal phasic events. A more quantitative study is required to establish the dynamic weights of each type of potential in the resulting EEG.

Dietmer (2001) suggests strategies for metabolic exchange between glial cells and neurons. A hypothesis is postulated which couples the transfer of energy and the conversion of CO<sub>2</sub> with the high-affinity glutamate uptake and other transport processes at glial and neuronal cell membranes. The transporters can be linked to glial signalling and may cooperate with each other at the cellular level. This could save energy, and would render energy exchange processes between glial cells and neurons more effective.

In the cortex of the strain of genetic absence epilepsy rats from Strasbourg (GAERS), increased glutamate-glutamine metabolism in neurons and astrocytes will lead to enhanced glutamergic output to the thalamus. This dysregulation leads to impaired thalamic filter function and hence reduced sensory input to cortex allowing the occurrence of spike wave discharges in the thalamocortical loop (Dufour *et al* 2001).

Hyperventilation has been used for decades to induce clinical absence attacks. Disturbances in GABAergic and glutamateric neurotransmission in the thalamocortical loop are involved in absence seizures. Does a “dysregulation” of metabolism which is triggered by a “hypocapnia cascade event” in patients with CAE lead to a clinical absence? Seizures are believed to originate in the thalamus, where there is an abundance of T-type calcium channels such as those



encoded by CACNA1H. However perhaps the propagation of astrocyte calcium wave in the glial syncytium is downregulated or suppressed contributing to the clinical absence events.

CO<sub>2</sub>-induced alteration in pH causes closure of the ATP-sensitive potassium channels due to hypocapnia-induced alkalosis (Nakahata *et al* 2003). pH shifts and brief pH transients may contribute to shape neuronal performance, and hence behaviour, at molecular and cellular levels. pH has a powerful modulatory action of GABAergic mechanisms (Kaila, 1994), which suggests a tight link between respiration-mediated regulation of pH/pCO<sub>2</sub> and neuronal functions at the whole-organism level. pH is a powerful physiological modulator of neuronal activity, and this has led to the hypothesis that H<sup>+</sup> ions have an important signalling function in brain tissue (Kaila and Ransom, 1998).

Observable BOLD–contrast fMRI signal changes in grey matter were shown to decrease approximately 30% more in subjects with intermittent rhythmic delta activity (IRDA) than in controls during the first 2 minutes of an EEG hyperventilation study by Makiranta (2004). The hyperventilation-induced physiological changes are thought to be a consequence of increased neuronal excitability and alteration of synaptic transmission resulting from the hypocapnia-induced alkalosis. This wave of cortical excitation could participate in mechanisms of a spreading paroxysmal depolarization shift leading to EEG slow wave build up when homeostasis of the neuronal-astrocyte–endothelial cells is dysregulated by brainstem/thalamic mediated constriction of cerebral vasculature by hypocapnia during the EEG hyperventilation exercise.

Posse *et al* (1997), using fMRI, demonstrated quiescence of the frontal and parietoccipital cortex, but not subcortical areas, during HV. They found no decrease in cerebral oxygen use during HV in normal subjects. Using transcranial magnetic stimulation (TMS) HV decreases intracortical inhibition (ICI) without changing intracortical facilitation were demonstrated by Sparing *et al* (2007), which suggests that low pCO<sub>2</sub> levels modulate in particular the intrinsic neuronal circuits of ICI, which are largely mediated by neurons containing GABA.

Kasischke *et al* (2004) showed that energy metabolism is compartmentalised between astrocytes and neurons especially during increased neuronal activity. Schurr *et al* (1999) concluded that lactate is a crucial aerobic energy substrate that enables neurons to endure activation. The work of Seigneur *et al* (2006) and Di Garbo *et al* (2007) supports neuron astrocyte coupling in the generation of neuronal firing patterns

The EEG activation procedure disturbs the homeostatic balance of the neural/glial/vascular network triad. Emerging evidence shows that neuronal activity can control microcirculation using astrocytes as a mediator. Patterns of synaptic connectivity, intrinsic cell properties and gap-junctional communication have been shown to combine to provide the rich temporal framework of activity typical of thalamocortical function *in vivo* (Traub *et al* 2005). Interactions within populations of GABAergic interneurons, and between these neurones and glial

cells can provide mechanisms which may underlie some classical EEG rhythms (theta, beta and gamma frequency activity in particular).

Winship *et al* (2007) demonstrated that rapid astrocyte calcium signals correlate with neuronal activity and onset of the hemodynamic response *in vivo*. Their data demonstrate that sensory-driven astrocyte  $\text{Ca}^{2+}$  oscillations, which have been proposed to modulate microvascular tone (Zonta *et al* 2003, Mulligan and MacVicar 2004, Takano *et al* 2006) can occur at short latencies necessary to facilitate hyperemia to the active cortex. These *in vivo* findings suggest that astrocytes can respond to sensory activity in a selective manner and process information on a subsecond time scale, enabling them to potentially form an active partnership with neurons for rapid regulation of microvascular tone and neuron-astrocyte network properties.

### **2.10.1 A novel hypothesis: the ‘hypocapnia cascade’ as the basis of the neurophysiological EEG response to spontaneous hyperventilation**

Fig 2.16 outlines in the form of a flow chart a novel hypothesis for a ‘hypocapnia cascade’ sequence which is supported by current research as a mechanism to explain the EEG slow wave changes noted during spontaneous EEG hyperventilation.

Once HV is initiated there is activation of both the sympathetic and parasympathetic ANS. The rostral ventrolateral medulla modulates cardioaccelerators and vasoconstrictors. There is an increase in heart rate and in blood pressure. Simultaneously the caudal ventrolateral medulla increases cardiac vagal tone to control the increased heart rate and BP. There is decreased activity in mesial reticular formation (MTR) + reticular activating system (RAS). Concurrent stimulation occurs to vagal afferents to the thalamus via nucleus tractus solitarius (NTS) + non-specific thalamic projection systems (NSTPS). Parallel to the activation in the brainstem ventrolateral medulla, hypocapnia is induced by the action of spontaneous HV. Hypocapnia leads to marked vasoconstriction, rapid reduction in cerebral blood flow and increased perivascular and intraneuronal pH. There is a shift in oxidation/reduction state of CNS. The conductivity of gap junctions in astrocytes increases. Astrocytic calcium waves signal the cerebral microvasculature, leading to increased cortical excitability and increased glucose consumption, a small increase in oxygen consumption and an increase in lactate/pyruvate production. There is closure of the ATP-sensitive K<sup>+</sup> channels due to hypocapnia induced alkalosis. The rate of

glutamate cycling is linked to the production of vasoactive elements. Neurovascular coupling is mediated by neuronal signalling mechanisms via glial endothelial pathways. The regulation of glutamate homeostasis in astrocytes is key to synaptic transmission and co-ordination at a neural network level. There is an increase in the oxygen extraction fraction of between 10-30% as HV continues. Early oxidative metabolism in neurons is sustained approximately 10 seconds later by astrocytic non-oxidative glycolysis via the astrocyte neuron lactate shuttle. There is now enhanced cortical excitability in widely distributed networks and a disturbance of homeostasis in neuron/interneuron/glial/vascular networks producing a decrease in intracortical inhibition without affecting cortical facilitation. Glial slow potential shifts, activity in neo-cortical interneurons coupled with GABAergic connections and ongoing synchronous activity from the NSTPS produces rhythmogenesis and the appearance of slow theta and delta activity is noted in the EEG.

## Hypothesis: Neurophysiology basis of HV EEG response

### **Hypocapnia Cascade**

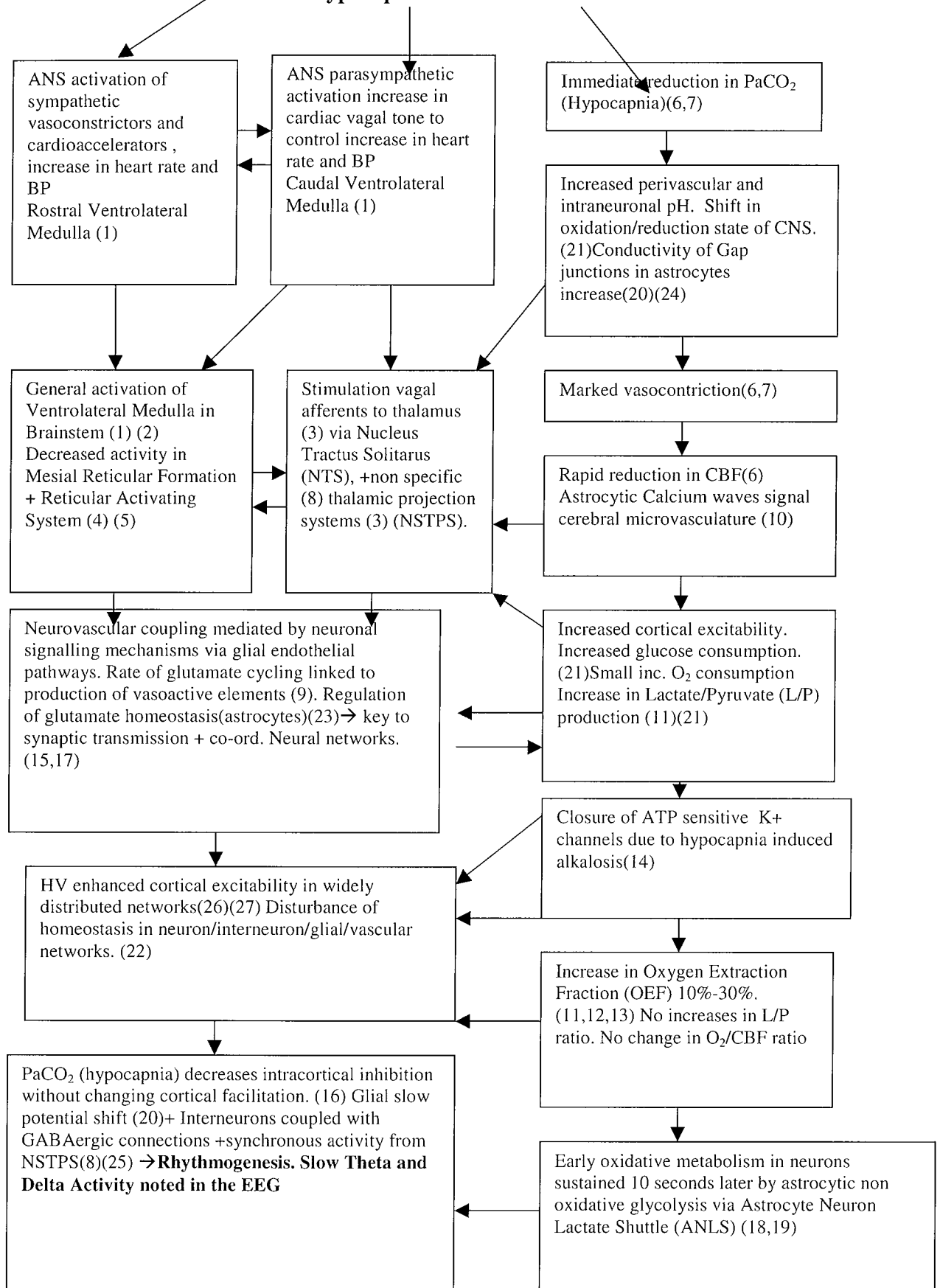


**Fig 2.16 Flow chart “hypocapnia cascade”:** hypothesis for a “hypocapnia cascade” sequence, which is supported by current research, to explain the EEG slow wave changes noted during a hyperventilation activation procedure.

NOTE: The numbered references in brackets, relate to the supporting literature

- (1) Julu *et al* (1997, 2005): Autonomic responses suggest that both rostral and caudal ventrolateral medulla are simultaneously activated during the Hyperventilation initiation process
- (2) Diehl *et al* (1998): close correlations existed between autoregulation and CO<sub>2</sub> induced vasomotor reactivity
- (3) Henry and Votaw (2006), Kanner (2008): 2 PET studies on Vagal Nerve Stimulation (VNS) showed thalamic activation
- (4) Patel and Maulsby (1987): Hypocapnia induced by hyperventilation decreased activity in mesencephalic reticular formation.
- (5) Bonvallet and Dell (1956): demonstrated that hypocapnia causes cortical depression by a direct effect on the mesencephalic reticular formation.
- (6) Gardner (1996): The degree of circulatory loss in the cerebral cortex is around 2% for each 1 mmHg drop in CO<sub>2</sub> pressure
- (7) Raichle and Plum (1972): A drop in CO<sub>2</sub> (hypocapnia), stimulates vasoconstriction by “*the most potent vasoconstrictive agent known*”
- (8) Marrosu *et al* (2000): SPECT study → slow activity on EEG is probably the result of synchronous activity in non specific thalamocortical projection systems
- (9) Raichle and Mintun (2006): A cascade of chemical events within the astrocyte may link rate of glutamate recycling to production of vasoactive chemical agents
- (10) Winship *et al* (2007): Rapid astrocyte calcium signals correlate with neuronal activity and onset of the haemodynamic response *in vivo*
- (11) Hutchinson *et al* (2002): HV significantly increases the OEF but does not increase the LP ratio. Compatible with ANLSH
- (12) Posse *et al* (1997): BOLD fMRI signal showed >10% reduction within 20 seconds of starting HV.

- (13) Makiranta *et al* (2004): BOLD fMRI signal changes in grey matter by 30% in subjects with IRDA on EEG
- (14) Nakahata *et al* (2003): CO<sub>2</sub> induced alteration of pH, induces closure of ATP-sensitive potassium channels
- (15) Amzica (2002), Amzica and Steriade (2001): Glial cells contribute to genesis of slow potential shifts. Field potentials result from complex interactions between neurons and glia. The state of the cortical networks modulates the interactions
- (16) Sparing *et al* (2007): HV increases intra cortical inhibition without changing intra cortical facilitation
- (17) Benarroch (2005): interactions between neurons and astrocytes are critical for signalling. Astrocytes participate in detection, propagation and modulation of excitatory synaptic signals, provide metabolic support to the active neurons and contribute to functional hyperemia in active brain tissue
- (18) Kasischke *et al* (2004): Energy metabolism is compartmentalised between astrocytes and neurons especially during increased neuronal activity
- (19) Pellerin and Magistretti (1994, 2004): ANLSH revised: Neuronal oxidative and then astrocyte non oxidative glycolysis
- (20) Zonta *et al* (2003): Astrocytes are intricately linked in the regulation of synaptic strength and provide a pathway for synaptic cross talk
- (21) Posse *et al* (1997): physiological effect of HV is to reduce arterial PaCO<sub>2</sub>, which increases perivascular and intra neuronal pH. Increased neuronal pH produces a shift in the oxidation/reduction state of central nervous system (CNS) tissue, increases neuronal discharge of both motor and sensory fibres and increases glucose consumption and lactate and pyruvate production.
- (22) Jensen *et al* (2002): HV enhances cortical excitability in widely distributed networks, and is known to lead to alterations in physiological and cognitive functions. Physiological changes are thought to be a consequence of increased neuronal/interneuron/glia/ endothelium excitability resulting from the hypocapnia induced alkalosis
- (23) Newman (2003), Hertz and Zeilke (2004): Glutamate binding triggers complex bi-directional neuron-astrocyte interactions that affect energy metabolism, excitability and transmission of signals within and between neuronal and astrocytic networks



- (24) Traub and Bibbig (2000), Spray (1981): conductivity of gap junctions increases with intracellular pH. It is possible that respiratory alkalosis could affect the gap junctions and thus the properties of the interneuronal network.
- (25) Palva *et al* (2000): experimental work suggests that networks of interneurons coupled with GABAergic connections are responsible for rhymogenesis and neuronal synchronizatio
- (26) Tomita-Gotoh and Hayashida (1996): recorded direct shifts in electrical potential from scalp electrodes when they induced hypocapnia and hypercapnia in human subjects. Hyperventilation increased cortical excitability with hypocapnia (decreased CO<sub>2</sub>). Kukumberg *et al* (1996) found increased cortical excitability in ten human subjects, noting changes of motor evoked potential amplitudes following magnetic stimulation after hyperventilation. Seyal *et al* (1998) showed widespread increased excitability as measured by motor evoked potentials with hyperventilation in six human subjects. Hyperventilation also increases the excitability of skin and motor nerves. In experimental animals, hyperventilation increases excitability of hippocampal neurons. The hippocampus is responsible for attention and orientation. Carbon *et al* (2000) have shown that fifteen minutes of hyperventilation increased sensorimotor cortex excitability measured by direct current magnetoencephalography
- (27) Dulla *et al* (2005): demonstrated that decreasing CO<sub>2</sub> levels reduced extracellular adenosine concentration and increased neuronal excitability via adenosine A<sub>1</sub> receptors, ATP receptors, and ecto-ATPase. They proposed that CO<sub>2</sub>-induced changes in neuronal function arise from a pH-dependent modulation of adenosine and ATP levels. These findings demonstrate a mechanism for the bidirectional effects of CO<sub>2</sub> on neuronal excitability in the forebrain.

## 2.11 Conclusions

In reviewing the vast body of literature pertaining to this subject different versions of the phrase “the mechanisms by which hyperventilation elicits slow wave activity in the EEG are not fully understood/are unclear/remains conjectural” etc. are frequently encountered. To this reviewer neuron-astrocyte interactions appear to be critical to understanding the mechanisms of the production of the build up of EEG slow wave activity during hyperventilation. A review of current literature indicates that voluntary hyperventilation elicits a “hypocapnia cascade” inducing vasoconstriction, and alterations in the pH of the cellular environment, which is mediated by mechanisms in the brainstem and thalamus. While an increase in the oxygen extraction fraction has been demonstrated during HV, there is no clear evidence of cerebral ischaemia/hypoxic changes related directly to the procedure. There is clear evidence that astrocytes, by releasing vasoactive molecules, mediate the neuron-astrocyte-endothelial signalling pathway and play a profound role in coupling blood flow to neuronal activity. Electrophysiological changes are hypothesized to be a consequence of increased neuronal-astrocytic-endothelial excitability and alteration of synaptic transmission at the neural network level. Neocortical interneurons appear to be crucial in modulating complex network oscillations and critically shaping population activity. The ANLSH may be a factor in the EEG “build up” phenomenon of slow theta and delta waves during hyperventilation activation and cortical excitation. The EEG is a sensitive method for real time temporal assessment of the functional state of the cortical neuron-glia networks during voluntary hyperventilation induced homeostatic

disturbances in baseline neurometabolic and neurovascular coupling the in the CNS.

Glial cells have not thus far gained centre-stage attention. The predominant investigative technology for most of the last century, electrophysiology, allowed the study of electrically excitable (to action potential) membranes but not of other forms of excitability. The recently developed technologies of live cell imaging and light excitation promise to reveal the detail of the astrocytic “excitable cytoplasm”. This work has already confirmed the ANLSH and has indicated a possible key role for astrocytes in seizure activity (Tian 2005). These technologies may be useful in assessing the interaction in the neural network of the “neurovascular units” of neuron, astrocyte and brain microvessels which contribute to the production of electrophysiological “slow waves” during hyperventilation; an activating procedure used routinely during EEG testing to precipitate seizure activity but whose mechanism of action has yet to be definitively described.

A hypothesis is outlined in section 2.10.1 which, while probable from a review of the current literature, requires elucidation in the controlled laboratory environment using new technologies of live cell imaging and light excitation, in conjunction with electrophysiological monitoring of neuronal fast electrical activity and astrocytic DC slow potential shifts both *in vitro* and *in vivo*. Unfortunately this experimental work is outside the remit of this work. “Gliologists” in specialist laboratories may soon be able to offer the definitive evidence of the generators of HV provoked sinusoidal rhythmogenesis in the EEG.

## References: Chapter 2

- Aaslid R, Lindegaard KF, Sorteberg W, Nornes H, 1989, Cerebral autoregulation dynamics in humans. *Stroke* 20: 45–52.
- Abbot NJ, 2002, Astrocyte-endothelial interactions and blood brain barrier permeability *J. Anat* 200: 629-638
- Abbot NJ, Ronnback L, Hansson E, 2006, Astrocyte-endothelial interactions at the blood brain barrier *Nat Rev Neurosci* 7(1): 41-53
- Alici K, W. Müller W, Heinemann U, 1996, Effects of glutamate receptor agonists on presumed presynaptic  $\text{Ca}^{2+}$ -signals in juvenile rat hippocampal area CA1. *Neurosci. Lett.* 214: 17-20
- Alpert NM, Buxton RB, Correia JA, 1988, Measurement of end-capillary  $\text{PO}_2$  with positron emission tomography. *J Cereb Blood Flow Metab* 8: 403-410
- Amzica F, Steriade M, 2001, Neuronal and glial membrane potentials during sleep and parosysmal oscillations in the neocortex. *J. Neurosci.* 20(17): 6648-6665
- Amzica F, 2002, In vivo electrophysiological evidences for cortical neuron-glia interactions during slow (<1Hz) and paroxysmal sleep oscillations. *J Physiol (Paris)* 96: 209-219
- Aram JA, Lodge D, 1987, Epileptiform activity induced by alkalosis in rat neocortical slices: block by antagonists of N-methyl-D-aspartate. *Neurosci Lett* 83: 345-350
- Balestrino M, and Somjen GG, 1988, Concentration of carbon dioxide, interstitial pH and synaptic transmission in hippocampal formation of the rat. *J Physiol (Lond)* 396: 247-266
- Balzamo E, Gayan-Ramirez G, Jammes Y, 1991, Quantitative EEG changes under various conditions of hyperventilation in the sensorimotor cortex of the anaesthetized cat. *Electroencephalogr Clin Neurophysiol* 78(2): 159-65.
- Barnes TC, Amoroso MD, 1947, The effects of age of the human brain on the EEG during hyperventilation. *Anat Rec* 99: 622
- Barros FL, Porras OH, Bittner CX, 2005, Why glucose transport in the brain matters for PET. *Trends in Neurosci* 28;3: 117-119
- Bauer HC, Bauer H 2002, Natural induction of the blood brain barrier: still an enigma *Cellular Mol. Neurobiol* 20: 13-28

Benarroch EE, 2005, Neuron-Astrocyte Interactions: Partnership for Normal Function and disease in the Central Nervous System *Mayo Clin Proc* 80(10): 1326-1338

Berger H, 1929, Über das Elektroenkephalogramm des Menschen. *Archiv für Psychiatrie und Nervenkrankheiten*, 87: 527-570

Berger H, 1933, Über das Elektroenkephalogramm des Menschen IX, *Arch Psychiatr. Nervenkr.* 101: 452-469

Bickford RG, 1979, Activation procedures and special electrodes. In *Current practice of Clinical electroencephalography*. Eds. Klass DW, Daly DD, pp.269-305. New York: Raven Press

Billinger TW, Frank GS, 1969, Effects of posture on EEG slowing during hyperventilation. *Am. J. EEG Technol* 9:1 22-27

Binks AP, Cunningham VJ, Adams L, Banzett RB, 2008, Grey Matter Blood Flow Change is Unevenly Distributed during Moderate Isocapnic Hypoxia in Humans *J Appl Physiol* 104: 212-217

Blaber AP, Bondar RL, Stein F, Dunphy PT, Moradshahi P, Kassam MS, 1997, Freeman R. Transfer function analysis of cerebral autoregulation dynamics in autonomic failure patients. *Stroke*. 28: 1686–1692.

Blinn KA, Noel WK, 1949, Continuous measurement of alveolar CO<sub>2</sub> tension during hyperventilation test in routine electroencephalography *Electroencephalogr Clin Neurophysiol* 1: 333-42

Blom S, and Heijbel J, 1975, Benign epilepsy of childrens with centro-temporal EEG foci. Discharge rate during sleep *Epilepsia* 16: 133-140

Bonvallet M, Dell P, 1956, Reflections on the mechanisms of the action of hyperventilation upon the EEG *Electroencephalogr clin Neurophysiol* 6: 119-44

Bonvento G, Herard AS, Voutsinos-Porche B, 2005, The astrocyte-neuron lactate shuttle: a debated but still valuable hypothesis for brain imaging. *J Cereb Blood Flow Metab* 25: 1394-1399

Boothby WM, 1912, Absence of apnoea after forced breathing *J Physiol (London)* 45: 328-333

Bostem FM, 1976, In: *Handbook of Electroencephalography and Clinical Neurophysiology*, Vol 3D, Ed: Remond A. Amsterdam: Elsevier 74-88

Brown AM, Tekkok SB, Ransom BR, 2003, Glycogen regulation and functional role in mouse white matter *J Physiol* 549: 501-512

Busija DW, Heistad DD, 2003, Factors involved in the physiological regulation of the cerebral circulation. *Rev Physiol Biochem Pharmacol.* 101: 161-211.

Buzáki G, Traub RD, Pedley TA, 2003, "*The Cellular Basis of EEG Activity*," in Current Practice of Clinical Electroencephalography, 3rd ed., J.S. Ebersole and T.A. Pedley Eds. Philadelphia: Lippincott Williams & Wilkins, 1-11.

Carbon M, Wubbler G, 2000, Hyperventilation-induced human cerebral magnetic fields non-invasively monitored by multichannel "direct current" magnetoencephalography *Neurosci Letts* 287: 227-230

Carlsson C, Nilsson L, Siesjö BK, 1974, Cerebral metabolic changes in arterial hypoxemia of short duration. *Acta Anaesthesiol Scand* 18: 104-113

Caspers H, Speckmann EJ, Lehmenkuhler A, 1987, DC potentials of the cerebral cortex. Seizure activity and changes in gas pressures. *Rev Physiol Biochem Pharmacol* 106: 127-178

Cataldo AM, Broadwell RD, 1986, Cytochemical identification of cerebral glycogen and glucose-6 phosphatase activity under normal and experimental conditions in Neurons and Glia. *J Electron Microscopy Technique* 3: 413-437

Charles A, 2005, Reaching Out Beyond the Synapse: Glial Inter-cellular Waves Coordinate Metabolism. *Sci. STKE*, 8 February 2005  
[DOI: 10.1126/stke.2702005pe6]

Charles AC, Giaume C, 2002, Inter-cellular calcium waves in astrocytes: underlying mechanisms and functional significance. In: *The Tripartite Synapse* (Volterra A, Magistretti PJ, Haydon P, eds) New York: Oxford University Press 110-26

Chesler M, 1990, The regulation and modulation of pH in the nervous system. *Progr. Neurobiol.* 34: 401-427.

Chih CP, Lipton P, Roberts EL Jr. 2001, Do active cerebral neurons really use lactate rather than glucose? *Trends Neurosci.* 24: 573-579

Chih CP, Roberts EL, 2003, Energy substrates for neurons during neural activity: a critical review of the astrocyte- neuron lactate shuttle hypothesis. *J Cereb Blood Flow Metab* 22: 1343-51

Corfield, DR, Morrell HJ, Guz A, 1995, The nature of breathing during hypoxemia in awake man. *Respiratory Physiology* 101: 145-159

Coughlan AJ, Mc Menamin J, 2008, The effects of posture on quantitative EEG and end tidal CO<sub>2</sub> during standardized hyperventilation in healthy adults. Abstract: Proc. BSCN Scientific Meeting, March 2008.  
In preparation for *J Clin Neurophys.*

Dallas M, Boycott HE, Atkinson L, Miller A, Boyle JP, Pearson HA, Peers C, 2007, Hypoxia Suppresses Glutamate Transport in Astrocytes *J Neuroscience*. 27(15): 3946-3955

Danober L, Deransart C, Depaulis A, Vergnes M, Marescaux C, 1998, Pathophysiological mechanisms of genetic absence epilepsy in the rat *Prog Neurobiol* 55: 27-57

Darrow CW, Green JR, Davis EW, Garol HW, 1944a, Parasympathetic regulation of high potential in the electroencephalogram. *J Neurophysiol* 7: 217-26

Darrow CW, Green JR, Davis EW, Garol HW, 1944b, Cholinergic influence on high potential slow waves of the EEG *Fed Proc Am Soc Exp Biol*. 3: 8

Darrow CW, Pathman JH, 1943, The role of blood pressure in electroencephalographic changes during hyperventilation. *Fed Proc Am Soc Exp Biol* 2: 9

Darrow CW, and Pathman JH, 1944, Relation of heart rate to slow waves in the EEG during over-ventilation. *Am J Physiol* 104: 583-8

Datta, A.K, Shea, R.L, Horner, R.L, 1991, The influence of induced hypocapnia and sleep on the endogenous respiratory rhythm in humans. *.Physiol (London)* 440: 17-33

Davis H, Wallace WM, 1942, Factors affecting changes produced in electroencephalograms by standardized hyperventilation. *Arch. Neurol Psychiatr.* 47: 606-625

Deitmer JW, 1992a, Evidence for glial control of extracellular pH in the leech central nervous system *Glia* 5: 43-47

Deitmer JW, Rose CR, 1996, pH regulation and proton signalling by glial cells. *Progr. Neurobiol.* 48: 73-103.

Deitmer JW, 2001, Strategies for metabolic exchange between glial cells and neurons. *Respir Physiol* 129(1-2): 71-81

Diehl RR, Linden D, Lücke D, Berlitz P, 1995, Phase relationship between cerebral blood flow velocity and blood pressure. A clinical test of autoregulation. *Stroke* 26: 1801-1804.1

Diehl RR, Linden D, Lucke D, Berlitz P, 1998, Spontaneous blood pressure oscillations and cerebral autoregulation. *Clin Auton Res.* 8: 7-12.

Diest IV, Stegen, de W, Schippers N, den Bergh OV, 2000, Hyperventilation and attention: effects of hypocapnia on performance in a stroop task. *Biol. Psychol* 53: 233-252

Di Garbo A, Barbi M, Chillemi S, Alloisio S, Nobile M, 2007, Calcium signalling in astrocytes and modulation of neural activity *Biosystems* 89: 1-3; 74-83

Diringer MN, Yundt K, Videen TO *et al*, 2000, No reduction in cerebral metabolism as a result of early moderate hyperventilation following severe traumatic brain injury. *J Neurosurg* 92(1): 7-13.

Djarova T, Ilkov A, Varbanova A, Nikiforova A, Mateev G, 1986, Human growth hormone, cortisol, and acid-base balance changes after Hyperventilation and breath-holding. *Int J Sports Med* 7(6): 311-5.

Drury I, 2000, Activation of seizures by hyperventilation. In: Luders HO, Noachtars, eds, *Epileptic seizures: pathophysiology and clinical semiology*, Philadelphia: Churchill & Livingstone, 575-9

Dufour F, Koning E, Nehlig A, 2003, Basal levels of metabolic activity are elevated in Genetic Absence Epilepsy Rats from Strasbourg (GAERS)—measurement of regional activity of cytochrome oxidase and lactate dehydrogenase by histochemistry. *Exp Neurol* 182: 346–352

Dufour F, Nalecz KA, Nalecz MJ, Nehlig A, 2001, Metabolic approach of absence seizures in a genetic model of absence epilepsy, the GAERS—study of the leucine–glutamate cycle. *J Neurosci Res* 66: 923–930

Dulla M, Dobelis P, Pearson T, Frenguelli BG, Staley KJ, Masino SA, 2005, Adenosine and ATP Link PCO<sub>2</sub> to cortical excitability via pH *Neuron* 48 (6): 1011-23

Dutuit M, Didier-Bazes M, Vergnes M, Mutin M, Conjard A, Akaoka H, Belin MF, Touret M, 2000, Specific alteration in the expression of glial fibrillary acidic protein, glutamate dehydrogenase, and glutamine synthetase in rats with genetic absence epilepsy. *Glia* 32: 15–24

Dutuit M, Touret M, Szymocha R, Nehlig A, Belin MF, Didier-Bazes M, 2002, Decreased expression of glutamate transporters in genetic absence epilepsy rats before seizure occurrence. *J Neurochem* 80: 1029–1038

Edvinsson L, MacKenzie ET, McCulloch J, 1993, Changes in arterial gas tensions, in *Cerebral Blood Flow and Metabolism*, eds. Edvinsson L, MacKenzie ET, McCulloch J. New York, Raven, 524–552

Eldridge, F.L, 1973, Post hyperventilation breathing: different effects of active and passive hyperventilation *J Appl Physiol* 34: 422-430



- Engel, G.L., Romano, J. *et al*, 1944, A simple method of determining frequency spectrums in the electroencephalogram. *Arch. Neurol, Psychiat.*, Chicago, 51: 134-146
- Engel J, Lubens P, Kuhl DE *et al*, 1985, Local cerebral metabolic rate for glucose during petit mal absences. *Ann Neurol* 17: 121-8
- Esquivel E, Chaussam M, Plouin P, Ponsot G, Arthuis M, 1991, Physical exercise and voluntary hyperventilation in childhood absence epilepsy. *Electroencephalogr Clin Neurophysiol* 79: 127-33
- Faraci FM, Sobey CG, 1998, Role of potassium channels in regulation of cerebral vascular tone. *J Cereb Blood Flow Metab.* 18: 1047-63.
- Fellin T, Pascual O, Haydon PG, 2006, Astrocytes coordinate synaptic networks: balanced oxidation and inhibition *Physiology (Bethesda)* 21; 208-215
- Filosa JA, Bonev AD, Nelson MT, 2004, Calcium dynamics in cortical astrocytes and arterioles during neurovascular coupling. *Circ Res* 95(10) 73-81. Epub 2004 Oct 21
- Fisahn A, Pike FG, Buhl .H, Paulsen O, 1998, Cholinergic induction of network oscillations at 40 Hz in the hippocampus in vitro. *Nature* 394, 186–189
- Friedman SD, Jensen JE, Frederick BB, Artru AA, Renshaw PF, Dager SR, 2007, Brain changes to hypocapnia using respidly interleaved phosphorus-proton magnetic resonance spectroscopy at 4TJ *Cereb Blood Flow Metab* 27(3): 646-53
- GaborAJ, Marsan CA, 1969, Co-existence of focal and bilateral diffuse paroxysmal discharges in epileptics: clinical-electrographic study *Epilepsia* 10: 453-72
- Gardner WN. 1996, The pathophysiology of hyperventilation disorders. *Chest* 109; 516-534
- Gardner WN, 2003, Hyperventilation: A practical guide *Medicine* 31;11: 7-8
- George AL, 2004, Inherited channelopathies associated with epilepsy. *Epilepsy Curr* 4(2); 65-70
- Gibbs EL, Gibbs FA, Lennox WG, Nims LF, 1942, Regulation of cerebral CO<sub>2</sub>. *Arch Neurol Psychiatry* 47 (7): 879-89
- Gibbs FA, 1942, Discussion. In: Davis H, Wallace W. Factors affecting changes in the human electroencephalogram by standardized hyperventilation. *Arch Neurol. Psychiatry.* 47: 606-25
- Gilbert C, 1999, Hyperventilation and the body. *Accident and Emergency Nursing* 7, 130-140

Gjedde A, Marrett S, 2001, Glycolysis in Neurons, Not Astrocytes, Delays Oxidative Metabolism of Human Visual Cortex During Sustained Checkerboard Stimulation *in Vivo J Cereb Blood Flow Metab* 21: 1384-1392

Golanov EV, Ruggiero DA, Reis DJ, 2000, A brainstem area mediating cerebrovascular and EEG responses to hypoxic excitation of rostral ventrolateral medulla in rat. *The Journal of Physiology* 529.2: 413-429

Gotoh F, Tazaki Y, Meyer JS, 1961, Transport of gases through brain and their extravascular vasomotor action. *Exp Neurol.* 4: 48-58.

Granholm L, 1971, Cerebral effects of Hyperventilation. *Acta Anaesthesia Scand.* (Suppl) ;45: 114-22

Granholm L, Lukjanova L, Siesjo BK, 1969, The effect of marked hyperventilation upon tissue levels of NADH, lactate, pyruvate, phosphocreatine and adenosine phosphates of rat brain. *Acta Physiol Scand* 77: 179-180

Granholm L, Siesjo BK, 1971, The effect of combined respiratory and nonrespiratory alkalosis on energy metabolites and acid-base parameters in the rat brain. *Acta Physiol Scand* 81: 307-314

Guaranha MSB, Garzon E, Buchpiguel CA, Tazima S, Yacubian EMT, Sakamoto AC, 2005, Hyperventilation Revisited: Physiological Effects and Efficacy on Focal Seizure Activation in the Era of Video-EEG Monitoring. *Epilepsia.* 46(1); 69-75

Gupta AK, Hutchinson PJ, Fryer T, 2002, Measurement of brain tissue oxygenation performed using positron emission tomography scanning to validate a novel monitoring method *J Neurosurg* 96: 263-268

Haldane JS, Priestly JG, 1905, The regulation of lung ventilation *J Physiol* (London) 32: 255-266

Harder DR, 1982, Effect of H<sup>+</sup> and elevated PCO<sub>2</sub> on membrane electrical properties of rat cerebral arteries. *Pflugers Arch.* 394: 182-5.

Harder DR, Alkayed NJ, Lange AR, Gebremedhin D, Roman RJ, 1998, Functional hyperemia in the brain: hypothesis for astrocyte-derived vasodilator metabolites. *Stroke; a journal of cerebral circulation* 29: 229-234

Haydon PG, Carmignoto G, 2006, Astrocyte control of synaptic transmission and neurovascular coupling *Physiol. Rev.* 86(3): 1009-31

Hattunen J, Tolvanen H, 1999, Effects of voluntary hyperventilation on cortical sensory responses, EEG and MEG studies *Exp Brain Res* 125(3) :248-254

Heinemann U, Lux HD, 1977, Ceiling of stimulus induced rises in extracellular potassium concentration in the cerebral cortex of cat. *Brain Res.* 120(2): 231-49

Henry T, Votaw L, 2006, Thalamic Blood Flow activation and electrocerebral delta-theta power reduction during acute vagus nerve stimulation *Clin Neurophysiol* 117 (supl 1): 12-13

Hertz L, Zielke HR, 2004, Astrocytic control of glutamatergic activity: astrocytes as stars of the show *Trends Neurosci.* 27: 735-743

Hood VL, Tannen RL, 1983, pH control of lactic acid and keto acid production: a mechanism of acid-base regulation. *Mineral Electrolyte Metabolism* 9: 317-325

Hoshi Y, Okuhara H, 1999, Re-evaluation of the hypoxia theory as the mechanism of hyperventilation –induced EEG slowing. *Paediatr. Neurol.* 21 (3): 638-43

Hutchinson JH, Gupta AK, Fryer TF, Al-Rawi PG *et al*, 2002, Correlation between cerebral blood flow, substrate delivery, and metabolism in head injury: a combined microdialysis and triple oxygen positron emission tomography study *J Cereb Blood Flow Metab* 22: 735-745

Jabs R, Paterson IA, Walz W, 1997, Qualitative analysis of membrane currents in glial cells from normal and gliotic tissue in situ: down-regulation of Na<sup>+</sup> current and lack of P2 purinergic responses. *Neuroscience* 81 (3): 847-60

Jaffe LF, 1991, The path of calcium in cytosolic calcium oscillations: a unifying hypothesis *Proc. Natl. Acad. Sci. USA* 88: 9883-9887,

Jensen O, Hari R, Kaila K, 2002, Visually evoked gamma responses in the human brain are enhanced during voluntary hyperventilation. *NeuroImage* 15: 575-586

Julu PO, Engerstrom IW, 2005, Assessment of the maturity-related brainstem functions reveals the heterogeneous phenotypes and facilitates clinical management of Rett syndrome. *Brain Dev* 27 (suppl): S43-S53

Julu PO, 1992, A linear scale for measuring vagal tone in man *J Auton Pharmacol* 12: 109-115

Julu PO, Kerr AM, Hansen S, Apartopoulos F, Jamal GA, 1997, Functional evidence of brain stem immaturity in Rett syndrome *Eur. Child. Adolesc. Psychiatry* 6 (suppl 1): 47-54

Kaila K, 1994, Ionic basis of GABAA receptor channel function in the nervous system, *Prog Neurobiol* 42: 489-537

Kaila K, Ransom BR, 1998, Concept of pH and its importance in neurobiology, in *pH and Brain Function*, eds. Kaila K, Ransom BR. New York, Wiley-Liss, 3-10

Kanner AM, 2008, Vagus nerve stimulation for generalized epilepsy? Show me the evidence! *Epilepsy Currents* 8(2): 35-36

Kasischke KA, Wishwasrao HD, Fisher PJ, Zipfel WR, Webb WW, 2004, Neural activity triggers neuronal oxidative metabolism followed by astrocytic glycolysis *Science* 305: 99-103

Kauppinen RA, Williams SR, 1998, Use of NMR spectroscopy in monitoring cerebral pH and metabolism during systemic and focal acid-base disturbances, in *pH and Brain Function*, eds. Kaila K, Ransom BR. New York, Wiley-Liss, 605-619

Kellaway P, 1985, Sleep and Epilepsy *Epilepsia* 26(Suppl 1): S15-S30

Kellaway P, 2000, The electroencephalographic features of benign centrottemporal (Rolandic) epilepsy of childhood *Epilepsia* 41: 1053-1056

Kerr AM, Julu POO, 1999, Recent insights into hyperventilation from the study of Rett syndrome *Arch Dis Child*, 80: 384-387

Kety SS, Schmidt CF, 1948, The effects of altered arterial carbon dioxide and oxygen on cerebral blood flow and cerebral oxygen consumption of normal young men. *J Clin Invest* 27: 484-49

Kogure K, Busto R, Matsumoto A *et al*, 1975, Effect of hyperventilation on dynamics of cerebral energy metabolism. *Am J Physiol* 228: 1862-1867

Konishi T, 1987, The standardization of hyperventilation on EEG recording in childhood I: The quantity of hyperventilation activation. *Brain Dev.* ) 9(1:) 16-20

Konishi T, 1987, The standardization of hyperventilation on EEG recording in childhood II: The quantitative analysis of build-up *Brain Dev.*)9(1:) 21-25,

Kontos HA, Raper AJ, Patterson JL, 1977, Analysis of vasoactivity of local pH, PCO<sub>2</sub> and bicarbonate on pial vessels. *Stroke* 8: 358-60.

Kontos HA, Wei EP, 1996, Arginine analogues inhibit responses mediated by ATP-sensitive K<sup>+</sup> channels. *Am J Physiol.* 271: H1498-H1506

Kontos HA, Wei EP, Raper AJ, Patterson JLJ, 1977, Local mechanism of CO<sub>2</sub> action of cat pial arterioles. *Stroke* 8: 226-9.

Kraaier V, Van Huffelen AC, Weineke GH, 1989, The hyperventilation induced ischaemia model in human neuropharmacology: Neurophysiological and psychometric studies of aniracetam and 3-OH aniracetam *Eur J Clin Pharmacol* 36: 605-611

Kukumberg P, Benetin J, Kuchar M, 1996, Changes of motor evoked potential amplitudes following magnetic stimulation after hyperventilation. *Electromyogr Clin Neurophysiol* 36(5): 271-3

Kujira T, Caramia MD, Rothwell JC, Day BL, Thompson PD, Ferbert A, Wroe S, Asselman P, Marsden CD, 1993, Corticocortical inhibition in human motor cortex *J Physiol* 471: 501-519

Kupferman R, Mitra PP, Hohenberg PC, Wang SS, 1997, Analytical Calculation of Intracellular Calcium Wave Characteristics *Biophys. J* 7: 2430-2442

Kuschinsky W, 1982, Role of hydrogen ions in regulation of cerebral blood flow and other regional flows. *Advances in Microcirculation* 11: 1-19

Lam TK, Gutierrez-Juarez R, Pocai A, Rossetti L, 2005, Regulation of blood glucose by hypothalamic pyruvate metabolism. *Science*. 309: 943-947

Lee JH, Taira T, Pihlaja P, Ransom BR, Kaila K, 1996, Effects of CO<sub>2</sub> on excitatory transmission apparently caused by changes in intracellular pH in the rat hippocampal slice. *Brain Res* 706: 210-216

Lehmenkuhler A, 1999, Hypoxia and hypercapnia-induced DC potential shifts in rat at the scalp and the skull are opposite in polarity to those at the cerebral cortex *Neurosci Lett*. 270: 67-70

Leusen I, Weyne J, 1976, Metabolic processes in the brain during respiratory and non-respiratory alkalosis and acidosis, in *Acid-Base Homeostasis of the Brain Extracellular Fluid and the Respiratory Control System*, ed. Loeschcke HH. Stuttgart, Thieme, 27-44

Ley R, 1999, The modification of breathing behavior. Pavlovian and operant control in motion and cognition. *Behav Modif* 23(3): 441-79.

Lubin AJ, Price JC, 1942, Effects of alkalosis and acidosis on cortical electrical activity and blood flow. *J Neurophysiol* 5: 261-8

Luther R, 1906, Propagation of chemical reactions in space. *Z. Elektrochem* 12: 596

Macefield G, Burke D, 1991, Paraesthesiae and tetany induced by voluntary hyperventilation. Increased excitability of human cutaneous and motor axons *Brain* 114: 527-540

Macmillan V, Siesjo BK, 1973, The influence of hypocapnia upon intracellular pH and upon some carbohydrate substrates, amino acids and organic phosphates in the brain. *J Neurochem* 21: 1283–1299

Mac Vicar BA, 1989, Transmitter and voltage activated ionic channels in astrocytes: possible role in extracellular ionic homeostasis *Acta Physiol Scand Suppl.* 582: 49

Magistretti PJ, Pellerin L, 1999, Cellular mechanisms of brain energy metabolism and their relevance to functional brain imaging. *Phil. Trans. R. Soc. London. B* 354: 1155-1163

Makiranta MJ, Ruohonen J, Suominen K, Sonkajarvi E, Salomaki T, Kiviniemi V, Seppanen T, Alahuhta S, Jantti V, Tervonen O, 2004, BOLD- contrast functional MRI signal changes related to intermittent rhythmic delta activity in EEG during voluntary hyperventilation-simultaneous EEG and fMRI study *Neuroimage*, 22(1): 222-31

Marrosu F, Puligheddu M, Giagheddu M, Cossu G, Piga M, 2000, Correlation between cerebral perfusion and hyperventilation enhanced focal spiking activity. *Epilepsy Res* 40(1): 79-86

Meeren H, van Luijtelaar G, Lopes da Silva FH, Coenen A, 2005, Evolving concepts on the pathophysiology of absence seizures—the cortical focus theory. *Arch Neurol* 62: 371–376

McHenry LC, Slocum HC, Bivens HE *et al*, 1965, Hyperventilation in awake and anesthetized man: effects on cerebral blood flow and cerebral metabolism. *Arch Neurol* 12: 270–277

Melo TM, Sonnewald U, Touret T, Nehlig A, 2006, Cortical Glutamate Metabolism is enhanced in a genetic model of absence epilepsy *J Cereb Blood flow Metab* 26: 1496-1506

Miley CE, Forster FM, 1977, Activation of partial Complex Seizures by hyperventilation, *Arch Neurol* 34 (6): 371-3

Mogyoros I, Kiernan MC, Burke D, Bostock H, 2000, Excitability changes in human sensory and motor axons during hyperventilation and ischaemia. *Brain* 120: 317-325

Morale MC, Gallo F, Tirulo C, Nesta N, Caniglia S *et al*, 2001, Neuroendocrine immune (NEI) circuitry from neuron-glia interactions to function: Focus on gender and HPA-HPG interaction on early programming of the NEI system. *Immun Cell Biol.* 79: 400-417

Morgan MD, Scott DF, 1970, EEG activation in epilepsies other than petit mal, *Epilepsia* 11: 255-61

Morrice JK, 1956, Slow wave production in the EEG with reference to hypernoea, carbon dioxide, and autonomic balance. *Electroenceph. Clin. Neurophysiol*, 8: 49-72

Muller K, 1971, Electrical picture of the brain under increased respiration in children. *Psychiatr. Neurol. Med. Psychol. Beih* 16: 1-146

Muller SM, Heistad DD, Marcus ML, 1977, Total and regional cerebral blood flow during hypotension, hypertension and hypocapnia. *Circulation Res.* 41: 350-536

Muller M, Somjen GG, 2000, Na<sup>+</sup> dependence and the role of glutamate receptors and Na<sup>+</sup> channels in ion fluxes during hypoxia of rat hippocampal slices. *J Neurophysiol* 84(4): 1869-80

Mulligan SJ, MacVicar BA, 2004, Calcium transients in astrocyte endfeet cause cerebrovascular constrictions. *Nature* 431: 195–199

Naganawa S, Norris DG, Zysset S, Mildner T, 2002, Regional differences of fMR signal changes induced by hyperventilation: comparison between SE-EPI and GE-EPI at 3-T. *J Magn Reson Imaging* 15(1): 23-30

Nakahata K, Kinoshita H, Hirano Y, Kimoto Y, Iranami H, Hatano Y, 2003, Mild hypercapnia induces vasodilation via adenosine triphosphate-sensitive K<sup>+</sup> channels in parenchymal microvessels of the rat cerebral cortex. *Anesthesiology* 99: 1333–9

Nedergaard M, Ransom BR Goldman S, 2003, New roles for astrocytes: Redefining the functional architecture of the brain (Review) *TINS* 26: 523-530

Nehlig A, Wittendorp-Rechenmann E, Lam CD, 2004, Selective uptake of [<sup>14</sup>C]2-deoxyglucose by neurons and astrocytes—high-resolution microautoradiographic imaging by cellular <sup>14</sup>C-trajectography combined with immunohistochemistry. *J Cereb Blood Flow Metab* 4: 1004–1014

Neidermeyer E, 1972, Focal and generalised seizure discharges in the electroencephalogram and their response to intravenous diazepam. *Int Med Dig* 7: 49-61

Newell DW, Grady MS, Sirotta P, Winn HR, 1989, Evaluation of brain death using transcranial Doppler. *Neurosurgery*. 24: 509–513

Newman EA, 1986, High potassium conductance in astrocyte endfeet. *Science*. 233(4762): 453-4.

Newman NM, 1995, Neuro-ophthalmology and systemic disease--Part I. An annual review *J Neuroophthalmol*. 15(2): 109-21

Newman EA, 2003, New roles for astrocytes: regulation of synaptic transmission. *Trends Neurosci*. 3226: 536-542

Nicholson C, 1995, Extracellular space as the pathway for neuron-glial cell interaction. In: *Neuroglia* (Kettenmann H, Ransom BR, eds), New York: Oxford University Press, 387-397

Nielsen S, Nagelhus EA, Amiry-Moghaddam, Bourque C, Agre P, Ottersen OP, 1997, Specialized membrane domains for water transport in glial cells: high resolution immunogold cytochemistry of aquaporin-4 in rat brain. *J Neurosci.* 17: 171-180

Nilson M, Hansson E, Ronnback L, 1992, Agonist-evoked  $\text{Ca}^{2+}$  transients in primary astroglial cultures :modulatory effects of valproic acid. *Glia* 5: 201-209

Nilsson L, Busto R, 1973, Controlled hyperventilation and its effects on brain energy and acid-base parameters. *Acta Anaesthesiol Scand* 17: 243–252

Nobili L, Baglietto MG, Beelke M, De Carli F, De Negri E, Rosadini G, De Negri M, Ferrillo F, 1999, Modulation of sleep interictal epileptiform discharges in partial epilepsy of childhood. *Clin Neurophysiol* 110: 839-845

Palva JM, Lamsa K, Lauri SE, Rauvala H, Kaila K, Taira T, 2000, Fast network oscillations in the newborn rat hippocampus in vitro. *J Neurosci.* 20: 1170-1178

Panerai RB, Chacon M Pereira R, Evans DH, 2004, Neural network modelling of dynamic cerebral autoregulation: assessment and comparison with established methods. *Med Eng Phys.* 26: 43–52.

Papp LA, Klein DF, Gorman JM, 1993, Carbon dioxide hypersensitivity, hyperventilation and panic disorder. *Am J Psychiatry* 150: 1149-1157

Patel VM, Maulsby RL, 1987, How hyperventilation alters the Electroencephalogram: A review of controversial viewpoints. *J Clin. Neurophysiol* 4(2): 101-120

Paulson OB, Strandgaard S, Edvinsson L, 1990, Cerebral autoregulation. *Cerebrovasc Brain Metab Rev.* 2: 161–192

Paulson OB, Sharborough FW, 1974, Physiologic and pathophysiologic relationship between the electroencephalogram and the regional cerebral blood flow. *Acta Neurol Scand.* 50: 194-220

Pellerin L, 2003, Lactate as a pivotal element in neuron-glia metabolic cooperation, *Neurochemistry International* 43: 331–338

Pellerin L, Magistretti PJ, 1994, Glutamate uptake into astrocytes stimulates aerobic glycolysis: a mechanism coupling neuronal activity to glucose utilisation. *Proc Natl Acad Sci.* 91; 10625-9



- Pellerin L et al, 1998, Evidence supporting the existence of an activity-dependent astrocyte-neuron lactate shuttle. *Dev. Neurosci.* 20: 291-299
- Pellerin L, Magistretti P J, 2003, How to balance the brain energy budget while spending glucose differently? . *Physiol.* 546: 325
- Pellerin L, Magistretti P J, 2004, Empiricism and rationalism: two paths toward the same goal. *J. Cereb. Blood Flow Metab.* 24: 1240 -1241
- Perez-Velazques JL, Valienta TA, Carlen PL, 1994, Modulation of gap junctional mechanisms during calcium-free induced field burst activity: a possible role for electrotonic coupling in epileptogenesis. *Neurosci* 14: 4308-4317
- Peters A, Palay SL, Webster HD, 1991, *The Fine Structure of the Nervous System: Neurons and their Supporting Cells*, 3<sup>rd</sup> Edition, New York: Oxford University Press
- Petroff OA, Prichard JW, Behar KL et al, 1985, Cerebral metabolism in hyper- and hypocarbia: <sup>31</sup>P and <sup>1</sup>H nuclear magnetic resonance studies. *Neurology* 35: 1681-1688
- Plum F, Brown HW, Snoep E, 1962, Neurologic significance of post hyperventilation apnoea *JAMA* 181: 1051-1055
- Posse S, Olthoff U, Weckesser M, Jancke L, Muller-Gartner HW, Dager SR, 1997, Regional dynamic signal changes during controlled hyperventilation assessed with blood oxygen level-dependant functional MR Imaging. *Am J Neuroradiol* 18: 1763-1770
- Prevett MC, Duncan JS, Jones T, Fish DR, Brooks DJ, 1995, Demonstration of thalamic activation during typical absence seizures using H2(15)O and PET. *Neurology* 45(7): 1396-402
- Raess C, 1974, Hyperventilation. *Am J Electroencephalogr Technol* 14: 166-72
- Raichle ME, Mintun MA, 2006, Brain work and brain imaging. *Annual review of neuroscience* 29: 449-476.
- Raichle ME, Plum F, 1972, Hyperventilation and cerebral blood flow. *Stroke* 3: 566-575
- Ransom BR, Sontheimer H, 1992, The Neurophysiology of Glial Cells. *J Clin Neurophysiol* 9: 224-251
- Reimann F, Ashcroft FM, 1999, Inwardly rectifying potassium channels *Curr Opin. Cell Biol.* 11; 503-508
- Reinhart CA, Gloor SM, 1997, Co culture blood brain barrier models and their use for pharmacotoxic screening *Toxicol. Vitro* 11: 513-518

Rivera C, Voipio J, Kaila K, 2005, Two developmental switches in GABAergic signalling: the  $K^+$ - $Cl^-$  cotransporter KCC2 and carbonic anhydrase CAVII J *Physiol* 562: 27-36

Rose CR, Deitmer JW, 1994, Evidence that Glial cells modulate extracellular pH transients induced by neuronal activity in the leech central nervous system *J Physiol* 481; 1-5

Rostrup E, Law I, Pott F, Ide K, Knudsen GM, 2002, Cerebral haemodynamics measured with simultaneous PET and near-infrared spectroscopy in humans. *Brain Res* 2002;(2): 183-93

Roy CS, Sherrington CS, 1890, On the Regulation of the Blood-supply of the Brain. *The Journal of physiology* 11, 85-158 117

Rudolf G, Therese BM, Godfrey F, Wilder P, Cox D, Lathrop M, Marescaux C, Gauguier D, 2004, Polygenic control of idiopathic generalized epilepsy phenotypes in the genetic absence rats from Strasbourg (GAERS). *Epilepsia* 45: 301-308

Schieve JF, Wilson WP, 1953, The changes in cerebral vascular resistance of man in experimental alkalosis and acidosis. *J Clin Invest* 32: 33-8,

Schipke CG, Kettenmann H, 2004, Astrocyte responses to neuronal activity. *Glia* 47: 226-32

Schurr A, Miller JJ, Payne RS, Rigor BM, 1999, An increase in lactate output by brain tissue serves to meet the energy needs of glutamate-activated neurons *J Neurosci* 19: 34-39

Seigneur J, Kroeger D, Dragos AN, Amzica F, 2006, Cholinergic action on cortical glial cells in vivo *Cereb. Cortex* 16(5): 655-668

Seyal M, Mull B, Gage B, 1998, Increased excitability of the human corticospinal system with hyperventilation. *Electroencephalogr Clin Neurophysiol* 109(3): 263-7

Sherwin I, 1965, Differential effects of hyperventilation on the excitability of intact and isolated cortex. *Electroencephalogr Clin Neurophysiol* 18: 599-607

Sherwin I, 1967, Alterations in the non-specific cortical afference during hyperventilation. *Electroencephalogr Clin Neurophysiol* 23: 532-8

Siesjo BK, 1978, *Brain Energy Metabolism*. New York, Wiley

Somjen GG, 1973, Electrogenesis of sustained potentials *Prog Neurobiol.* 1(3): 201-37

Somjen GC, Allen BE, Balestrino M, Aitken PG, 1987, Pathophysiology of pH and  $\text{Ca}^{2+}$  in bloodstream and brain. *Can J Physiol Pharmacol* 65: 1078-1085

Sparing R, Dafotakis M, Buelte D, Meister IG, Noth J, 2007, Excitability of human motor and visual cortex before, during and after hyperventilation *J Appl Physiol* 102: 406-411

Spray DC, Harris AL, Bennett MV, 1981, Gap junctional conductance is a simple and sensitive function of intracellular pH. *Science* 211: 712-715

Strandgaard S, Barry DI, Paulson OB, 1984, Converting enzyme inhibition and autoregulation of cerebral blood flow in spontaneously hypertensive and normotensive rats. *Scand J Urol Nephrol Suppl.* 79: 35–38

Stenkamp K, Palva JM, Uusisaari M *et al*, 2001, Enhanced temporal stability of cholinergic hippocampal gamma oscillations following respiratory alkalosis in vitro *J Neurophysiol* 85(5): 2063-9.

St John WM, 1990, Neurogenesis, control and functional significance of gasping. *J Appl Physiol* 68: 1305-1315

Swanson AG, Stavney LS, Plum F, 1958, Effects of Blood pH and carbon dioxide on cerebral electrical activity. *Neurology* 8: 787-92

Takahashi T, 2004, 5<sup>th</sup> Ed. Chapter 14: Activation Methods, in *Electroencephalography: Basic principles, clinical applications, and related fields*. Eds Neidermeyer E, Lopes da Silva F. Pg.261-262. Lippincott Williams and Wilkins  
ISBN-13: 9780781751261

Takano T, Tian GF, Peng W, Lou N, Libionka W, Han X, Nedergaard M, 2006, Astrocyte-mediated control of cerebral blood flow. *Nat Neurosci* 9: 260–267

Thomas SH, Orf JRN, Wedel SK, Conn AK, 2002, Hyperventilation in traumatic brain injury patients: Inconsistency between consensus guidelines and clinical practice *J Trauma inj infection crit care* 52(1): 47-53

Tian GF, Azmi H, Takano T, Xu Q, Peng W, Lin J, Oberheim NA, Wang X, Zielke HW, Kang J, Nedergaard M, 2005, An astrocytic basis of epilepsy *Nature Medicine* 11: 973-981

Toda N, Hatano Y, Mori K, 1989, Mechanisms underlying response to hypercapnia and bicarbonate of isolated dog cerebral arteries. *Am J Physiol.* 257: H141-H146

Tombaugh GC, Somjen GC, 1998, In : pH and Brain function, Eds. Kaila K, Ransom BR Pub: Wiley  
Chap 21 ;pH modulation of voltage gated ion channels

Tomita-Gotoh S, Hayashida Y, 1996, Scalp-recorded direct current potential shifts induced by hypocapnia and hypercapnia in humans. *Electroencephalogr Clin Neurophysiol* 99(1): 90-7

Traub RD, Bibbig A, LeBeau FEN, Cunningham MO, Whittington MA, 2005, Persistent gamma oscillations in superficial layers of rat auditory neocortex: experiment and model *J Neurophysiol* 262.1: 3-8

Traub RD, Bibbig A, 2000, A model of high-frequency ripples in the hippocampus based on synaptic coupling plus axon-axon gap junctions between pyramidal neurons. *J Neurosci* 20: 2086-2093

Traynelis SF, 1998, *pH modulation of ligand-gated ion channels*, In : pH and Brain function Eds. Kaila K, Ransom BR, Wiley

Treier R, Steingoetter A, Weishaupt D, et al 2006. Gastric motor function and emptying in the right decubitus and seated body position as assessed by magnetic resonance imaging. *J Mag Res Image* 22(3);331-338

Van der Worp, H.B Kraaier V, Wieneke GH, Van Huffelen AC, 1991, Quantitative EEG during progressive hypocarbia and hypoxia. Hyperventilation-induced EEG changes reconsidered. *Electroencephalogr. Clin. Neurophysiol.* 79(5): 335-41

Van Diest I, Stegen K, Van de Woestijne KP, Schippers N, Van den Bergh O, 2000, Hyperventilation and attention: effects of hypocapnia on performance in a stroop task. *Biol Psychol* 53(2-3): 233-52.

Van Rijen PC, Luyten PR, Berkelbach Van Der Sprenkel JW *et al*, 1989, <sup>1</sup>H and <sup>31</sup>P NMR measurement of cerebral lactate, high energy phosphate levels and pH in humans during voluntary hyperventilation: associated EEG, capnographic, and Doppler findings. *Magn Reson Med* 10: 182-193

Vanucci SJ, Maher F, Simpson IA, 1997, Glucose transporter proteins in brain: delivery of glucose to neurons and glia. *Glia* 21: 2-21

Vidiendal Olsen N, Christensen H, Klausen T *et al*, 1998, Effects of hyperventilation and hypocapnic/normocapnic hypoxemia on renal function and lithium clearance in humans. *Anesthesiology* 89(6): 1389-400.

Voipio J, Kaila K, Tolvanen H, Heinonen E, 1995, Negative shift in DC-EEG linked to a fall in end tidal CO<sub>2</sub> during voluntary hyperventilation. *Soc Neurosci Abstr* 21 :969

Volterra A *et al*, 2002, *The Tripartite Synapse. Glia in Synaptic Transmission*, Oxford University Press

Walz W, 1989, Role of glial cells in the regulation of the brain ion microenvironment *Prog Neurobiol.* 33(4): 309-33

- Walz W, Mac Vicar B, 1988, Electrophysiological properties of glial cells: comparison of brain slices with primary cultures. *Brain Res.* 443(1-2): 321-4
- Wei EP, Kontos HA, 1990, Blockade of ATP-sensitive potassium channels in cerebral arterioles inhibits vasoconstriction from hypocapnic alkalosis in cats. *Stroke* 30: 851-3.
- Wender R, Brown AM, Fern R, Swanson RA, Farrell K, Ranson BR, 2000, Astrocytic glycogen influences anion function and survival during glucose deprivation in central white matter. *J Neurosci.* 20: 6804-6810
- White HS, Skeen GA, Edwards JA, 1992, Pharmacological regulation of astrocytic calcium channels: for the treatment of seizure disorders. *Prog Brain Res* 94: 77-87.
- Winship IR, Plaa N, Murphy TH, 2007, Rapid Astrocyte Calcium Signals Correlate with Neuronal Activity and Onset of the Hemodynamic Response *In Vivo*. *The Journal of Neuroscience*, 27(23): 6268-6272;
- Wolff HG, Forbes HS, 1928, The cerebral circulation: Observations of the pial circulation during changes in intracranial pressure. *Arch Neurol Psychiat* 20: 1035-1047
- Wolff JR, 1970, Quantitative aspects of macroglia. In: *Proceeding of the sixth international congress of neuropathology* pp327-352 Paris Masson
- Yamatani M, Konishi T, Murakami M, Okuda T, 1994, Hyperventilation activation on EEG recording in Childhood *Epilepsia*. 35(6): 1199-203
- Yamatani M, Konishi T, Murakami M, Okuda T, 1995, Hyperventilation activation on EEG recording in children with epilepsy *Paed. Neurol.* 13(1): 42-45
- Young RS, Yagel SK, 1984, Cerebral physiological and metabolic effects of hyperventilation in the neonatal dog. *Ann Neurol* 16: 337-342
- Young JK, Baker JH, Montes MI, 2000, The brain response to 2-deoxy glucose is blocked by a glial drug. *Pharmacol. Biochem. Behav.* 67: 233-239
- Zhang R, Zuckerman JH, Giller CA, Levine BD, 1998, Transfer function analysis of dynamic cerebral autoregulation in humans. *Am J Physiol.* 274: H233-H241
- Zonta M, Angulo MC, Gobbo S, Rosengarten B, Hossmann KA, Pozzan T, Carmignoto G, 2003, Neuron-to-astrocyte signaling is central to the dynamic control of brain microcirculation. *Nat Neurosci* 6: 43-50

Zwiener U, Lobel S., *et al*, 1998, Quantitative topographical analysis of EEG during non-standardized and standardized Hyperventilation. *J Clin. Neurophysiol.* 15 (6): 521-8

## **Bibliography**

Buzáki G, Traub RD, Pedley TA, 2003, "The Cellular Basis of EEG Activity," in Current Practice of Clinical Electroencephalography, 3rd ed., JEbersole JS, Pedley TA Eds. Philadelphia: Lippincott Williams & Wilkins, pp. 1-11

Degen R, Degen HE, 1992, Contribution to the genetics of Rolandic epilepsy: wking and sleeping EEGs in siblings. In Degan R, Dreifuss FE, Eds., Benign localized and generalized epilepsies of early childhood, Elsevier Science; New York

Deitmer JW, 1998, Chap 11 in "Glial cells:Their Role in Behavior. Acid/alkaline transients and pH regulation by glia (page 16)

Guyton AC, Hall JE, 2000, Textbook of Medical Physiology, 10<sup>th</sup> edition, WB Saunders Company. An Imprint of Elsevier Science  
ISBN 0-7216—8677-X

Heinemann U, Walz W, 1998, Chapter 10 in "Glial Cells: Their Role in Behavior" Eds. LamingPR, Sykova E. Cambridge University Press

Jakovcevic J, Harder DR, 2007, Chapter 4 in: "Current topics in developmental biology" Role of astrocytes in matching blood flow to neuronal activity Elsevier, Amsterdam

Julu POO, Engerstrom W, 2005, Assessment of the maturity related brainstem functions reveals the heterogeneous phenotypes and facilitates clinical management of Rett syndrome  
*Brain Dev. Suppl 1*: S43-S53

Kaila K, Ransom BR, 1998, Chapter 1 in : pH and Brain Function, Concept of pH and its Importance in Neurobiology

Laming PR, Sykova E, Reichenback A, Hatton GI, Bauer H, 1998, Glial cells:their role and behavior. Cambridge University Press

Plum F, Leigh RJ, 1981, In: Regulation of Breathing, Ed. Hornbein TF: Abnormalities of central mechanisms

DaleP, Augustine GJ, Fitzpatrick D, Hall WC, LaMantia AS, McNamara, JO White LE, 2008, *Neuroscience. 4th ed.*. Sinauer Associates. pp. 128-9. ISBN 978-0-87893-697-7

Santiago Ramon y Cayal, 1928, *Degeneration and Regeneration of the Nervous System*. London: Oxford University Press; Humphrey Milford

Sharpey-Schafer EP, 1965 In: W.F. Hamilton, Editor, *Handbook of Physiology*, Effect of respiratory acts on the circulation

Traynelis SF, 1998, pH modulation of ligand-gated ion channels  
In: Kaila K, Ransom BR (eds). *pH and Brain Function*. Wiley-Liss, New York, pp 395-416

## CHAPTER 3

# MATERIALS, METHODS AND RESULTS

### Methodology

This prospective study examines the effects of posture on the scalp recorded EEG, pETCO<sub>2</sub>, pO<sub>2</sub>, heart rate, and vCBF (in a sub-group of 5 subjects) during optimal hyperventilation conditions in a study group of healthy adult volunteers. 22 healthy subjects were recruited to this study following approval from the local Research Ethics Committee and after informed written consent had been obtained from the volunteers. Possible side effects of optimal hyperventilation such as dizziness, paraesthesia, facial flushing, sweating and tetany were discussed at this time.

The author used students paired *t*- tests and to compare two paired sets of quantitative data with a definite relationship between each pair of data points. An *a priori* power calculation indicating a power greater than 0.99 was based on acquiring for pETCO<sub>2</sub>

$n = 22$  paired samples

$\delta = 5.0$  a difference in population means (in mmHg)

$\alpha = 0.05$  Type I error probability for a two sided test



$\sigma = 0.9$  For paired designs  $\sigma$  is the standard deviation of difference in the response of matched pairs.

An *a priori* power calculation for EEG frequency in Hz assuming a 1 Hz difference in population means ( $\delta$ ) indicated a power greater than 0.99 (same  $n$ ,  $\alpha$  and  $\sigma$ )

The study population comprised 22 subjects (14 females, 8 males) with a mean age of 29.5 years (range 19-51). They were recruited from DIT college students and work colleagues. 19 had never smoked. 3 had smoked (2 female, 1 male) but had ceased at least one year before the study. All subjects were fit and well with no history of cardiovascular disease, metabolic and endocrine disease or respiratory disease. The subjects were tested in a dedicated quiet examination room. An optimal hyperventilation (OHV) breathing exercise was performed in two trials by each subject in two positions, supine, (180 degrees), and sitting upright (90 degrees). All subjects undertook both protocols (supine and sitting), and the sequence was assigned randomly.

The subjects performed the OHV exercise in these two different positions for 4 minutes; at a respiratory rate of 30/minute producing a three fold elevation of expired volume per minute (VE), one breath being defined as a full inspiration and expiration cycle. This standardisation of the hyperventilation method was shown by Konishi in 1987 to effectively elevate the VE to produce optimal hyperventilation. When carried out by adults, such hyperventilation causes an air exchange of 20-50 litres/min and a drop in  $PCO_2$  (partial pressure of carbon dioxide, P representing pressure) in the range of 4-7% (Morrice 1956). In response to this procedure the characteristic EEG change is a fluctuating

increase of bilaterally synchronous slow theta (5.0-7.0 Hz) and delta (0.5-4.0 Hz) activity, and a slowing of alpha (8.0-12.0 Hz) and beta (13.0-20.0 Hz) activity. There is also an overall increase in the background amplitude of the recorded waveforms.

OHV has been shown to cause hyperventilation induced high amplitude rhythmical slowing (HIHARS) in adult subjects with end-tidal  $p\text{CO}_2$  ( $p\text{ETCO}_2$ ) of  $2.0 \pm 0.1$  kPa ( $15.4 \pm 0.8$  mm Hg) (Zweiner *et al* 1998). This study uses the criteria described by Lum *et al* (2002) to define an epoch of HIHARS. These are:

1. high amplitude EEG ( $>100\mu\text{V}$ )
2.  $\sim 2.5$ -5.0 Hz generalized rhythmic EEG slowing
3. duration of greater than or equal to 3 seconds.

A full set of silver/silver chloride (Ag/AgCl) EEG electrodes were applied using skin preparation and electrode paste (as per 10-20 system) plus ECG, EOG, sub-mental chin EMG, and respiration using a piezo-electric chest crystal respiration belt for confirmation of respiration rate and effort. A set of nasal prongs was applied and the subjects reminded to expire only through the nose. This was to ensure that the expired  $\text{CO}_2$  could be measured using a hand held capnometer. The total test period for each position was 8 minutes, i.e. 4 minutes of optimal hyperventilation and 4 minutes of post-hyperventilation. There was a rest period of 20 minutes between testing protocols. The subjects hyperventilated under capnographic control. Expired  $\text{CO}_2$  and respiration rate were monitored continuously via nasal prongs and side stream measurement by

the “Poet LT” Capnometer using non-dispersive infrared technology with auto-calibration. PO<sub>2</sub> was monitored using an infra red finger probe attached to a Datex Ohmeda 3900 series oximeter. Resting blood pressure was taken before the testing commenced in both the supine and seated position. A metronome was used to maintain a respiration rate of 30/minute. Subjects had eaten no less than one hour before testing and finger stick blood sugars were within the normal range.

Every 30 seconds before, during and after optimal HV measurements of heart rate, respiration rate, SpO<sub>2</sub>, and pETCO<sub>2</sub>, were noted on the recording system. Therefore the study consisted of 4 parts:

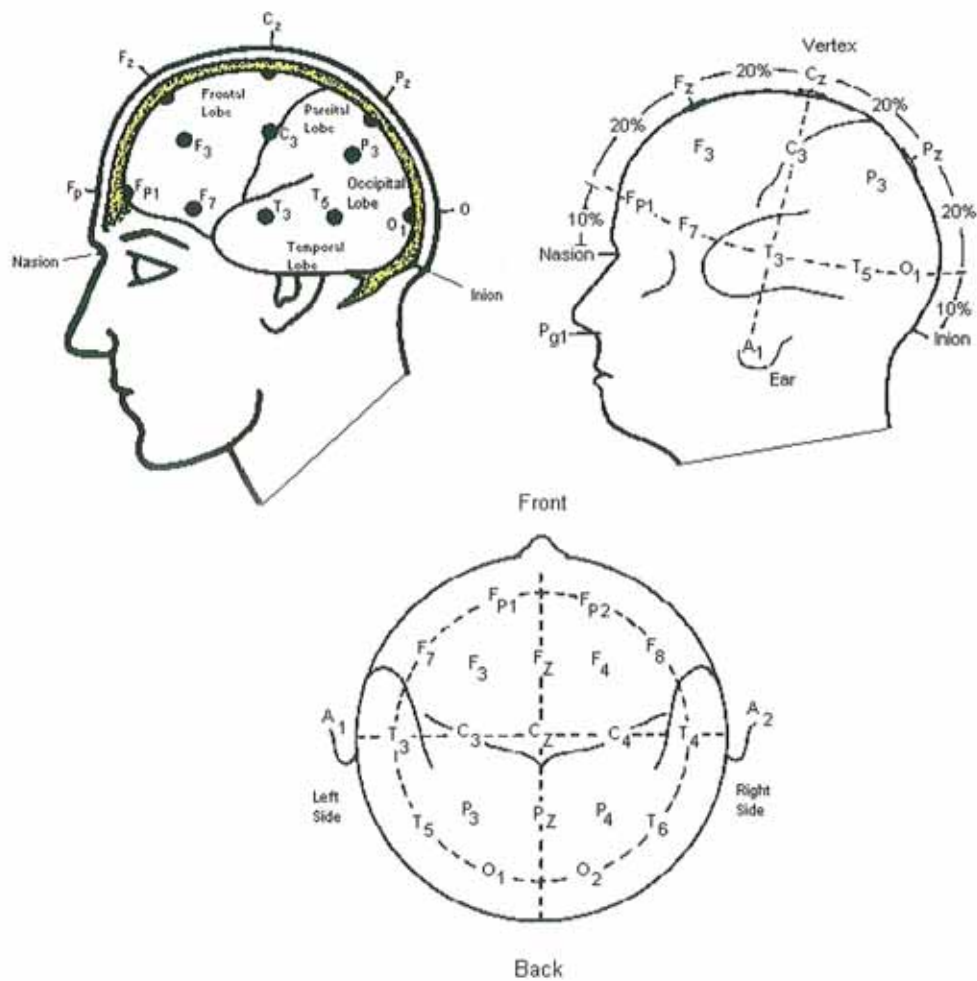
- seated at rest (stR)
- seated optimal hyperventilation (stOHV) protocol
- supine at rest (spR)
- supine optimal hyperventilation (spOHV) protocol.

### **3.1 Electrode application method**

The “10-20” system is the gold standard for EEG electrode placement and is used internationally (Harner and Sannitt 1974). It is based upon 10% and 20% distances taken from the head circumference, and coronal and para-sagittal measurements through the vertex, using the inion, nasion, and pre-auricular points as bony landmarks on the individual head as position indicators. Correct measurement ensures that that prescribed electrodes overly specific areas of the brain. For example Cz is the vertex position where C denotes central position

and z denotes over the midline. T4 is the right mid-temporal electrode etc. (see Fig 3.1)

**Fig 3.1: International 10-20 system of electrode placement for routine scalp EEG (Harner and Sannit 1974)**



The subjects head was initially measured as called for in the 10-20 system and the electrode positions marked with a skin pencil. The skin was then prepped with an abrasive paste, and the electrode cup filled with an electrolyte such as “elifix”. The impedance of each electrode should not exceed 5 K $\Omega$  to ensure a good EEG signal is obtained. The electrodes are connected to the EEG system via the input head-box which usually contains the pre-amplifiers. The raw EEG analogue signal is suitably amplified and filtered and passed through an ADC (analogue to digital converter), and the digital signal displayed on a monitor. Data are stored in memory during acquisition. Data may be kept on the main database or archived down to various digital storage media from which they are available for review and post processing, if required.

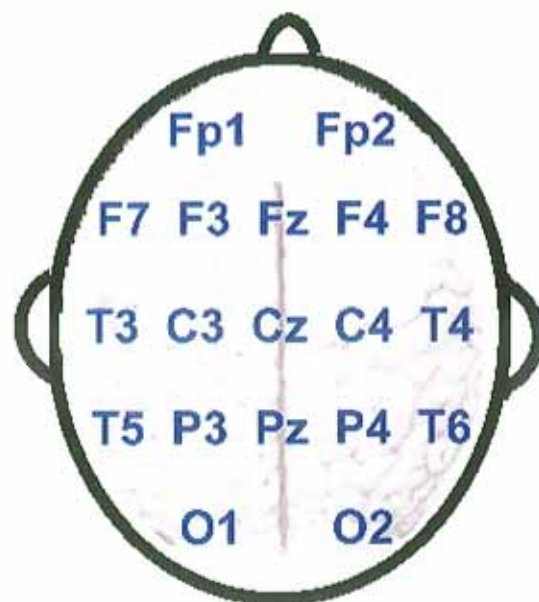


**Fig. 3.1.2: International 10/20 system. Electrode positions superimposed on brain image**

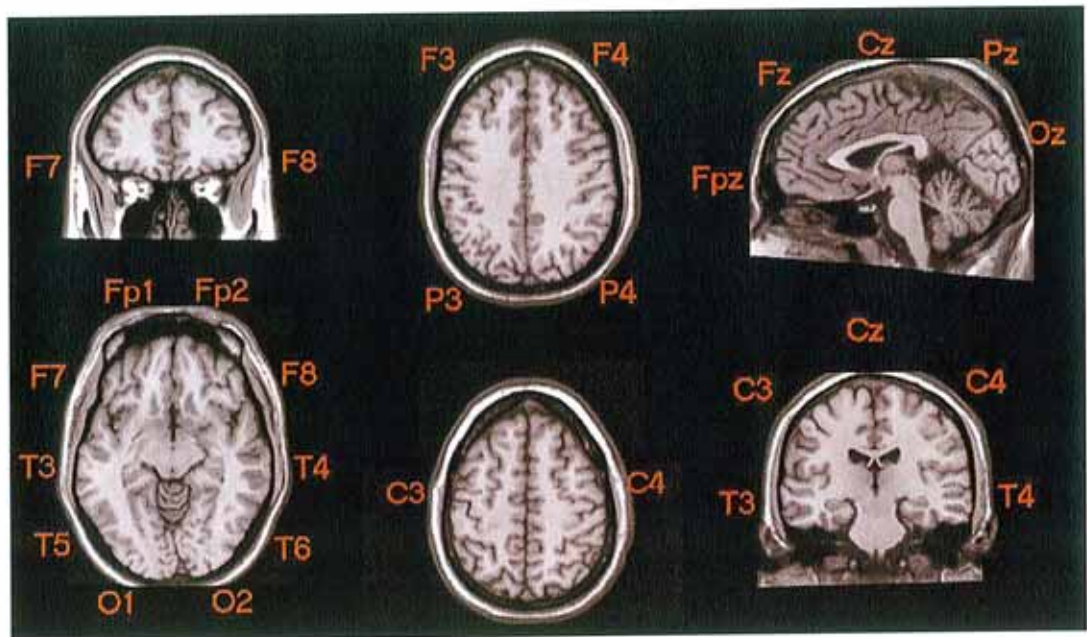


**Fig. 3.1.3: MRI slices nearest the international 10/20 electrode positions**

In most clinical applications, 21 recording electrodes (plus ground and system reference) are used. Additional electrodes can be added to the standard set-up when a clinical or research application demands increased spatial resolution for a particular area of the brain. High-density arrays (typically via cap or net) can contain up to 256 electrodes more-or-less evenly spaced around the scalp.

Each electrode is connected to one input of a differential amplifier (one amplifier per pair of electrodes). A common system reference electrode is connected to the other input of each differential amplifier. These amplifiers amplify the voltage between the active electrode and the reference (typically by a factor of 1,000-100,000, or + 60-100 dB of voltage gain). Filtering is normally implemented within the amplifier chain. Typical settings for the high and low

pass filters are 0.5-1.0 Hz and 15.0-70.0 Hz respectively. The high-pass filter typically filters out slow artefact such as sweat and movement, whereas the low-pass filter filters out high-frequency artefact, such as electromyographic (muscle) signals. An additional 50 Hz notch filter is typically used to remove artefact caused by electrical power lines.

A typical adult human EEG signal is about 10  $\mu$ V to 100  $\mu$ V in amplitude when measured from the scalp and is about 10-20 mV when measured from subdural electrodes.

The amplified analogue signal is digitised via an analogue-to-digital converter, after being passed through an anti-aliasing filter. Sampling preparatory to analogue-to-digital conversion typically occurs at 256-512 Hz in clinical scalp EEG; sampling rates of up to 10 kHz are used in some research applications.

Since an EEG voltage signal represents a voltage difference between two electrodes, the display of the EEG for the reading encephalographer may be set up in one of several ways. The representation of the EEG channels is referred to as a montage.

### **3.2 Physiological signals measured**

During the optimal hyperventilation breathing exercise the following physiological signals were monitored:

- scalp electroencephalogram (EEG)

- electrocardiogram (ECG), a modified lead II ECG, to monitor heart rate
- electro-oculogram (EOG) obtained by placing electrodes above and below the outer canthus of the right and left eyes. Slow rolling eye movements (SEM) are indicative of drowsiness, which is not desirable in a subject supposed to be concentrating upon optimal hyperventilation. If slow eye movements were noted the subject was roused to continue the hyperventilation exercise.
- electromyogram (EMG). Sub-mental (Below the chin) EMG, i.e. electromyogram or muscle recordings are also useful in determining the subject's state of arousal and their effort being made during the hyperventilation exercise.
- respiration rate and flow. A respiration belt is attached around the upper abdomen to obtain the respiration rate and display this with the EEG, ECG, EOG, and EMG on the monitoring screen.
- partial pressure of end-tidal carbon dioxide in expired air (pETCO<sub>2</sub>)
- saturation of peripheral oxygen (SpO<sub>2</sub>)
- blood pressure
- cerebral blood flow (velocity) in middle cerebral artery (sub-group only)
- total expired volume per minute (VE) (sub-group only)

### **3.3 Equipment**

- The electroencephalogram and polygraphic inputs were recorded using a "Nicolet" Digital Video EEG recording system (Alliance Works), with full post processing capabilities



- Expired CO<sub>2</sub> and respiration rate were monitored continuously via nasal prongs and side stream technology by the “Poet LT” Capnometer using non-dispersive infrared technology with auto-calibration
- pO<sub>2</sub> was monitored using an infrared finger probe and an Ohmeda Oximeter (Model 3900 series)
- A metronome was used to mark time and ensure that the subject breathed at the required 30 breaths per minute.
- A set of silver/ silver chloride (Ag/AgCl ) non polarisable disc electrodes to record EEG, ECG, EOG and EMG
- Digital automatic blood pressure measurement cuff
- Respiration rate obtained using a Nicolet respiration belt with inbuilt piezoelectric strain gauge

CBF (velocity) in the middle cerebral artery was monitored using a Nicolet transcranial Doppler system (Companion III).

### **3.4 EEG montage**

For the purpose of this study a specific “montage” (arrangement of EEG and polygraphic inputs) was designed containing 20 channels of EEG, right and left eye EOG, respiration, and ECG (Fig. 3.2.).

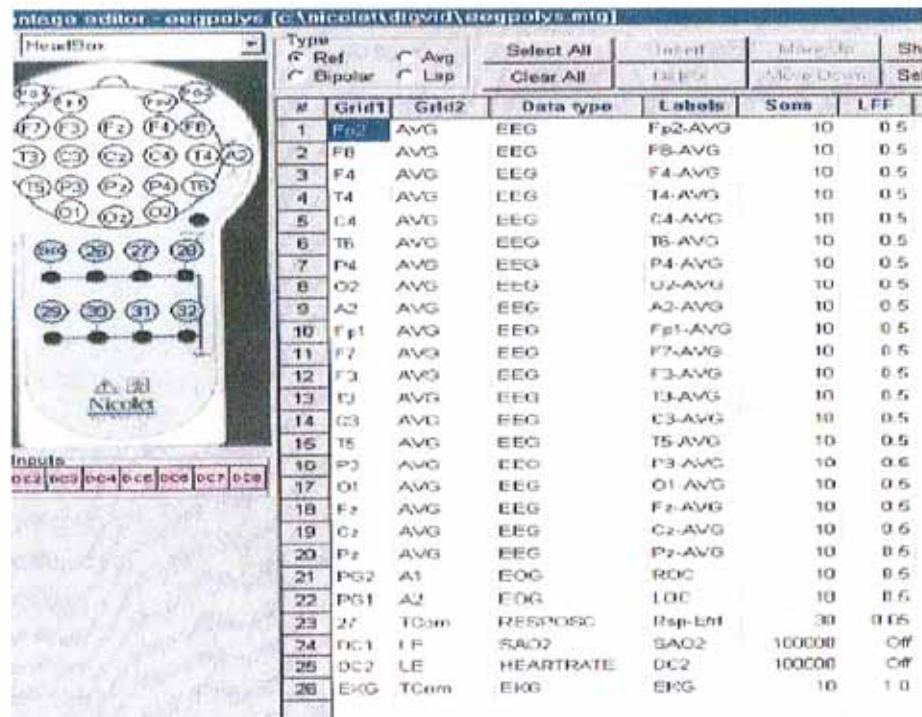
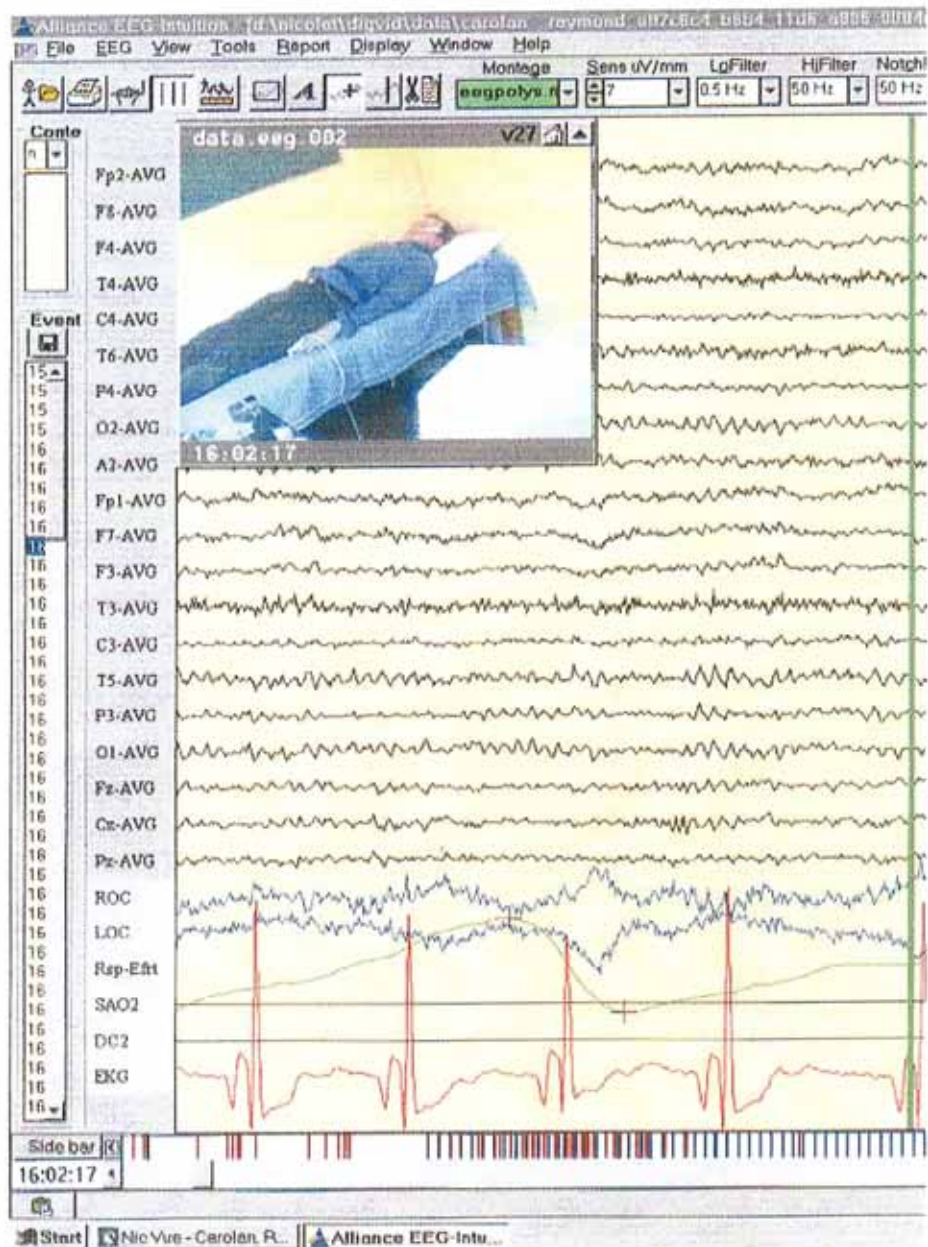


**Fig. 3.2: EEG montage for posture hyperventilation study**

These were input through the AC inputs of the headbox. The SaO<sub>2</sub> (saturated arterial Oxygen) input was via a DC input through the Ohmeda Oximeter. The Montage uses a common reference for all EEG input electrodes. This is to facilitate the digital signal processing performed on the information after acquisition.

A digital video image of the subject is acquired during the test using a colour JVC camera and the digital image displayed in real time on the monitor screen alongside the EEG and polygraphic information (Fig 3.3). This captures a visual record of the posture in which the resting EEG and the period of optimal hyperventilation is recorded. A zoom option on the camera is useful to view clinically visible physiological changes such as facial flushing, sweating and muscle twitching or tetany that may be induced by the HV exercise. This is also available off-line during the review phase.



Flashing display  
 RR 16/100  
 HR 65/100  
 O2 100%

Fig. 3.3: Digital video EEG

### 3.5 Capnography

Capnography is the monitoring of the concentration or partial pressure of carbon dioxide (CO<sub>2</sub>) in the respiratory gases. The capnogram is a direct measure of the inhaled and exhaled concentration or partial pressure of CO<sub>2</sub>, and an indirect measure of the CO<sub>2</sub> partial pressure in the arterial blood. In healthy individuals, the difference between arterial blood and expired gas CO<sub>2</sub> partial pressures is very small. Capnographs usually work on the principle that CO<sub>2</sub> absorbs infrared radiation. A beam of infrared light is passed across the gas sample to fall on a sensor. The presence of CO<sub>2</sub> in the gas leads to a reduction in the amount of light falling on the sensor, which changes the voltage in a circuit. The analysis is rapid and accurate, but the presence of nitrous oxide in the gas mix changes the infrared absorption via the phenomenon of collision broadening. This must be corrected for. End-tidal CO<sub>2</sub> (ETCO<sub>2</sub>) is the level of carbon dioxide released at the end of expiration.

Monitoring of pCO<sub>2</sub>/pETCO<sub>2</sub> is achieved by a hand held Criticare "Poet LT" capnometer, which uses a CO<sub>2</sub> breath-detection algorithm, with N<sub>2</sub>O compensation, and with a numeric display of respiration rate and a trend option measuring in 30-second intervals. It has an option for a serial output to printer of pETCO<sub>2</sub>, and respiration rate.

### 3.6 Oxygen Saturation

Oxygen saturation ( $\text{SO}_2$ ), commonly abbreviated as "sats", measures the percentage of haemoglobin binding sites in the bloodstream occupied by oxygen. At low partial pressures of oxygen, most haemoglobin is deoxygenated. At around 90% oxygen saturation it increases according to an oxygen-haemoglobin dissociation curve and approaches 100% at partial oxygen pressures of  $>10$  kPa. A pulse oximeter relies on the light absorption characteristics of saturated haemoglobin to give an indication of oxygen saturation. A  $\text{SaO}_2$  (arterial oxygen saturation) value below 90% is termed hypoxemia. This may be due to various medical conditions. Saturation of peripheral oxygen ( $\text{SpO}_2$ ) is an estimation of the oxygen saturation level usually measured with a pulse oximeter device. Pulse oximetry is a non-invasive method allowing the monitoring of the oxygenation of a patient's haemoglobin.

Pulse oximetry was developed in 1972 by an engineer, Takuo Aoyagi, working for the Nihon Kohden corporation (Tremper 1992) using the ratio of red to infrared light absorption of pulsating components at the measuring site. A sensor is placed on a thin part of the patient's anatomy, usually a fingertip or earlobe, and a light containing both red and infrared wavelengths is passed from one side to the other. Changing absorbance of each of the two wavelengths is measured, allowing determination of the absorbances due to the pulsing arterial blood alone, excluding venous blood, skin, bone, muscle and fat. Based upon the ratio of changing absorbance of the red and infrared light caused by the difference in color between oxygen-bound (bright red) and oxygen unbound (dark red or blue, in severe cases) blood haemoglobin, a measure of oxygenation (the per cent of

haemoglobin molecules bound with oxygen molecules) can be made. Pulse oximetry has limitations. It is a measure solely of oxygenation. The metabolism of oxygen can be readily measured by monitoring expired  $\text{CO}_2$ . Saturation figures also give no information about blood oxygen content. A patient can be severely anaemic but still be fully saturated. Pulse oximetry only reads the percentage of bound haemoglobin. It can be bound to other gases such as carbon monoxide and still read high even though the patient is hypoxic. Although pulse oximetry is used to monitor oxygenation, it cannot determine the metabolism of oxygen, or the amount of oxygen being used by a patient. For this purpose, it is necessary to also measure carbon dioxide ( $\text{CO}_2$ ) levels.

### **3.7 Transcranial Doppler ultrasonography (TCD) procedure**

Transcranial Doppler ultrasonography (TCD) was first described by Rune Aaslid in 1982 as a method of obtaining blood velocity information in intracranial vessels. During TCD measurement identification of the different arteries is based on the following factors relative to the skull surface:

- depth of the sample volume from the surface of the skull
- direction of flow
- angle of probe with respect to the skull

TCD using “blind” Doppler has its limitations as it is not possible to know the angle of insonation (AoL) except for the middle cerebral artery (MCA) in which the AoL is assumed to be close to 0 degrees. For the purpose of this study measurements of velocity of cerebral blood flow are taken from the MCA. The MCA is identified by the depth of the sample volume from the surface of skull,

the direction of flow (MCA is towards the probe) and the angle of the probe with respect to the skull.

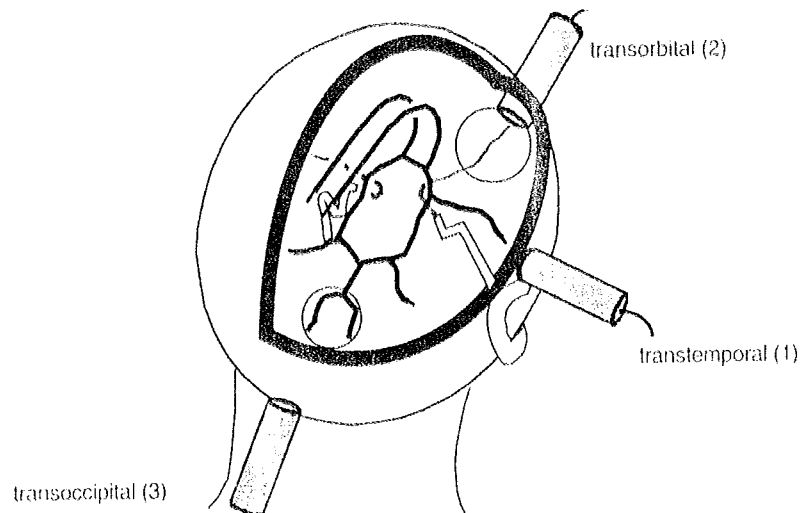


**Fig. 3.4a: TCD the transtemporal window (1), the transorbital window (2) and the transoccipital window (3) (Aaslid *et al* 1982)**

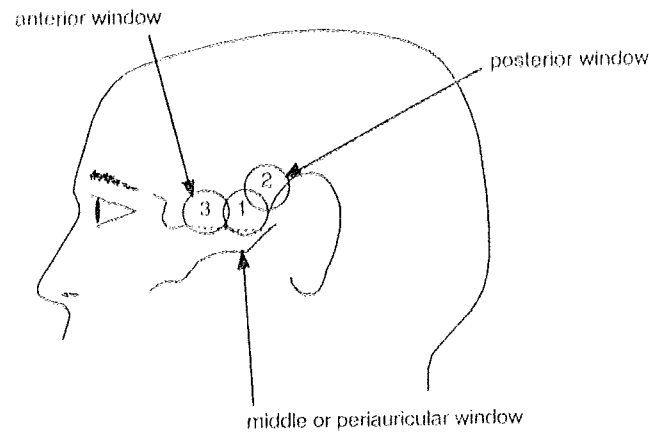


**Fig. 3.4b: TCD 3 positions through the transtemporal window (Aaslid *et al* 1982)**

There are three specific areas in the cranium, which are relatively thin and allow penetration of an ultrasound beam (Fig. 3.4a). These are referred to as the “acoustic windows”. There is the transtemporal window, the transorbital window and the transoccipital window. Measurements of vCBF in the MCA for this study are obtained by insonating through the transtemporal window using a 2 MHz pulsed Doppler probe (Fig. 3.4b). Velocity of CBF varies with age. There is a peak of approximately  $100 \text{ cm s}^{-1}$  at 4-6 years of age. VCBF is approximately  $70 \text{ cm s}^{-1}$  from 10-29 years (Fig. 3.4 c). Hypocapnia results in cerebral vasoconstriction reducing the vCBF. (see chapter 3 section 3.18)



Age (Years)	MCA
10-29	70 ± 6.4
30-49	57 ± 11.2
50-59	51 ±9.7
60-70	41 ± 7.0
Insonated depth (mm)	50-55

**Fig. 3.4c: VCBF in MCA with age (adapted from Aaslid *et al* 1982)**

A subgroup of 5 subjects had TCD screening. vCBF measurements were obtained in 4 test conditions, producing 20 data sets.

- Baseline supine resting (condition A)
- Baseline sitting resting (condition B) (Fig 3.4 d)
- Supine optimal hyperventilation (condition C)
- Sitting optimal hyperventilation (condition D)

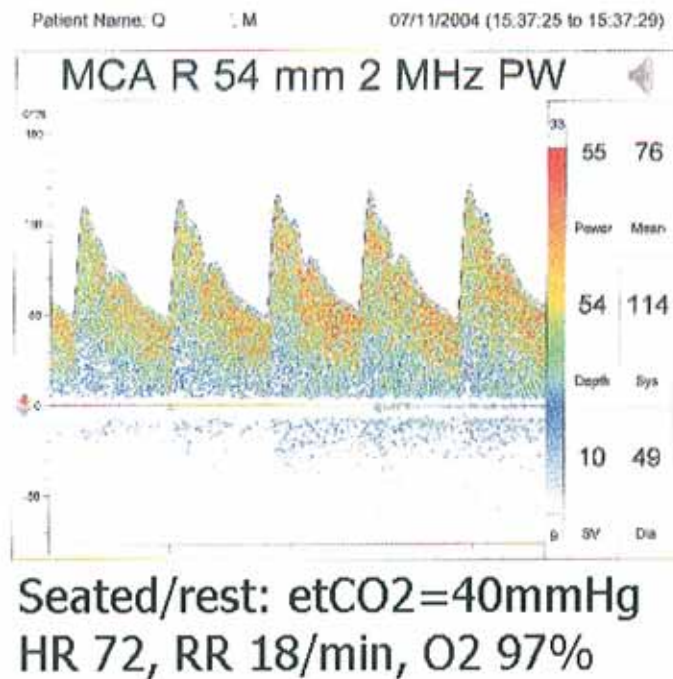


**Fig. 3.4d: Sample of TCD waveform with subject seated at rest**

### 3.8 Acquisition of each data set

- Full explanation and demonstration of the optimal hyperventilation technique to the subject before commencing the first hyperventilation activation. After this a signed informed consent is obtained.
- A resting record of 5 minutes duration performed initially with periods of eye opening and closure to obtain a baseline with which to compare any changes elicited during hyperventilation.
- A standardized method of hyperventilation was used (see Section 3.0)

- The test periods separated by a minimum of 20 minutes and the two positions randomly administered to control for order effects and to ensure that any difference in response is not due to an incomplete recovery from the first trial.
- EEG measurements continue for 6 minutes after each period of hyperventilation. Bilaterally synchronous slow activity has been reported to occur at 5 minutes post hyperventilation during the post hyperventilation phase.

### **3.9 Quantitative Analysis**

Quantitative digital EEG changes in the subjects in the resting state and during optimal hyperventilation, obtained while in the supine and seated position are reviewed, using linear and log spectral analysis of all channels, examining in particular, frequency and power spectra alterations during hyperventilation activation. Topographic maps of the power spectra of EEG frequencies from 0.5 Hz through 30.0 Hz are generated. During data review, re-montaging, re-filtering, and digital post-processing of data is possible.

Pre-hyperventilation baseline EEG, peri-optimal hyperventilation and post-optimal hyperventilation changes in the frequency, amplitude, topography and symmetry, of EEG waveforms are analysed using quantitative digital EEG (QEEG) methods. Topographical quantitative EEG changes in the mean spectral power density of the delta, theta, alpha, and beta frequency bands during and after optimal hyperventilation are compared to the baseline resting activity.

Changes in the power ratios between the four EEG frequency bands are measured using fast Fourier transform. Pre-, peri-, and post- optimal hyperventilation measurements of end-tidal  $p\text{CO}_2$ ,  $\text{SpO}_2$ , and the respiration rate are analysed for both supine and seated positions.

4-8 second sample epochs were analyzed every 30 seconds, i.e. 9 samples of 8 seconds each over the 4-minute hyperventilation period. (Post- hyperventilation monitoring continued for 6 minutes as it has been shown that  $p\text{O}_2$  falls to a nadir at about 5 minutes post-hyperventilation). These were compared to 4 x 8 second epochs of baseline EEG with eye closure in the resting postural state before hyperventilation commenced initially. The hyperventilation epoch during which the minimal  $p\text{ETCO}_2$  was obtained in each position, compared with baseline resting epoch, and examined for changes using appropriate statistical methods.

The most artefact-free epochs were chosen for analysis. Each epoch was subjectively screened for excessive eye movement or EMG artefacts before analysis.

### **3.10 EEG analysis software**

The “Persyst EEG suite” analysis software was used to analyse the EEG data. It consists of a package of analysis programs (“Insight, Spike Detector, and Prism”, Version 4.0) and can support multiple EEG system formats. This means that digital EEG (DEEG) data acquired on the Nicolet alliance platform can be reviewed using the analysis program. The software is used for EEG review, for

patient demographics, and can read recording system events, such as slow wave, seizure, and spike detection. The Insight program was used to review the EEGs, mark sections of interest, and apply speed, sensitivity, zoom, re-montaging and digital filtering adjustments to the EEG. It can also be used to copy data samples from selected channels to a spreadsheet for further analysis. Spike detector was used to automatically mark rhythmic bursts and manually reviewed the data afterward. Spike detector and review are accessed through Insight. The detection sensitivity can be adjusted after the record is scanned and re-analysed. Prism uses EEG power tools for voltage and spectral mapping. The power spectrum can be displayed by channel or by frequency band. Prism was used to create frequency band tables with up to eight bands and distinct colours for each band. The topograph plots can be animated to see spatial changes in frequency content over time (e.g. during optimal hyperventilation). Hemisphere differences are clearly illustrated with topograph symmetry plots. Prism was also used to show the pair-wise correlation and lag between numbers of channels simultaneously and the correlation plot was animated to see the onset of correlated activity.

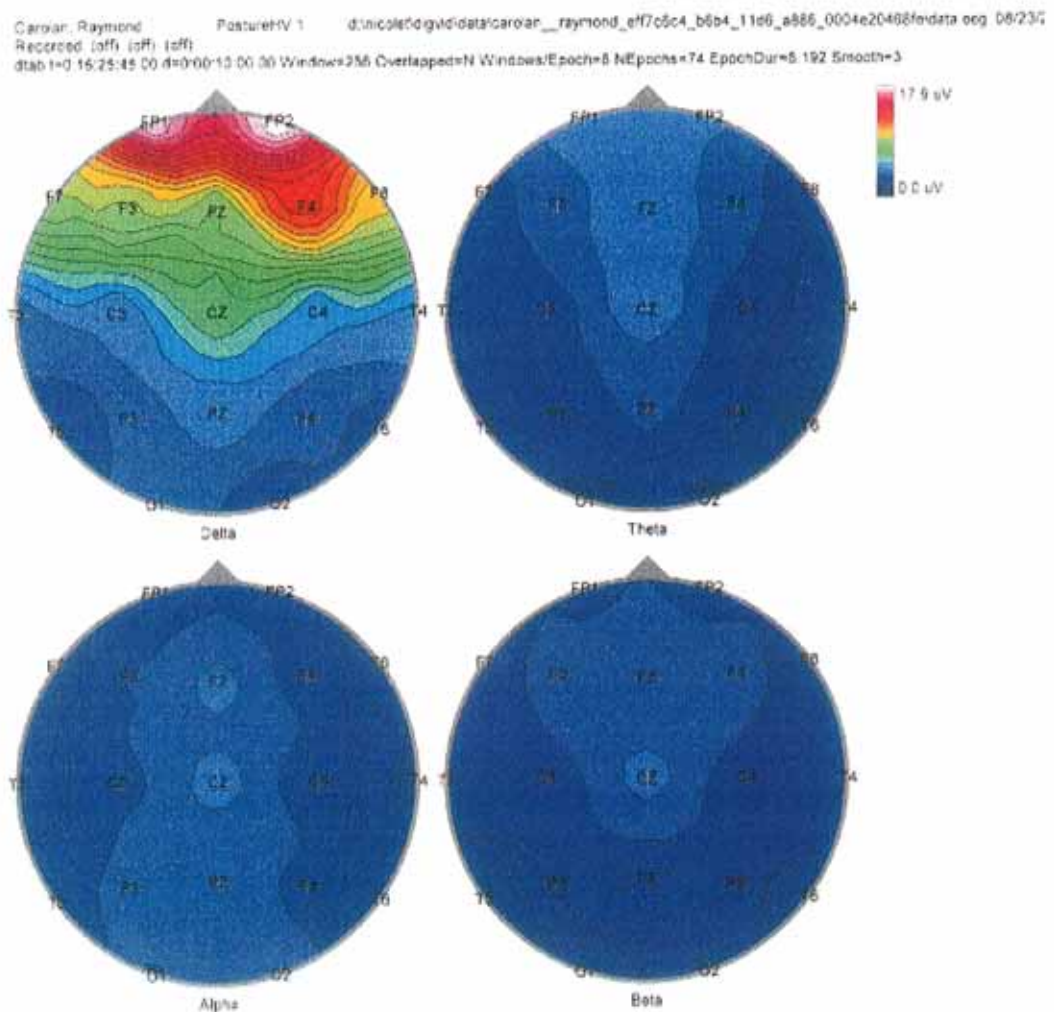
The fast Fourier transform (FFT) calculation for signal analysis is controlled via the points per window, windows per epoch, overlapping windows, and smoothing. Artefacts were removed from the spectral calculation by using multiple manually selected segments.

### **3.10.1 Topograph contour creation (Fig. 3.5)**

The contours in the topographs are created using the standard nearest point interpolation algorithm (Current Practice of Clinical Electroencephalography, 3<sup>rd</sup>

ed, 2003, Ebersole J, Pedley T). The number of electrodes used can be adjusted as can the number of points on the interpolation grid, as well as the interpolation order (linear, squared or cubed). Only the active electrodes, i.e those in the current montage, are used when determining the nearest electrodes.

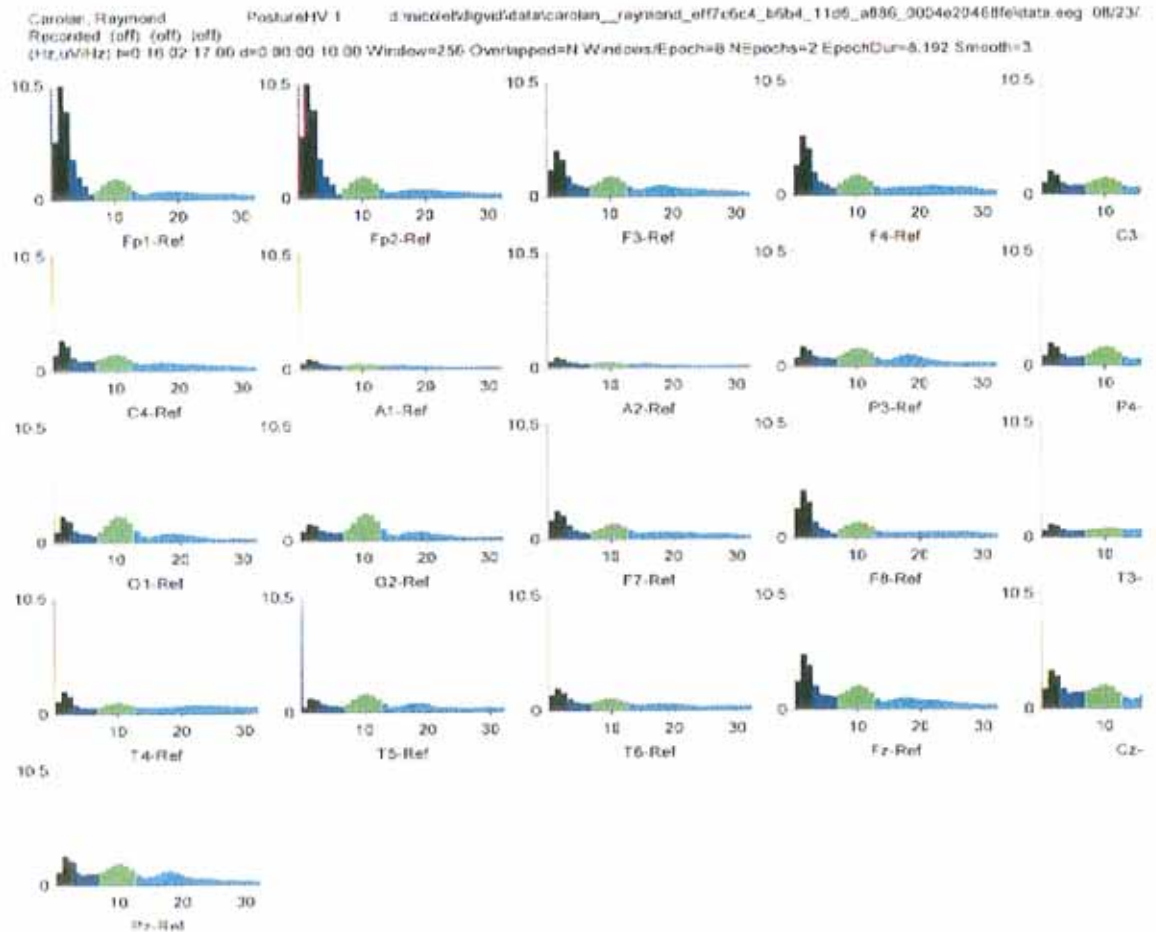
**Fig. 3.5: Sample of topographic plot of delta, theta, alpha and beta EEG frequency bands**



### **3.10.2 Power Spectrum (Fig. 3.6)**

To describe a given signal uniquely both an amplitude spectrum and a phase spectrum are required. Often the amplitude values are squared and the result is then called a “power spectrum”. The sum of the values of the power spectrum is equal to the total power or mean square value of the original signal (Parseval's theorem). This is why power or variance measures are often used instead of amplitude measures in signal analysis

**Fig. 3.6: Sample of power spectrum (Hz,  $\mu\text{V}/\text{Hz}$ ) of 10-20 scalp electrodes**



### 3.10.3 Fast Fourier transform (FFT) calculation

The standard FFT calculation is used to compute the power spectra (Current Practice of Clinical Electroencephalography 3rd ed. 2003). The power spectrum for a window is computed with “points per window” data samples. The spectrum for an epoch is created by averaging the “windows per epoch” spectra. When using “overlap windows” each FFT computation is shifted by only half



the number of points per window. The waveform data filters are Butterworth IIR, i.e. single order low and high pass, double order notch filters.

### **3.11 RESULTS**

All variables were distributed normally and differences between the normocapnia and supine hypocapnia, normocapnia and seated hypocapnia, and supine and seated hypocapnia studies were analysed with paired students *t*-tests.

### **3.12 Subjective symptoms**

Subjects reported the symptoms they experienced while engaged in the standardised OHV exercise: (percentages are rounded off)

- Feeling light headed or dizzy 21%
- Paraesthesia, tingling or other sensations in hands, feet or peri-oral area  
18%
- Feeling hot /sweaty 5%
- Feeling cold/sweaty 17%
- Shivering 17%
- Goosebumps 17%
- Muscle cramp 1%
- Headache 4%

The 22 subjects in the study population, who performed the OHV exercise in the seated posture reported a total of 102 subjective symptoms. 38 mixed subjective

symptoms were experienced by 8 males and 64 by 14 females during St OHV (Table 3.2). The same 22 subjects who performed the OHV exercise in the supine posture reported a total of 87 subjective symptoms. A mixture of 36 subjective symptoms were experienced by 8 males and 51 by 14 females during SpOHV (Table 3.3). Wilcoxon signed-rank test comparing the symptoms experienced during HV in the two positions yields a  $p < 0.001$  (Table 3.5). This indicates that performing the SOHV exercise in the seated posture has some degree of statistical significance with regard to the symptoms reported by the subjects. Similar symptoms are reported in the literature in patients with anxiety and panic disorders. These conditions are commonly associated with hyperventilatory symptoms. Sheikh *et al* (2002) reported that studies of panic disorders with respiratory symptoms consistently noted a higher incidence in women than in men. There was no significant difference in the subjective symptoms experienced by males and females during hyperventilation in this study population. The subjects in this study did not report any heart palpitations, shortness of breath or chest pain which are commonly noted in patients with panic disorder. There is conflicting evidence in the literature that hyperventilation causes panic attacks (Roth 2005). None of the subjects in this study became unduly distressed by their subjective symptoms and no episodes of anxiety or panic were induced. None of the subjects had a past history of anxiety disorder, but the fact that the hyperventilation exercise was performed in a “safe and controlled” environment may have contributed to a positive bias in preventing the onset of anxiety related symptoms.

Age	Male	Female
50-54	0	1
45-49	1	2
40-44	0	1
35-39	0	1
30-34	0	1
25-29	2	3
20-24	4	5
16-19	1	0
<b>Total</b>	<b>8</b>	<b>14</b>

**Table 3.1: Age and gender of study population**

	Male:38 symptoms	Female: symptoms	64	Total: Symptoms	102
<b>Light headed/Dizzy</b>	<b>8 (21%)</b>	<b>14 (21.5%)</b>		<b>22 (21.8 %)</b>	
<b>Paraesthesia</b>	<b>6 (15.7%)</b>	<b>13 (20.3%)</b>		<b>19 (18.63%)</b>	
<b>Tetany</b>	<b>0 (0%)</b>	<b>0 (0%)</b>		<b>0 (0%)</b>	
<b>Hot/sweaty</b>	<b>2 (5%)</b>	<b>3 (4.84%)</b>		<b>5 (4.90%)</b>	
<b>Cold/sweaty</b>	<b>7 (18%)</b>	<b>10 (15.87%)</b>		<b>17 (16.66%)</b>	
<b>Shivering</b>	<b>7 (18%)</b>	<b>10 (15.86%)</b>		<b>17 (16.66%)</b>	
<b>Goosebumps</b>	<b>7 (18%)</b>	<b>10 (15.87%)</b>		<b>17 (16.66%)</b>	
<b>Muscle cramp</b>	<b>0 (0%)</b>	<b>1 (1.58%)</b>		<b>1 (1.01%)</b>	
<b>Headache</b>	<b>1 (3%)</b>	<b>3 (3.17%)</b>		<b>4 (3.98%)</b>	
<b>No symptoms</b>	<b>0 (0%)</b>	<b>0 (0%)</b>		<b>0 (0%)</b>	

**Table 3.2: Subjective symptoms by gender during seated OHV (StOHV)**

Paired students *t*-test of the percentage of symptoms experienced by males compared to females during seated optimal hyperventilation did not reach significance ( $p < 0.806$ )

	Male:36 symptoms	Female: 51 symptoms	Total symptoms: 87
Light headed/Dizzy	6 (16.69%)	10 (19.6%)	16 (18.39%)
Paraesthesia	5 (13.88%)	11 (21.56%)	16 (18.39%)
Tetany	0 (0%)	0 (0%)	0 (0%)
Hot/Sweaty	1 (2.77%)	1 (1.97%)	2 (2.30%)
Cold/Sweaty	8 (22.2%)	9 (17.65%)	17 (19.54%)
Shivering	8 (22.2%)	9 (17.65%)	17 (19.54%)
Goosebumps	8 (22.2%)	9 (17.65%)	17 (19.54%)
Muscle cramp	0 (0%)	0 (0%)	0 (0%)
Headache	0 (0%)	2 (3.93%)	2 (2.30%)
No symptoms	0 (0%)	0 (0%)	0 (0%)

**Table 3.3: Subjective symptoms by gender during supine OHV (SpOHV)**

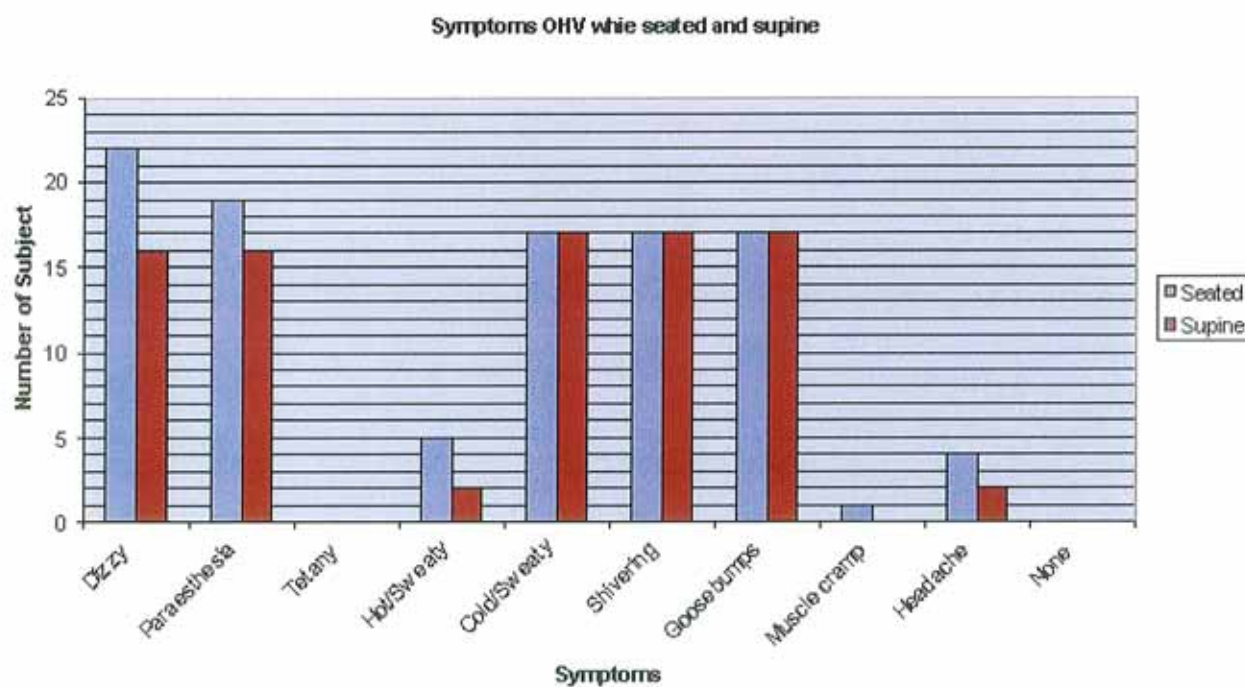
Paired students *t*-test of the percentage of symptoms experienced by males compared to females during supine optimal hyperventilation did not reach significance ( $p < 0.977$ )

**Table 3.4 : Total subjective symptoms, seated OHV and supine OHV**

Wilcoxon Signed-Rank test  $p < 0.001$

Symptoms	Seated : 102	Supine: 87
Light Headed/Dizzy	22 (21.5%)	16 (18.39%)
Paraesthesia	19 (18.63%)	16 (18.39%)
Tetany	0 (0%)	0 (0%)
Hot/Sweaty	5 (4.9%)	2 (2.3%)
Cold/Sweaty	17 (16.66%)	17 (19.54%)
Shivering	17 (16.66%)	17 (19.54%)
Goosebumps	17 (16.66%)	17 (19.54%)
Muscle Cramp	1 (1.01%)	0 (0%)
Headache	4 (3.98%)	2 (2.3%)
No Symptoms	0 (0%)	0 (0%)

**Fig. 3.7: Total of subjective symptoms, seated OHV and supine OHV**



### **3.13 Analysis**

44 separate trials were obtained on the 22 subjects each with a period of optimal HV in the seated and supine position as previously described.

Initially the raw data were examined and sample epochs of 4 –8 seconds duration taken every 30 seconds for analysis. Some epochs were excluded as they contained biological artefacts such as large eye blinks or excessive muscle activity. Eye blinks are slow frequency components of a non-cerebral nature that would therefore fall into the EEG delta range if not manually extracted from the analysis. Muscle activity is a fast frequency and is viewed by the analysis program as falling into the beta range if not manually excluded.

The epochs at which the subject recorded the lowest level of pETCO<sub>2</sub> and the most marked slowing in EEG frequencies were noted for further analysis. It was noted that the lowest pETCO<sub>2</sub> always corresponded with the epoch which contained the slowest EEG activity in the theta and occasionally in the delta range.

The “persyst EEG suite” analysis program (section 3.11) was used to define epochs for quantitative analysis.

### **3.14 Box Plots**

A box plot, or a “box and whiskers” plot is a graphic display that uses descriptive statistics based on percentiles (Tukey 1977). It simultaneously displays the median, the interquartile range (IQR), and the smallest and largest values for a group (Norusis 1998). The length of the box corresponds to the IQR; that is the box begins with the 25<sup>th</sup> percentile and ends with the 75<sup>th</sup> percentile. A line within the box indicates the location of the median or 50<sup>th</sup> percentile. Thus the box provides information about the central tendency and the variability of the middle 50% of the distribution. The “Whiskers” of the plot extend to the smallest and largest values that are not minor or extreme outlying values. Individual scores between 1.5 times the IQR and 3 times the IQR away from the edges of the box are minor outlying values. These are denoted on the box plot with the symbol “O”. The box plot is particularly well suited for comparisons among several groups.

### **3.15 Comparison of partial end tidal CO<sub>2</sub> (pETCO<sub>2</sub>) following 4 minutes of optimal hyperventilation controlled for posture**

44 separate trials of standardised hyperventilation were obtained from 22 subjects in both the supine (SpOHV) and seated (StOHV) positions. The mean value of pETCO<sub>2</sub> achieved during SpOHV was 23.5 mmHg (SD1.28). The mean value of pETCO<sub>2</sub> obtained during StOHV was 14.4 mmHg (SD 0.996). Using students paired *t*- test the probability of this result supporting the null hypothesis, is <0.0001 (CI 95%).

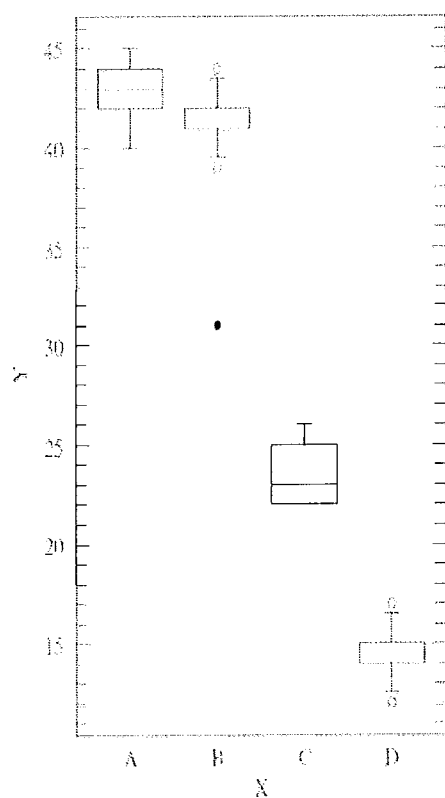


**Table 3.5 Paired student's *t*-test: results  
end-tidal CO<sub>2</sub>, supine OHV and seated OHV**

	<b>StOHV</b>	<b>SpOHV</b>	<b><i>p</i> value</b>
<b>Mean (SD)</b>	<b>14.11 (0.996)</b>	<b>23.5 (1.28)</b>	<b>0.0001</b>
<b>N=</b>	<b>44</b>	<b>44</b>	

**Fig. 3.8: Box plot of pETCO<sub>2</sub> at rest and during Sp OHV and StOHV**  
Y axis are units in mmHg

Posture	A=Supine Rest	B=Seated Rest	C=Sp OHV	D=St OHV
Range	40-45 mmHg	39- 44mmHg	22-26 mmH g	12-17 mmHg
Mean	42.6mmHg	41.4mmHg	23.5 mmH g	14.4mmHg
Standard Dev.	1.63	0.972	1.28	0.996



### 3.16 Comparison of EEG frequency in Hz, following 4 minutes of optimal hyperventilation controlled for posture

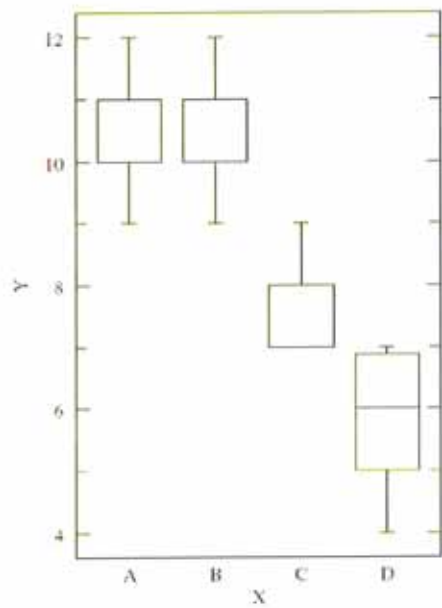
44 separate trials of standardised hyperventilation were obtained from 22 subjects in both the supine (SpOHV) and seated (StOHV) positions. The mean value of EEG frequency achieved during SpOHV was 7.7 Hz (SD 0.650). The mean value of EEG frequency obtained during StOHV was 5.91 Hz (SD 0.878). Using students paired *t*- test the probability of this result supporting the null hypothesis, is <0.0001 (CI 95%).

**Table 3.6 Paired student's *t*-test: results  
EEG frequency in Hz, seated OHV and supine OHV**

	<b>StOHV</b>	<b>SpOHV</b>	<b><i>P</i> value</b>
<b>Mean (SD)</b>	<b>5.91(0.878)</b>	<b>7.7 (0.650)</b>	<b>0.0001</b>
<b>N=</b>	<b>44</b>	<b>44</b>	

**Fig. 3.9: Box plot of EEG in Hz at rest and during Sp OHV and StOHV Y axis units are Hz**

Posture	A=Supine Rest	B=Seated Rest	C=Sp OHV	D=St OHV
Range	9-12Hz	9-12Hz	7-9Hz	4-7Hz
Mean	10.5 Hz	10.5Hz	7.7Hz	5.91Hz
Standard Dev.	0.728	0.728	0.650	0.878



### 3.17 Change in heart rate with SpOHV and StOHV

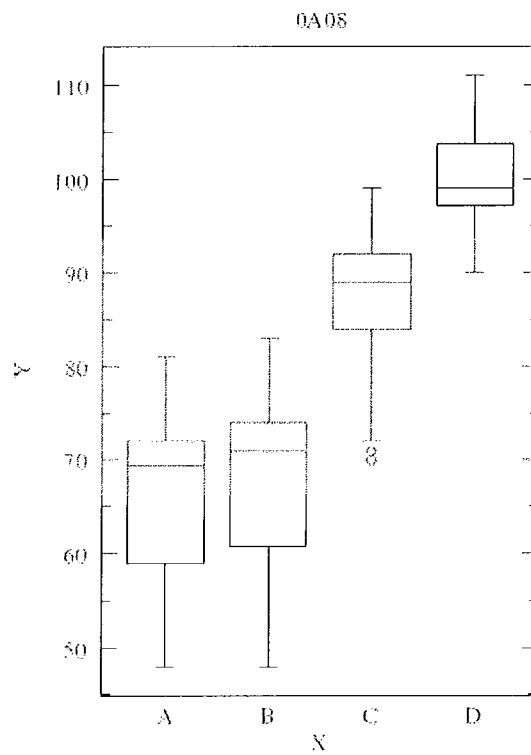
Using a standard of 30 breaths per minute, one cycle to include a full inspiration and full nasal expiration, the mean heart rate measured during SpOHV was 87.9 beats per minute (bpm) (SD 7.1). Under the same breathing regime, the mean heart rate measured during StOHV was 100 bpm (SD 4.7). There is a mean difference of +12.1 bpm in the heart rate of the subjects when undertaking the standardized HV exercise while in the seated position compared to the supine position.

**Table 3.7 Paired student's *t*-test: results**  
**Heart rate in bpm, seated OHV and supine OHV**

	StOHV	SpOHV	<i>p</i> value
<b>Mean (SD)</b>	<b>100(4.7)</b>	<b>87.9 (7.1)</b>	<b>0.0001</b>
<b>N=</b>	<b>44</b>	<b>44</b>	

**Fig. 3.10: Box plot of heart rate in bpm at rest and during SpOHV and StOHV** Y axis units are bpm.

Posture	A=Supine Rest	B=Seated Rest	C=Sp OHV	D=St OHV
Range	48-81	48-83	70-99	90-111
Mean	67	68.6	87.9	100
Standard Dev.	8.4	8.8	7.1	4.7



### **3.18 Transcranial Doppler ultrasound measurement of the velocity of cerebral blood flow (vCBF)**

A sub-group of the study population also had TCD performed to assess vCBF at rest while supine and seated, and during SpOHV and StOHV. There were 5 subjects in the sub-group and two trials were obtained from each, producing 10 data sets. A Nicolet Pioneer III TCD system was available to the investigator for one week, during which time the 5 subjects were studied (subjects 3, 4, 5, 6, 7). A 2MHz Doppler pulse wave probe was used to measure the vCBF in the right middle cerebral artery, as described in chapter 3, section 3.8. The velocity of CBF was measured at the minimal pETCO<sub>2</sub> reached by each subject during SpOHV and StOHV. The mean blood velocity (in cm s<sup>-1</sup>) in the MCA, for subjects aged between 10-29 years is 70 ± 6.4 (Newell *et al* 1992). Decreases in the vCBF between 31-42% compared to baseline values, have been identified during hyperventilation (Jibiki *et al* 1992). In this group the mean vCBF while supine at rest is 68.8 cm s<sup>-1</sup>. The mean vCBF while seated at rest is 68.3 cm s<sup>-1</sup>. There is no significant difference between the mean vCBF at rest while supine and seated (p=0.751). However during the standardised HV exercise the mean vCBF while supine is 38 cm s<sup>-1</sup>, and while seated is 29.5 cm s<sup>-1</sup>. There is a decrease of 8.5 cm s<sup>-1</sup> in the velocity of the cerebral blood flow seen during standardised optimal hyperventilation in the seated position (StOHV) (p<0.001). Decreases in the vCBF of between 44.7% while seated and 56.8% while supine are identified in this group compared to baseline values. There is an association between the efficacy of optimal hyperventilation in the seated position and the increase in the power frequency spectra of the slower theta and delta EEG

frequencies. The cause would appear to be the reduction in  $p\text{CO}_2$ . However this is a small group with only 10 trials on 5 subjects, and so the power is low. A more extensive study is required to confirm these findings.

**Table 3.8 Paired student's *t*-test: results  
vCBF in  $\text{cm s}^{-1}$ , supine OHV and seated OHV**

	<b>StOHV</b>	<b>SpOHV</b>	<b><i>P</i> value</b>
<b>Mean (SD)</b>	<b>29.5 (4.3)</b>	<b>38 (3.1)</b>	<b>0.001</b>
<b>N=</b>	<b>10</b>	<b>10</b>	



**Fig. 3.11: Box plot of vCBF in  $\text{cm s}^{-1}$  during Sp OHV( sample in Fig. 3.14) and StOHV (sample in Fig. 3.15). Y axis is in  $\text{cm s}^{-1}$ ( $p<0.001$ )**

Posture	A=Supine Rest	B=Seated Rest	C=Sp OHV	D=St OHV
Range	65.91-71.81	65.19-71.21	35.81-40.19	26.37-32.63
Mean	68.8	68.2	38	29.5
Standard Dev.	4.21	4.21	3.06	4.34

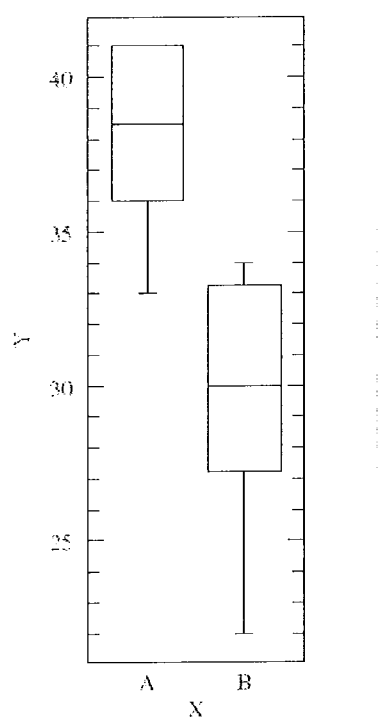


Fig. 3.12: Trial 1 subject 6 trial 1 . TCD of right MCA supine at rest

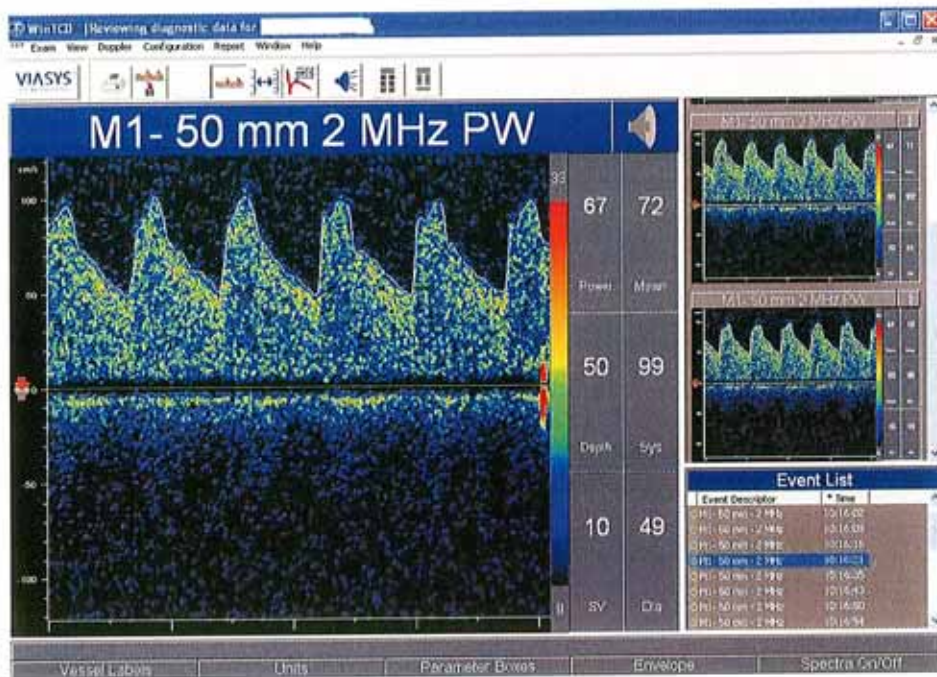
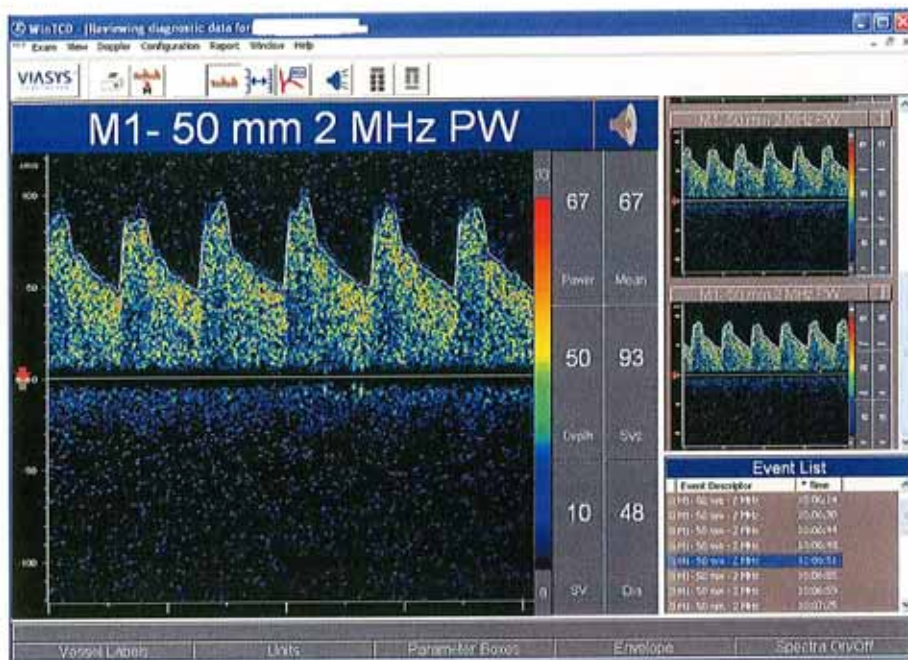
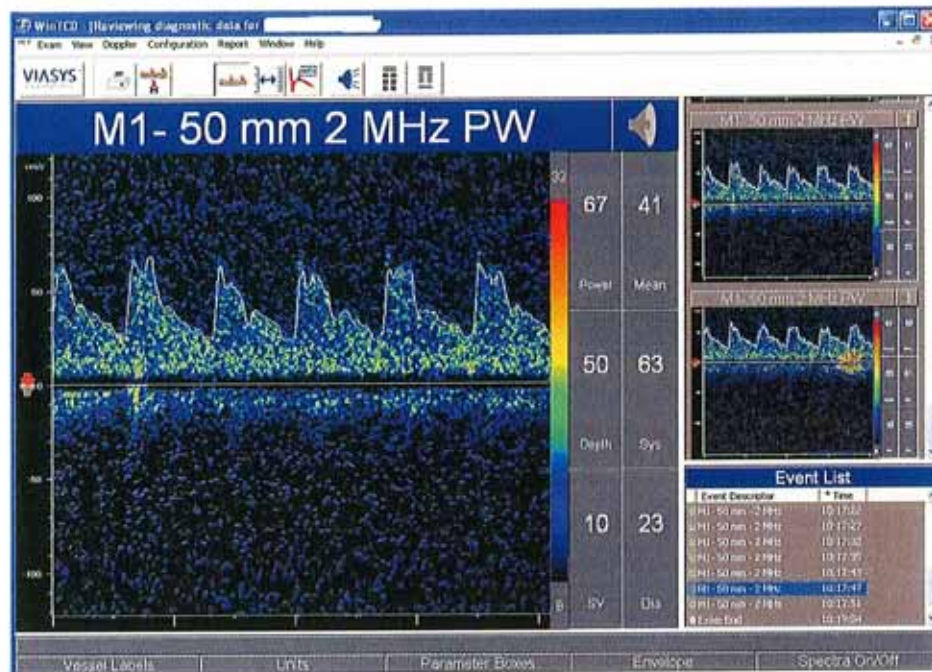


Fig. 3.13: Trial 1 subject 6. TCD of right MCA seated at rest

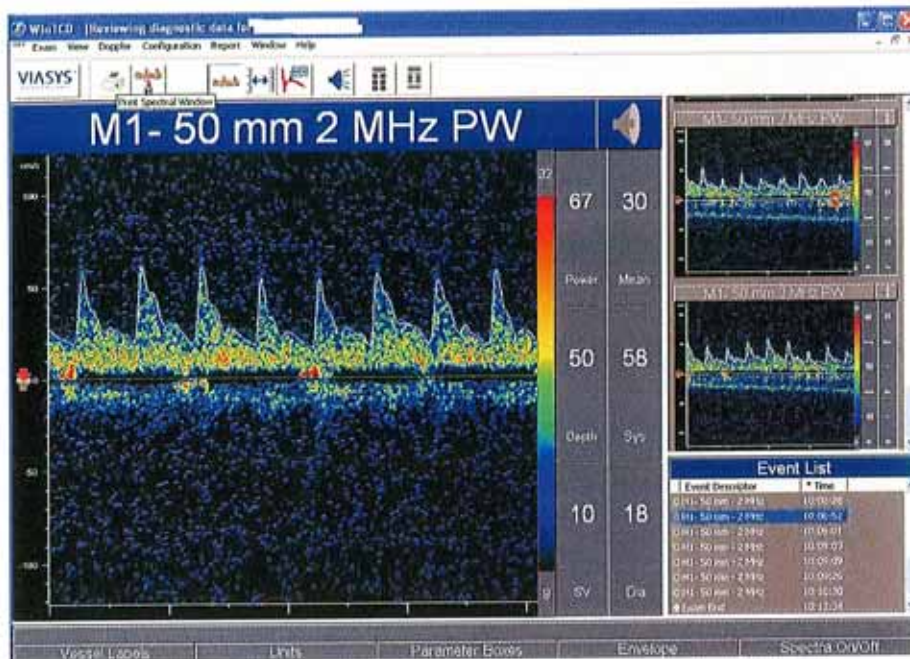


**Fig. 3.14: Trial 1 subject 6. TCD of right MCA supine during SOHV, at pETCO<sub>2</sub> of 22 mmHg**





**Fig. 3.15: Trial 1 subject 6. TCD of right MCA seated during SOHV, at pETCO<sub>2</sub> of 13 mmHg**



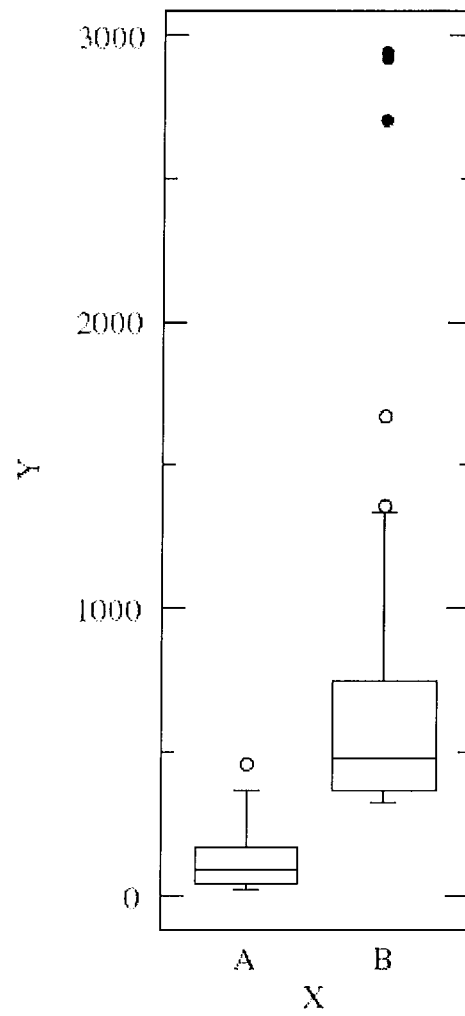
### 3.19 Power density of low frequency bands

The power density of EEG low frequency bands 3.0-7.5 Hz showed a highly significant increase during StOHV ( $p < 0.002$ ).

**Table 3.9 Paired student's *t*-test: results**  
**Power density of low frequency bands in EEG ( $\mu V^2$ ), supine OHV and seated OHV**

	StOHV	SpOHV	<i>p</i> value
Mean (SD)	877 (861)	133 (119)	0.001
N=	44	44	

**Fig. 3.16: Box plot of power density of low frequency bands**  
Y axis is power density in  $\mu V^2$



### **3.20 Case presentation, Subject 3 (27-year-old male)**

This study generated large quantities of data. A case presentation is utilized to illustrate the data acquired for each subject and each trial, and the analysis performed on that data to produce the reported results. The case presented equates closely to the median of results obtained. This subject was included in the sub-group of 5 subjects who had transcranial Doppler ultrasound of the middle cerebral artery (MCA) performed. Details of the entire data set and test results are available for reference in the CD which is attached to the back inside cover of this thesis (Appendix 6, file 1).

The subject 3 is a 27-year-old male. Data from this subject's second trial is presented (Trial no. 6 in a total series of 44 trials). Each subject's results were entered into an excel workbook. This detailed all the measurements made (Table 3.11).

**Table 3.10 Sample from Excel file of data on each subject  
(this is subject 3, trial no. 6)**

**End-tidal CO<sub>2</sub> in mmHg**

<b>Trial No</b>	<b>Sp Rest</b>	<b>St Rest</b>	<b>Sp OHV</b>	<b>St OHV</b>
<b>6</b>	<b>45</b>	<b>41</b>	<b>23</b>	<b>15</b>

**Dominant EEG frequency in Hz**

<b>Trial No</b>	<b>Sp Rest</b>	<b>St Rest</b>	<b>Sp OHV</b>	<b>St OHV</b>
<b>6</b>	<b>11</b>	<b>11</b>	<b>7</b>	<b>6</b>

**Heart rate per minute (bpm)**

<b>Trial No</b>	<b>Sp Rest</b>	<b>St Rest</b>	<b>Sp OHV</b>	<b>St OHV</b>
<b>6</b>	<b>48</b>	<b>48</b>	<b>74</b>	<b>99</b>

**Respiration rate per minute**

<b>Trial No</b>	<b>Sp Rest</b>	<b>St Rest</b>	<b>Sp OHV</b>	<b>St OHV</b>
<b>6</b>	<b>16</b>	<b>19</b>	<b>30</b>	<b>30</b>

**vCBF in cm s<sup>-1</sup> measured with TCD**

<b>Trial No</b>	<b>Sp Rest</b>	<b>St Rest</b>	<b>Sp OHV</b>	<b>St OHV</b>
<b>6</b>	<b>72</b>	<b>67</b>	<b>37</b>	<b>34</b>

**Peak power spectra of low frequencies from 2.0-7.5 Hz (in  $\mu\text{V}^2$ )**

<b>Trial No</b>	<b>Sp Rest</b>	<b>St Rest</b>	<b>Sp OHV</b>	<b>St OHV</b>
<b>6</b>	<b>72</b>	<b>72</b>	<b>81</b>	<b>603</b>



**Fig. 3.17: pETCO<sub>2</sub> (mmHg) and EEG (Hz) in both postures at rest and during HV**

**Subject 3. Note decrease in both pETCO<sub>2</sub> and EEG frequencies during HV.**

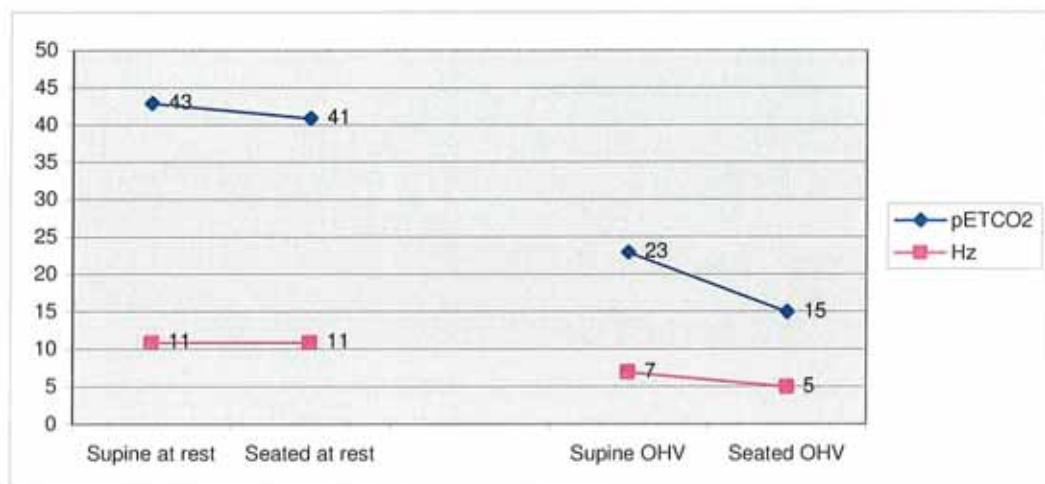


**Fig. 3.18: pETCO<sub>2</sub>(mmHg) and heart rate (bpm) in both postures at rest and during HV, subject 3. Note increase in heart rate and concomitant decrease in pETCO<sub>2</sub> during HV.**

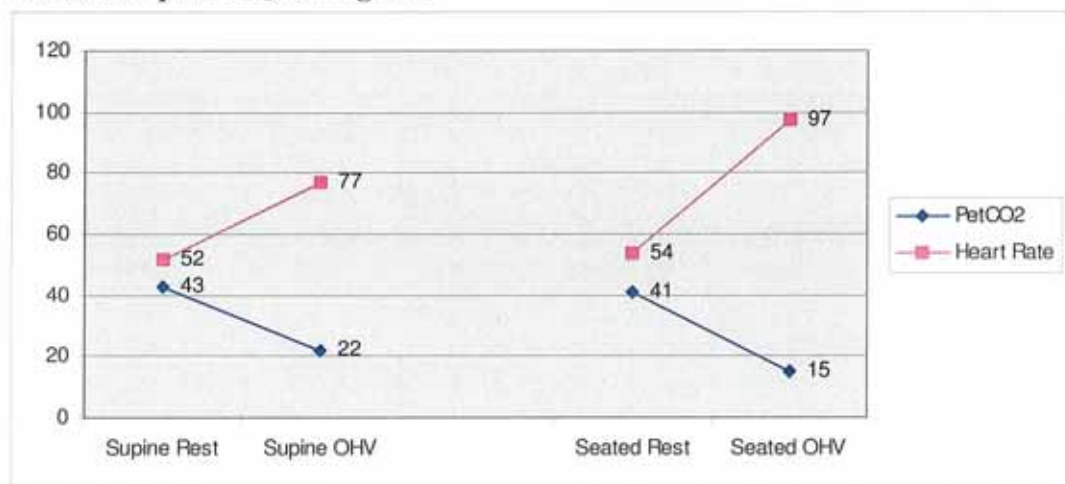


**Fig. 3.18: pETCO<sub>2</sub>(mmHg) and heart rate (bpm) in both postures at rest and during HV** The decrease in both pETCO<sub>2</sub> and EEG frequencies is reproducible over two trials in the same subject

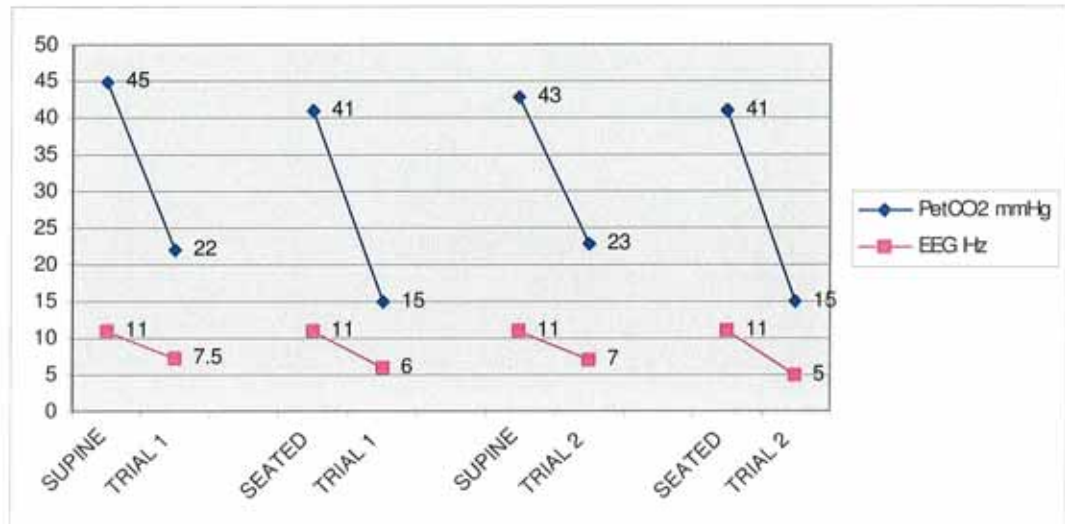
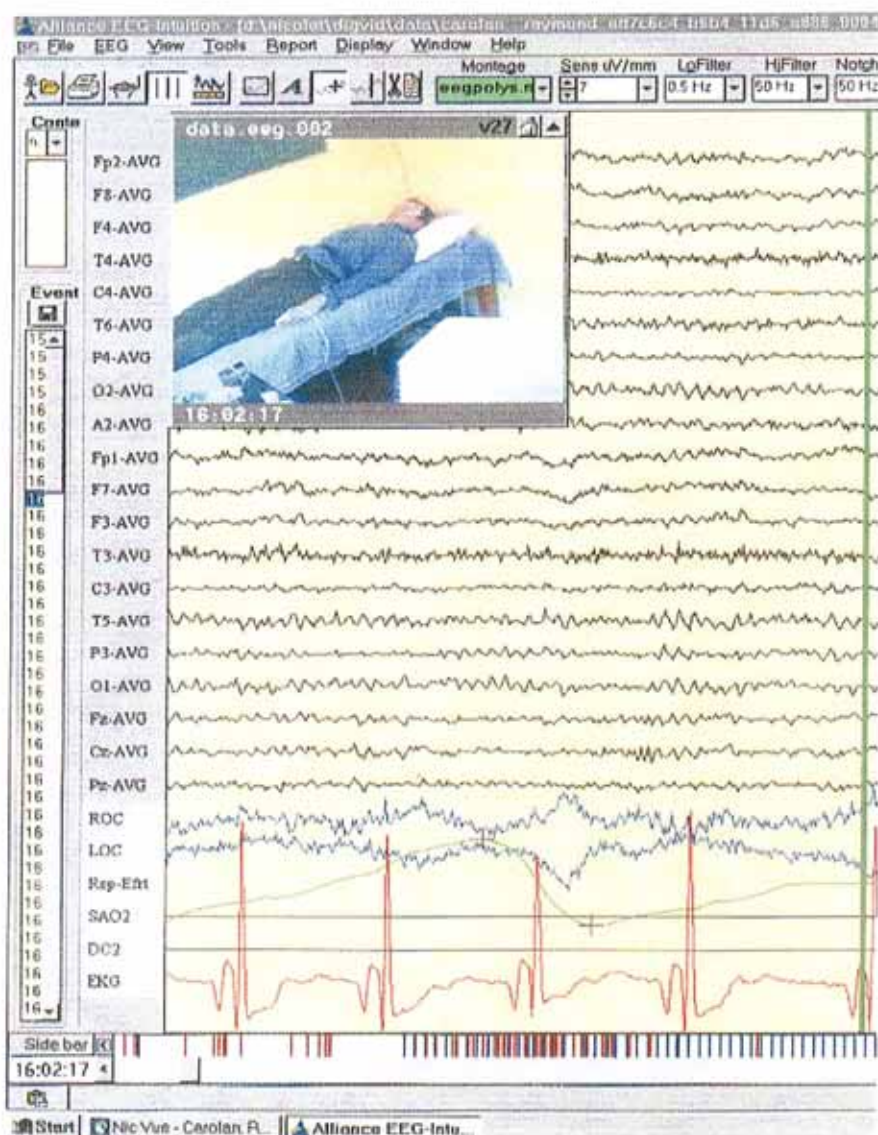
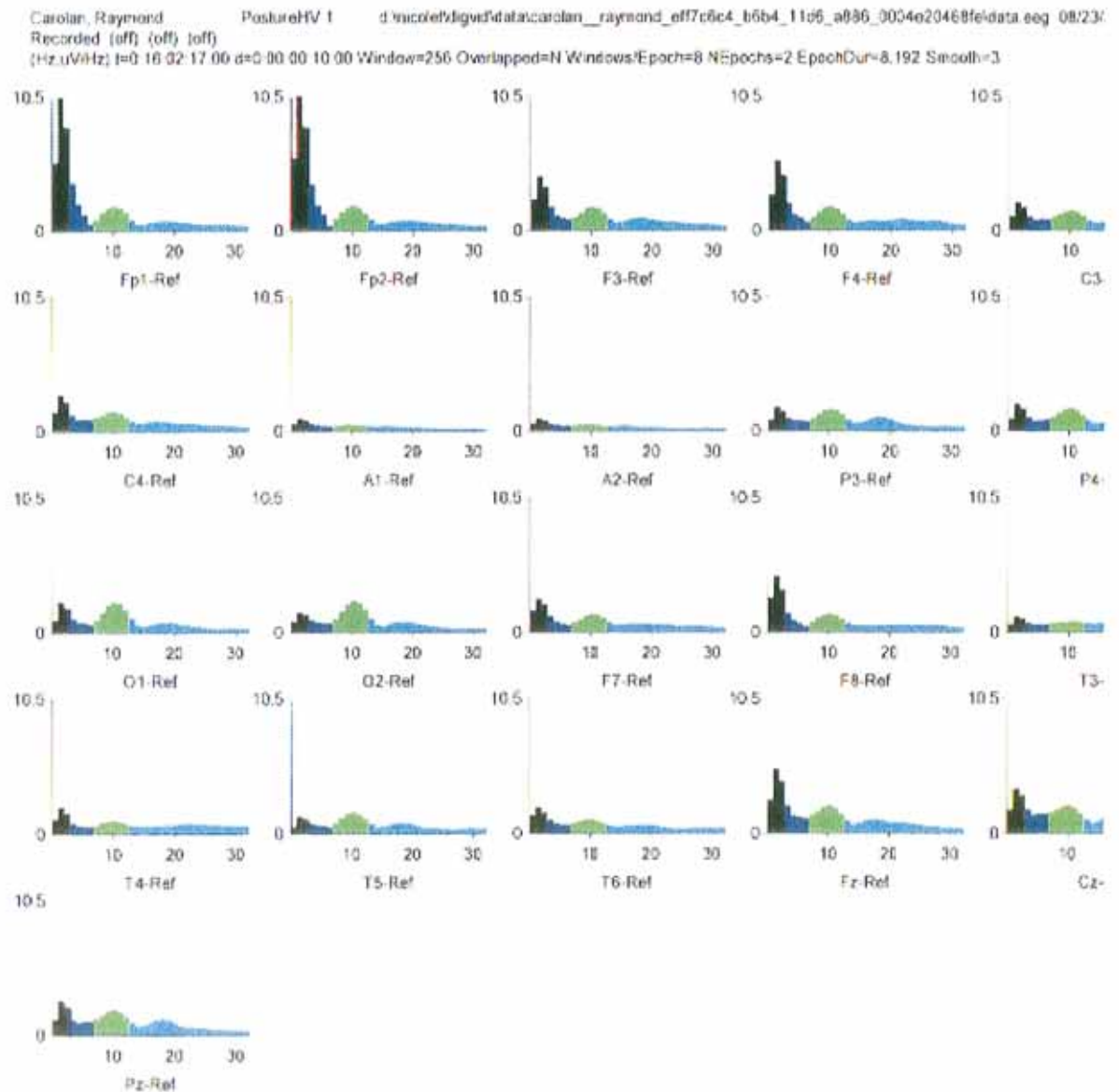


Fig. 3.19: Digital EEG/video image, subject supine and resting. Raw EEG, EOG, respiration and ECG data



Resting stage  
RR 10/min CO2 4.5 mmHg  
HR 121/min  
SpO2 100%

**Fig. 3.20: Power spectrum of Fig. 3.19 with subject supine and resting**  
 Frontal leads contaminated by eye movement artefact, giving an erroneous peak in the delta range (0-4 Hz colour: Black). Note the dominant posterior alpha rhythm at 10 Hz (Green)



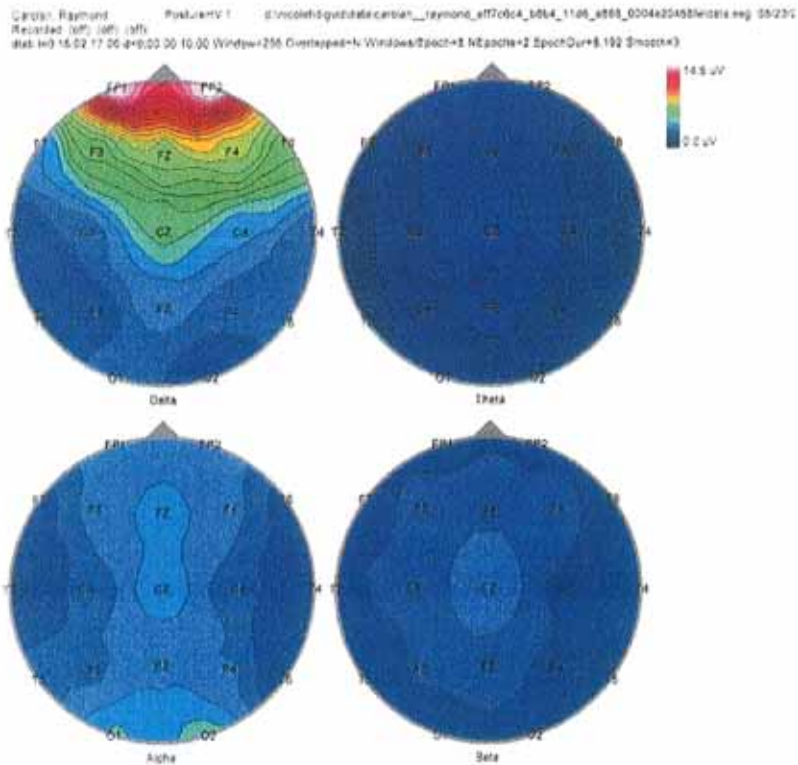


**Fig. 3.21: Topographic map of alpha, beta, theta and delta frequency bands from power spectrum in Fig. 3.19, supine resting**

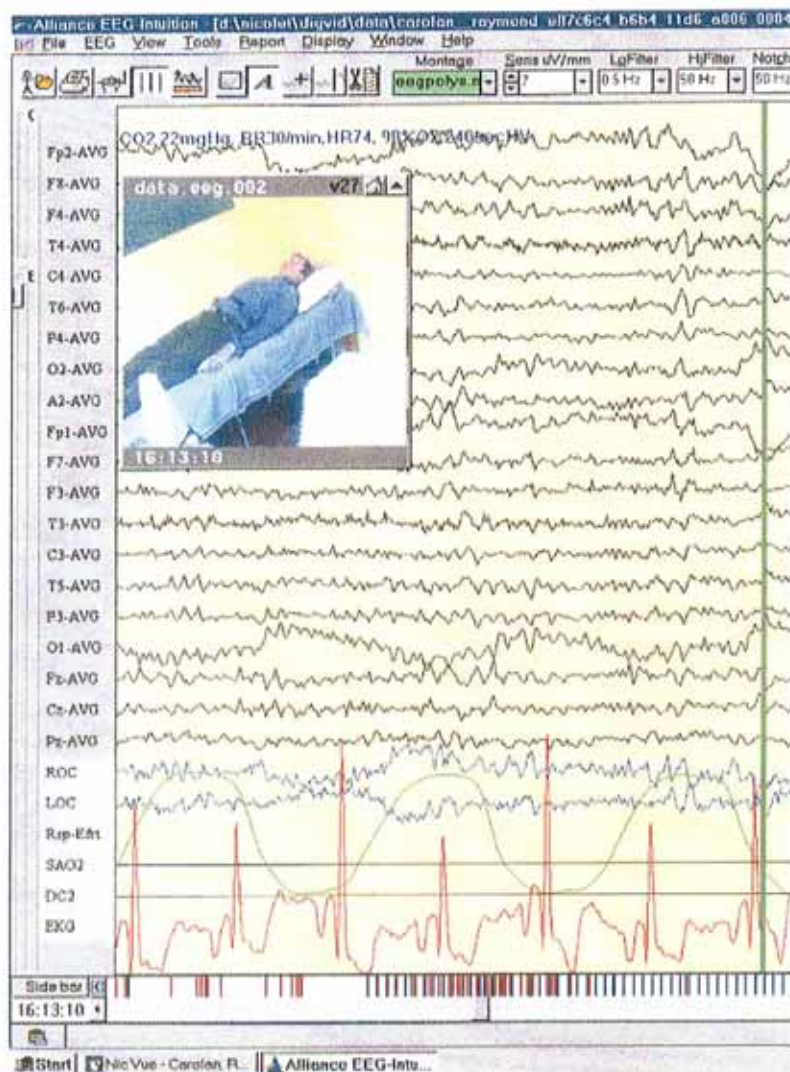
Biological eye movement artefact at 2 Hz from electrodes FP1, FP2, F8, and F7 noted in the delta range map. This is not significant as its origin is not cortical in nature.

Note the alpha peak in the occipital area from electrodes O1 and O2. This is normal resting background topographic map (range from 0 to 14.6  $\mu$ V).



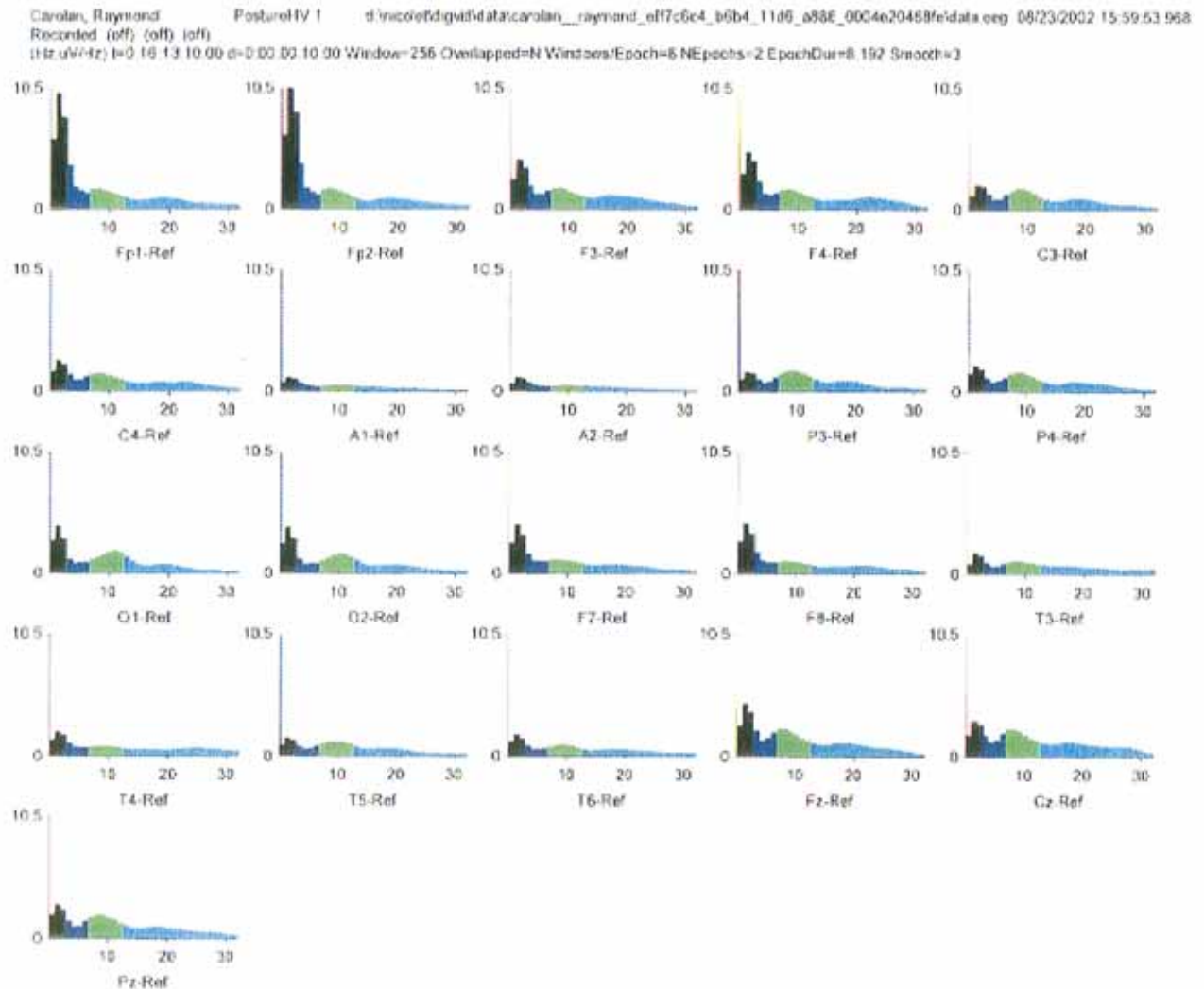
**Fig. 3.22: Supine OHV digital video EEG**

Note drop in frequency of background dominant EEG frequency to 7 Hz (theta range), increase in respiration rate and effort, and increased heart rate on ECG



*High resolution EEG*

**Fig. 3.23: Power spectrum of EEG data in Fig. 3.22**  
 Note increase in slow wave spectra during supine OHV



*Overlaid - 100 Hz*

Carlier, Raymond      Posture: V      d:\nicolab\gvid\data\carlier\_...\_raymond\_slf7c5c4\_b5b4\_11b5\_a005\_0004e20468\evdata.eeg 05/23/2  
 recorded: (off) (off) (off)  
 state: 1=0 15 13 12 00 d=0.0000 10 00 Window: 256 Overlapped: 4 Window: Epoch: 5 NEpochs: 2 EpochDur: 8 192 Smooth: 3

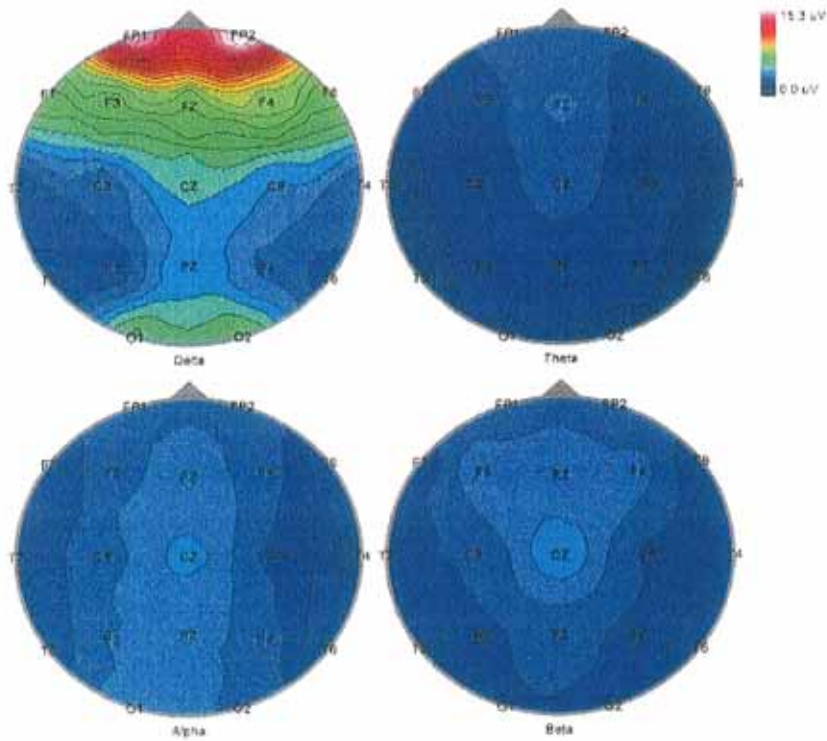


**Fig. 3.24: Topograph of alpha, beta, theta, delta bands of Fig. 3.22, supine with optimal hyperventilation. Note increase of power in theta and delta bands, frontally and in the occipital area.**



**Fig. 3.25: Comparison of raw EEG data, supine resting and OHV**

Note slowing of background frequencies to 7hz while hyperventilating with increased respiratory effort and respiratory rate changes from 16/min to 30/min. Heart rate has increased from a resting value of 48 beats per minute to 74 beats per minute during supine optimal hyperventilation.

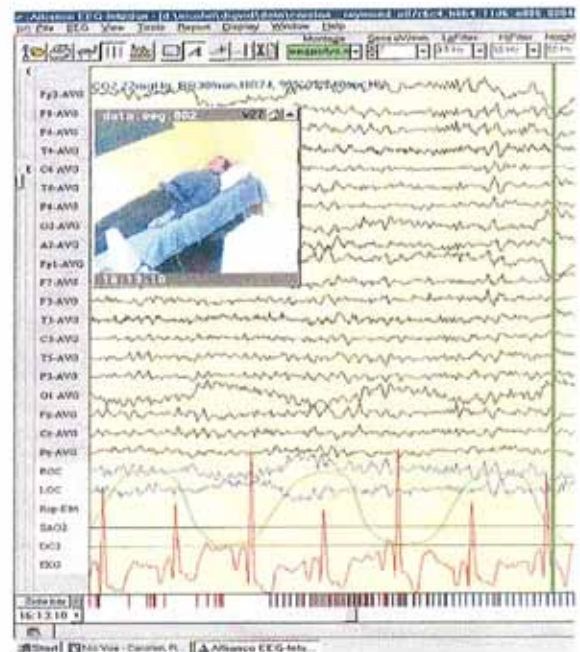
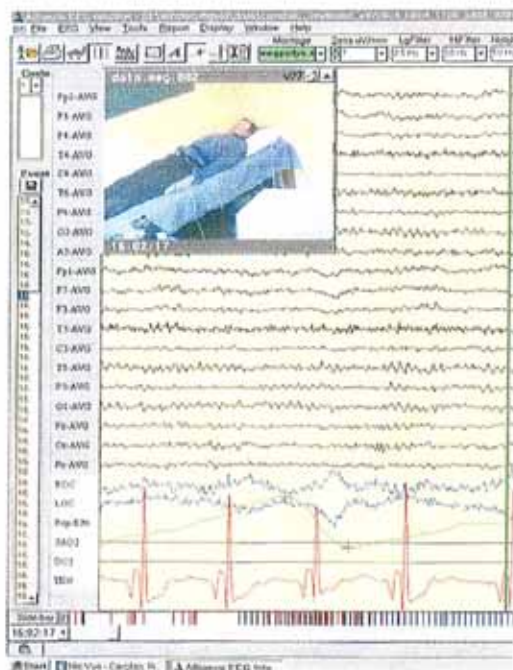
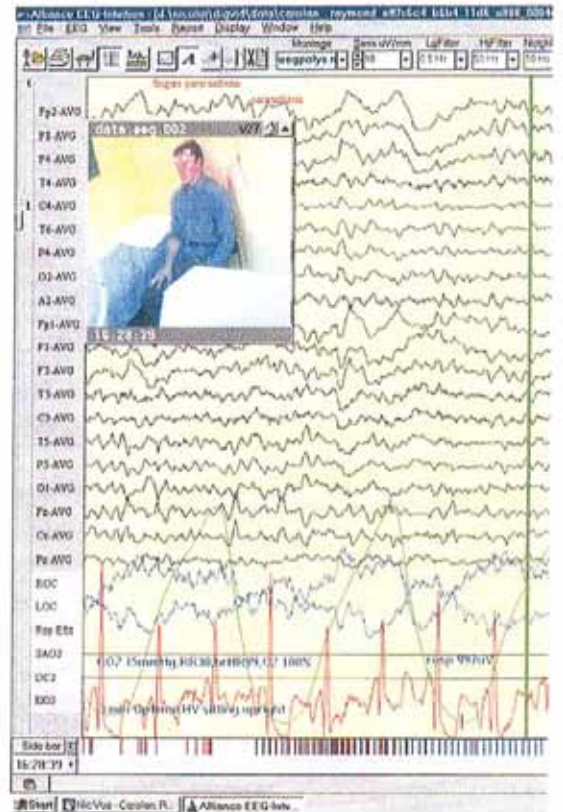
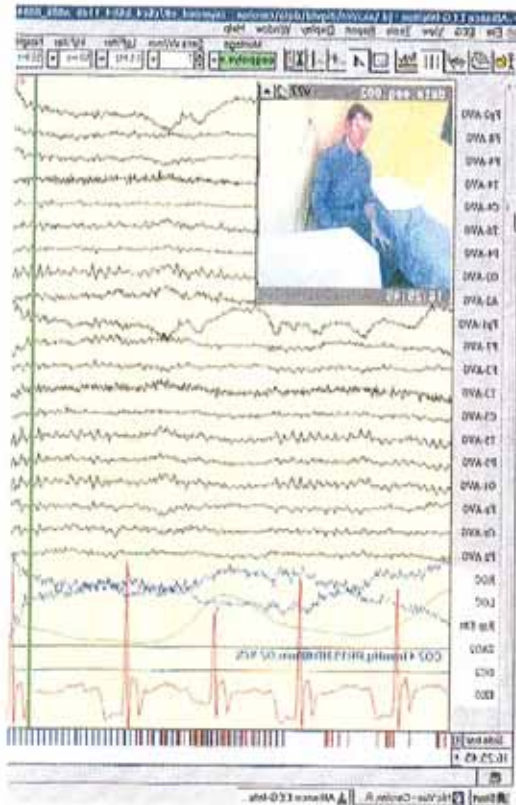
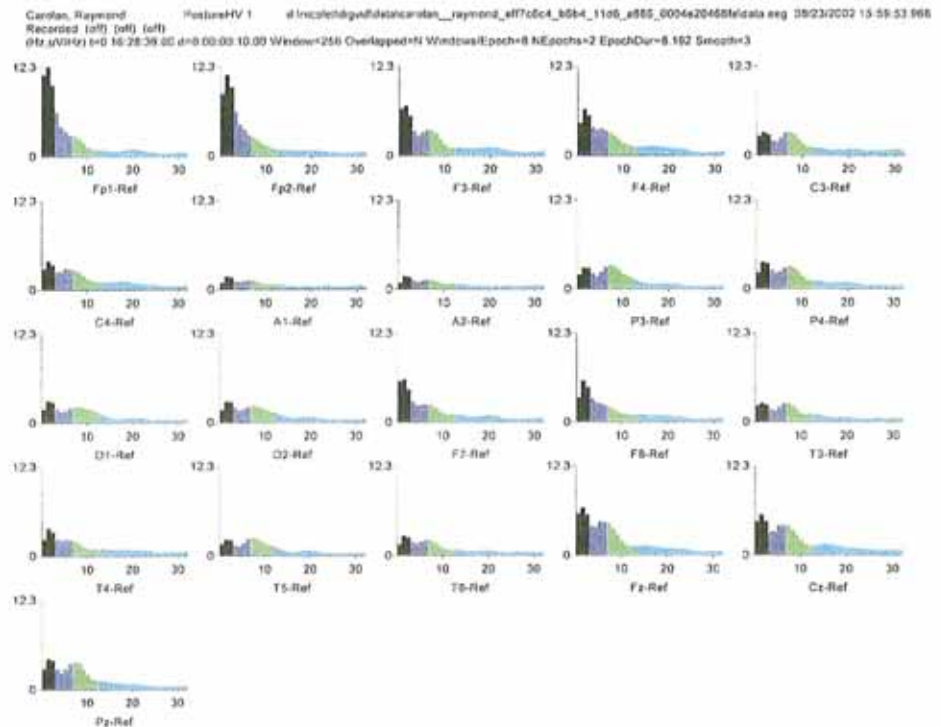


Fig. 3.26: Raw digital EEG seated at rest

Fig. 3.27: Raw digital EEG seated and hyperventilating

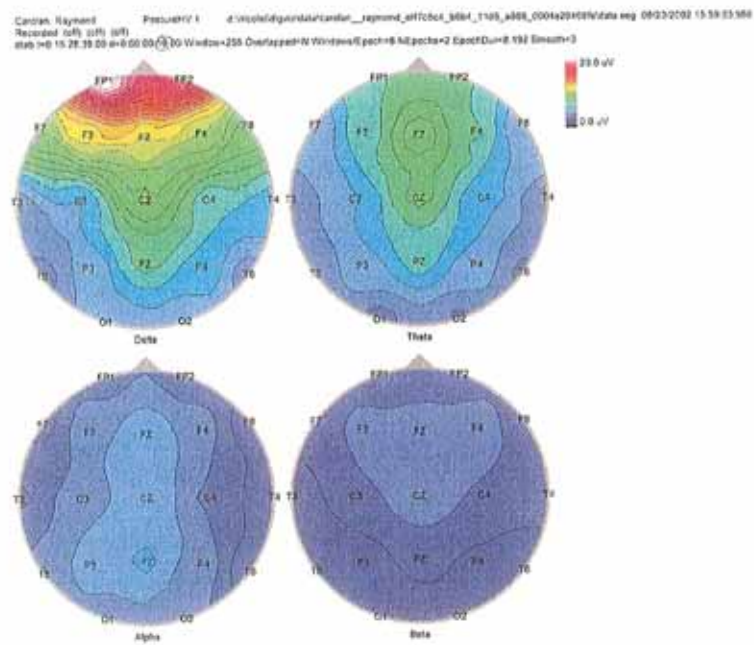


Viewing images of the EEG activity side by side demonstrates clearly the marked change in background EEG frequencies (5Hz), increase in respiratory rate (30 BPM) and effort (amplitude of Resp excursions 997  $\mu$ V >> expired volume), and increase in heart rate ( 99 bpm ) elicited by optimal hyperventilation in the upright seated position.



**Fig. 3.28: Power spectrum of EEG during seated OHV (Fig. 3.27)**  
Note increase in slow wave spectra, i.e. frequencies under 8 Hz, during seated OHV compared to Fig. 3.22 (supine OHV)

**Fig. 3.29: Topograph of alpha, beta, theta, delta bands of Fig. 3.27 during seated OHV. Note increase of power in theta and delta bands particularly in the frontal and central area, also the absence of alpha activity in the occipital leads**



### **3.21 Discussion**

The major experimental aim of the research reported in this thesis was to determine if a standardized optimal method of performing a hyperventilation exercise in two different postures had a measurable quantifiable effect upon a collection of defined physiological variables in a study group of healthy adult volunteers. The initial trigger for this research was the observation by the author, over many years experience in clinical neurophysiology, that during EEG testing the hyperventilation exercise was generally performed in a non-standardized manner in the supine position. Hyperventilation is an activation method that provokes physiological slowing of brain waves, and may trigger inter-ictal epileptiform discharges and seizure activity, most especially in idiopathic generalized epilepsies.

According to the literature there are four factors which influence the magnitude of the hyperventilation response on the EEG (Takahasi 2004).

- vigorous exchange of air
- the age of the subject
- the blood glucose levels
- posture.

A review of the literature showed that it has been reported in only three papers since 1944, that an erect position as compared with a reclining position enhances the effect of hyperventilation on the EEG. The original observation on the efficacy of upright hyperventilation was made in 1944 by Engel and Romano attempting to determine frequency spectra in the EEG. Morrice in 1956 writing on EEG, CO<sub>2</sub> and autonomic balance reported that hyperventilation in the seated

position was found to be most effective, (Chapter 1 Section 1.2) Billinger and Frank in 1969 formally set out to study the effects of posture on EEG slowing during hyperventilation. They used analogue EEG and subjective analysis to confirm that the build-up of EEG slow rhythms was better when the subject was seated rather than when supine. Therefore on the basis of 3 papers, only one of which actually intended to study the phenomenon, the efficacy of seated hyperventilation became one of the 4 tenets affecting the magnitude of the physiological over-breathing response on the EEG.

Personal clinical and educational experience in numerous neurophysiology departments indicated that while the patient's age, a vigorous effort, and awareness of blood glucose levels were considered as significant factors in EEG hyperventilation the role of posture was largely ignored. Most EEGs are carried out with the patient in the supine position, generally while reclining on a bed or couch. This position facilitates relaxation and encourages the patient to sleep, both of which are advantageous in achieving good quality EEG data. The method of hyperventilation is not standardized across neurophysiology departments. The duration of the exercise may vary from 3-5 minutes and is subject to the EEG practitioner encouraging the patient to make a vigorous effort. The effort is usually subjectively graded as fair, good, very good, or excellent. In the current era of standard operational protocols (SOPs), laboratory accreditation of best practice, and quality assurance, a more scientific and standardised method of EEG hyperventilation is required. Following ethics approval research commenced on “the effects of posture on quantitative EEG



(QEEG) and end-tidal CO<sub>2</sub> during standardised optimal hyperventilation in healthy adults”.

The study population of 14 females and 8 males undertook a standardised hyperventilation protocol as described earlier in section 3.0.

They reported subjective symptoms during the SpOHV and StOHV exercises and analysis of these indicated that standardized HV in the seated position was weakly statistically significantly more likely to induce symptoms. ( $p < 0.001$ ). The gender of the subject was not found to be a significant factor. They reported that they found performing the standardized HV exercise easier while seated. (see Chapter 1 section 1.2 “The effect of of postur on respiratory activity”) These subjective effects of hyperventilation may be the result of altered function of the numerous receptors, channels, transporters, and enzymes in neurons that are highly sensitive to increases in pH, rather than the result of hypoxia (Kaila and Ransom 1998).

Hyperventilation induces hypocapnia indicated by the partial end-tidal carbon dioxide expired by the subjects. The mean pETCO<sub>2</sub> (14.4mmHg) achieved in the seated position was 9.1 mmHg less than the mean (23.5mmHg) achieved during standardized SpOHV (Fig 3.8). StOHV was found to be significantly more effective than SpOHV ( $p < 0.001$ ) at inducing hypocapnia.

Hyperventilation induces a build up of slow EEG frequencies, moving the posterior dominant rhythm from the alpha range into the theta and occasionally the delta range, the effect reported to be related to the age of subject, and being

most prominent in children. The measurements indicated that StOHV was significantly more effective ( $p<0.0001$ ) than SpOHV in reducing the mean EEG frequency and in producing HHHARS patterns. The mean EEG frequency (5.9 Hz) achieved in the seated position was 1.8 Hz lower than the 7.7 Hz measured during standardized SpOHV (Fig 3.9).

QEEG analysis of the power density of the low frequency bands from 2.0-7.5 Hz in the EEG also showed a highly significant increase during StOHV ( $p<0.001$ ) (Fig 3.16).

These reductions in the frequency of EEG activity and in pETCO<sub>2</sub> were found to be accompanied by an increase in the heart rate. Using the steady respiration rate of 30 per minute a mean increase of 12.1 bpm in the heart rate of the subjects during StOPV compared with SpOHV ( $p<0.001$ ). This reflects the increased physiological effort possible while hyperventilating in the upright posture (fig 3.10).

Hypocapnia is known to induce cerebral vasoconstriction. StOHV was indeed found to reduce the pETCO<sub>2</sub> to a mean of 14.4 mmHg. In the 5 subjects who had TCD ultrasonography of the MCA at rest and during StOHV and SpOHV, the flow velocity in the MCA decreased from a mean baseline value of 68 cm s<sup>-1</sup> to a mean of 30.3 cm s<sup>-1</sup> during StOHV. This was 8.2 cm s<sup>-1</sup> slower than the mean flow velocity found during SpOHV (38.7 cm s<sup>-1</sup>) ( $p<0.001$  (fig 3.11)). Thus CO<sub>2</sub> acts as a regulator of cerebrovascular tone and cerebral blood flow. The posterior dominant EEG rhythm was found to change concomitant with the onset of hypocapnic changes from a mean of 10.6 Hz at rest to a mean of 5.7 Hz



during seated optimal hyperventilation. This is a significant lowering of the EEG frequencies with the reduction in  $p\text{ETCO}_2$ . Konishi (1987) reported that EEG changes were independent of a reduction in CBF. The results of this, admittedly small study would tend to support an association of global alteration/reduction in cerebral function as indicated by reduction of the EEG frequencies with the concomitant reduction of  $v\text{CBF}$ . Emerging evidence indicates that neuronal activity can control microcirculation using astrocytes as a mediator. In general, neuronal activation is accompanied by a local increase in cerebral blood flow and in cerebral metabolic rate of oxygen consumption  $\text{CMRO}_2$  attributed to neurovascular and neurmetabolic coupling. It would be of clinical interest to investigate whether or not, in the inverse situation, a decrease in CBF and an associated decrease in the  $\text{CMRO}_2$  would suggest a “de-activation” or inhibition of neuronal activity. Is it possible that the slow EEG pattern seen during HV a reflection of such an inhibition? Is the rhythmicity, attributed in large part to the breakthrough of the nonspecific thalamic activation system (NSTAS), a reflection of the astrocytic influence on the ECS, and the induction of an “edge of sleep state” as suggested by Patel and Mulsby (1987)?

$p\text{O}_2$  was found to show a consistent increase during SOHV from a mean of 98% at rest to a mean of 100% while the subject was actively hyperventilating down to levels of 14 mmHg  $p\text{ETCO}_2$ .  $\text{SpO}_2$  is a measure of peripheral partial pressure of oxygen. It is by no means a direct indicator of the cerebral levels of  $\text{O}_2$ , but the increase to 100% during StOHV does not support the argument in favour of a role for hypoxia in the global alteration of cerebral function indicated by the reduction in the posterior dominant rhythms in the EEG. Besides, reviews of experimental studies of brain metabolism during hyperventilation have

concluded that hyperventilation leading to a  $p\text{CO}_2$  as low as 14 mmHg does not produce brain hypoxia (Seisjo 1978, Kuschinsky 1982, Hood and Tannen 1983).

Hyperventilation causes a large increase in arterial pH but only a small increase in brain pH (Van Rijen *et al* 1989, Petrof *et al* 1985). Various biochemical studies (Granholt *et al* 1969, Granholt and Seisjo 1971, Nilsson and Busto 1974, Carlsson *et al* 1974, Kogure *et al* 1975, Young and Yagel 1984) and spectroscopic studies (Van Rijen *et al* 1989, Petroff *et al* 1985) have shown that high-energy phosphate levels (ATP and PCr) remain unchanged during hyperventilation that produces  $p\text{CO}_2$  levels of approximately 14 mmHg. Studies of cerebral oxygen consumption ( $\text{CMRO}_2$ ) during hyperventilation also typically show no reduction in  $\text{CMRO}_2$  (Young and Yagel 1984, Macmillan and Siesjo 1973). Overall, the evidence suggests that respiratory alkalosis leading to a  $p\text{CO}_2$  of  $\geq 14$  mmHg produces a rise in brain lactate as a result of increased glycolysis in the service of regulating intracellular pH, and that brain hypoxia does not occur.

The cortical activity reflected in the EEG results from complex interactions within neurons and glial cells. Manipulation of glial cell volume and thus of extracellular volume affects neuronal hypersynchrony. Transmembrane currents of both type of cells summate in the interstitial space. Hyperventilation produces an EEG “build up” phenomenon which consists of low frequency high amplitude hypersynchronous activity in the theta and delta range. The age of the subject is considered a significant factor in the characteristic EEG “build up” response. Using non-standardised HV such responses are considered to be difficult to elicit in adults (Takahasi 2004). This study has found that using a

standardised OHV protocol, high amplitude rhythmic slowing may be induced a normal adult population.

Sir Charles Sherrington the English physiologist published the initial work on the physiology of posture in 1926 in “The Lancet”. Over the next 30 years he demonstrated the physiological significance of muscle tone and the factors governing its maintenance, which he described as the raw material of posture. Posture is essentially the position of the body in space, the relationship of the body parts—head, trunk, and limbs—to each other. Changes in posture occur when any part of the body is moved. The effects of posture can be far reaching, involving respiratory, digestive and circulatory systems as well as the musculoskeletal system. Posture control involves static and phasic reflex activities:

- *static reflexes* involve sustained contraction of the musculature
- dynamic short-term *phasic reflexes* involve transient movements.

Both types of reflex are integrated at various levels in the central nervous system (CNS) from the spinal cord to the cerebral cortex and are largely effected through extrapyramidal motor pathways.

Postural reflex patterns from reflexes result in a coordination of many joint movements and combinations of muscle actions. The integrative pattern of posture is predominantly automatic and unconscious, resulting from the incessant shifting of weight (postural sway). Postural corrections are continuously mediated by spinal reflexes. Posture is further mediated by the visual, labyrinthine, neck-righting reflexes and by the interplay of joint reflexes.

While the control of posture is primarily controlled by various reflex mechanisms, there is also extensive input from the higher centres of the nervous system (Guyton and Hall 2000).

Change in posture from sitting to horizontal position *per se* causes a decrease in effort-dependent inspiratory and expiratory flow rates (Talwar *et al* 2002). The effect of posture on intracranial physiology can be quantified by MRI. Posture-related changes in intra-cranial compliance and intra-cranial pressure strongly affect the dynamics of cerebral blood and CSF flows (Alperin *et al* 2005). Treier *et al* (2003), in an MRI study investigating the influence of posture on gastric physiology, reported that differences in gastric relaxation and retained intragastric air volume were observed in the seated and right decubitus body position (lying on right side).

Caldwell in 1999 reported that an upright posture increases EEG arousal and may be useful for counteracting fatigue in sleep-deprived individuals. Neidermeyer (2004) writing on non-epileptic attacks stated that in patients with orthostatic syncope accompanied by dizziness, EEG recording in an erect position is not helpful in early stages. Subjective dizziness and light headedness are unassociated with significant EEG changes. Marked slowing induced by orthostatic posture in the EEG is however noted in patients with Shy-Drager syndrome (SDS). This is a rare condition that causes progressive damage to the autonomic nervous system in which the patients lack compensatory heart rate changes. Heart rate remains stable while BP falls dramatically giving rise to considerable cerebral ischaemia. The use of the postural tilt test during EEG is extremely conducive to syncopal manifestations.

This research has demonstrated the practical efficacy of the use of a standardised optimal protocol with the subject in the seated posture during EEG activation. In the seated posture the patient makes a greater effort (heart rate increases significantly), the vCBF shows a significant decrease, the pETCO<sub>2</sub> shows a significant decrease and the posterior dominant rhythm of the EEG is markedly slower than when the subject hyperventilates in the supine position.

Therefore the physiological measurement of a number of variables (EEG, heart rate, expired carbon dioxide, and velocity of cerebral blood flow) during a standardised hyperventilation exercise, while controlling for posture, indicates that in a group of normal adults the seated position is significantly more effective. The use of a standardised operational protocol demonstrated the reproducibility of the results in this group of 22 normal adults. Adoption of such a standardised operational protocol for the hyperventilation exercise during routine EEG would maximise the efficacy of the procedure, remove the operator bias intrinsic in the current non-standardised methods in common use in EEG laboratories and facilitate the exchange of clinical results from different laboratories. This study has confirmed that the position in which hyperventilation is performed is a highly significant ( $p < 0.001$ ) factor in the magnitude of the HV response on the EEG and justifies the inclusion of posture amongst the factors which directly influence this response. The adoption of a standard operational protocol (SOP) for the HV activation exercise is recommended within a set of guidelines, in order to ensure best practice in neurophysiology departments engaged in EEG testing.

## References: Chapter 3

- Aaslid R, Markwalder TM, Nornes H, 1982, Noninvasive transcranial Doppler ultrasound recording of flow velocity in basal cerebral arteries *J Neurosurg.* ;57(6): 769–774.
- Alperin N, Lee SH, Sivaramakrishnan A, Hushek SG, 2005, Quantifying the effects of posture on intracranial physiology in humans by MRI flow studies. *J Mag Res Imag* 22(5): 591-596
- Billinger TW, Frank GS, 1969, Effects of posture on EEG slowing during hyperventilation. *Am. J. EEG Technol* 9(1): 22-27
- Cadwell JA, Prazinko BF, Hall KK, 2000, The effects of body posture on resting electroencephalographic activity in sleep-deprived subjects. *Clin Neuro* 111 (3): 464-470
- Carlsson C, Nilsson L, Siesjo BK, 1974, Cerebral metabolic changes in arterial hypoxemia of short duration. *Acta Anaesthesiol Scand* 18: 104–113
- Engel GL, Romano J *et al*, 1944, A simple method of determining frequency spectrums in the electroencephalogram. *Arch. Neurol, Psychiat., Chicago*, 51: 134-146
- Granholm L, Lukjanova L, Siesjo BK, 1969, The effect of marked hyperventilation upon tissue levels of NADH, lactate, pyruvate, phosphocreatine and adenosine phosphates of rat brain. *Acta Physiol Scand* 77: 179–180
- Granholm L, Siesjo BK, 1971, The effect of combined respiratory and nonrespiratory alkalosis on energy metabolites and acid-base parameters in the rat brain. *Acta Physiol Scand* 81: 307–314
- Harner PF, Sannit T, 1974, A Review of the international Ten-Twenty System of electrode placement *Grass Instrument company (copyright)*
- Hood VL, Tannen RL, 1983, pH control of lactic acid and keto acid production: a mechanism of acid-base regulation. *Mineral Electrolyte Metabolism* 9: 317–325
- Jibiki I, Kurokawa K, Matsuda H, Fukushima T, Yamaguchi N, Hisada K, 1992, Widespread reduction of regional cerebral blood flow during hyperventilation-induced EEG slowing ('buildup'). Observation from subtraction of brain imaging with single photon emission computed tomography using technetium-99m hexamethyl-propyleneamine oxime. *Neuropsychobiology*. 26(3): 120-4.
- Kaila K, Ransom BR, 1998, Concept of pH and its importance in neurobiology, in *pH and Brain Function*, eds. Kaila K, Ransom BR. New York, Wiley-Liss, pp 3–10

Kogure K, Busto R, Matsumoto A *et al*, 1975, Effect of hyperventilation on dynamics of cerebral energy metabolism. *Am J Physiol* 228: 1862–1867

Konishi T, 1987, The standardization of hyperventilation on EEG recording in childhood I: The quantity of hyperventilation activation *Brain Dev.* 9(1): 16-20

Konishi T, 1987, The standardization of hyperventilation on EEG recording in childhood II: The quantitative analysis of build-up *Brain Dev.* 9(1): 21-25

Lum LM, Connolly MB, Farrell K, Wong PKH, 2002, Hyperventilation – Induced High Amplitude Rhythmic Slowing with altered awareness: A video EEG Comparison with Absence seizures. *Epilepsia* 43(11): 1372-1378

Morrice JK, 1956, Slow wave production in the EEG with reference to hypernoea, carbon dioxide, and autonomic balance. *Electroenceph. Clin.Neurophysiol*, 8: 49-72

Macmillan V, Siesjo BK, 1973, The influence of hypocapnia upon intracellular pH and upon some carbohydrate substrates, amino acids and organic phosphates in the brain. *J Neurochem* 21: 1283–1299

Neidermeyer E, 2004, 5<sup>th</sup> Ed. Chapter 26 : Non Epileptic Attacks, in *Electroencephalography: Basic principles, clinical applications, and related fields*. Eds. Neidermeyer E, Lopes da Silva F. pp 261-262. Lippincott Williams and Wilkins  
ISBN-13: 9780781751261

Newell DW, Aaslid R, Stooss R, Reulen HJ, 1992, The relationship of blood flow velocity fluctuations to intracranial pressure B waves. *J Neurosurg* 76: 415-421

Nilsson L, Busto R, 1973, Controlled hyperventilation and its effects on brain energy and acid-base parameters. *Acta Anaesthesiol Scand* 17: 243–252

Norusis M J, 1998, Straight talk about data analysis and SPSS Version 8.0 . Englewood Cliffs: Prentice Hall.

Patel VM, Maulsby RL, 1987, How hyperventilation alters the Electroencephalogram: A review of controversial viewpoints. *J. Clin.Neurophysiol* 4(2): 101-120

Petroff OA, Prichard JW, Behar KL *et al*, 1985, Cerebral metabolism in hyper- and hypocarbia: <sup>31</sup>P and <sup>1</sup>H nuclear magnetic resonance studies. *Neurology* 35: 1681–1688

Roth WT, 2005, Physiological markers for anxiety: panic disorder and phobias. *Int J psychophysiol* 58(2-3): 190-8 (Review)

Sheikh JI, Leskin GA, Klein DF, 2002, Gender differences in panic disorder: Findings from the national comorbidity survey. *Am J Psychiatry* 159: 55-58

Siesjo BK, 1978, *Brain Energy Metabolism*. New York, Wiley

Takahashi T, 2004, 5<sup>th</sup> Ed. Chapter 14: Activation Methods , in *Electroencephalography: Basic principles, clinical applications, and related fields*. Eds. Neidermeyer E, Lopes da Silva F. pp 261-262. Lippincott Williams and Wilkins

Talwar A, Sood S, Sethi J, 2002, Effect of body posture on dynamic lung functions in young non-obese Indian subjects. *Indian Journal of Medical Science* 56(12): 607-12

Tremper KK, 1992, Noninvasive monitoring of oxygenation and ventilation. 40 years in development. *West J Med.* 156(6): 662–663.

Tukey JW, 1977, "*Exploratory Data Analysis*". Addison-Wesley, Reading, MA.

Van Rijen PC, Luyten PR, Berkelbach Van Der Sprenkel JW *et al*, 1989, <sup>1</sup>H and <sup>31</sup>P NMR measurement of cerebral lactate, high energy phosphate levels and pH in humans during voluntary hyperventilation: associated EEG, capnographic, and Doppler findings. *Magn Reson Med* 10: 182-193

Young RS, Yagel SK, 1984, Cerebral physiological and metabolic effects of hyperventilation in the neonatal dog. *Ann Neurol* 16: 337–342

Zwiener U, Lobel S, *et al*, 1998, Quantitative topographical analysis of EEG during non-standardized and standardized Hyperventilation. *J Clin. Neurophysiol.* 15(6): 521-8

## **Bibliography**

Ebersole JS, Pedley TA, Eds. 1993, Current Practice of Clinical Electroencephalography, 3rd ed. Lippincott, Williams.



## **CHAPTER 4**

# **STANDARDIZED HYPERVENTILATION DURING EEG IN CHILDREN WITH ABSENCE EPILEPSY AND ATTACK DISORDER**

The research work outlined in Chapters 3 proved that in a group of healthy adults a standardised method of hyperventilation, controlling for posture and end tidal CO<sub>2</sub>, was statistically significantly more effective in eliciting high amplitude rhythmic slowing of brain wave activity than the non-standardised supine method of hyperventilation in general use in EEG/Neurophysiology departments. The Research Ethics committee of Our Lady's Children's Hospital, Crumlin (OLCHC), Dublin approved a follow-on study on the hyperventilation exercise during EEG testing in children. The standardised method of HV was used in a prospective study of

1. Patients with childhood absence epilepsy (CAE)
2. Patients at first presentation with undiagnosed episodes of “fits, faints, and funny turns”, i.e. “not yet diagnosed” (NYD) episodes of attack disorder (AD)

The aim of the study was to examine if the standardised method was a more effective clinical tool than a non-standardised method in eliciting positive EEG findings in these two groups.

The EEG is commonly used as a first-line diagnostic screening test when there is a clinical suspicion that a patient may be experiencing epileptic events. It is

non-invasive, relatively cheap, and offers a window into the functional activity of the brain with high temporal resolution. The clinical events can be captured during EEG with simultaneous digital video recording either during a routine study or using EEG long term monitoring. This facilitates correlation of the clinical events with the alterations in the electrophysiological brain wave activity, which is of significant diagnostic assistance to the reporting clinician. In addition to the ongoing resting background activity three activation procedures are used to provoke physiological alterations in the EEG. These are photic stimulation, recording of a period of sleep, and hyperventilation (Takahashi 2004). Hyperventilation constitutes a classic activation procedure of the EEG and it usually provokes physiological slowing of the brain rhythms, more intense and abrupt in children from 8-12 years old (Gibbs *et al* 1943, Takahashi 2004, Guaranha *et al* 2005). This effect, while observed in normal individuals, is more prevalent and more pronounced in patients with epilepsy.

The definitive mechanisms involved in the effects of HV are not yet clear. However it was observed as far back as 1924 by that HV could precipitate seizures in individuals with epilepsy. In patients with epilepsy, hyperventilation may activate interictal discharges and frank clinical seizures. Dalby (1969) and Drury (2000) reported the provocation of 3 Hz spike and wave complexes in approximately 80% of patients with idiopathic generalised epilepsies and slow spike and wave complexes in approximately 50% of patients with symptomatic generalised epilepsies. Positive activation of the EEG has been reported in 6-11% of individuals with focal epilepsy (Gabor and Marsan 1969, Morgan and Scott 1970, Miley and Forster 1977). This seizure precipitating effect on the

EEG was originally discovered by Berger in 1934. There have been few quantitative studies concerning the ability of HV to elicit focal seizures. There are no studies in the literature on the efficacy of standardised HV controlling for posture and end tidal CO<sub>2</sub> in patients with epilepsy. Engel and Romano (1944) noted that hyperventilation produced greater EEG slowing when the subjects were in an upright position than when they were in the recumbent position. In 1956 Morrice mentioned position as one of the factors influencing the HV response. Billinger and Frank in 1969 examined the effects of posture on EEG slowing during hyperventilation using analog 8 and 16 channel recording instruments and subjective grading of the responses into four possible categories using three judges scoring the tracings. These studies were performed on normal volunteers and not on patients with attack disorder.

Wirrel *et al* (1996) in a study on 12 untreated children with newly diagnosed absence epilepsy found that in 67% of subjects, absence seizures were reliably provoked by hypocapnia. They found that the critical pCO<sub>2</sub> varied among children with absence. All of their subjects had their own critical pCO<sub>2</sub>, ranging from 19 to 28 mmHg. The posture in which hyperventilation was performed was not given in the paper.

There is an ongoing debate in the literature as to the efficacy of hyperventilation in induction of seizure events. Holmes *et al* (2005) found that HV rarely evokes seizures (0.5% of patients) or spikes (3.4% of patients) during standard EEGs in 383 patients with unequivocal focal epilepsy. Anti-epileptic medication was maintained in the Holmes *et al* study which included 433 consecutive patients in

total with most of them adults. 9.2% of the subjects were aged from 10-18 years. A generalised epilepsy syndrome was present in 49 (11.9%), 25 of whom had absence seizures. The HV protocol was “5 minutes of maximal effort from the subject, with monitoring of respiratory excursions and encouragement by the EEG technologist”. The posture in which the exercise was performed was not reported. They concluded that their results constituted evidence contrary to the notion that HV is an effective “activating “ procedure for the majority of patients with epilepsy. *“voluntary hyperventilation in patients with unequivocal epilepsy is rarely associated with either clinical seizures or an increase in the frequency of epileptiform discharges”* (Holmes *et al* 2005).

A caveat was given in that this conclusion may not apply to younger children, especially those with typical absence epilepsy, in whom the evidence for provocation of seizures is strongest. They called for a re-examination of the role of HV in routine clinical EEG studies and the concepts that link hypocapnia to seizure provocation. Guaranha *et al* (2005) also explored the effectiveness of HV in eliciting clinical and electrographic seizures during Video EEG monitoring on medically intractable focal epilepsies. All patients had their anti-epileptic drugs tapered and discontinued during the evaluation. The reported HV protocol is described as” vigorously breathing for 5 minutes, at a minimum breath frequency of 20 excursions per minute”. The HV procedure was repeated approximately every 3 hours (on LTM EEG patients). The posture in which the exercise is performed was not reported. 97 patients were included in the study, 24 of whom had positive seizure activation. 28.3% of all of the seizures recorded were activated by hyperventilation. The maximum activation was

observed at 4 minutes into HV. The authors concluded that contrary to the results of the study by Holmes *et al* in 2004, "*Hyperventilation is a safe and effective method of seizure activation during EEG Long Term Monitoring*" (Guaranha *et al* 2005).

They found that it did not modify any of the characteristics of the seizures and allowed ictal single photic emission computerised tomography (SPECT) to be performed. They found that HV was clinically relevant and had the potential to shorten pre-surgical evaluation, reducing costs and increasing the number of candidates for epilepsy surgery. Blume (2006) reviewed and critiqued the divergent results of the Holmes and Guaranha studies. He reported that while the HV procedures were similar, anti-epileptic medication was maintained in the Holmes *et al* report while it was tapered to omission for in-patient video EEG telemetry in the Guaranha *et al* study. He noted that while in the Guaranha *et al* study the data appeared to be competently gathered, he stated that evaluating how effective HV is as an activation agent would have been better assessed using an age-matched control group. Efficacy could also have been evaluated by comparing the number of seizures during HV with those spontaneously occurring during resting, wakefulness and sleep, using 10 minute epochs as denominators. He concluded that in the Guaranha *et al* study HV did appear to effectively activate clinical and electrographic seizures in Video-EEG LTM temporal lobe patients for whom anti-epileptic drugs had been reduced or omitted. Its value for other focally originating seizures remains less certain. He further commented that the mechanism by which HV can precipitate seizures and augment or evoke theta and delta activity remains unresolved; but he stated

that it is probably because of alkalosis and decreases that occur in cerebral blood flow,  $pO_2$  and  $pCO_2$ .

The HV protocols used in the Holmes *et al* and in the Guaranha *et al* studies were subjective. There was no quantitative or objective measure of respiratory rate or effort, (given as 20 excursions per minute in Guaranha study). There was no measurement of expired gases or analysis of EEG frequencies reported.

Posture is one of the four criteria which determine the magnitude of the hyperventilation response (Takahashi 2004). The posture in which the HV protocol was performed was not reported in either study. The inconclusive nature of the debate evaluating the efficacy of HV as an activation procedure of the EEG renders the subject of this study both topical and timely. The methodology used here is both objective and quantitative in nature.

#### **4.1 Aim of Study**

The major aims of the clinical trial was to compare the results using a standardised optimal hyperventilation (SOHV) protocol with the results of a non-standardised HV (nsHV) method as currently in general use in EEG/Neurophysiology departments, with subjects both seated and supine, and, in particular, to examine the effectiveness of the SOHV method in eliciting:

- diagnostic EEG “3 per second spike and wave” changes of epileptogenic significance in patients with probable childhood absence epilepsy (CAE)
- hyperventilation induced high amplitude rhythmic slowing (HIHARS) related to the level of end-tidal  $CO_2$  in both CAE patients and NYD patients

- whether or not the SOHV method reduces the amount of EEG investigations required
- Whether or not the SOHV method shortens the time to diagnosis and treatment

Patient with childhood absence epilepsy (CAE) were chosen for the study to seek to achieve the following

- Elucidate the possible role of T-type calcium currents in the generation of absence seizures and HHARS. In CAE, abnormal oscillatory rhythms are believed to develop in thalamo-cortical pathways. This involves GABA-B-mediated inhibition alternating with glutamate-mediated excitation. The cellular mechanism is believed to involve T-type calcium currents.
- Clinical absence seizures are common and brief causing little distress to the patient. If the standardised seated hyperventilation method effectively induced an increase in the amount of seizures this would not have a negative effect upon the patient, as absence events rarely progress to more major events. This factor was significant in gaining approval for the study from the Research Ethics Committee in OLCHC
- Patients with CAE usually experience a period of motor arrest, staring, eyelid flutter and occasionally some simple automatisms. They are not likely to become mobile and move out of the range of the video camera during the event. Therefore the entire event can be recorded using digital video EEG.

- Adams and Lueders (1981) found that for analysis of epileptiform activity, 5 minutes of controlled ventilation recording was more reliable than 6-hour recording as a predictor of clinical seizure frequency in the evaluation of absence seizures.
- Patients with first presentation with “not yet diagnosed “ (NYD) events were included because:
  - They acted as a control group matched for age and sex with the CAE group
  - If they did have positive EEG findings, in particular if they had evidence of focal epilepsy, the results could be evaluated for the effectiveness of the standardised seated HV method in eliciting focal EEG changes prospectively.

## **4.2 Childhood absence epilepsy**

In accordance with the recommendations of the Commission on Classification and Terminology of the International League Against Epilepsy (ILAE 1989), absence epilepsy is defined as a generalised form, which means that the abnormal electrical activity encompasses both hemispheres of the brain and each seizure is accompanied by a complete loss of consciousness. Absence epilepsy can be subdivided further into typical and atypical forms. The incidence of absence epilepsy is relatively low and affects between 2 and 8 out of every 100,000 children up to the age of 16 years, with a prevalence suggested to be between 2 and 10% of children with any form of epilepsy (Crunelli and



Leresche 2002). Typical absence seizures are characterised behaviourally by a paroxysmal loss of consciousness of abrupt onset and termination that is associated with a bilateral synchronous spike and wave discharge (SWD) measuring ~ 3 Hz on the EEG.

Children with idiopathic generalized epilepsies may present with a history of staring spells, but infrequent absence seizures may not be diagnosed until a generalized tonic clonic (GTC) seizure has occurred. Other symptoms, such as behavioural problems, may be the presenting complaint. Although the brief attacks are unrecognized, the lapses of awareness interfere with following up what is happening; as a result, the child often becomes frustrated. Decline in school performance may be an indication of the onset or breakthrough of absence seizures. On clinical examination, typical absence seizures appear as brief staring spells. Patients have no warning or post-ictal phase, and if engaged in gross motor activity, such as walking, may stop and stand motionless or may continue to walk. Children are not responsive during the seizure and have no memory of what happened during the attack; they are generally unaware that a seizure has occurred.

No deaths result directly from absence seizures. The morbidity from typical absence seizures is related to the frequency and duration of the seizures, as well as to the patient's activities; effective treatment ameliorates these factors. Educational problems and behavioural problems are sequelae of unrecognized, frequent seizures. No racial predilection is known. Absence seizures are generally believed to be more common in females than in males, with some

studies showing a 2:1 female-to-male ratio. Other studies have shown no difference between the sexes.

Type of Clinical Seizure	EEG Findings
<p>Typical Absence:</p> <p>Impairment of Consciousness only</p> <p>Mild Clonic Components</p> <p>Atonic Components</p> <p>Tonic Components</p> <p>Automatisms</p> <p>Autonomic component</p>	<p>Usually regular and symmetrical 3Hz, possible 2- to 4 Hz spike and slow wave complexes, and possible multiple spike and slow wave complexes.</p>
<p>Atypical Absence:</p> <p>Changes in tone more pronounced than those of typical absence seizure.</p> <p>Non abrupt onset and/or cessation abrupt</p>	<p>EEG more heterogeneous than in typical absence, may include irregular spike and slow wave complexes, fast activity, or other paroxysmal activity</p> <p>Abnormalities bilateral but often irregular and asymmetric</p>

**Table 4.1: Clinical and EEG findings in typical and atypical absence seizures\***

\* May be seen alone or in combination

Adapted from Dreifuss, 1977

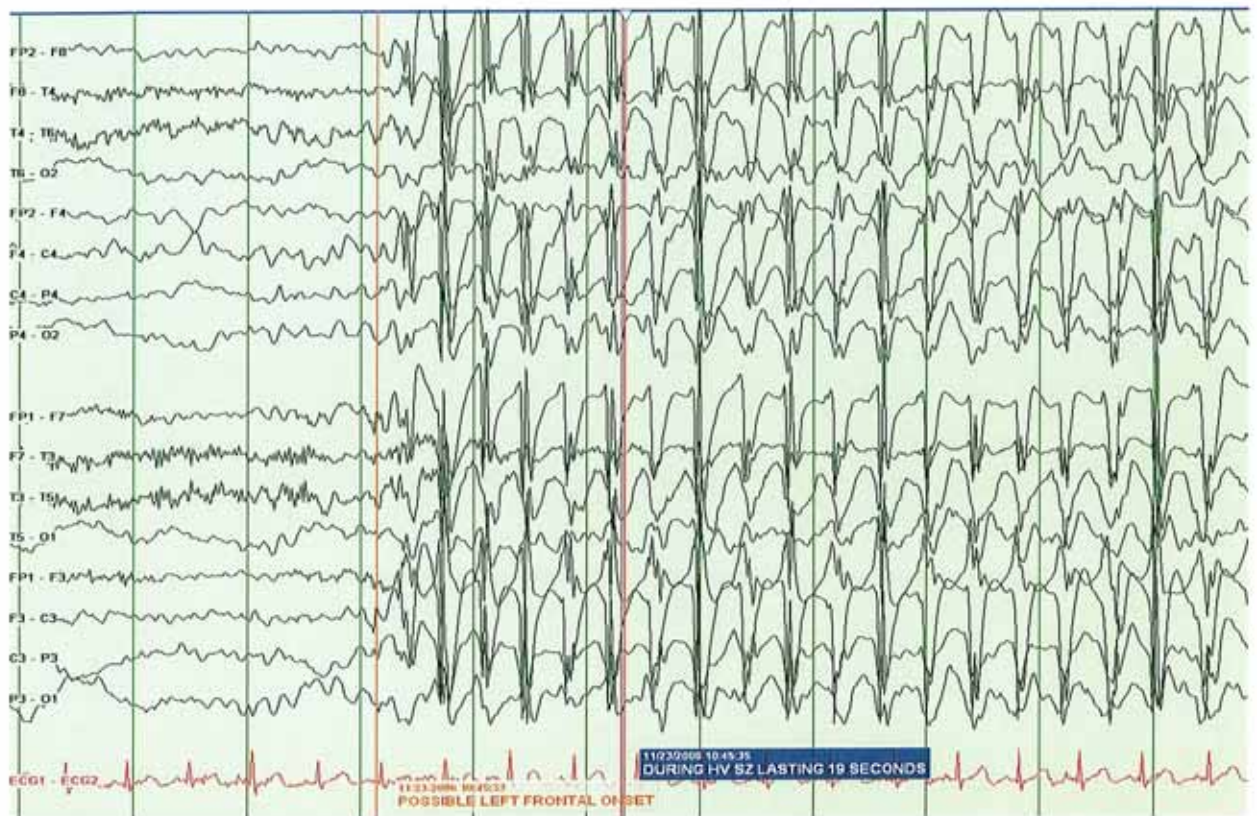


**Fig 4.1: Typical 3 per second (3 Hz) spike and wave discharges seen in CAE (From EEG/Neurophysiology Department Our Lady's Children's Hospital, Crumlin, Dublin)**

### 4.3 Pathogenesis of absence epilepsy

The pathophysiology of absence seizures is not fully understood. The involvement of a thalamocortical circuit, particularly the contribution of the ventrobasal thalamus (VB) and reticular thalamic nucleus (RTN) in the propagation of absence seizures is known (Penfield and Jasper 1947, Avoli and Gloor 1982, Vergnes *et al* 1987, Gloor and Fariello 1988). The basic underlying mechanism of CAE appears to involve thalamo-cortical circuitry and the

generation of abnormal oscillatory rhythms from that particular neuronal network due to a channelopathy with malfunction of calcium channels (Snead 1995). Perturbation of this network may be achieved by hyperventilation and the classic “3 per second spike and wave” pattern appears on the EEG accompanied by a brief clinical absence event in the patient (Esquivel *et al* 1991).

Absence seizures are a type of generalized seizures. They were first described by Poupart in 1705, and later by Tissot in 1770, who used the term *petit access* to describe them. In 1824, Calmeil used the term *absence*. In 1935, Gibbs, Davis and Lennox described the association of impaired consciousness and 3-Hz spike-and-slow-wave complexes on EEGs. Absence seizures occur in both idiopathic and symptomatic generalized epilepsies. Among the idiopathic, or primary, generalized epilepsies (i.e. with age-related onset) absence seizures are seen in childhood absence epilepsy (CAE), juvenile absence epilepsy (JAE), and juvenile myoclonic epilepsy (JME). The seizures in these conditions are called typical absence seizures and usually associated with 3-Hz spike-and-slow-wave complexes on EEG. In CAE, seizures are frequent and brief, lasting just a few seconds. Some children can have hundreds of such seizures per day.

In 1947, Jasper and Droogleever-Fortuyn electrically stimulated nuclei in the thalami of cats at 3 Hz and produced bilaterally synchronous spike-and-wave discharges on EEG. In 1953, bilaterally synchronous spike-and-wave discharges were recorded by using depth electrodes placed in the thalamus of a child with absence seizures. In 1977, Gloor *et al* demonstrated that the bilaterally synchronous 3-Hz spike-wave discharges in the feline penicillin model of

absence seizures were generated in the cortex. This led to the corticoreticular theory of primarily generalized seizures.

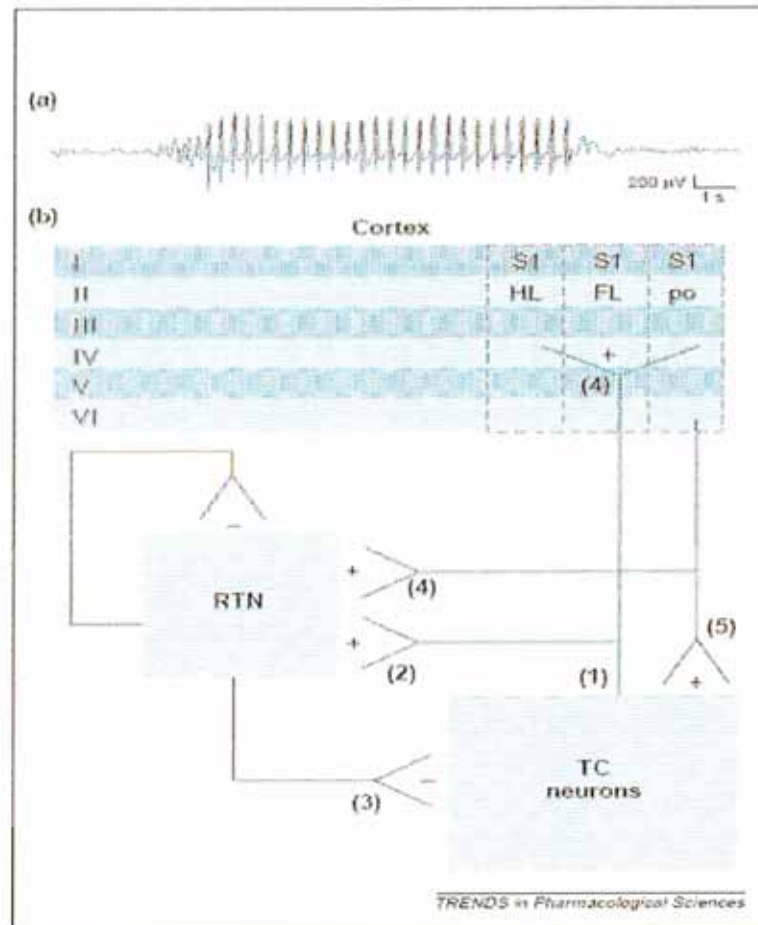


**Figure 4.2 :** (a)An EEG recording of a generalised absence seizure showing the synchronous spike and wave discharge (SWD) (b) The classic view of absence seizure pathophysiology is shown. Activation of a low threshold transient  $\text{Ca}^{2+}$  current ( $I_t$ ) within thalamocortical neurons (1) enable neurons of the reticular thalamic nuclei (RTN) to produce high frequency burst of action potentials spontaneously (2). GABA is subsequently released onto TC neurons in the thalamic relay nuclei, resulting in the production of a series of inhibitory post synaptic potentials (IPSPs) that increasingly removes the inactivation from the T-type  $\text{Ca}^{2+}$  channels (3). The ensuing  $\text{Ca}^{2+}$  mediated rebound burst discharge facilitates the release of excitatory amino acids via axon collaterals that evoke excitatory postsynaptic potentials (EPSPs) in the RTN, peri-oral region of the primary somatosensory cortex (S1po) and the forelimb (S1FL) and hind-limb (S1HL) regions of the somatosensory cortex (4). Further activation of the RTN and TC neurons then comes from descending cortical projections (5). The contemporary view of the circuit would suggest that activation of ( $I_t$ ) within the thalamic neurons occurs as a result of initial activity within the S1po (Meeren *et al* 2002)). Red indicates inhibitory GABA- containing neurons and green indicates excitatory glutamate-containing neurons. The layers of the cortex are indicated by roman numerals. (after Panayiotopoulos 2002).

Abnormal oscillatory rhythms are believed to develop in thalamocortical pathways. Meeren *et al* (2002) suggested that CAE seizures might be initiated at a specific cortical site, S1po (primary somato- sensory cortex, peri-oral area). This involves GABA-B-mediated inhibition alternating with glutamate-mediated excitation. The cellular mechanism is believed to involve *T-type calcium currents*. T channels of the GABAergic reticular thalamic nucleus neurons appear to play a major role in the spike-wave discharges of the GABAergic thalamic neurons. GABA-B inhibition appears to be altered in absence seizures, and potentiation of GABA-B inhibition with the anti-epileptic drugs (AEDs), tiagabine, vigabatrin, and possibly gabapentin, results in exacerbation of absence seizures. Ethosuxinimide is a suxinimide AED effective only against absence seizures. It has no effect on generalised tonic clonic (GTC), myoclonic, atonic, or partial seizures. The mechanism of action is based on reducing current in T-type calcium channels on thalamic neurons. (The spike-and-wave pattern during absence seizures is thought to be initiated in thalamocortical relays by activation of these channels). Enhanced burst firing in selected corticothalamic networks may increase GABA-B receptor activation in the thalamus, leading to generalized spike-wave activity. Several mutations of genes which encode protein subunits in various ion channels have been found in patients and family members with idiopathic epilepsies. Some forms of JME and absence epilepsy have been shown to result from mutations in Ca<sup>+</sup> channels.

Childhood absence epilepsy (CAE) is a complex polygenic disorder. There is an association between mutations in CACNA1H gene and CAE. These mutations

cause increased channel activity and associated increased neuronal excitability. CAE seizures are believed to originate in the thalamus, where there is an abundance of T-type calcium channels such as those encoded by CACNA1H.

Many of the CACNA1H mutations have a measurable effect on channel kinetics, including activation time constant and voltage dependence, deactivation time constant, and inactivation time constant and voltage dependence. Many of these mutations should lead to neuronal excitability, though others may lead to hypoexcitability. The full impact of ion channel dysfunction in the idiopathic generalized epilepsies, including absence epilepsy, is however incompletely understood.

The hypothesis discussed in Chapter 2 section 10.1, for a “hypocapnia cascade” with involvement of the neuron/glia/endothelial network in the generation of EEG rhythmogenesis postulates a role for the astrocytically generated “calcium wave”.

Childhood absence epilepsy (CAE) may provide an example of the astrocytic etiology of epilepsy. CAE seizures can often be provoked by hyperventilation. After several minutes of hyperventilating the pH of the child's blood becomes slightly alkaline as a consequence of the respiratory depletion of carbon dioxide. With this shift toward the alkaline, the CAE seizure begins as evidenced by a characteristic three-per-second spike-wave pattern on the EEG. In addition to their many other roles, astrocytes near the capillaries of cerebral cortex envelop these blood vessels with their cytoplasmic extensions. The exposure of these perivascular astrocytes, which also control synaptic domains of influence, to the

sudden alkaline shift in the blood may result in primary perivascular calcium wave activation and secondary perivascular synaptic synchrony. Indeed, the three-per-second spike-wave pattern seen on the EEG may reflect the synaptic (spike) and astrocytic (wave) oscillations the theory proposes, with unusually high frequency calcium waves resulting from the effects of alkalosis combined with secondarily coordinated neurotransmitter release. Of additional interest is the demonstration that many of the medications used in the treatment of epilepsy are astrocytic calcium wave inhibitors (White 1992, Nilson 1992).

#### **4.4 Differentiating features of absence seizures and complex partial seizures**

Absence seizures may be confused with complex partial seizures, especially in cases of prolonged seizures with automatisms (Table 4.2). The occurrence of automatisms is dependent on duration of the seizure; the longer the seizure, the more likely automatisms are to occur. Atypical absence seizures, which occur in patients with symptomatic generalized epilepsies, are usually longer than typical absences and often have more gradual onset and resolution. Although absence seizures may share many clinical features with complex partial seizures, the abrupt ending of typical absence seizures, without a post-ictal phase, is the most useful clinical feature in distinguishing the two conditions.



<i>Feature</i>	<i>Complex Partial</i>	<i>Absence</i>
Onset	May have simple partial onset	Abrupt onset of event
Duration	Usually > 30 seconds in duration	Usually < 30 seconds in duration
Automatisms	Present	Duration dependent
Awareness	No	No
Ending	Gradual post- ictal phase	Abrupt end to event.

**Table 4. 2. Differentiating features of complex partial and absence seizures**

#### **4.5 Childhood absence epilepsy and hyperventilation-induced high amplitude rhythmic slowing**

Hyperventilation-induced high amplitude rhythmic slowing (HIHARS) in normal children may be associated with clinical episodes of altered awareness (Engel *et al* 1947). The presence of automatisms has been proposed as a distinguishing feature that helps to differentiate absence seizures from non-epileptic causes of decreased responsiveness. A review by Lum *et al* (2002) found that automatisms are common in both HIHARS and absence seizures (Fig 4.4). Yawning, smiling and particularly fidgeting occur more commonly, and eye opening and eyelid flutter less commonly, in HIHARS. However, episodes of HIHARS with loss of awareness clinically mimic absence seizures, and these conditions can be distinguished reliably only by EEG.



**Fig 4.3 : HIHARS during hyperventilation (Sample from EEG dept. OLCHC)**

Optimal hyperventilation has been demonstrated to produce HIHARS in adult subjects with end-tidal  $p\text{CO}_2$  ( $p\text{ETCO}_2$ ) of  $2.0 \pm 0.1$  kPa ( $15.4 \pm 0.8$  mm Hg). (Zwiener *et al* 1998). In this study see chapter 3 section 3.16. Lum *et al* (2002) used the following criteria to define HIHARS (in a video EEG study on HIHARS with altered awareness)

1. high amplitude ( $> 100\mu\text{V}$ )
2.  $\sim 2.5\text{-}5.0$  Hz generalised rhythmic slowing
3. duration of greater than or equal to 3 seconds.

These are the criteria for the definition of an epoch of HIHARS activity used in this study.

Reduction in consciousness during voluntary hyperventilation was first reported by Davis and Davis (1939), when failure to respond to commands was observed with 2- to 3 Hz high voltage sinusoidal activity. Clinical testing during episodes of HIHARS may demonstrate altered awareness, which prompted speculation that these episodes might be epileptic (Lee and Kirby 1988, Silva *et al* 1995). However, the episodes of HIHARS with altered awareness resolve spontaneously in most patients, and it is generally accepted that these episodes do not have an epileptic basis (Epstein *et al* 1994, North 1990, Lum *et al* 2002) (Fig 4.4).

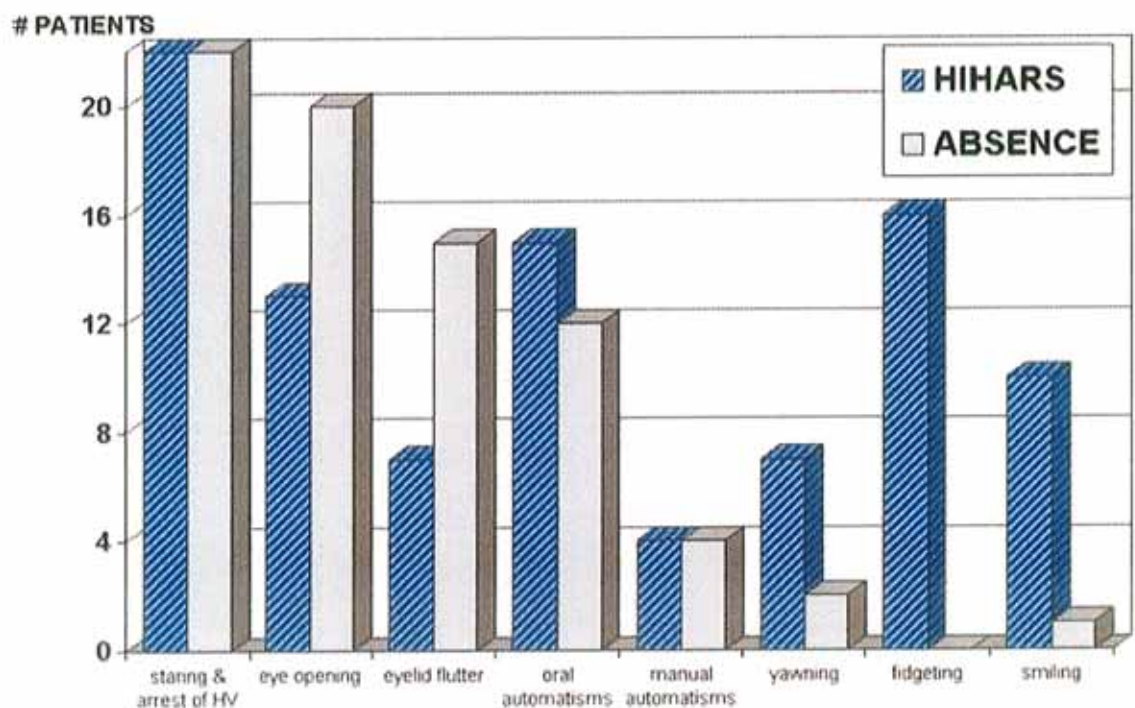


**Fig 4.4: Frequency and type of clinical features observed in episodes of HIHARS with altered awareness and in absence seizures (after Lum *et al* 2002)**

## 4.6 Methodology

In designing the clinical trial on patients with childhood absence epilepsy and first presentation of undiagnosed episodes to pursue the aims set out in section 4.1 above, the critiques of the Holmes *et al* (2005) and Guaranha *et al* (2005) were addressed. The study design consisted of:

- A prospective clinical trial involving two sample cohorts
- A group of patients with *childhood absence epilepsy* matched for age and sex with a group of patients at first presentation with *undiagnosed “events”* which may or may not be of epileptiform origin
- Patients presented sequentially to the Neurophysiology/EEG department of Our Lady’s Children’s Hospital, Crumlin, Dublin, commencing in June 2007
- If the patients were taking anti-epileptic drugs (AEDs) at presentation they were not reduced or discontinued
- Aim was to enrol 15 patients into each group
- Patients undertook two episodes of hyperventilation during their EEG test
  1. The current non-standardised 3 minutes of HV while supine with eye closure
  2. The new standardised protocol, seated, standardised optimal hyperventilation (SOHV) with eyes closed achieving an end-tidal CO<sub>2</sub> of 22-15 mmHg
- Each patient therefore acts as their own control

The acquisition of electrophysiological data was achieved by the method described in Chapter 3. Briefly this consisted of:

- A full head of EEG electrodes as per 10-20 system with simultaneous digital video recording
- Hypocapnia measurement with nasal prongs and capnometer
- Respiration effort, excursion, and rate recorded on EEG system using respiration belt
- ECG recorded using modified lead II
- Oximetry measured using finger probe
- Cerebral blood flow (CBF) measured at rest and at base hypocapnia level using transcranial Doppler measurement probe at temple (sub-group)

Assesment of the efficacy of the methodology was achieved by comparison of :

- number of absence seizures
- number of epochs of spike and wave activity
- number of epochs of HIHARS

which occurred during hyperventilation in the supine non-standardised protocol and in the seated standardised optimal hyperventilation protocol, with those spontaneously occurring during resting, wakefulness, and sleep, using 8 minute epochs as denominators. (4 minutes of SOHV and 4 minutes post-HV).

## References: Chapter 4

- Adams DL, Lueders H, 1981, Hyperventilation and 6-hour EEG recording in evaluation of absence seizures. *Neurology* 31(9): 1175-7
- Annegers JF, Coan SP, 1999, SUDEP: overview of definitions and review of incidence data *Seizure* 8: 347-52
- Avoli M, Gloor P, 1982, Interaction of the cortex and thalamus in spike wave discharges of feline generalised penicillin epilepsy *Exp.Neurol* 76: 196-217
- Berger H, 1934, Uber das Electrenkephalogram des Menschen IX Arch Psychiatr. Nervenkr.
- Billinger TW, Frank G S, 1969, Effects of posture on EEG slowing during hyperventilation. *Am. J. EEG Technol* 9(1): 22-27
- Blume WT, 2006, Hyperventilation, more than just hot air *Epilepsy Currents*, 6(3): 76-77
- Crunelli V, Leresche N, 2002, Childhood absence Epilepsy: genes, channels, neurons and networks. *Nat Rev Neuosci* 3: 371-382
- Dalby MA, 1969, Epilepsy and three per second spike and wave rhythms: a clinical electroencephalographic and prognostic analysis of 346 patients. *Acta Neurol Scand* suppl 40: 1-180
- Davis H, Davis PA, 1939, Electrical activity of the brain: its relationship to physiological states and states of impaired consciousness. *Res Publ Assoc Nerv Ment Dis* 19: 50-80
- Donner EJ, Smith CR, Snead OC 3<sup>rd</sup>, 2001, Sudden unexplained death in children with epilepsy. *Neurology* 57: 430-34
- Dreifuss FE, 1997, Classification of epileptic seizures. In: Engel J Jr, Pedley TA, eds. *Epilepsy: A Comprehensive Textbook*. Philadelphia: Lippincott-Raven
- Drury I, 2000, Activation of seizures by hyperventilation. In: Lueders HO, Noachtars, eds, *Epileptic seizures: pathophysiology and clinical semiology*, Philadelphia: Churchill & Livingstone, 575-9
- Earnest MP, Thomas GE, Eden RA, Hossack KF, 1992, The sudden unexplained death syndrome in epilepsy; demographic, clinical, and postmortem features. *Epilepsia* 33: 310-16

Engel GL, Romano J, 1944, A simple method of determining frequency spectrums in the electroencephalogram. *Arch. Neurol, Psychiat., Chicago*, 51: 134-146

Engel GJ, Ferris EB, Logan M, 1947, Hyperventilation: analysis of clinical symptomatology. *Ann Intern Med* 27: 683-704

Epstein MA, Duchowney M, Jayakar P *et al*, 1994, Altered responsiveness during hyperventilation induced EEG slowing: a non epileptic phenomenon in normal children *Epilepsia* 35: 1204-7

Esquivel E, Chaussam M, Plouin P, Ponsot G, Arthuis M, 1991, Physical exercise and voluntary hyperventilation in childhood absence epilepsy. *Electroencephalogr Clin Neurophysiol* 79: 127-33

Ficker DM, 2000, Sudden unexplained death and injury in epilepsy. *Epilepsia* 41(suppl 2): S7-12

Foerster O, 1924, Hyperventilationsepilepsie. *Z Neurol Psychiatrie*, 38: 289-93

GaborAJ, Marsan CA, 1969, Co-existence of focal and bilateral diffuse paroxysmal discharges in epileptics:clinical-electrographic study *Epilepsia* 10: 453-72

Gibbs FA, Davis H, Lennox WG, 1935, The EEG in epilepsy and in conditions of impaired consciousness. *Arch Neurol Psychiat* 34: 1134-48

Gibbs FA, Gibbs EL, Lennox WG, 1943, Electroencephalographic response to overventilation and its relation to age. *J Pediatrics* 23; 497-505

Gloor P, Fariello RG, 1988, Generalised epilepsy: some of its cellular mechanisms differ from those of focal epilepsy. *Trends Neurosci* 11: 63-68

Gloor P, Quesney LF, Zumstein H, 1977, Pathophysiology of generalized penicillin epilepsy in the cat: the role of cortical and subcortical structures. II. Topical application of penicillin to the cerebral cortex and to subcortical structures. *Electroencephalogr Clin Neurophysiol* 43(1): 79-94

Guaranha MSB, Garzon E. Buchpiguel CA, Tazima S, Yacubian EMT, Sakamoto AC, 2005, Hyperventilation Revisited: Physiological Effects and Efficacy on Focal Seizure Activation in the Era of Video-EEG Monitoring. *Epilepsia*. 46(1): 69-75

Holmes MD, Dewaraja AS, Vanhatalo S, 2005, Does hyperventilation elicit epileptic seizures? *Epilepsia* 46: 69-75

ILAE 1989. Commission on Classification and Terminology of the International League Against Epilepsy, Proposal for revised classification of epilepsies and epileptic syndromes. *Epilepsia* 30: 389-399

Jasper HH, Droogleever-Fortuyn J, 1947, Experimental studies on the functional anatomy of petit mal epilepsy. *Assoc Res Nerv Ment Dis* 26: 272-98

Kloster R, Engelskjøn T, 1999, Sudden unexpected death in epilepsy (SUDEP): a clinical perspective and a search for risk factors *J Neurol Neurosurg Psychiatry* 67: 439-44

Langan Y, 2000, Sudden unexpected death in epilepsy (SUDEP): risk factors and case control studies. *Seizure* 9: 179-83

Langan Y, Nashef L, Sander JW, Fish DR, Shorvon SD, 2000, Sudden unexpected death in epilepsy; a series of witnessed deaths. *J Neurol Neurosurg Psychiatry* 68: 211-13

Lee SI, Kirby D, 1988 Absence seizure with generalised rhythmic delta activity. *Epilepsia* 29: 262-7

Leestma JE, Kalelkar MB, Teas SS, Jay GW, Hughes JR, 1984, Sudden unexpected death associated with seizures; analysis of 66 cases. *Epilepsia* 25: 84-88

Lum LM, Connolly MB, Farrell K, Wong PKH, 2002, Hyperventilation – Induced High Amplitude Rhythmic Slowing with altered awareness: A video EEG Comparison with absence seizures. *Epilepsia* 43(11): 1372-1378

Meeren HK *et al*, 2002, Cortical focus drives widespread cortico-thalamic networks during spontaneous absence seizures in rats. *J Neurosci* 22: 1480-1495

Miley CE, Forster FM, 1977, Activation of partial Complex Seizures by hyperventilation *Arch Neurol* 34 (6): 371-3

Morgan MD, Scott DF, 1970, EEG activation in epilepsies other than petit mal, *Epilepsia* 11: 255-61

Morrice JK, 1956, Slow wave production in the EEG with reference to hypernoea, carbon dioxide, and autonomic balance. *Electroenceph. Clin. Neurophysiol*, 8: 49-72

Nashef L, Garner S, Sander JW, Fish DR, Shorvon SD, 1998, Circumstances of death in sudden death in epilepsy: interviews of bereaved relatives. *J Neurol Neurosurg. Psychiatry* 64: 349-52

Nei M, Ho RT, Sperling MR, 2000, EKG abnormalities during partial seizures in refractory epilepsy *Epilepsia* 41: 542-48

Nilson M, Hansson E, Ronnback L, 1992, Agonist-evoked  $Ca^{2+}$  transients in primary astroglial cultures :modulatory effects of valproic acid. *Glia* 5: 201-209



- Nilsson L, Farahmand BY, Perssen PG, Thiblin I, Temsen T, 1999, Risk factors for sudden unexpected death in epilepsy: a case control study *Lancet* 353: 888-93
- North KN, Ouvrier RA, Nugent M, 1990, Pseudoseizures caused by hyperventilation resembling absence epilepsy. *J Child Neurol* ;5: 288-94
- Opeskin K, Harvey AS, Cordner SM Berkovic SF, 2000, Sudden unexplained death in Victoria. *J Clin Neurosci* 7: 34-37
- Panayiotopoulos CP, 2002, *A Clinical guide to epilepsy syndromes and their treatment*. Bladon Medical Publishing, Oxford
- Pedley T, Hauser WA, 2002, Sudden Death in epilepsy: a wake up call for management.  
Pub online May 21, 2002. *The Lancet*  
<http://image.thelancet.com/extras/o2cmt85web.pdf>
- Penfield WG, Jasper HH, 1947, Highest level seizures. *Assoc Nerv Ment dis Prioc* 26: 252-271
- Silva DF, Lima MM, Anghinah R *et al*, 1995, Atypical EEG pattern in children with absence seizures. *Arq Neuropsiquiatr* 53: 258-61
- Simon RP, 1997, Epileptic sudden death; animal models *Epilepsia* 38 (suppl 11): S35-37
- Snead OC, 1995, Basic Mechanisms of Generalised Absence Seizures *Ann Neurol* 37(2): 146-57
- So EL, Sam MC, Lagerlund TL, 2000, Postictal central apnea as a cause of SUDEP; evidence from near-SUDEP incident. *Epilepsia* 41: 1494-97
- Takahashi T, 1987, Activation Methods, In Niedermeyer E, Lopes Da Silva F, eds., *Electroencephalography: Basic principles, clinical applications, and related fields*. Baltimore: Urban& Schwarzenberg, pp 209-27
- Terrence CF Jr. Wisotzkey HM, Perper JA, 1975, Unexpected, unexplained, death in epileptic patients. *Neurology* 25: 594-98
- Vergnes M Marescaux C, Depaulis A, Micheletti G, Warter JM, 1987, Spontaneous spike and wave discharges in thalamus and cortex in a rat model of genetic petit mal like seizures. *Exp Neurol* 96: 127-136
- Walczak TS, Leppik IE, D'Amelio M *et al*, 2001, Incidence and risk factors in sudden unexplained death in epilepsy: a prospective cohort study. *Neurology* 56: 519-25

White HS, Skeen GA, Edwards JA, 1992, Pharmacological regulation of astrocytic calcium channels: for the treatment of seizure disorders. *Prog Brain Res* 94: 77-87

Wirrell EC, Camfield PR, Gordon KE, Camfield CS, Dooley JM, Hanna BD, 1996, Will a critical level of hyperventilation induced hypocapnia always induce an absence seizure? *Epilepsia* 37(5): 459-62

Zwiener U, Lobel S *et al*, 1998, Quantitative topographical analysis of EEG during non-standardized and standardized Hyperventilation. *J Clin. Neurophysiol.* 15 (6): 521-8

## **CHAPTER 5**

### **RESULTS FOR STANDARDIZED**

### **HYPERVENTILATION DURING EEG IN**

### **CHILDHOOD ABSENCE EPILEPSY AND ATTACK**

### **DISORDERS**

The data were acquired and analysed as described in chapter 3. The EEG system used was an XLTEK neuroworks 5.0. Please see Appendix 6 on CD attached to this thesis for entire data set and original files.

37 patients were enrolled in this clinical pilot study, 18 (48.6%) males and 19 (51.4%) females. The age range of males was from 7-16 years, while the age range of females was 5-17 years. The mean age of males was 9.5 years and of females was 9.7 years. The patients presented sequentially to the neurophysiology department of Our Lady's Children's Hospital, Crumlin (OLCHC), Dublin between June 2007 and May 2008. There were 16 patients in the childhood absence epilepsy (CAE) Group, 16 patients in the "not yet diagnosed" (NYD) Group, and 5 patients with absence epilepsy, which was atypical or accompanied by generalised tonic clonic or partial seizures in addition, designated as "Absence+". The total number of patients in the CAE and Absence+ group is 21.

5 of the patients in the CAE group were not on any medication at the time of their EEG (31.2%). 10 of the patients in this group were on anti-epileptic

medication (AED) at the time of their EEG (62.5%). One patient in the CAE group was on Ritalin only at the time of EEG for attention deficit hyperactivity disorder (6.25%). In the Absence+ group 4 patients (80%) were taking AEDs and 1 (20%) was on no medication. In the NYD group 2 patients were taking AEDs (12.5%) and 14 were on no medication (87.5%) (Figs. 5.1, 5.2). The two patients on AED in the NYD group were referred to OLCCH as a tertiary referral centre from a regional hospital. They had been commenced on medication before the OLCCH attendance and their first EEG and were therefore considered to not yet have a diagnosis. The AEDs included Ethosuximide, Oxcarbazepine, Lamotrigine, Na Valproate, Topiramate, and Levetiracetam. Most patients were on monotherapy, but in the CAE group there were 2 patients taking 3 AEDs. In the Absence+ group one patient was taking 2 AEDs and one patient was taking 3 AEDs. Overall 54% of the patients were not taking anti-epileptic medication, 43% were taking AEDs, and 3% were taking other medication ( methylphenidate for ADHD) (Fig. 5.3).

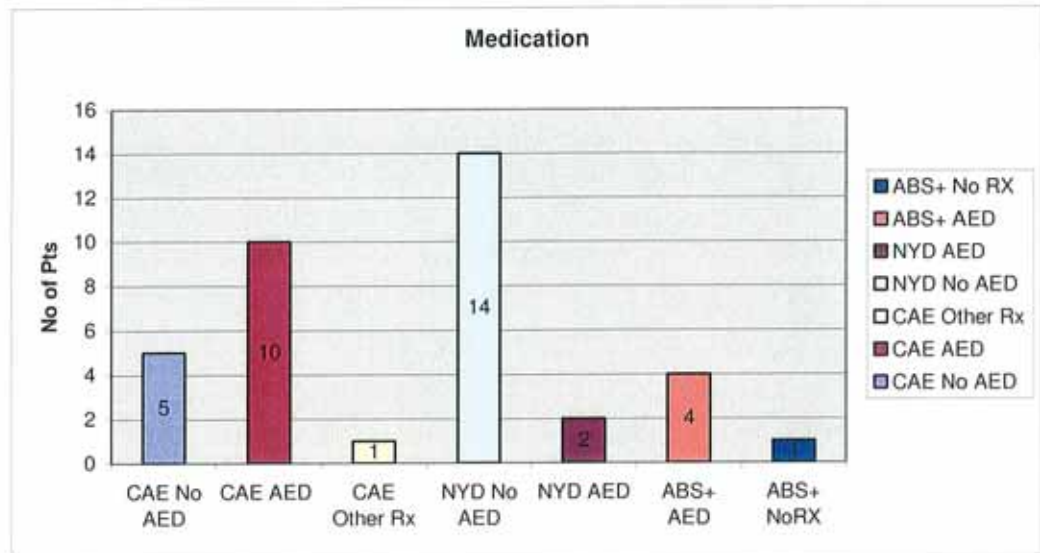


**Fig. 5.1: Medication; number of patients in each group taking AED, not taking AED, and on other medications**

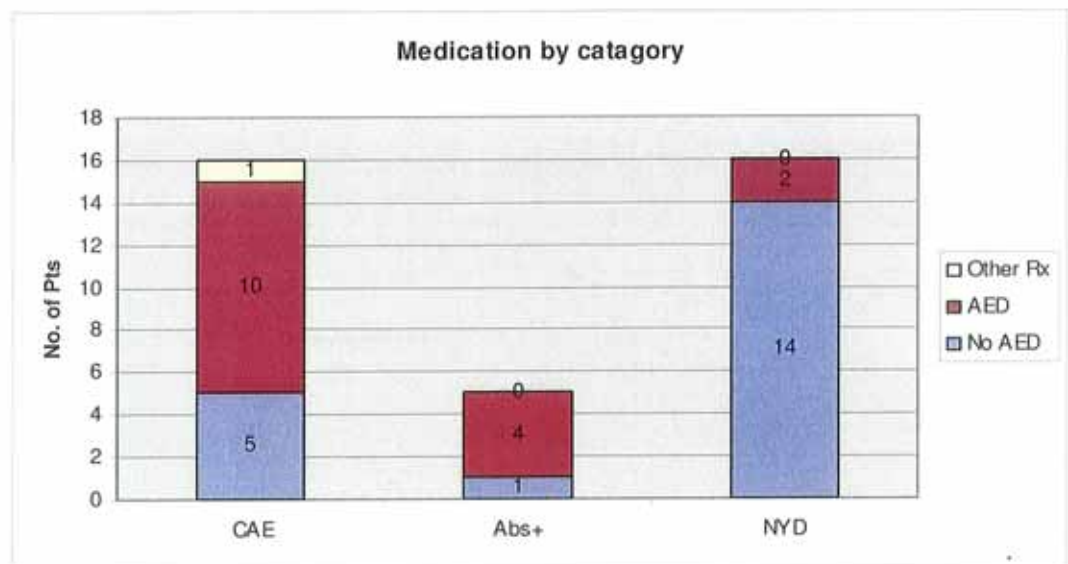


**Fig. 5.2: Medication by category**

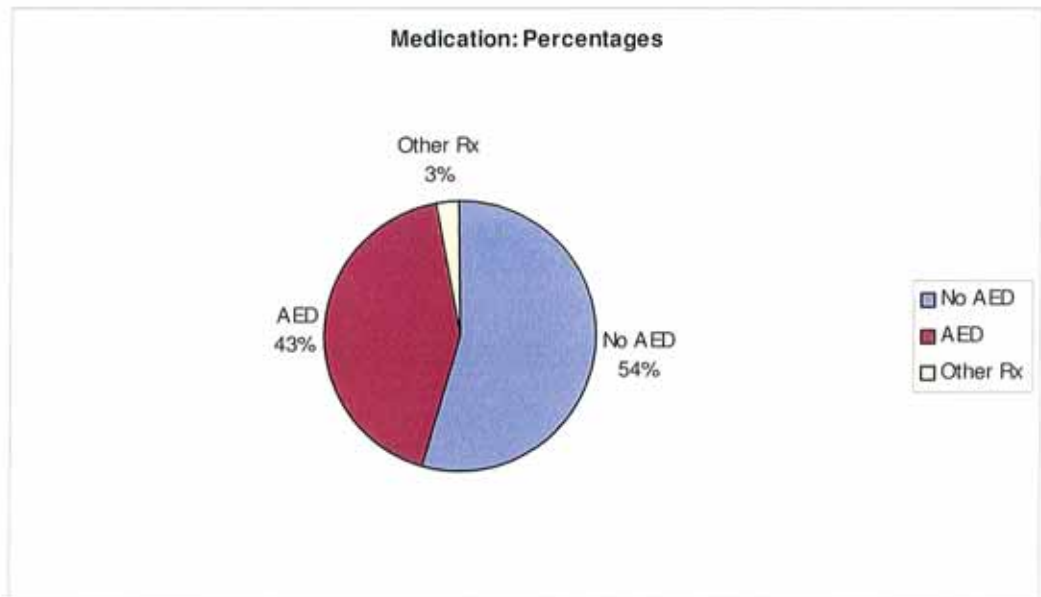


**Fig. 5.3: Medication percentages**

The co-operation / effort of the patients with the standardised hyperventilation exercise was subjectively graded by the author using the following scale:

- 1 poor effort
- 2 erratic/fair effort
- 3 good effort
- 4 very good effort
- 5 excellent effort.

This is the rating scale used by all EEG practitioners in the neurophysiology dept. of Our Lady's Children's Hospital, Crumlin, Dublin. All patients were assessed by the author thus removing any inter-rater bias. The possibility of intra-rater bias is acknowledged.

31 patients were assessed as making an excellent effort (83.7%), 3 made a very good effort (8.1%), 1 made a good effort (2.7%), and 2 made an erratic effort (5.4%). The two patients who made an erratic effort were one 7-year-old male in the CAE group, and one 5-year-old female with mild learning disability in the CAE group (Fig. 5.4).

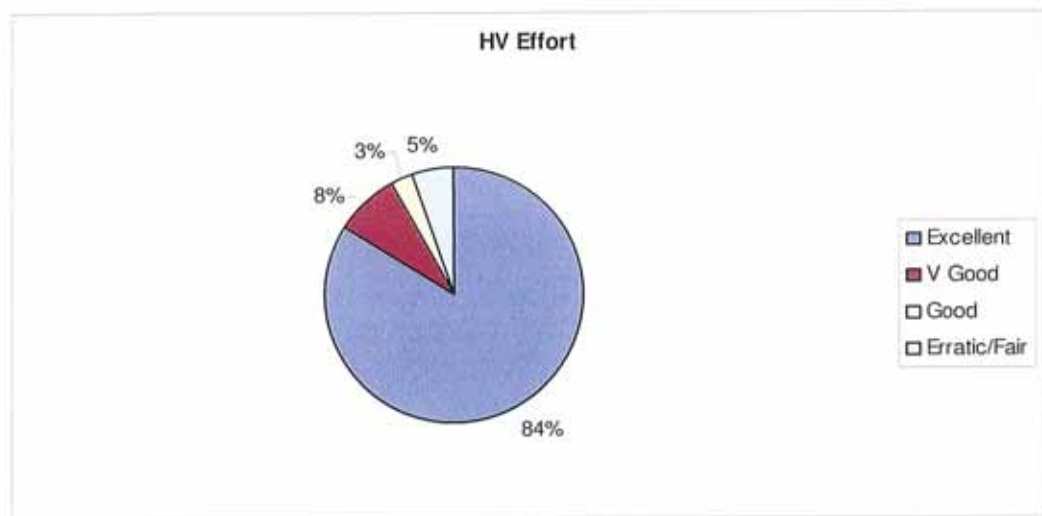


**Fig. 5.4: HV effort**

## 5.1 Analysis of the data

The author used student paired t test to compare two small paired sets of quantitative data with a definite relationship between each pair of data points

An *a priori* power calculation indicating a power greater than 0.8 was based on acquiring

$N = 16$  paired samples

$\delta = 0.3$  a difference in population means

$\alpha = 0.05$  Type I error probability for a two sided test

$\sigma = 0.4$  For paired designs  $\sigma$  is the standard deviation of difference in the response of matched pairs.

## 5.2 “At rest” EEG

The resting EEG background in 31 (83.7%) of the patients contained posterior dominant rhythms (PDR) in the alpha range from 8.0-10.0 Hz. In 6 (16.2%) of the patients the EEG background activity was slower than expected for age and state with frequencies from 6.0-8.0 Hz. 5 of these subjects were in the CAE group (comprised 31.25% of CAE group) and 1 in the Absence + group (comprised 20% of Absence+ group). All of the patients in the NYD group had normal resting background posterior dominant rhythms. The mean PDR of the 37 patients in the waking resting state with eye closure was 9.0 Hz.



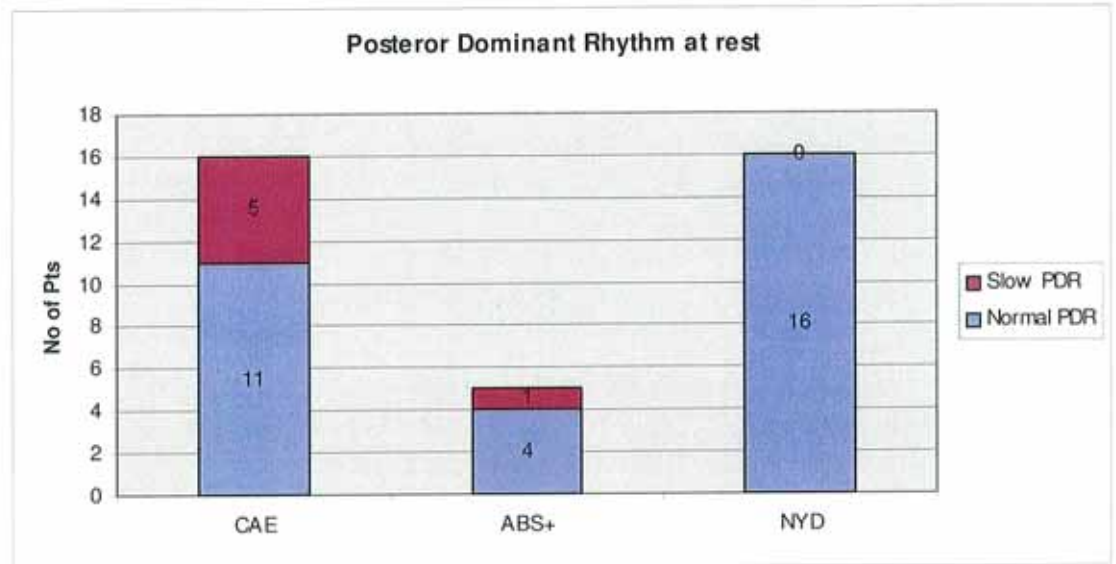


**Fig. 5.5: Posterior dominant rhythm (PDR) at rest**

28 patients (75.6%) became drowsy during the EEG. In 7 (18.9%) of these there was an exacerbation of epileptiform discharges in the drowsy state. Of these 7 patients, 5 (13.5%) were in the CAE group, 1 (2.7%) in the Absence + group and 1 (2.7%) in the NYD group. 27 patients (72.9%) subsequently slept. 8 of the patients (21.6%) who slept showed epileptiform activity in the sleeping state. One patient had a primary generalised tonic clonic seizure during the EEG with onset in stage II NREM sleep. This patient had a clinical absence of 17 seconds duration in the resting state, was in the Absence+ group and was on 3 AEDs at the time of the EEG study. Two patients showed epileptiform activity only in the drowsy and sleeping states at rest. These two patients did not demonstrate an epileptiform abnormality in either non-standardised HV (nsHV) or in standardised optimal HV (SOHV).

In 13 patients (35.1%) the resting EEG was normal for age and state, 3 of these (8.1%) from CAE group, 1 (2.7%) from Absence+ group and 9 (24.3%) from the NYD group.

In total, 20 episodes of epileptiform EEG activity which was focal, multifocal, and/or generalised in type occurred spontaneously in the resting state in 15 patients. 7 patients (18.9%) had a generalised dysrhythmia and 9 patients (24.3%) had a focal dysrhythmia. 5 patients had EEG changes indicative of both generalised and focal dysrhythmia. Details of EEG changes observed at rest are given in Fig. 5.6.

5 patients (13.5%) had 7 episodes of spontaneous clinical absence events during the resting EEG, 4 of these from the CAE group and 1 from the Absence+ group. 2 patients had 2 CAE seizures and 3 patients had 1 CAE seizure. The duration of the clinical absences was from 4 seconds to 30 seconds, accompanied electrographically by classical 3 per second spike and wave discharges on the EEG. 5 patients (13.5%) had discharges of 3 per second spike and wave and spike and wave paroxysms at other frequencies in the resting EEG without any clinical changes. The total duration of the 7 spontaneous CAE seizures experienced by 5 patients during the resting phase of the EEG was 101 seconds, with a mean duration of 14.4 seconds.

**Fig. 5.6: Number of EEG changes observed at rest in 37 subjects**

Focal/Multi focal epileptiform abnormalities: focal/multi

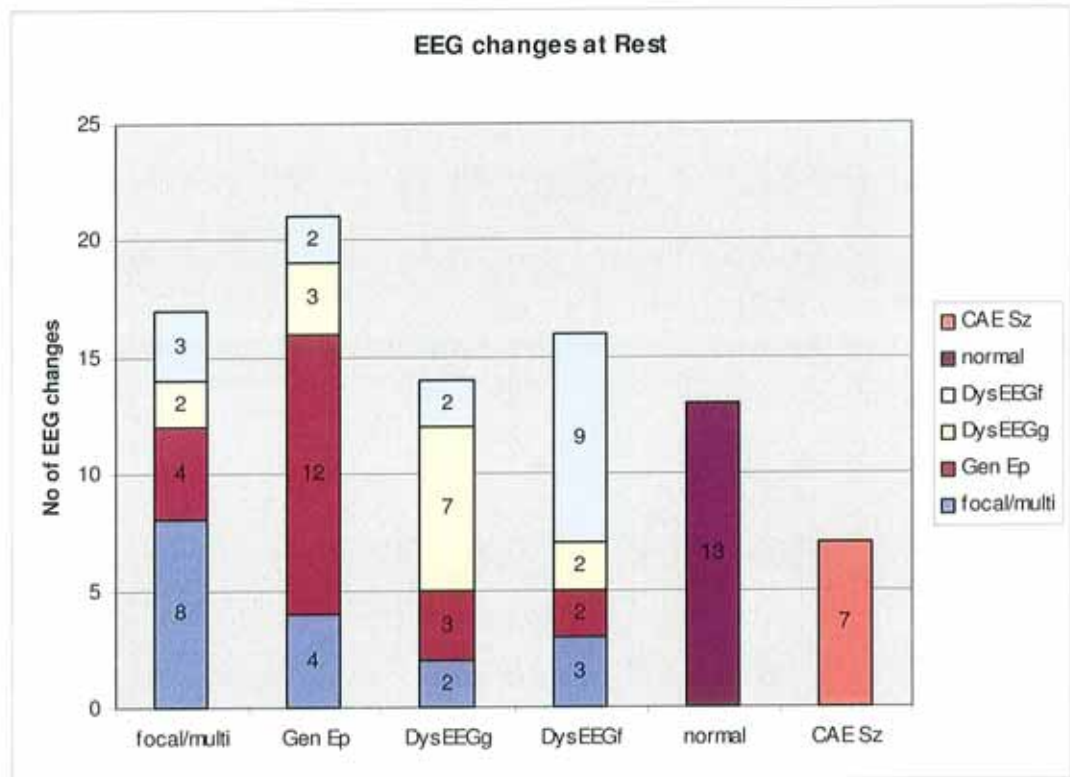
Generalised epileptiform abnormalities: Gen Ep

Dysrhythmic EEG, generalised: DysEEGg

Dysrhythmic EEG, Focal: DysEEGf

Normal EEG: normal

CAE Sz: Absence Seizure



### 5.3 Non Standardised Hyperventilation

The non-standardised hyperventilation (nsHV) exercise consisted of 3 minutes of vigorous hyperventilation by the patient with eyes closed. Expiration was generally buccal and the EEG practitioner demonstrated HV and encouraged the patient throughout. Hyperventilation induced high amplitude rhythmic slowing (HIHARS) reduced the mean PDR achieved by the 37 patients to 5.5 Hz.

In 14 patients (37.8%) the EEG did not show any abnormality during nsHV, 3 of these (8.1%) from CAE group, 2 (5.4%) from Absence+ group and 9 (24.3%) from the NYD group.

In total 19 episodes of epileptiform EEG activity, which was focal, multifocal, and/or generalised in type, (51% EEG changes seen in 37 patients) were elicited during nsHV hyperventilation. 6 EEGs (16.2%) had a generalised dysrhythmia and 4 EEGs (10.8 %) had a focal dysrhythmia. Details of EEG changes observed during non-standardised hyperventilation are given in Fig. 5.7.

7 patients (18.9%) had 10 episodes of spontaneous clinical absence events during the nsHV EEG exercise, 5 of these from the CAE group and 2 from the Absence+ group. 3 patients had 2 CAE seizures and 4 patients had 1 CAE seizure. The duration of the clinical absences was from 4 seconds to 19 seconds, accompanied electrographically by classical 3 per second spike and wave discharges on the EEG. 7 patients (18.9%) had discharges of 3 per second spike and wave during HV without any clinical changes, 4 of whom also had CAE events and 3 did not. The total duration of the 10 CAE seizures experienced by 7 patients during non-standardised HV was 104 seconds, with a mean duration of 10.4 seconds.

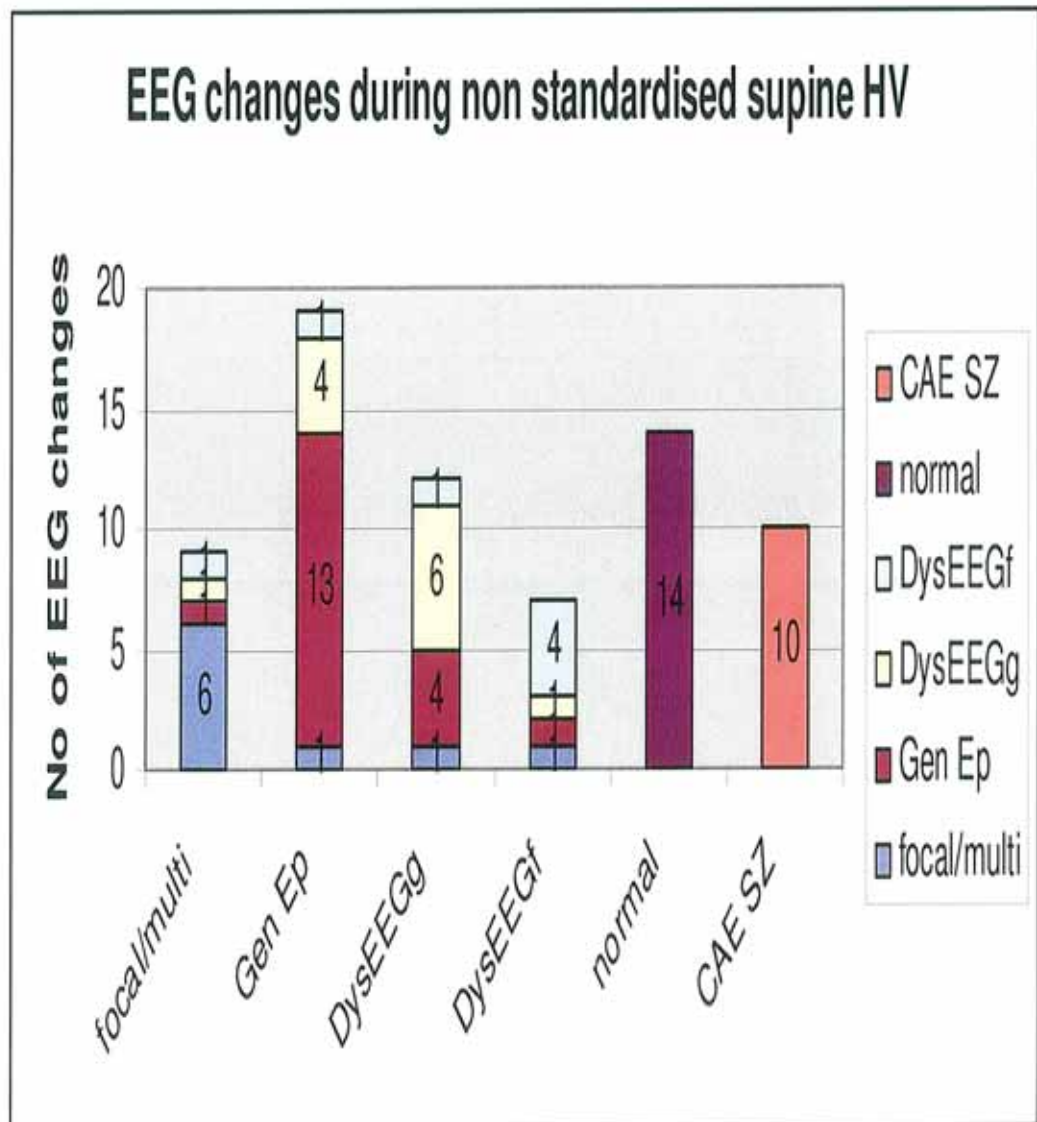


**Fig. 5.7: Number of EEG changes observed during non-standardised supine HV**

Focal/Multi focal epileptiform abnormalities: focal/multi

Generalised epileptiform abnormalities: Gen Ep

Dysrhythmic EEG, generalised: DysEEGg

Dysrhythmic EEG, Focal: DysEEGf

Normal EEG: normal

CAE Sz: Absence Seizures

## **5.4 Standardised seated optimal hyperventilation (SOHV)**

The SOHV exercise consisted of 4 minutes of vigorous hyperventilation in the seated position at a controlled breathing rate of 30 per minute by the subject with eyes closed, as described previously in this work. Expiration was generally nasal and the EEG practitioner demonstrated SOHV and encouraged the patients throughout. HIHARS reduced the mean PDR achieved by the 37 patients to 3.9 Hz.

In 13 patients (35.1%) the EEG did not show any abnormality during SOHV, 4 of these (10.8%) from CAE group, 1 (2.7%) from Absence+ group and 8 (21.6%) from the NYD group.

In total 21 patients (56.7%) demonstrated epileptiform EEG activity (focal, multifocal, and/or generalised in type) during hyperventilation. 7 patients (18.9%) had a generalised dysrhythmia and 8 patients (21.6%) had a focal dysrhythmia. Details of EEG changes observed during SOHV are given in Fig. 5.8.

11 patients had 27 episodes of spontaneous clinical absence seizures during the SOHV exercise, 9 of these from the CAE group and 2 from the Absence + group. 7 patients (18.9%) had discharges of 3 per second spike and wave during HV without any clinical changes. 6 of these 7 patients also had frank absence events during SOHV. 1 patient only had generalised spike and wave discharges without clinical absence during SOHV. The duration of the clinical absences

was from 4-25 seconds, accompanied electrographically by classical 3 per second spike and wave discharges on the EEG. Two patients had 5 episodes of CAE, 3 patients had 3 episodes of CAE, 2 patients had 2 episodes of CAE, and 4 patients had one episode of CAE during SOHV.

The total duration of the 27 clinical absence seizures experienced by 11 patients was 314 seconds, with a mean duration per CAE seizure of 11.6 seconds.

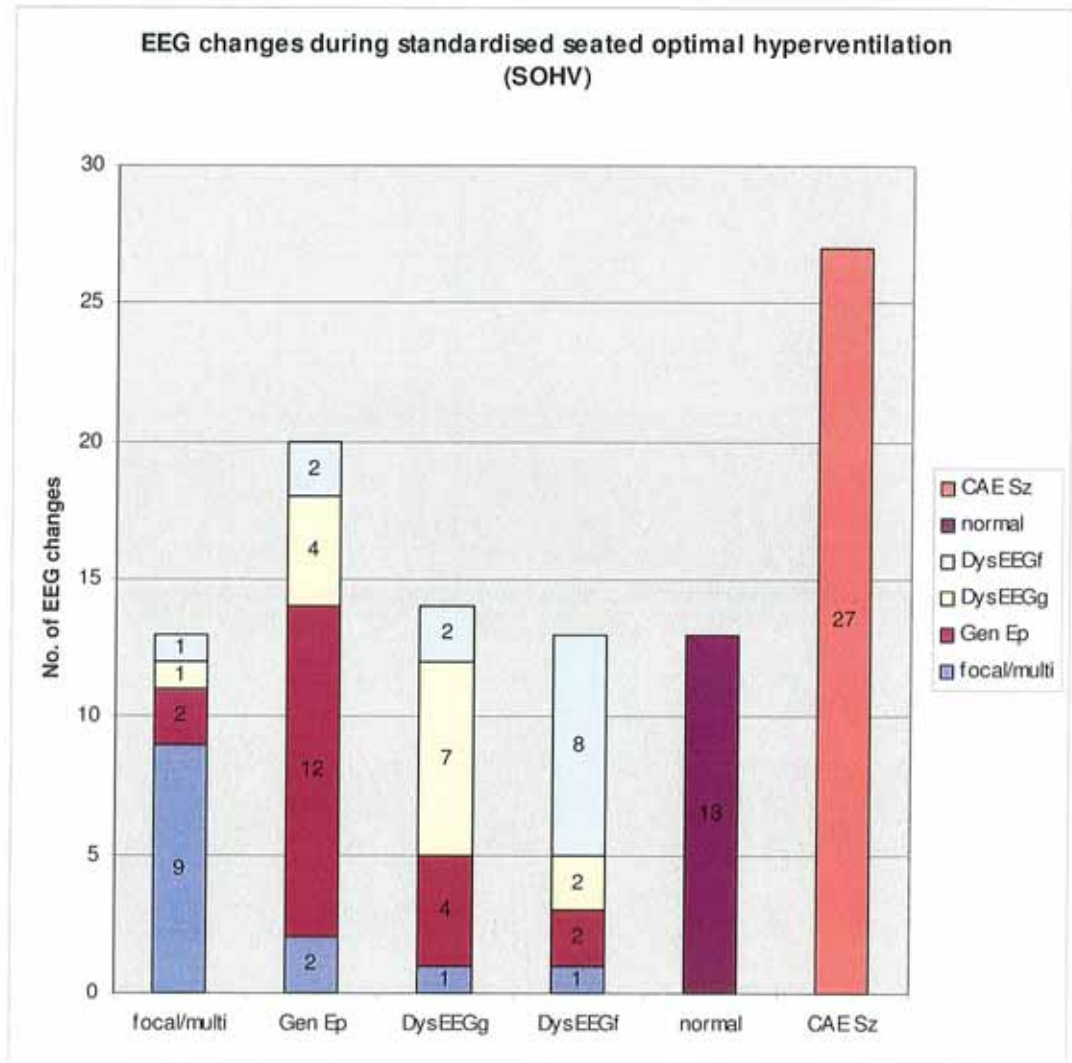


**Fig. 5.8: Number of EEG changes observed during standardised supine hyperventilation (SOHV) in 37 subjects**

Legend:

Focal/Multi focal epileptiform abnormalities: focal/multi

Generalised epileptiform abnormalities: Gen Ep

Dysrhythmic EEG, generalised: DysEEGg

Dysrhythmic EEG, Focal: DysEEGf

Normal EEG: normal

CAE Sz: Absence Seizures



## 5.5 Posterior dominant rhythms and hyperventilation

Performing standardised optimal hyperventilation for 4 minutes in the seated position is significantly more effective in producing HIHARS on the patient's EEG. Student's *t*-test gives a  $p < 0.001$ . The mean EEG frequency in Hz achieved using the routine non-standardised supine method is 5.5 Hz. The mean frequency achieved using SOHV is 3.9 Hz (Table 5.1, Fig. 5.8). This result is in concordance with the results described in section 3.16 Table 3.7 and Fig. 3.9 (the normal adult SOHV study). Frequencies are generally lower in the study on children as their background frequencies have not yet reached adult values and they have a marked response to hyperventilation as previously reported (Takahasi 2004).

**Table 5.1: Comparison of PDR during nsHV and SOHV**

<i>p</i> < 0.001	nsHV	SOHV
<b>Mean</b>	<b>5.5</b>	<b>3.9</b>
<b>95% CI for Mean</b>	<b>5.031-5.943</b>	<b>3.438-4.318</b>
<b>SD</b>	<b>1.4</b>	<b>1.3</b>

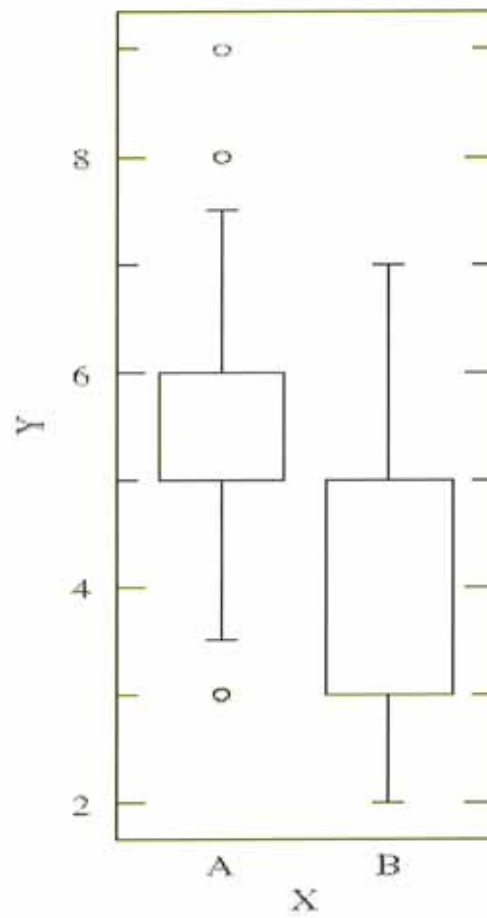


**Fig. 5.9:** Box plot, range, mean and standard deviation of the change in posterior dominant rhythm in EEG during nsHV (group A) and SOHV (group B). Y axis is EEG frequency in Hz.

The changes in PDR from the frequencies found in the resting state, to those achieved during nsHV and SOHV were also analysed using Analysis of Variance (ANOVA) in the 3 states ( $p < 0.0001$ ). The results were comparable with the paired student's t-test applied to the nsHV and SOHV group (Table 5.2, Fig. 5.9).

**Table 5.2: ANOVA of PDR at rest, during nsHV, and SOHV**

<b>p&lt;0.0001</b>	<b>At Rest</b>	<b>nsHV</b>	<b>SOHV</b>
<b>Mean</b>	<b>9.0</b>	<b>5.5</b>	<b>3.9</b>
<b>95% CI for Mean</b>	<b>8.6-9.4</b>	<b>5.06-5.9</b>	<b>3.45-4.3</b>
<b>SD</b>	<b>1.2</b>	<b>1.4</b>	<b>1.3</b>
F 149.9			

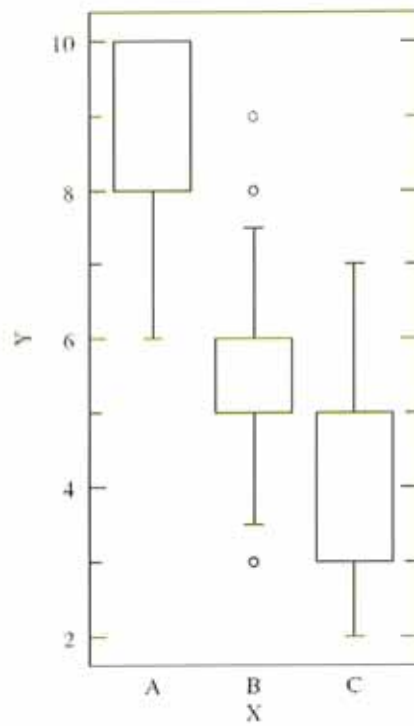


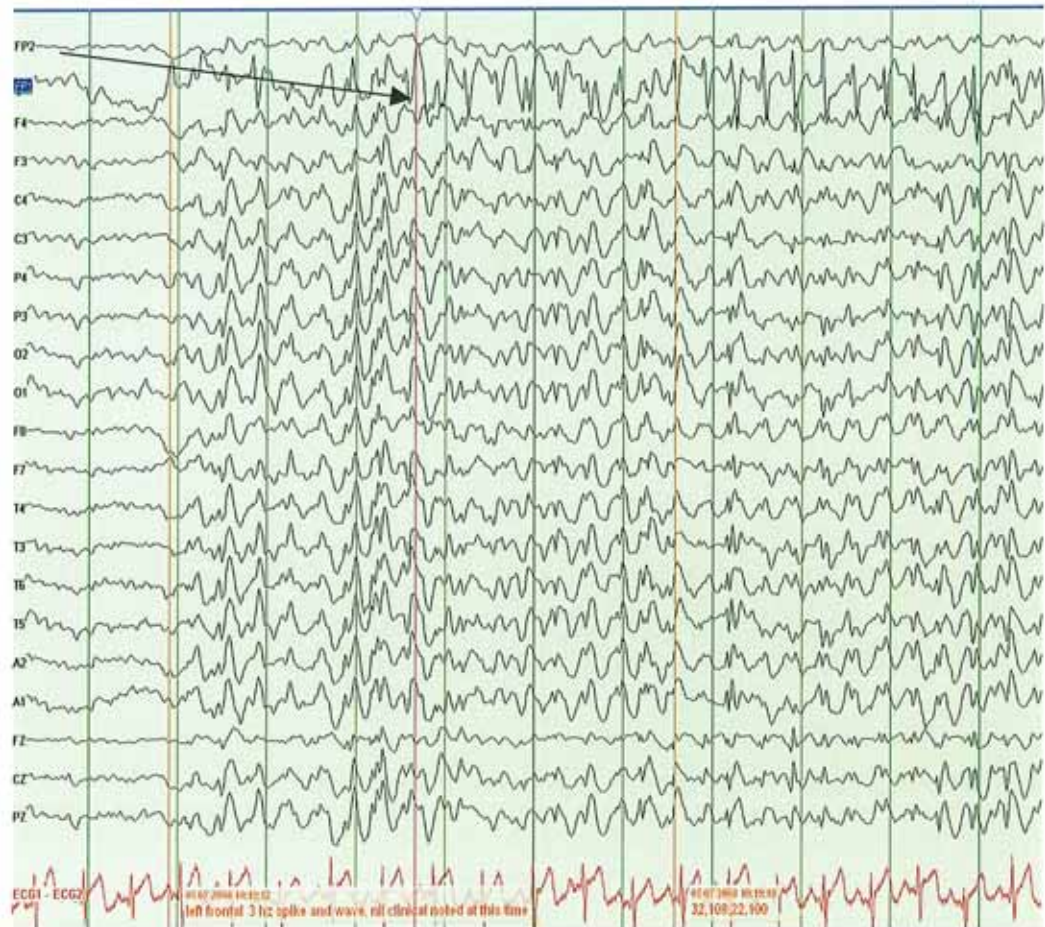
**Fig. 5.10: Box plot of group means, range and SD of PDR, with 95% confidence intervals**  
 (A) At Rest, (B) nsHV, (C) SOHV. Y axis is the EEG frequency in Hz

## 5.6 Efficacy of SOHV in induction of absence seizures

5 patients had 7 spontaneous CAE seizures at rest. 7 patients had 10 CAE seizures elicited by nsHV. 11 patients had 27 CAE seizures elicited by SOHV. The frequency and duration of the CAE seizures increased significantly during SOHV (Figs. 5.11, 5.12).

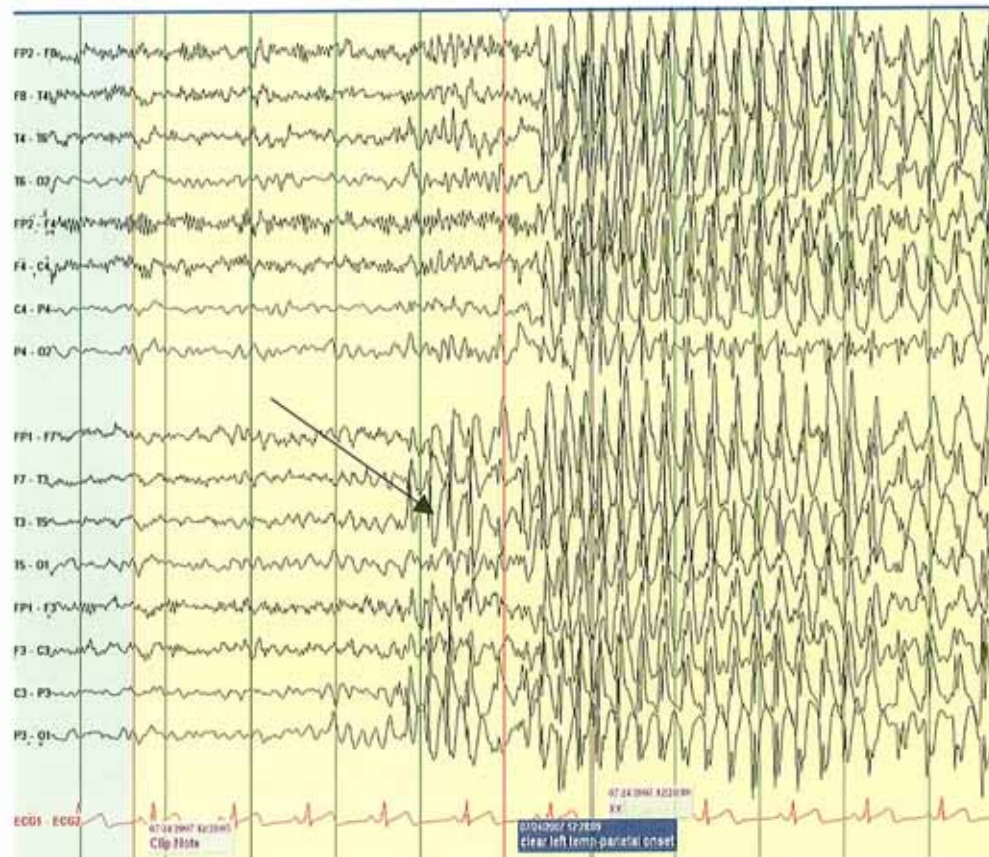
In 3 patients absence seizures were elicited only during SOHV. All 3 of these patients were in the CAE group. The inclusion of standardised seated optimal hyperventilation therefore contributed directly to a positive diagnosis of primary generalised epilepsy in 8.1% of the patients in this study. This result is clinically and statistically significant. Paired student's *t*- test comparing the number of CAE seizures induced during nsHV and SOHV yields  $p < 0.0008$  (Table 5.3). Paired student's *t*- test comparing the total duration of the CAE seizures induced during nsHV and SOHV yields  $p < 0.014$  (Table 5.4). ANOVA comparing the duration of CAE seizures in the 3 states (at rest, nsHv, SOHV) gives a  $p < 0.064$  (Table 5.5, Fig. 5.13), and the results are comparable for mean and standard deviation with the paired student's *t*-test applied to the nsHV and SOHV group (Table 5.4). The 3 patients who showed clinical absence discharges only during StOHV were a 16-year-old male, a 10-year-old male and a 13-year-old female. In both of the male patients StOHV induced additional focal electrographic EEG activity. In the 16-year-old male left frontal polar focal slow theta and a phase reversing spike discharge was noted. An MRI has been booked on this patient (EEG sample 5.1).

**EEG sample 5.1: left frontal polar focal slow theta and a phase reversing spike**



In the 10-year-old male clinical CAE events were preceded on occasion by left temporal focal epileptiform discharges (EEG Sample 5.2)

### EEG Sample 5.2: Left sided onset



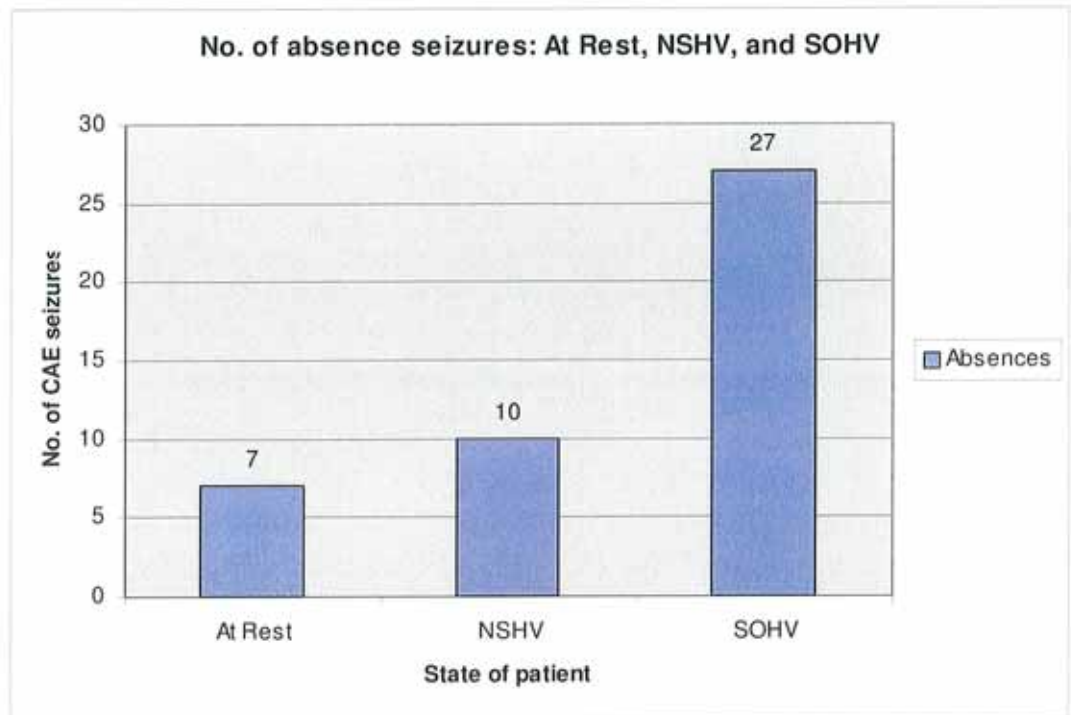


**Fig. 5. 11: Number of childhood absence seizures captured spontaneously “at rest”, during non-standardized HV (nsHV), and during standardized HV (SOHV)**



**Table 5.3: Number of absence seizures induced during nsHV and SOHV paired student's t test.  $p < 0.008$**

<i>P</i> < 0.008	nsHV	SOHV
Mean	0.270	0.73
95% CI for Mean	0.217-0.4729	0.2671-1.192
SD	0.608	1.39

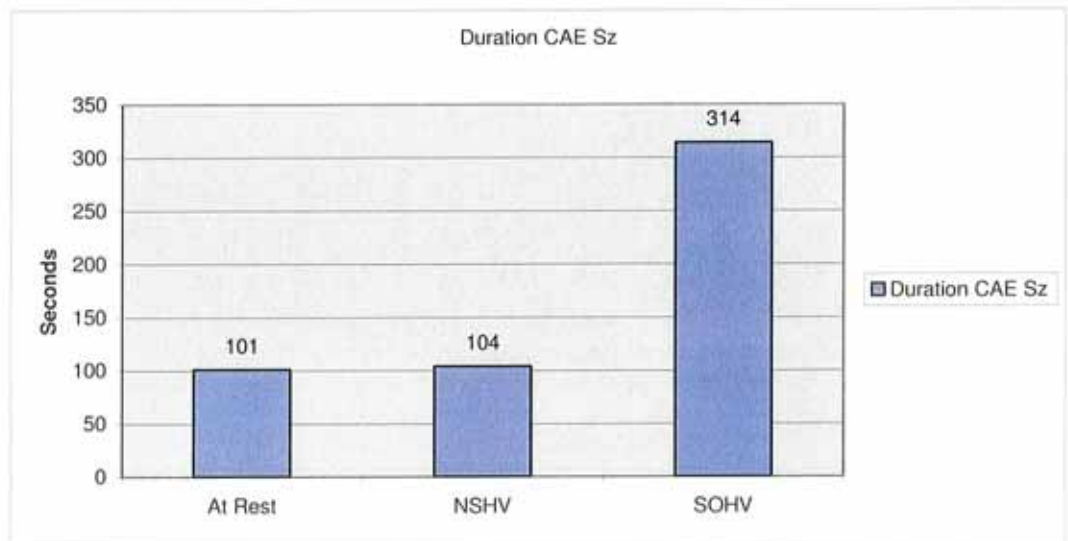


**Fig. 5.12: Total duration of CAE seizures; at rest 101 seconds, during non-standardised HV (nsHV) 104 seconds, and during standardised HV (SOHV) 314 seconds**

**Table 5.4: Paired *t*-test duration of CAE seizures, nsHV, SOHV**

<b><i>p</i>&lt;0.014</b>	<b>nsHV</b>	<b>SOHV</b>
<b>Mean</b>	<b>2.81</b>	<b>8.49</b>
<b>95 % CI for mean</b>	<b>0.4718- 5.150</b>	<b>2.656- 14.32</b>
<b>SD</b>	<b>7.02</b>	<b>17.5</b>

**Table 5.5: ANOVA comparison of duration of CAE events, at rest (A), nsHV (B), SOHV (C)**

<b>p&lt;0.064</b>	<b>At Rest</b>	<b>nsHV</b>	<b>SOHV</b>
<b>Mean</b>	<b>2.72</b>	<b>2.81</b>	<b>8.48</b>
<b>95 % CI for Mean</b>	<b>-1.165-6.624</b>	<b>-1.083-6.705</b>	<b>4.592-12.38</b>
<b>SD</b>	<b>8.57</b>	<b>7.02</b>	<b>17.5</b>
<b><u>F 2.82</u></b>			

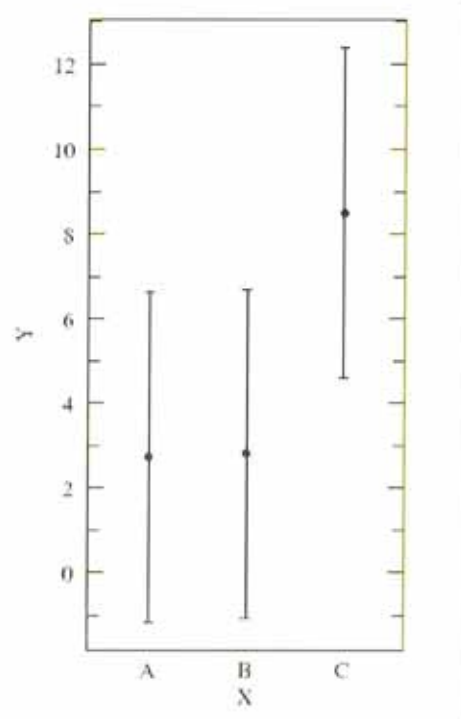


**Fig. 5.13: Plot of group means 95% CI. Y axis duration of events in seconds**

## 5.7 Spontaneous CAE seizures “at rest” and CAE seizure induction during nsHV

There is no statistical difference between the total duration of the spontaneous CAE seizure noted at rest (101 seconds) and the total duration of CAE seizures which were induced during nsHV (104 seconds). Student's *t*-test yields a *p* value of 0.964 which does not reach statistical significance (Table 5.6). However in 2 patients who did not show epileptiform abnormalities in the resting state, clinical and EEG evidence of CAE seizures were triggered by nsHV. 2 patients who slept in the “at rest” state had epileptiform discharges only while sleeping and not during nsHV. Therefore performing the nsHV exercise proved to be clinically significant in 2 patients with CAE.

**Table 5.6: Paired *t*-test spontaneous CAE Seizures “at rest” and during nsHV**

<i>p</i> <0.964	At Rest	nsHV
Mean	2.73	2.81
95 % CI for Mean	-0-1284-5.588	0.4718-5.150
SD	8.57	7.02

## 5.8 Gender Differences

15 females and 10 males had abnormal EEGs. Females with abnormal EEGs were in the following groups: 9 CAE, 4 NYD, 2 Absence +. Males with abnormal EEGs were in the following groups: 5 CAE, 3 NYD, 2 Absence + (Figs. 5.14, 5.15). In this group 44% more females than males were diagnosed with childhood absence epilepsy. 33% more females had abnormal EEGs. There is generally no difference reported in the incidence of idiopathic generalised epilepsies although a 1996 report from the Minnesota epidemiology of epilepsy study (Hauser *et al* 1996) found that *"the age-adjusted incidence of epilepsy per 100,000 person-years characterised primarily by absence seizures was 3 and was higher for females than for males"*. A 2005 study by a Danish group (Christensen *et al*) found that generalised epilepsy was more frequent in women and the percentage of CAE in their population was 63% for females and 37% for males.

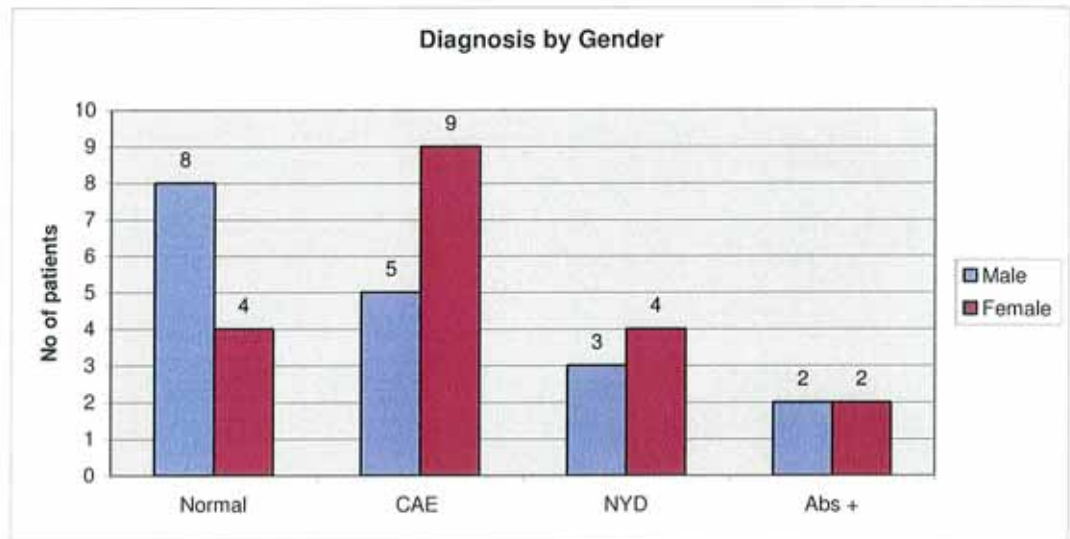


**Fig. 5.14: Diagnosis by gender (following EEG)**

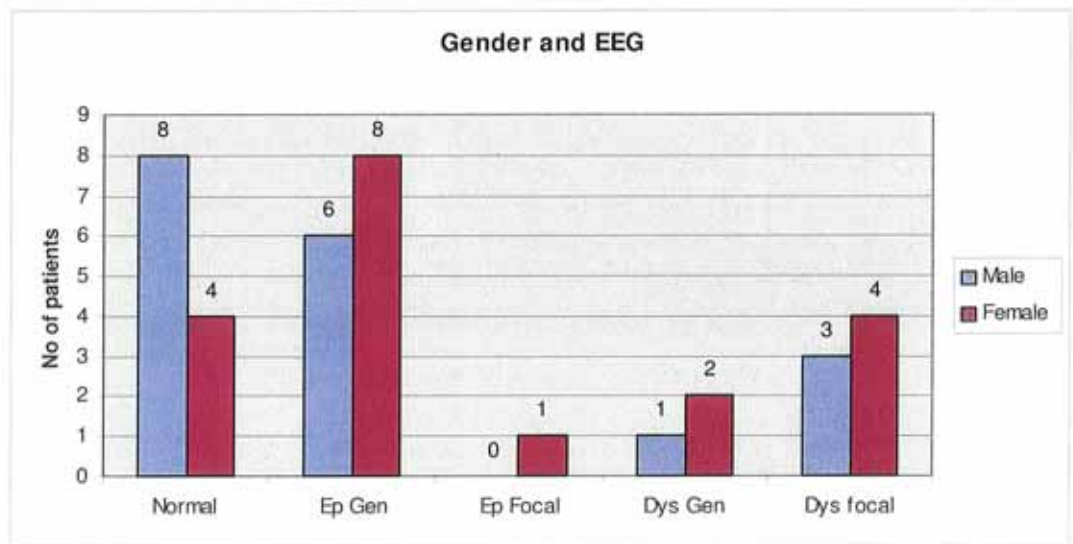


**Fig. 5. 15: Gender and EEG findings**

## 5.9 Discussion

While making a diagnosis of epilepsy is based on the clinical history, the EEG is the first line diagnostic test used by the clinician who may suspect that a patient is experiencing epileptic seizures. A normal EEG does not exclude the possibility that the patient does have the condition. Subsequent follow up studies which may include a period of sleep, long term ambulatory EEG, or video EEG monitoring are often requested to capture an event or electrographic epileptiform abnormalities. An abnormal EEG, which contains spike or spike and wave discharges is often diagnostic of the condition and clarifies if the attacks have a generalised or a focal onset. Increasing the specificity of the EEG test would therefore have a universally positive effect on the both the patient and the treating clinician. A reduction in the time to diagnosis and treatment may be facilitated by increasing the efficacy of the hyperventilation activation procedure during the patient's EEG test.

In this group of 37 patients, which included 16 patients with CAE, matched for age and gender with 16 patients with NYD events, and 5 Absence+ patients, the SOHV method has been proven to be statistically and clinically more effective than nsHV in eliciting diagnostic epileptiform EEG abnormalities.

2 patients in the CAE group who were being treated with the AED Ethosuximide showed epileptiform activity only in drowsiness and sleep (5.4% of the total patient group). 12 of the 37 patients had normal EEGs (32.4% of the total group), 11 of whom were in the original NYD group. The other single

patient with a normal EEG was in the CAE group and on no medication, and was a first presentation with staring episodes which were queried as being behavioural in origin. It was considered unlikely that this patient would have a positive diagnosis of CAE following the EEG. Of the 5 remaining patients in the NYD group who had abnormal EEGs 4 showed mild focal dysrhythmia and one a generalised dysrhythmia. Presenting symptoms included episodes of confusion, unexplained loss of consciousness, faints and anxiety. 15 patients had frank epileptiform abnormalities on their EEGs, which were focal, multifocal, or generalised in type. 10 were in the CAE group, 4 in the Absence + group and 1 in the NYD group (presenting with 1<sup>st</sup> seizure). 10 further patients had focal and /or generalised slow rhythms (dysrhythmias) which were not appropriate for the age and state of the patient. A significant difference was seen between the genders in this group. 44% more females were diagnosed with CAE and 33% more females had abnormal EEGs. However the numbers are small and therefore the strength of this finding can not be high.

Hyperventilation induced high amplitude rhythmic activity (HIHARS) was induced both by nsHV and by StOHV. The posterior dominant rhythm of the EEG was 1.6 Hz slower during the seated OHV protocol at 3.9 Hz ( $p < 0.001$ ). Runs of activity were of sudden onset, of higher amplitude and more continuous during StOHV. There were no episodes of non-epileptic altered awareness experienced by the patients. Lum *et al* (2002) reported that HIHARS in children may be associated with clinical episodes of altered awareness. They noted this phenomenon in a review of 6,564 patients 22 of whom demonstrated episodes of loss of awareness (0.33%) with fidgeting, smiling and yawning, with arrest of



activity, staring and oral and manual automatism. As clinical episodes of HIHARS mimic true absence seizures, these conditions can be distinguished dependably only by video EEG. Given the rarity of this finding of absence of non-epileptic clinical HIHARS in the Lum study, it is perhaps not surprising that no such patients were found in this study. However following the cessation of collection of data for this study a case, which did fulfil the criteria for clinical HIHARS with loss of awareness presented for EEG with a differential diagnosis of CAE. The StOHV SOP protocol was used in conjunction with digital video and it was possible to clearly differentiate that this patient did not have CAE. Smiling and loss of awareness with automatisms were the primary clinical presentations. The EEG showed high amplitude bilaterally synchronous 3.5-4.0 Hz slow wave activity but no spikes or other epileptiform activity.

Childhood absence epilepsy (CAE) may provide an example of the astrocytic etiology of epilepsy. Epilepsy investigators frequently have theorized that a dysfunction in glial cells, and not in neurons or synapses, may be the initiating cause of epilepsy. This proposition has been based on several observations:

- Reactive gliosis is necessary to induce post traumatic epilepsy (Penfield 1929).
- Astrocytes play a critical role in ion homeostasis and thus in neuronal excitability (Orkand *et al* 1966).
- Manipulation of glial cell volume and therefore of extracellular volume affects neuronal hypersynchrony (Lux *et al* 1986, Hochman 1995).
- Astrocytes have a direct role in the regulation of synaptic strength and neuronal excitability (Araque *et al* 1998, Newman and Zahs 1998).

Astrocytes can generate oscillatory intracellular calcium waves which can propagate through the astrocyte network, releasing neuroactive transmitters such as glutamate (Cornell-Bell *et al* 1990). Recent work by Tian *et al* (2005) has provided direct evidence that activation of a single astrocyte by photolytic uncaging of intracellular  $\text{Ca}^{2+}$  induces paroxysmal depolarisation shifts (PDS). They found that astrocyte calcium waves have properties that could facilitate seizures. Calcium waves have a propagation velocity comparable to that of spreading depression. The cellular mechanism involved in the development of absence seizures (and possibly of HIRARS) is believed to involve T-type calcium currents. Abnormal oscillatory rhythms involving GABA-B mediated inhibition alternating with glutamate-mediated excitation develops in thalamo-cortical pathways. This study has demonstrated the efficacy of StOHV and low pETCO<sub>2</sub> levels in triggering more numerous clinical absence seizures and extending their duration. It is interesting to postulate whether or not there is relationship between these factors and a pathophysiological irritability of the glial/neuronal networks producing abnormal oscillatory rhythms in a thalamo-cortical circuit that mainly involves the neocortical pyramidal cells, the reticular nucleus, and the relay nuclei of the thalamus.

In 3 patients from the CAE group diagnostic childhood absence seizures with 3 per second spike and wave discharges on their EEG, accompanied by a clinical absence, were *only* captured during the standardised optimal hyperventilation exercise. Therefore 8.1% of the 37 patients in the whole group, or 18.8% of the patients in the CAE group would *not* have been diagnosed with that condition if the SOHV exercise had not been performed.. Incorporating this standard operational protocol (SOP) of seated optimal hyperventilation

significantly increased the specificity of EEG testing in patients with primary idiopathic childhood absence epilepsy ( $p=0.008$ ). The StOHV method in this group therefore reduced the amount of EEG investigations required to make the diagnosis, increasing the sensitivity of the test for positive identification of indicative epileptiform activity. In 18.8% of patients with a differential diagnosis of CAE it was possible to make a positive conclusion on the basis of their first EEG, reducing the time to achieve diagnosis and commencement of suitable treatment. The continuation of untreated episodes of CAE, in which the child may have several or multiple episodes each day, can greatly interfere with a child's ability to learn and play. In addition to interference with daily activities absences present a serious risk of accidental injury (Wirrell *et al* 1996). Childhood absence epilepsy has the potential to negatively impact upon learning and academic performance. Affected children need to take precautions to prevent injury during absence, and should refrain from activities that would put them at risk if seizures occurred (e.g. climbing heights, swimming unsupervised, or cycling without a helmet or on busy roads). They also may increase their risk of injury because of the frequent impairment of consciousness and the fact that they occur without any warning. In one study, 27% of children with absence epilepsy reported accidental injury during an absence seizure. Bicycle accidents, being struck by a car, and mild head injury were the greatest risks (Wirrell *et al* 1996).

Absence seizures generally respond promptly to treatment with conventional anti-epileptic drugs (Browne *et al* 1983). A positive EEG during which a clinical absence seizure is captured confirms the diagnosis. A negative EEG may mean

that the patient does not receive a diagnosis and continues to experience CAE events with the risk of injury outlined above. Adams and Lueders (1981) found that for the analysis of epileptiform activity, 5 minutes of controlled ventilation during EEG was more reliable than an extended 6 hour recording as a predictor of clinical seizure frequency in the evaluation of absence seizures.

Sudden unexpected death in epilepsy (SUDEP) is generally defined as an *“uncommon and non-traumatic death that occurs suddenly and unexpectedly in a person with epilepsy who was otherwise perfectly healthy”*. It is without any obvious clinical or pathological explanation. SUDEP is the most common cause of seizure related mortality in people with chronic epilepsy. Depending on the cohort studied, SUDEP is responsible for 2% to 18% of all deaths in patients with epilepsy (Ficker 2000, Walczak *et al* 2001). In the general population of people with epilepsy the incidence of SUDEP is of the order of 1:1000 per year. This is at least 10 times the sudden death rate found in the general population. Increasing the sensitivity and efficacy of the EEG may contribute to management of the risk factors for SUDEP. Pedley and Hauser (2002) in a commentary on a UK audit of SUDEP in the Lancet stated that *“Because continuing seizures...are one of the most important associations with SUDEP, early and aggressive treatment is essential. Patients whose seizures do not respond promptly to treatment should be referred early to a neurologist for classification of seizure type and epilepsy syndrome, appropriate diagnostic testing,*

*“Appropriate diagnostic testing”* should include the most effective proven method of hyperventilation activation of epileptiform abnormalities on the

EEG, which would contribute significantly to the “*classification of seizure type and epilepsy syndrome*”.

In this thesis the initial study (Chapters 1-3) demonstrated the efficacy of using a standardised operational protocol (SOP) during the HV EEG exercise in normal adults ( $p>0.0001$ ). The significant decrease in the frequency of the posterior dominant rhythms noted in the adult study is confirmed in the clinical trial on patients with CAE and attack disorders. The SOP for HV has also been clearly demonstrated to be statistically and clinically significant in increasing the diagnostic yield of the EEG test in patients with primary generalised epilepsy (Fig. 5.11, Table 5.3). On the basis of this research the adoption of an SOP using the standardised seated OHV protocol during routine EEG and is recommended for all clinical neurophysiology departments, both paediatric and adult.

## **5.10 Final conclusions and summation**

There is currently no “Gold Standard” method of hyperventilation activation of EEG brain wave activity. This research was carried out to assess a novel methodological approach to the HV exercise during EEG testing. A standardized operational protocol (SOP), which controls for posture is most effective. In a clinical trial of patients with epilepsy it increased the diagnostic sensitivity of the test.

The initial study aimed to develop a standardised operational protocol for the hyperventilation exercise during EEG in adults. Testing was done while controlling for posture (seated: StOHV, and supine: SpOHV).

The StOHV protocol was shown to be effective by eliciting more pronounced EEG slow activity, increasing significantly the power density of EEG low frequency bands between 3.0 and 7.5 Hz, producing lower end-tidal CO<sub>2</sub>, and increasing the blood flow velocity in intracerebral arteries. The subjects were able to make a greater effort in the seated posture. This effort was reflected in the increase in heart rate during StOHV and the presence of more physical symptoms in response to the over-breathing. Therefore in a group of normal adults the study demonstrated the importance of position in developing a standardized hyperventilation response during EEG.

The method was shown to be statistically significantly more effective by reproducibly eliciting alterations in measured physiological variables as detailed in this thesis.

On the basis of these results, generalised adoption of such a standardised operational protocol (SOP) is recommended as a guideline for clinical best practice in adult EEG/Neurophysiology laboratories.

The aim of the follow-on study was to evaluate the StOHV method with the non-standardised HV (nsHV) method in clinical practice, in a group of children with childhood absence epilepsy (CAE), which is classified as an idiopathic generalised epilepsy, and another group of children with attack disorder

episodes, which had not yet been diagnosed (NYD). As this study was on children with a mean age of 9.6 years, co-operation with the over-breathing exercise was a possible variable. 87% of the patients were assessed to have made an excellent effort. As previously seen in the study on normal adults there was a significant increase in the amount of slow EEG activity elicited during the StOHV method. Hyperventilation induced high amplitude rhythmic slow activity (HIHARS) was induced both by nsHV and StOHV, but the mean PDR was 1.6 Hz slower during StOHV in both the CAE and AD/NYD group.

With regard to the efficacy of the method in eliciting epileptiform changes on the EEG and in inducing clinical events, the StOHV method is shown to be statistically and clinically more effective than nsHV. At rest 7 episodes of spontaneous clinical absence were captured with a total duration of 101 seconds and a mean duration for each event of 14.4 seconds. During nsHV, 10 episodes of clinical absence were captured with a total duration of 104 seconds and mean duration for each event of 10.4 seconds. During StOHV 27 episodes of clinical absence were captured with a total duration of 314 seconds and a mean duration for each event of 11.6 seconds. The number of absence seizures during nsHV-StOHV was statistically significant ( $p < 0.008$ ).

Significantly, 8.1% of the total group or 18.75% of the patients in the CAE group would not have been diagnosed with CAE if the StOHV exercise had not been performed.

Thus the two reported studies support the generalised adoption of such a standardised operational protocol (SOP), which is recommended as a guideline for clinical best practice in both paediatric and adult EEG/Neurophysiology laboratories

The method has also proven effective in eliciting additional diagnostic changes in the EEG of almost one fifth of patients in a group with probable idiopathic epilepsy. The HV SOP method described has been adopted in clinical practice in all EEGs performed in Our Lady's Children's Hospital, Crumlin, Dublin. It has now been in use by 6 different EEG practitioners since October 2008. There has been a greater than 15% improvement in the diagnostic yield of epileptiform EEGs with no significant difference in inter-practitioner results. It is proving to be a robust clinical tool. The author intends to audit the outcome of the adoption of the HV SOP after 6 months, preparatory to publishing the outcome in the academic and clinical literature.

In addition to the two reported clinical studies, this thesis also introduces a novel hypothesis: the 'Hypocapnia Cascade' (Chapter 2), which incorporates available data from the literature and suggests a comprehensive theory in which there is interaction and feedback within the ANS, brainstem, thalamus and CNS, triggered initially by hypocapnia and subsequent alkalosis induced by spontaneous hyperventilation, as the basis of the alterations in neuron/glial neocortical network that influence the degree of the neurophysiological EEG response to the over-breathing exercise.



## References Chapter 5:

- Adams DL, Lueders H, 1981, Hyperventilation and 6-hour EEG recording in evaluation of absence seizures. *Neurology* 31 (9): 1175-7
- Araque A, Sanzgiri RP, Parpura V, Haydon PG, 1998, Calcium elevation in astrocytes causes an NMDA receptor-dependent increase in the frequency of miniature synaptic currents in cultured hippocampal neurons. *J Neurosci* 18: 6822-6829
- Browne TR, Dreifuss FE, Penry JK, Porter RJ, White BG, 1983, Clinical and EEG estimates of absence seizure frequency. *Archives of Neurology* 40: 469-472
- Christensen J, Kjeldsen MJ, Andersen H, Friis ML, Sidenius P, 2005, Gender differences in Epilepsy. *Epilepsia* 46 (6): 956-960
- Cornell-Bell AH, Finkbeiner SM, Cooper MS, Smith SJ, 1990, Glutamate induces calcium waves in cultured astrocytes: long-range glial signalling. *Science* 247: 470-473
- Ficker DM, 2000, Sudden unexplained death and injury in epilepsy. *Epilepsia* 41(suppl 2): S7-12
- Hauser WA, Annegers JF, Rocca WA, 1996, Descriptive Epidemiology of Epilepsy: Contributions of Population-Based Studies from Rochester, Minnesota. *Mayo Clin Proc.* 71: 576-586
- Hochman DW, Baraban SC, Owens JW, Schwartzjroin PA, 1995, Dissociation of synchronization and excitability in furosemide blockade of epileptiform activity. *Science* 270: 99-102
- Lum LM, Connolly MB, Farrell K, Wong PKH, 2002, Hyperventilation – Induced High Amplitude Rhythmic Slowing with altered awareness: A video EEG Comparison with absence seizures. *Epilepsia* 43(11): 1372-1378
- Lux HD, Keinemann U, Dietzel I, 1986, Ionic changes and alterations in the size of the extracellular space during epileptic activity. *Adv Neurol* 44: 619-639
- Newman EA, Zahs KR, 1998, Modulation of neuronal activity by glial cells in the retina. *J Neurosci* 18: 4022-4028
- Orkand RK, Nicholls JG, Kuffner SW, 1966 Effect of nerve impulses on the membrane potential of glial cells in the central nervous system of amphibia. *J Neurophysiol* 29 (4): 788-806
- Pedley T, Hauser WA, 2002, Sudden Death in epilepsy: a wake up call for management.  
Pub online May 21, 2002. *The Lancet*  
<http://image.thelancet.com/extras/o2cmt85web.pdf>

Penfield W, 1929 The mechanisms of cicatricial contraction in the brain. *Brain* 50: 499-515

Takahashi T, 2004, 5<sup>th</sup> Ed. Chapter 14: Activation Methods , in *Electroencephalography: Basic principles, clinical applications, and related fields*. Eds. Neidermeyer E, Lopes da Silva F. pp 261-262 Lippincott Williams and Wilkins

Tian GF, Azmi H, Takano T, Xu Q, Peng W, Lin J, Oberheim N, Lou N, Wang X, Zeilke HR, Kang J, Negergaard M, 2005, An astrocytic basis of epilepsy *Nat Med* 11: 973-981

Walczak TS, Leppik IE, D'Amelio M *et al*, 2001, Incidence and risk factors in sudden unexplained death in epilepsy: a prospective cohort study. *Neurology* 56: 519-25  
Wirrell E, Camfield PR, Camfield CS, Dooley JM, Gordon KE, 1996, Accidental injury is a serious risk to children with typical absence epilepsy. *Archives of Neurology* 53: 929-932

## **Appendices**

**Appendix 1:** Research Ethics committee (REC Letter of approval, May 2002)

**Appendix 2a and 2b:** Research Ethics committee (REC Letters of approval, December 2006, March 2007)

**Appendix 3:** Information leaflets for clinical optimal hyperventilation study

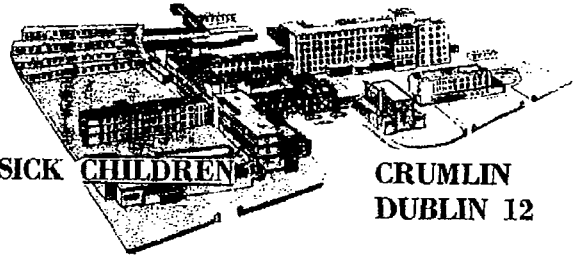
**Appendix 4:** Consent forms for clinical optimal hyperventilation study

**Appendix 5:** Data sheets for clinical optimal hyperventilation study

**Appendix 6:** A CD attached to the rear inside cover of the thesis, which contains the entire data set for both studies in the thesis

- 1) Adult HV study, excel workbook file, and subjects samples
- 2) CAE study, excel workbook file, and patient samples

## Appendix 1



**OUR LADY'S HOSPITAL FOR SICK CHILDREN**

TELEPHONE 409 8100 FAX 455 8873

**CRUMLIN  
DUBLIN 12**

REF. CR/ML

8<sup>th</sup> May 2002

Ms Ann Coughlan  
Chief Neuro-Technologist  
Our Lady's Hospital for Sick Children  
Crumlin  
Dublin 12

**Re: Neurological Study – The Effects of Posture on Quantitative EEG & Multivariate Analysis During Optimal Hyperventilation Activation in Healthy Adults.**

**Principal Investigator: Ms. Ann Coughlan, Chief Neuro-Technologist**

Dear Ms Coughlan

I write to advise you that the Ethics Committee Meeting held on Tuesday, 7<sup>th</sup> May 2002 approved the above Research Project.

Yours sincerely

A handwritten signature in cursive script, appearing to read 'Claire Rice', with a small star-like mark at the end.

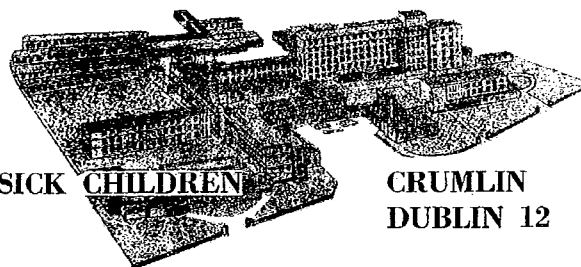
**CLAIRE RICE  
SECRETARY  
ETHICS COMMITTEE**

CC: Professor Joe McMenamin  
Dr. David Webb

## Appendix 2a

**OUR LADY'S HOSPITAL FOR SICK CHILDREN**

TELEPHONE 409 6100 FAX 455 8873



**CRUMLIN  
DUBLIN 12**

REF.

**RESEARCH ETHICS COMMITTEE OFFICE**  
Tel: (01) 409 6307/6243

**Ms Ann Coughlan**  
**Chief Neurophysiology Technologist**  
Children's Neuroscience Centre  
Neurophysiology/EEG Department  
Medical Tower  
Our Lady's Children's Hospital  
Crumlin  
Dublin 12

**13<sup>th</sup> December 2006**

**REC Reference: SAC/91/06**

**EudraCT No.: N/A**  
(Please quote REC reference and EudraCT numbers on all correspondence)

**Re: The hyperventilation exercise during EEG testing in children.  
Is a change to the hyperventilation method more effective at  
eliciting positive EEG findings in patients with childhood  
absence epilepsy and undiagnosed episodes?**  
*Chief Investigator: Ms. Ann Coughlan*

Dear Ms Coughlan

The Recognised Ethics Committee reviewed the above application at its meeting held on 12<sup>th</sup> December 2006.

The Committee has given a favourable ethical opinion for the Project based on the application form, protocol and supporting documentation submitted and **subject to receipt by the Secretary** of the following amended documentation and review of same by Chairperson:

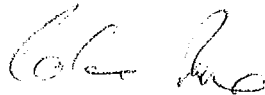
- Documentation for the Research Project to be kept separate from the hospital's appointment/tests notification to parents.
- Age related Information Leaflets/Consent Forms to be provided.

-2-

- Mention to be made in the above documentation of confidentiality and anonymity, in any publication resulting from the Study.

Please forward the above amended documentation to the Secretary **as soon as possible** for review by the Chairperson and to complete our files.

Yours sincerely



**Claire Rice**  
**Secretary**  
**Research Ethics Committee**

E-mail: [ethics.committee@olhsc.ie](mailto:ethics.committee@olhsc.ie)

Appendix 2b

OUR LADY'S HOSPITAL FOR SICK CHILDREN

TELEPHONE 409 6100 FAX 455 8873

CRUMLIN  
DUBLIN 12

RESEARCH ETHICS COMMITTEE OFFICE  
Tel: (01) 409 6307/6243

REF

Ms Ann Coughlan  
Chief Neurophysiology Technologist  
Children's Neuroscience Centre  
Neurophysiology/EEG Department  
Medical Tower  
Our Lady's Children's Hospital  
Crumlin  
Dublin 12

13<sup>th</sup> March 2007

REC Reference: SAC/91/06

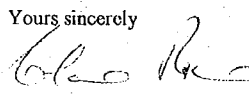
Re: The hyperventilation exercise during EEG testing in children.  
Is a change to the hyperventilation method more effective at  
eliciting positive EEG findings in patients with childhood  
absence epilepsy and undiagnosed episodes?  
Chief Investigator: Ms. Ann Coughlan

Dear Ms Coughlan

Thank you for forwarding the amended documentation in relation to the above project, which was requested following the Ethics Committee meeting of 12<sup>th</sup> December 2006.

The Chairperson, Professor Andrew Green, has reviewed these documents and has requested one further minor alteration i.e. please insert an additional line for "Witness Signature" on the Consent Forms. This now completes our file on this project.

Yours sincerely

  
Claire Rice  
Secretary  
Research Ethics Committee

E-mail: [ethics.committee@olhsc.ie](mailto:ethics.committee@olhsc.ie)

CC: Dr. David Webb

### Appendix 3: Information Leaflets for various age groups



**Information Leaflet.  
For children aged 4 to 8 Years  
Optimal Hyperventilation during the Video- EEG test with Trans Cranial Doppler  
measurement of blood flow**

Dear \_\_\_\_\_

Your appointment for Video – EEG test is on \_\_\_\_\_ at \_\_\_\_\_

The Video-EEG test is a test which measures your “Brain Wave” activity.

It takes about 1 hour to do the test. It does not hurt. During the EEG test we ask children to take deep breaths for 3 minutes with the eyes closed while lying down on a bed. Sometimes this makes you feel a little dizzy or you might get “pins and needles” in your fingers while you are taking the deep breaths.

As part of a project we would also like you to do the deep breathing again but this time while sitting in a comfy armchair. We will ask you to breathe 30 times per minute. We will measure how fast you are breathing using a little button under your nose.

We think this new way of doing the breathing test may be better

We would also like to put a different button on your forehead for a few minutes to listen to the blood flowing while you are taking the deep breaths. This is all really easy and it doesn't hurt at all. We will be taking a video of you during your EEG. If we use any of your brain wave measurement results in papers we might write about the new way of doing the breathing test your name is always kept totally private.

We will answer any questions you may have when you attend for the EEG test.

If you don't wish to take part in this project we will only do our routine EEG study.

Many Thanks

Ann

---

Ann Coughlan MSc, Chief Neurophysiology Technologist  
Prof J. Mc Menamin, Consultant Paediatric Neurologist  
Dr. D Webb, Consultant Paediatric Neurologist





**Information Leaflet.**  
**For children aged 8 to 12 Years**  
**Optimal Hyperventilation during the Video- EEG test with Trans Cranial Doppler**  
**measurement of blood flow**

Dear \_\_\_\_\_

Your appointment for Video – EEG test is on \_\_\_\_\_ at \_\_\_\_\_

The Video-EEG test is a test which measures your "Brain Wave" activity.

It takes about 1 hour to do the test. It does not hurt. During the EEG test we ask children to take deep breaths for 3 minutes with the eyes closed while lying down on a bed. Sometimes this makes you feel a little dizzy or you might get "pins and needles" in your fingers while you are taking the deep breaths.

As part of a project we would also like you to do the deep breathing again but this time while sitting in a comfy armchair. We will ask you to breathe 30 times per minute. We will measure how fast you are breathing using a little button under your nose.

We think this new way of doing the breathing test may be better

We would also like to put a different button on your forehead for a few minutes to listen to the blood flowing while you are taking the deep breaths. This is all really easy and it doesn't hurt at all. We will be taking a video of you during your EEG

We will answer any questions you may have when you attend for the EEG test.

If you don't wish to take part in this project we will only do our routine EEG study.

Many Thanks

Ann

---

Ann Coughlan MSc. Chief Neurophysiology Technologist  
Prof J. Mc Menamin, Consultant Paediatric Neurologist  
Dr. D Webb, Consultant Paediatric Neurologist



**Information Leaflet.**  
**For children/teenagers aged 12-18 years**  
**Optimal Hyperventilation during the Video- EEG test with Trans Cranial Doppler**  
**measurement of blood flow**

Dear \_\_\_\_\_

Your appointment for Video – EEG test is on \_\_\_\_\_ at \_\_\_\_\_

The Video-EEG test is a test which measures your "Brain Wave" activity.

It takes about 1 hour to do the test. It does not hurt. During the EEG test we ask you to take deep breaths for 3 minutes with the eyes closed while lying down on a bed. Sometimes this makes you feel a little dizzy or you might get "pins and needles" in your fingers while you are taking the deep breaths.

As part of a research project we would also like you to do the deep breathing a second time while sitting upright in a comfy armchair. We will ask you to breathe 30 times per minute. We will measure how fast you are breathing using soft plastic nasal prong placed just under your nose.

We think this new way of doing the breathing test may be better and more useful to your doctor.

We would also like to put a small microphone on your forehead for a few minutes to listen to the blood flowing while you are taking the deep breaths. This is all really easy to do and it doesn't hurt at all. We will be taking a video of you during your EEG and the breathing exercise.

If you have any questions about the EEG test or the new way of doing the breathing test while sitting call me at 4096632. We can also answer any questions you may have when you attend for the EEG test. If you don't wish to take part in this project we will only do our routine EEG study.

All of the information collected is totally confidential and anonymous if used in any publication resulting from the study. You may choose to withdraw from the study at any time.

A consent form is attached which your parents need to sign if you wish to take part in this research.

Many Thanks

Ann

---

Ann Coughlan MSc. Chief Neurophysiology Technologist  
Prof J. Mc Menamin, Consultant Paediatric Neurologist  
Dr. D Webb, Consultant Paediatric Neurologist



**Information Leaflet for Parents**  
**Optimal Hyperventilation during the Video- EEG test with Trans Cranial Doppler measurement of blood flow**

Dear \_\_\_\_\_

Your child's appointment for Video – EEG test is on \_\_\_\_\_ at \_\_\_\_\_

The Video-EEG test is a painless test which measures "Brain Wave" activity. It takes approximately 1 hour to perform. During the EEG test we routinely ask children to over breathe (hyperventilate) for a period of 3 minutes. This involves breathing quickly and deeply for 3 minutes with the eyes closed while lying down. During this breathing exercise some children feel light headed, get a tingling sensation in their fingers or toes or face and feel hot or cold. This is a normal response to taking deep breaths and will go away within 30 seconds once the over breathing ceases.

As part of a research study we would also like your child to perform an additional 3 minute period of over breathing while sitting upright in a comfortable armchair. This will involve breathing 30 times per minute while we measure the amount of a gas called carbon dioxide breathed out through the nose through soft nasal prongs. We think this new way of doing the breathing test may be more effective and useful to your doctor in making a diagnosis and choosing treatment.

Using an ultrasound probe we would also like to measure the speed of blood flow through the forehead. This measurement is called a Trans Cranial Doppler (TCD) test. It does not hurt in any way.

We routinely video the EEG so that any spells or changes in facial colour can be recorded. If there are no such events the video is deleted and is not retained.

If you have any questions about the EEG test or about the new way of doing the breathing test while sitting upright please call me at 4096632. We can also answer any questions you may have when you attend for the EEG test. If you do not wish your child to take part in this research we will only perform our routine EEG study. All the EEG information collected will be totally confidential and completely anonymous if used in any publication resulting from the study. You may withdraw from inclusion in the study at any time.

A consent form is attached. If you and your child are willing to take part in this research please sign the consent form and bring it with you on the day of the EEG test.

Many Thanks

---

Ann Coughlan MSc. Chief Neurophysiology Technologist  
Prof J. Mc Menamin, Consultant Paediatric Neurologist  
Dr. D Webb, Consultant Paediatric Neurologist

#### Appendix 4: Consent forms for various age groups



##### Consent form (Parents) Video EEG with seated hyperventilation

I give consent for my child \_\_\_\_\_

To perform a period of Hyperventilation while seated during their Video –EEG test .

I give consent for the recording of a Video-EEG on my child.

I give consent for a measurement of blood flow using Trans Cranial Doppler

Signed\_\_\_\_\_

Witness\_\_\_\_\_

Date\_\_\_\_\_



**Consent form  
Age 12-18 years  
Video EEG with seated hyperventilation**

NAME: \_\_\_\_\_

I \_\_\_\_\_ give my consent to:

- perform a period of Hyperventilation while seated during my Video –EEG test .
- I give consent for the recording of my Video-EEG .
- I give consent for a measurement of blood flow using Trans Cranial Doppler

Signed \_\_\_\_\_

Witness -----

Date \_\_\_\_\_

**Appendix 5: Data Sheets for Clinical SOHV study**

NAME	DOB	EEG #	PROC DATE	HEIGHT	<u>WEIGHT</u>	SUPINE BP	SEATED BP
At Rest	Seated	ClinHx:					<u>Co-op ?</u>
Time	RespRate	HrtRate	ETCO2	O2	EEG @	vCBF avg	
HV1	SOPHV	4 min					
Time	RespRate	HrtRate	ETCO2	O2	EEG@	vCBF peak	<u>Co-op ?</u>
Absence Events							
At Rest	Supine						
Time	RespRate	HrtRate	ETCO2	O2	EEG@	vCBF avg	Co-op ?
HV 2	Supine,SOPHV	4 min					
Time	RespRate	HrtRate	ETCO2	O2	EEG@	vCBF peak	Co-op ?
Absence Events							
HV 3	Supine, non standardised HV	3 min					
Time	RespRate	HrtRate	ETCO2	O2	EEG@	vCBF peak	Co-op ?
							t

